

STUDIES OF CELL DISRUPTION  
IN HIGH PRESSURE HOMOGENISERS

by

ELAHEH KESHAVARZ

A thesis submitted for the degree  
of Doctor of Philosophy at The  
University of London

SERC Centre for Biochemical Engineering  
Department of Chemical and Biochemical Engineering  
University College London

1990

ProQuest Number: 10609867

All rights reserved

INFORMATION TO ALL USERS

The quality of this reproduction is dependent upon the quality of the copy submitted.

In the unlikely event that the author did not send a complete manuscript and there are missing pages, these will be noted. Also, if material had to be removed, a note will indicate the deletion.



ProQuest 10609867

Published by ProQuest LLC (2017). Copyright of the Dissertation is held by the Author.

All rights reserved.

This work is protected against unauthorized copying under Title 17, United States Code  
Microform Edition © ProQuest LLC.

ProQuest LLC.  
789 East Eisenhower Parkway  
P.O. Box 1346  
Ann Arbor, MI 48106 – 1346

I would like to express my special thanks to my supervisor, Professor Peter Dunnill for his invaluable advice and continuous encouragement of new thoughts and ideas in the course of this study. I also wish to thank Dr. Mike Hoare for his constructive and helpful comments, and the members of the research and technical team for their support. I would like to extend my thanks to the SERC for their financial support, and to the members of APV-Gaulin and APV-Baker specially Messrs. Dick Kinney and Peter Davies for their cooperation.

*"E pur si muove!"*  
(But it does move!)

Attributed to Galileo Galilei; after he  
recanted his assertion that the earth  
moved round the sun.

## ABSTRACT

In this study several aspects of cell disruption in high pressure homogenisers were investigated. Firstly, the kinetics of disruption of Rhizopus nigricans, a filamentous fungus, was shown to exhibit major differences from those of unicellular microorganisms. The release of soluble protein was a weak function of pressure and number of passes. The maximum level of soluble protein release ( $R_m$ ) which appeared to vary with pressure was shown to be associated with micronisation of cell debris. A more specific assay for a soluble enzyme (ADH) showed no such apparent variation. The major effect of cell concentration was not on disruption kinetics but on structural characteristics of the suspension which resulted in homogeniser blockage at relatively low cell concentrations (20–22 g/L dry weight) and also influenced the harvesting and resuspension processes.

Another aspect of cell disruption examined was the effect of valve assembly configuration on the disruption of both unicellular and filamentous microorganisms. Six valve units were characterised and several parameters were shown to be critical. Impact distance was an important factor in the disruption of filamentous R. nigricans cells, whilst valve geometry did not appear to have any notable effect. Valve unit configuration had a significant effect on the disruption of the unicellular microorganism, bakers' yeast. Maximum performance was observed with a 'knife-edge' valve seat configuration and valve geometries consisting of a flat valve seat and flat valve rod gave lowest yields. A reduction in the "land" width gave improved performance. Changing the valve rod to a cone shape also resulted in higher protein release. As with filamentous microorganisms, variation in the impact distance had a major effect on the performance of the homogeniser.

The effect of homogenisation on the size distribution of yeast cell debris and microsomal fractions obtained from R. nigricans cells was also investigated. A reduction of at least 10% was observed in the size of the microsomes from one to 2 passes with no further decrease up to 4 passes. For all valve units tested, as the number of passes was increased, a reduction in the proportion of larger yeast debris particles was noted. In general, higher protein release was associated with a higher percentage of smaller particles except for a marginal trend observed for the 'flat valve' unit giving larger particles for equivalent protein release compared to other valves.

Based on the findings for bakers' yeast an explanation of the mechanism of cell disruption was sought. A modified Bernoulli equation was used to define the flow velocities through the valve rod and valve seat for different valve unit configurations. The main disruption mechanism was shown to be impingement, the rate of cell breakage being related to the stagnation pressure or the maximum wall stress of the fluid jet. Decreased valve gap width and decreased impact distance both contributed to an increased cell disruption rate, the performance of the homogeniser being related to the product of these two dimensions for the range of valve seats and impact distances studied. Further experimental work to test the proposals has been defined.

The design of an integrated homogenisation system consisting of a new commercial homogeniser and various ancillary items of equipment was undertaken to provide a suitable process unit for further research, taking into account the additional elements needed for containment.

<u>TABLE OF CONTENTS</u>	<u>PAGE</u>
TITLE PAGE	1
ACKNOWLEDGMENTS	2
ABSTRACT	4
TABLE OF CONTENTS	6
 1. INTRODUCTION	 12
1.1 Methods of cell disruption	12
1.1.1 Small scale disruption	13
1.1.1.1 Non-mechanical methods	13
1.1.1.2 Mechanical methods	14
1.1.1.2.1 Sonication	15
1.1.1.2.2 Explosive decompression	16
1.1.1.2.3 Extrusion	16
1.1.1.2.4 Agitation	19
1.1.2 Large scale disruption	19
1.1.2.1 High speed bead mill	20
1.1.2.2 High pressure homogenisers	23
1.1.3 Recent developments in mechanical devices for cell disruption	25
1.1.3.1 New concepts in the design of high pressure homogenisers	25
1.1.3.2 Microfluidisers	26
1.2 Kinetics of cell disruption	27
1.2.1 Development of a kinetic model	27
1.2.2 Effect of $R_m$ on the kinetics model	30
1.2.3 Disruption kinetics of filamentous microorganisms	32
1.2.4 Effect of operating parameters	33
1.2.4.1 Valve design	34
1.2.4.2 Cell characteristics	36

1.2.4.2.1	Conditions of cell growth	36
1.2.4.2.2	Effect of cell wall structure	36
1.2.4.2.3	Cell concentration	46
1.2.4.3	Pressure and number of passes	47
1.2.4.4	Temperature	48
1.2.4.5	Flow rate	49
1.3	Disruption mechanism in high pressure homogenisers	50
1.3.1	Stress	50
1.3.1.1	Normal stress	52
1.3.1.2	Impingement	53
1.3.1.3	Shear	54
1.3.2	Magnitude and rate of pressure drop	55
1.3.3	Turbulence and velocity changes	55
1.3.4	Cavitation	56
1.3.5	Explosive decompression	57
1.4	Cell particle and cell debris formation	58
1.4.1	Cell debris	59
1.4.2	Inclusion bodies	60
1.4.3	Microsomal fractions	60
1.5	Scope of the study	63
2.	MATERIALS AND METHODS	64
2.1	Materials	64
2.2	Microorganisms	64
2.3	Growth medium for <u>Rhizopus nigricans</u>	65
2.4	Growth of <u>Rhizopus nigricans</u> in shake flasks	65
2.5	Growth of <u>R. nigricans</u> in fermenters	66
2.5.1	Equipment	66
2.5.1.1	Fermenters	66
2.5.1.2	Instrumentation and sterilisation	66
2.5.2	Conditions of growth	67
2.5.2.1	Filamentous growth	67
2.5.2.2	Pelleted growth	68



2.6	Harvesting	68
2.6.1	Nylon Mesh	68
2.6.2	Basket centrifuge	68
2.7	Preparation of microorganisms for disruption	69
2.7.1	Bakers'yeast	69
2.7.2	<u>Rhizopus nigricans</u>	69
2.8	High pressure homogenisation	69
2.8.1	Equipment	69
2.8.2	Changing of valve assembly	70
2.8.3	Disruption procedure	73
2.9	Microsomal preparation	74
2.9.1	Homogenate	74
2.9.2	Gel filtration	74
2.9.3	'Sugar cushioning'	75
2.10	Particle size measurement	75
2.10.1	Sample types	75
2.10.2	Photon correlation spectroscopy	75
2.10.2.1	Equipment	75
2.10.2.2	Sample preparation	77
2.10.2.3	Instrument settings	78
2.10.3	Electrical sensing zone	78
2.11	Gel electrophoresis	78
2.12	Protein assay	79
2.12.1	Bakers'yeast	79
2.12.2	<u>R.nigricans</u>	80
2.13	Alcohol dehydrogenase activity assay	80
2.14	Dry weight measurements	80
2.15	Microscopy	81
3.	DISRUPTION CHARACTERISTICS OF <u>RHIZOPUS NIGRICANS</u>	82
3.1	Effect of pressure and number of passes	82
3.1.1	Shake flask culture	82
3.1.2	Fermenter cultures	84

3.1.3	Maximum protein release	84
3.2	Effect of cell concentration	90
3.3	Effect of up-stream processing conditions	90
3.3.1	Cell growth	90
3.3.2	Harvesting and storage	92
3.4	Discussion	93
3.4.1	Micronisation	93
3.4.2	Cell related conditions	98
3.4.3	Disruption kinetic	98
4.	SIGNIFICANCE OF MECHANICAL PARAMETERS IN CELL DISRUPTION	100
4.1	Valve unit characterisation	100
4.2	Effect of valve unit geometry on disruption of <u>R.nigricans</u>	102
4.3	Effect of impact distance on disruption of <u>R.nigricans</u>	107
4.4	Discussion	107
4.5	Effect of valve unit geometry on disruption of bakers' yeast	110
4.5.1	Effect of geometry of valve seat central orifice	110
4.6	Effect of impact distance on disruption of bakers' yeast	114
4.7	Effect of scoring of the valve seat	114
5.	PARTICLE AND CELL DEBRIS FORMATION	121
5.1	Microsomal fractions from <u>R. nigricans</u>	121
5.1.1	Microsomal preparation	121
5.1.2	Effect of cell disruption on microsomes	124
5.1.3	Sugar cushioning for microsomal separation	127
5.2	Effect of homogenisation on yeast debris formation	129

5.2.1	Effect of multiple passes	129
5.2.2	Effect of valve unit geometry	129
5.2.3	Comparison between CD and CR valve units	142
5.2.4	Effect of impact distance	148
6.	MECHANISM OF CELL DISRUPTION	153
6.1	Theoretical considerations	153
6.2	Discussion	158
6.2.1	Effect of impact ring	160
6.2.2	Effect of valve geometry	161
6.3	Concluding remarks on the mechanism of disruption	162
7.	BIOCHEMICAL ENGINEERING DESIGN OF AN INTEGRATED HOMOGENISATION SYSTEM	165
7.1	Background	165
7.2	Design philosophy	166
7.3	The homogeniser	167
7.3.1	Main features	167
7.3.2	Additional features for the integrated system	169
7.4	Plan of the auxiliary equipment	170
7.5	Design of hoppers	172
7.5.1	Level control	172
7.5.2	Instrumentation	173
7.6	Pipework, fittings and valves	175
7.7	Heat exchanger unit	176
7.8	Control panel	180
7.9	Steam sterilisation and CIP	180
7.10	Conclusion – future containment	184

8. CONCLUSION – FUTURE WORK	186
8.1 Mechanism of cell disruption	186
8.2 Particle sizing and valve design	187
APPENDIX A Growth of <u>Rhizopus nigricans</u> in fermenters	188
APPENDIX B Application of photon correlation spectroscopy	195
NOMENCLATURE	213
REFERENCES	215

## 1. INTRODUCTION

The recovery of intracellular materials, such as enzymes, from microorganisms has gained a fresh momentum over the past decade as a result of new commercial applications in the food and pharmaceutical industries and the prospects of further product development by genetic engineering.

The design and operation of large scale extraction and isolation systems for intracellular proteins and enzymes have been constrained by the denaturation and loss of activity of products during processing. Better understanding of each step from product formation in fermenters to cell breakage, separation and purification has been shown to improve the development of industrial techniques (Dunnill 1983). Cell disruption constitutes the first stage in the isolation of intracellular materials. It is a crucial step in downstream processing because any damage to the product at this initial phase will invalidate subsequent design and make operational refinement to other plant equipment irrelevant. On the other hand high disruption yield will allow more flexibility in the follow up treatment of the product.

### 1.1 Methods of cell disruption

Over the past twenty years several reviews have been published on the methods available for cell disruption (Wimpenny 1967; Edebo 1969; Wiseman 1969; Hughes et al. 1971; Edebo and Magnusson 1973; Coakley et al. 1977; Engler 1985; Chisti and Moo-Young 1986). These methods can be divided into two categories, small scale techniques for laboratory applications and large scale techniques for industrial uses.

### 1.1.1 Small scale disruption

Techniques in laboratory work are numerous and entail both mechanical and non-mechanical approaches. A wide range of non-mechanical methods are available including enzymic lysis, chemical lysis, phage lysis, heat treatment, osmotic shock, freezing and thawing and utilisation of temperature sensitive or wall deficient microbial mutations.

#### 1.1.1.1 Non-mechanical methods

Enzymic lysis is one of the most widely studied laboratory methods. It constitutes the most gentle way to release the cell membrane intact (Hughes et al. 1971; Kitamura and Tanabe 1982; Asenjo et al. 1985). The enzyme attacks only specific bonds in the cell wall structure of microorganisms leaving the rest of the cell undamaged. It can also be used to weaken the cell wall prior to mechanical disruption in order to reduce the resulting mechanical shear applied on the intracellular constituents of the microorganism (Liu et al. 1988).

The method is at present limited for several reasons. A prerequisite in the application of enzymic lysis is the selection of appropriate enzyme system and determination of appropriate reaction conditions for efficient lysis (Engler 1985; Zomer et al. 1987). The use of previously untested lytic enzymes would therefore entail considerable input of time and effort. Commercially available lytic enzymes may be a mixture of reagents containing degradative enzymes to which intracellular contents of interest may be susceptible. The costs of lytic enzymes is a further restrictive element in their usage. The immobilisation of lytic enzymes on insoluble supports to extend their use, although highly desirable, is limited by steric hindrance of their activity (Asenjo and Dunnill 1981). The use of a soluble support has been shown to be feasible (Dunnill 1972) but may

prove difficult for processing filamentous fungi due to fouling of the filtration membrane at the separation stage.

Autolysis is attractive because it is volume independent (Chisti and Moo-Young 1986), however it is affected by many parameters including temperature, pH, buffer molarity and is therefore difficult to control (Hughes et al. 1971). Phage infection is also a difficult process to control and may result in altered cellular constituents (Engler 1985).

Chemical lysis by treatment with acids, alkalis, surfactants or solvents may be expensive and results in contamination of the product with the chemical (Chisti and Moo-Young 1986). It is also generally accompanied by considerable protein denaturation (Dunnill and Lilly 1975).

Osmotic shock is another gentle method for cell disruption although most microorganisms cannot be disrupted by it alone. The method is therefore often used in conjunction with other techniques (Wimpenny 1967).

Physical methods such as repeated freezing and thawing, heating and drying although reported successful (Hughes et al. 1971), usually have low yields (Dunnill and Lilly 1975) and are susceptible to denaturation (Engler 1985). In the case of temperature sensitive mutants or microorganisms containing inducible phages, the time lag involved in temperature changes in fermenters require careful engineering to avoid premature lysis (Dunnill 1983).

#### 1.1.1.2 Mechanical methods

Mechanical methods employed in cell disruption are based on shearing action which may involve solids with or without abrasives, such as in the Hughes Press and in the X Press, or a grinding action as with

a pestle and mortar or in a ball mill. Otherwise the French Press, ultrasonication or vibration with beads may be employed.

#### 1.1.1.2.1 Sonication

One of the most frequently used mechanical methods for cell disruption on laboratory scale is sonication (Wiseman 1969; Engler 1985). As the input sonic energy increases, microbubbles form at various nucleation sites during the rarefaction phase of the sound wave and then in the compression phase, the bubbles collapse releasing shock waves which propagate in the medium. The phenomenon is called cavitation. Mechanical forces that can cause cell disintegration could arise prior to the collapse of bubbles. Microstreaming near the bubble surface generates stresses caused by velocity gradients strong enough to disrupt cells (Hughes and Cunningham 1963). In the collapse phase of cavitation, a large quantity of sonic energy is released as elastic waves. Doulah (1977) proposed that shear stresses responsible for cell disruption arise from elastic waves. The principal determinant of susceptibility to ultrasonic cell disruption was reported to be the mean volume of the cell irrespective of culture conditions (Wase and Patel 1985). However this observation may be the result of changes in wall strength brought about by varying fermentation conditions (e.g. impeller speed) which were implemented to obtain different cell volumes, and not the cell volume itself.

The technique is limited to small scale operation for several reasons. There are difficulties of transmitting sufficient power to large volumes of liquid (Scawen et al. 1980) and providing adequate cooling (Lilly and Dunnill 1969); the process may cause significant degradation of enzymes (Engler 1985) and also may produce very fine debris which may lead to subsequent processing problems (Chisti and Moo-Young 1986). Furthermore, sonication has proved to be an inefficient method of disruption of fungi (Edebo 1983).



#### 1.1.1.2.2 Explosive decompression

In this technique, an inert gas (e.g. nitrogen) is dissolved into cells under high pressure until equilibrium is reached. The pressure is then suddenly released causing rupture of cell wall and membranes due to high internal and external cellular pressure difference (Fraser 1951). The technique is gentle, no oxidation occurs since an inert gas is used and, rapid adiabatic decompression results in minimal overall temperature increase. However, it is only applicable to fragile cells and is difficult to scale up (Nissinen and Markkanen 1986).

#### 1.1.1.2.3 Extrusion

Extrusion of microorganisms through an orifice by pressure is the basis of operation for Hughes Press, X Press and the French Press. The former two devices extrude material that has been frozen, and do not require a valve to adjust pressure. The French Press handles unfrozen cells and consists of a steel cylinder having a small orifice, with a needle valve at its base. A hydraulically driven gas piston pressurises the content of the piston up to 210 MPa (Hughes et al. 1971). The press is precooled to 0-5° C. At the chosen pressure the valve is opened and pressure is maintained by pumping. Similar devices with precise orifice size control were later designed.

In 1951, Hughes developed a method for breaking microorganisms by forcing a frozen suspension or paste of cells through a narrow slit at very high pressures (200 MPa). Later on Edebo modified the apparatus such that the cell suspension would undergo several passes. This device, referred to as an X Press, consisted of two identical cylindrical axial chambers separated by a disk with a central circular orifice of about 1-2 mm diameter. Different theories have been put forward for the mechanism of cell disruption

by this technique, with little agreement amongst researchers.

Hughes et al. (1971) attributed the disintegrative effect to the abrasive action of ice crystals during compression and the re-gelation brought about by the pressure drop at discharge, with a resultant decrease in volume. Early work by Edebo in the 1960's however had suggested that a major contribution factor was the conformational change when ice crystals changed phases under pressure; the pressure required for initiation of flow being related to the phase boundaries of water. The flow through the orifice was in discontinuous short pulses accompanied by sharp bangs. Further experimentation by Hughes et al. (1971) indicated that when the plunger of a Hughes press was given sufficient pressure (the value of which was not disclosed) to produce the cracking sound associated with the phase change and to force about 2 mm of a 3 cm plug of frozen cells through the slit into a reservoir, over 95% disintegration was noted in the cells in the reservoir, 80% at both ends of the plug and almost none at the centre of the plug. Hughes took this as evidence for the abrasive action of ice when ice and cells moved across the gap from cylinder to reservoir. No mention was made of mechanisms which may be related to the size or shape of the gap or to the kinetics of the process. Further detailed studies were carried out using an X Press (Magnusson and Edebo 1976a, 1976b). Although much data was obtained on the effects of salts and gelatin, on cell concentration, on differing freezing temperatures and on changes in the hydraulic press design (manual versus motor driven), no conclusive results to explain the mechanism of disruption emerged. The main result was that more concentrated samples tended to flow more smoothly and that disintegration was enhanced by a lower temperature and a higher velocity of flow through the orifice.

Scully and Wimpenny (1974) carried out a set of experiments with yeast suspension (50% w/w) at -27° C in which Hughes Press was filled with alternating layers of different colours before compression.

After an initial compression during which the mixture became compact due to the release of intra-crystalline air, the solid moved down inside the cylinder in plug flow until the gap was reached. By examining the layers deposited in the reservoir and the last layers remaining in the press, it was shown that only the lowest zone had extruded radially. The conclusion was therefore that the flow regime was plug flow followed by radial flow. Comparative experiments at ambient temperature using gelatine, plasticine and sand each coloured in layers resulted in the flow properties similar to that pertaining in the Hughes Press. Disruption was therefore modelled on the basis of plastic flow of thin layers under compression through an orifice. This theoretical treatment was to be followed by experimental work with various microorganisms and varying gap width and temperature, however no published data is available on these studies.

The scale up of the X Press based on a semi-continuous operation of the equipment was developed by Magnusson and Edebo (1976c). However no industrial sized freeze press is known to be commercially available (Chisti and Moo-Young 1986).

The major advantage of freeze pressing is its effectiveness in disrupting cells. At a sample temperature of  $-35^{\circ}\text{C}$  and a press temperature of  $-20^{\circ}\text{C}$ , about 90% disruption was achieved in a single passage of bakers' yeast paste through the orifice (Magnusson and Edebo 1976c). Furthermore cell wall membrane preparations by this method are relatively intact (Wimpenny 1967). Although Edebo (1983) stated that minimal enzyme inactivation occurs during this process relative to other procedures, Hughes et al. (1971) had commented that the technique was not suitable for enzymes sensitive to freezing and thawing.

#### 1.1.1.2.4 Agitation

Rapid agitation of a cell suspension with glass beads as a means of cell disruption has been extensively applied to both laboratory and industrial scale operations. For laboratory applications, blenders (e.g. Waring blender) have been used although the shear forces produced are not large enough to break many strains of bacteria (Wimpenny 1967). Better results were obtained by introducing ballotini beads into the suspension. The rapid increase in sample temperature during disruption has to be offset by means of a cooling system.

Recently, it has been reported that a mixer mill (traditionally used for dry milling of minerals, textiles etc.) may be modified for cell disruption on microscale level (Schutte and Kula 1988). The mill is equipped with two horizontally positioned grinding chambers of 12.5 mL capacity each, in which beads (less than 1 mm) are accelerated to a three dimensional movement. The most significant parameters affecting disruption are similar to those identified for the large scale bead mills (Section 1.1.2.1). One advantage of this technique is the low temperature increase ( $0.12^{\circ}\text{C/min}$  at a vibration frequency of  $1800\text{ min}^{-1}$ ), which eliminates the need for an external cooling system.

#### 1.1.2 Large scale disruption

Attempts at scaling up laboratory disruption methods for large scale operations have been mainly concentrated on mechanical techniques, specifically high speed bead mills and high pressure homogenisers. With the advent of modern recombinant DNA technology for the manufacture of mammalian proteins in microorganisms, it is necessary to operate cell disruption equipment in a contained fashion and with the possibility of in-place cleaning and sterilisation. These two disruption techniques are well geared to meet such requirements.

High speed bead mills are particularly effective against those microbial cells which are resistant to other methods. The smaller models can be readily mounted and operated in safety cabinets and therefore used for the disruption of potentially pathogenic microorganisms (Scawen et al. 1980). However, according to Darbyshire (1981), the technique has rarely been used for large scale enzyme preparation. Scawen et al. (1980) carried out a survey of large scale enzyme purification techniques undertaken in the 1970's. Data on twenty seven enzymes, seventeen of which were from bacterial or fungal sources were collected. It was found that out of the twenty one large scale purification procedures reported, eleven utilised an APV-Gaulin homogeniser, two a French Press and only one a bead mill. This could be attributed to two possible factors. Firstly, bead mills may be limited by the minimum size of beads that can be used in commercial scale units (Schutte et al. 1983). Homogenisers, on the other hand, are very flexible. Their only limitation is that blockage may occur with concentrated mycelial suspensions. However research has been carried out to investigate and overcome this problem (Thomas 1988). Secondly, with homogenisers, there are fewer operating parameters to consider than with high speed ball mills (Engler 1985).

#### 1.1.2.1 High speed bead mill

Originally bead mills were used in industry for fine grinding and dispersion of dyestuffs and pigments. Zetelaki (1969) briefly described the use of a bead mill for the disruption of Aspergillus and Currie et al. (1972) examined the disruption of yeast cells using a similar mill. No machine was constructed at the time specifically with a view to cell disruption. The development of bead mill equipment and research carried out in their design are reviewed by Dunnill and Lilly (1975), Engler (1985), and Chisti and Moo-Young (1986).

The design of bead mills depends on the size of the unit and the manufacturer. They consist of either a vertical or a horizontal grinding chamber containing rotating disks mounted on a motor driven shaft. The grinding action is provided by beads typically occupying 80–85% of the free working volume of the chamber. The disks may be mounted concentrically or off-centred. The units must be equipped with high capacity cooling systems for processing temperature sensitive materials. Horizontal units are generally preferred for cell disruption. The grinding action in vertical mills is reduced due to fluidising effects of the upward fluid flow on the beads. Furthermore horizontal mills are fed from above so that there is no need for a screen at the feed end to retain the beads inside the chamber as is the case in a vertical mill.

A large number of factors affect the operation of the bead mill. These include the agitator speed and the number of disks, the design of disks, bead material, diameter and loading of beads, residence time, temperature, cell concentration and cell type. The kinetics of the cell disruption process was first studied by Currie et al. in (1972) and was further investigated in detail by Limon-Lason et al. (1979). First order kinetics were noted for yeast cells, where the rate of disruption as measured by the soluble protein release was directly proportional to the amount of unreleased protein. The data fitted the model for 0.6 and 5 litres horizontal mills and covered a range of impeller speeds. In the larger mill, at higher impeller tip speed (above 10 m/s) disruption did not follow first order kinetics. Difficulties with temperature control in batch experiments led to inconclusive results. The continuous disruption in the 5 L mill was adequately modelled as a CSTR in series with the number of tanks corresponding to the number of impellers. For the smaller mill (0.6 L), the model was modified to include backflow in order to obtain good agreement with experimental data. Currie et al. (1972) reported that for a range of bead diameter studied (0.5–2.8 mm), the smaller beads were more effective. However the effect is dependent on the cell concentration. For a 30% yeast slurry small beads were

favoured while above a concentration of 60% their advantage was reduced. The variation of disruption efficiency with yeast concentration for the different size beads was similar and no special effect of large beads on thick yeast suspensions was observed. Schutte et al. (1983) indicated that for yeast cells, the location of an enzyme within a cell influenced the optimum bead size. Larger beads could be used to recover enzymes located in the periplasmic space and smaller ones to release the cytoplasmic material. These findings suggest that smaller beads are more effective in achieving complete cell disintegration. The disintegration of other microorganisms has been reported in the literature, such as a variety of bacteria (Woodrow and Quirk 1982; Schutte et al. 1983), algae (Hedenskog and Mogren 1973), and filamentous fungi (Zetelaki 1969). The disintegration of bacteria in a glass bead mill was hampered by the small dimensions of the cells (approximately 1/10 the size of a yeast cell) (Schutte et al. 1983). Although the use of smaller beads would seem appropriate, its application is limited by the tendency of small beads to float at high cell concentrations as noticed by Currie et al. (1972).

Increased disruption with increased bead loading was reported (Currie et al. 1972). However greater cooling is required as greater temperature rise was recorded (Schutte et al. 1983).

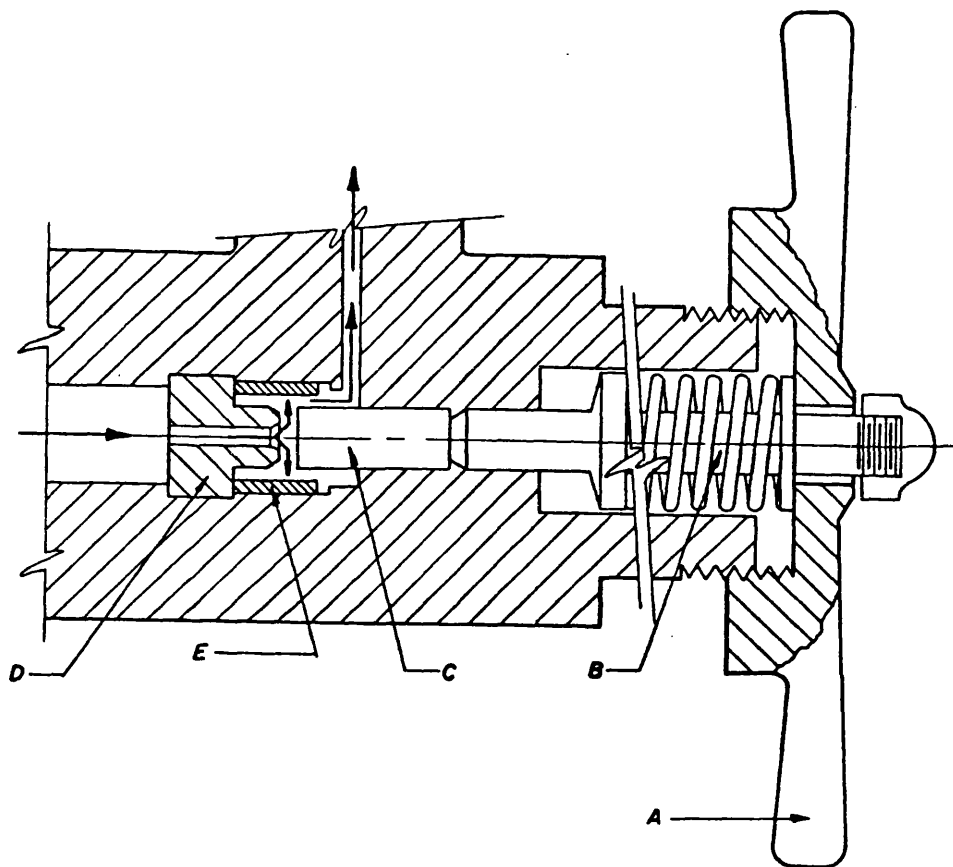
Limon-Lason et al. (1979) showed that the disruption rate constant was independent of cell concentration at higher concentrations of yeast (greater than 30% w/v) for stainless steel impellers; but for polyurethane impellers, it continuously decreased with increasing yeast concentration. The results were attributed to, firstly, the variations in the rheological behaviour of the suspension and secondly to the differences in the design of the two impellers. Schutte et al. (1983) reported an optimum concentration for low impeller speeds but noticed little effect of concentration on disruption at higher speeds (8 m/s). In a review by Engler (1985) it was stated that E.coli was more difficult to disrupt than A.niger or

Basidomyces species. Candida utilis was noted to be harder to disintegrate than bakers' yeast. The effects of cell type and conditions of growth are not limited to disruption in a bead mill. The importance of cell characteristics and growth history is discussed in Section 1.2.4.2.

#### 1.1.2.2 High pressure homogenisers

High pressure homogenisation is the most widely used method for large scale cell disruption (Scawen et al. 1980). The equipment consists of a high pressure reciprocating positive displacement pump with one or more adjustable, restricted orifice valves. All commercial models operate on the same principle and are distinguished by their capacity, the type of homogeniser valve, pressure range, drive mechanism and number of pistons. A diagram of a discharge valve assembly is shown in Figure 1.1. Cell suspensions is drawn through a check valve into the pump cylinder and on the return of the piston, is forced through the discharge valve assembly. The discharge pressure is controlled by a handwheel assembly, which through a spring-loaded shaft positions the valve rod in relation to the valve seat. During discharge the suspension passes between the valve rod and its seat and impinges on an impact ring. The pressure is shown on a gauge mounted on top of the cylinder. In the case of a single piston homogeniser, fluctuations in pressure measurements are reduced by a dampener assembly. In the subsequent sections, different aspects of cell disruption in this type of equipment are described in detail.





- A. Handwheel for pressure control
- B. Spring-loaded shaft
- C. Valve rod
- D. Valve seat
- E. Impact ring

**Figure 1.1** Schematic diagram of a homogeniser valve assembly

### 1.1.3 Recent developments in mechanical devices for cell disruption

#### 1.1.3.1 New concepts in the design of high pressure homogenisers

The first high pressure homogenisers appeared before the turn of the century for the processing of high fat products such as artificial butter. Since then, many changes and modifications have been made in the equipment, with the main emphasis on the design of the valve unit. This includes flat valves, tapered valves, grooved valves, tapered and grooved valves, and highly chamfered or knife-edged valves. The reason for all these changes is to increase the efficiency of homogenisation. In the context of milk product homogenisation, this has meant the generation of the smallest average fat globule size with the least expenditure of energy. In terms of cell disruption efficiency, whilst the aim is to maximise the release of the desired product from the cells with minimum energy expenditure, other factors need to be considered such as cell debris size (see Section 1.4).

In the homogenisation of milk products, the efficiency at flow rates less than 760 L/h was not maintained when a design was scaled up to handle flow rates in excess of 11000 L/h, which are common in the milk industry. This is because at high flow rates, the cross sectional area between the valve rod and the valve seat must increase in order to maintain pressure and accommodate flow. This may be accomplished by either increasing the gap between the valve rod and the valve seat or by increasing the diameter of the valve rod and seat. In the former instance, efficiency is decreased; in the latter, actuation of the assembly is difficult. Furthermore close tolerance machining of large diameter valves is difficult (Pandolfe 1982). The problem was resolved with the design of the Gaulin Micro-Gap™ valve. The main feature of this design is that the flow is divided into equal parts by stacking the homogenising valves in parallel. The valve assembly has a knife-edge on one side, which

is the seat, and a flat surface on the other side, which acts as the valve plate; thus each valve disc is a valve seat and a valve. The gap distance between the valve and seat is fixed. The size and the number of the valves are selected to achieve the best homogenizing conditions at the required flow rate.

The importance of valve geometry in cell disruption is now well known even though the amount of research reported in the open literature is limited and the mechanism not well understood. This is discussed in greater length in Section 1.2.4.1.

Another important design feature in high pressure homogenisers is the strength of material used in the manufacture of the valve unit. Continuous operation specially at high pressures results in rapid wear of the valve unit; in particular the knife-edge types. This has led to extensive research with the result that the tungsten-carbide units are now superseded by valves made of a ceramic composite material capable of withstanding much wear (APV-Gaulin 1985).

More attention is now being paid to the specific application of cell disruption and its related requirements such as equipment sterilisation and containment. Features of new equipment dealing with such issues are detailed in Chapter 7 as part of a design study for an integrated homogenisation system.

#### 1.1.3.2 Microfluidisers

The microfluidiser is a relatively new development in the disruption and emulsification technology, based on the submerged jet principal. A hydraulically operated high pressure pump forces the fluid through an "interaction chamber" at pressures up to 160 MPa. The interaction chamber is the core of the instrument and consists of a system of channels in a ceramic block, which splits the fluid into two streams. These are then forced through narrow rectangular slits and

are recombined to impinge against one another at high velocity (Figure 1.2). Several sizes of the instrument are available. The manufacturers claim that a major advantage of the technology is the ease of scale up; all that is required is to make the slits in the interaction chamber wider in order to increase the throughput without altering the disruption process (Washington 1987; Washington and Davis 1988).

A preliminary comparison of the extent of disruption of yeast and bacteria by this technique and by other mechanical methods has indicated that microfluidisers are not suitable for yeast disruption. At least 30 passes were required at 60 MPa to achieve 90% cell breakage (as measured by viable cell count). With B. subtilis, percentage breakage in the microfluidiser and in an APV-Gaulin single piston homogeniser were similar at the same pressure, however the levels of protein release were different (Seva et al. 1986). More recent studies based on a similar principle have indicated that similar disruption levels as those obtained with conventional mechanical techniques may be obtained but at lower pressures and fewer passes if the design parameters such as the distance between the jet nozzles are optimised (Kramer and Bomberg 1988a, 1988b). Further research is required to fully assess the merits of this equipment.

## 1.2 Kinetics of cell disruption

### 1.2.1 Development of a kinetics model

Several operating parameters have been identified to affect the performance of high pressure homogenisers. Hetherington et al. (1971) elucidated the effects of some of these factors such as pressure, number of passes, temperature, cell concentration and put forward a kinetic model for the disruption of yeast cells.

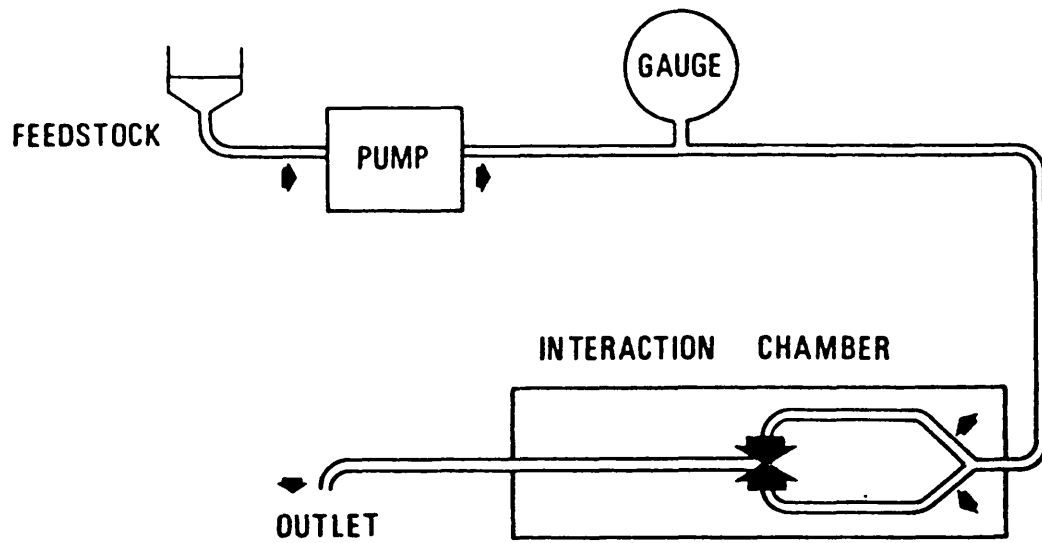


Figure 1.2(a) Schematic diagram of the Microfluidiser

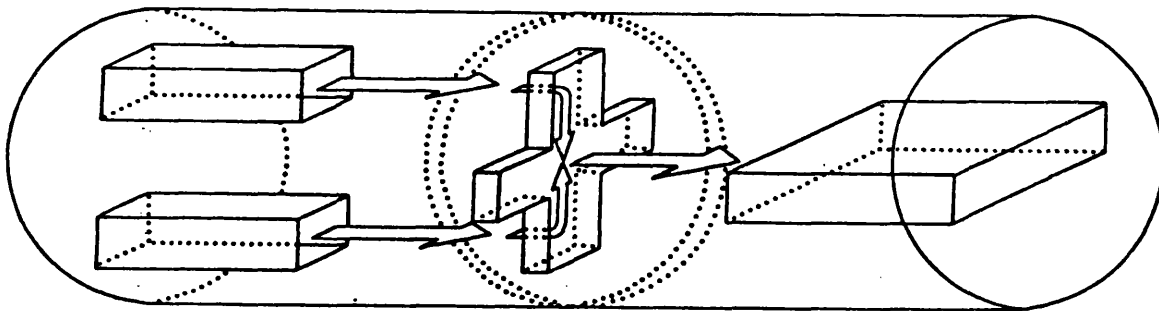


Figure 1.2(b) Microfluidiser interaction chamber

The disruption followed first order kinetics with respect to the number of passes and could be described by the general equation:

$$\text{Log} \left[ \frac{R_m}{R_m - R_p} \right] = K.N = (k.P^a).N \quad (1.1)$$

where  $R_m$  is the maximum soluble protein available for release and  $R_p$  is the soluble protein release after a number of discrete passes,  $N$ , through the valve.  $K$  is a dimensionless rate constant which, as indicated, is principally a function of the pressure drop,  $P$ , across the valve seat;  $k$  is a constant which is a function of temperature and maybe a function of cell concentration; both  $k$  and the pressure exponent " $a$ " are a function of cell type. Hetherington et al. (1971) found a value of 2.9 for the pressure exponent " $a$ ", using a suspension of bakers' yeast. The kinetics of  $\beta$ -galactosidase and protein release by constitutive mutant of E. coli growing in batch and continuous cultures have been examined (Gray et al. 1972). The first order kinetics fitted the model for both protein and enzyme release. A value of 2.2 was reported for the pressure exponent in the kinetic expression for  $\beta$ -galactosidase release.

The kinetics of enzyme release have been shown to be first order for bakers' yeast, but the rate of release of the enzyme varies with its location in the cell (Follows et al. 1971). Acid phosphatase located outside the cell membrane was released faster than the overall protein release, but fumarase, reported to be present in the mitochondria, was released more slowly than the overall protein release. For most enzymes tested no significant loss in activity was detected after several passes through the homogeniser at temperatures at or below 30° C.

Work by Augenstein et al. (1974) indicated that the enzyme complex

which forms the cyclic decapeptide antibiotic, gramicidin S, degraded rapidly when cells of B. brevis were subjected to homogenisation. They therefore put forward a kinetic equation which included an enzyme degradation exponent for the pressure. Their results were contrary to the findings that water soluble intracellular enzymes and other globular proteins were stable with respect to shear (Virkar et al. 1981). It now seems likely that gramicidin synthetase may be a membrane associated enzyme and the discrepancy is explained by the work of Talboys and Dunnill (1985) who reported that membrane associated enzymes were highly shear sensitive.

#### 1.2.2 Effect of $R_m$ on the kinetics model

The application of the kinetics equation is dependent on the value of  $R_m$ , the maximum amount of protein available for release. The  $R_m$  value determined by Hetherington for Bakers' yeast (96 mg protein/g packed yeast) obtained by trial and error was in close agreement with published data (the total protein content of packed cells was given as 120 mg/g yeast, 85% of which was released into solution (Harrison 1967; Hughes 1961)).

Work carried out by Whitworth (1974b) on Candida lipolytica, a mixture of filamentous and elongated ovoid cells, showed that protein release ( $R_p$ ) was a function of the number of passes in the pressure range 30-56 MPa. It was not clear from the data provided whether the same  $R_m$  value for each given pressure was reached or not. It appeared that the maximum R value achieved varied with different operating pressures. The highest value obtained at 56 MPa after 6 passes was only 30.5% of the total protein content of the yeast, given as 91 mg protein/g yeast cake. The authors were therefore unable to describe the release of protein in terms of a first order rate expression of the type derived for bakers' yeast where  $R_m$  is independent of pressure. A previous study by the same author

(Whitworth 1974a) on the kinetics of disruption of spent brewery yeast had confirmed the Hetherington model although a different pressure exponent was calculated. No alternative model for C. lipolytica was put forward.

Engler (1979) studied the disruption kinetics of Candida utilis in a specially designed high pressure impingement device. Although the results did not show a maximal soluble protein value after 4 passes at pressures up to 88 MP, the author obtained an  $R_m$  value for each set of data based on the total nitrogen content of the cells for that particular experiment. This treatment of the data resulted in a first order kinetics expression for the disruption of C. utilis. It may be argued that firstly, the total soluble protein available for release is not equal to the total protein content of the cells, and secondly the results are based on different experiments with varying values of  $R_m$ . It must however be noted that the highest protein value obtained experimentally was 77% of the estimated maximum protein release. The value is therefore high enough to make the estimated  $R_m$  value a reasonable approximation.

Engler replotted the data of Whitworth using only the protein released after one pass at each given pressure. He deduced a first order kinetics expression. The methodology is not clear as he infers that it is possible to obtain the  $R_m$  values by knowing the protein released after the first pass. To incorporate the dependence of  $R_m$  on the operating pressure, it would have been more reasonable to assess the protein released as a function of pressure for each pass.

The dependence of  $R_m$  value on pressure in the study of C. lipolytica may be attributed to two factors. Firstly, it is likely that at higher pressures intracellular material such as insoluble complex protein, peptide, glycopeptide and amino acids are released by micronisation of the cell debris (Limon-lason et al. 1979). Secondly, it has been reported that C. lipolytica grown in a hydrocarbon culture medium accumulates hydrocarbons around and



inside the cell wall structure and that the cytoplasmic membrane becomes thicker and more deeply invaginated (Tsang et al. 1979). This could interfere with the complete rupture of the cell wall and membrane and thus with the release of protein at lower pressures. Other cell characteristics such as age of culture, morphology, and conditions of growth may also contribute to the effects observed. One piece of evidence is that different batches of C. utilis cells showed inconsistent total nitrogen cell content (Engler 1979).

### 1.2.3 Disruption kinetics of filamentous microorganisms

Little data is available in the literature on the disruption kinetics of filamentous microorganisms. The study by Zetelaki (1969) compared the extent of disruption of Aspergillus niger achieved by different methods. It was concluded that bead mills and the X Press resulted in highest yields with few cellular fragments remaining in the suspension. High pressure homogenisation was not found to be a suitable technique as a result of poor disruption (at over 50 MPa, 2 passes) and blockage of the equipment even at low concentrations (50 g/L wet weight). However, further investigation indicated that it was possible to disrupt A. niger at 35 MPa at much higher concentrations of 700 g/L wet weight (Lilly and Dunnill 1969). Data obtained only gave a preliminary indication that first order kinetics may be applicable.

Hanisch (1978) reported on the disruption of Rhizopus nigricans in a high pressure homogeniser and a bead mill. According to his results, the homogeniser released only 13% soluble protein at 50 MPa after 4 passes, in comparison with 26% after 30 seconds in the bead mill operating under optimised conditions. No study of the kinetics was carried out.

Only recently has there been an interest in investigating the disruption of filamentous microorganisms. Thomas (1988) studied the

release of soluble protein from R. nigricans. Preliminary work indicated that for this microorganism, contrary to previously reported results, high pressure homogenisation was a more effective method of disruption than bead milling. Subsequent data on high pressure homogenisation indicated that firstly the soluble protein release was very rapid even at low pressures. Secondly, the  $R_m$  value varied with the pressure as it was previously observed for C. lipolytica by Whitworth (1974b) (Section 1.2.2). By using a weighted linear least square technique, the protein release was described by a first order relationship. The pressure exponent (0.57) was however much lower than that quoted for unicellular microorganisms (Section 1.2.1). The maximum protein available for release,  $R_m$ , was given to be proportional to  $P^{0.14}$ .

As part of the work the release of the membrane bound enzyme progesterone 11 $\alpha$ -hydroxylase was characterised. Activity release followed first order kinetics, but was less rapid than the soluble protein release. Furthermore, the maximal enzyme release was not found to be a function of pressure. This led to a review of the model for the protein release, in which cytoplasmic, wall and membrane release were taken into account. The use of this model for other filamentous microorganisms may prove difficult since it is based on the premise that  $R_m$  is inevitably pressure dependent and also that it requires a knowledge about compartmentalised release of proteins from the cells.

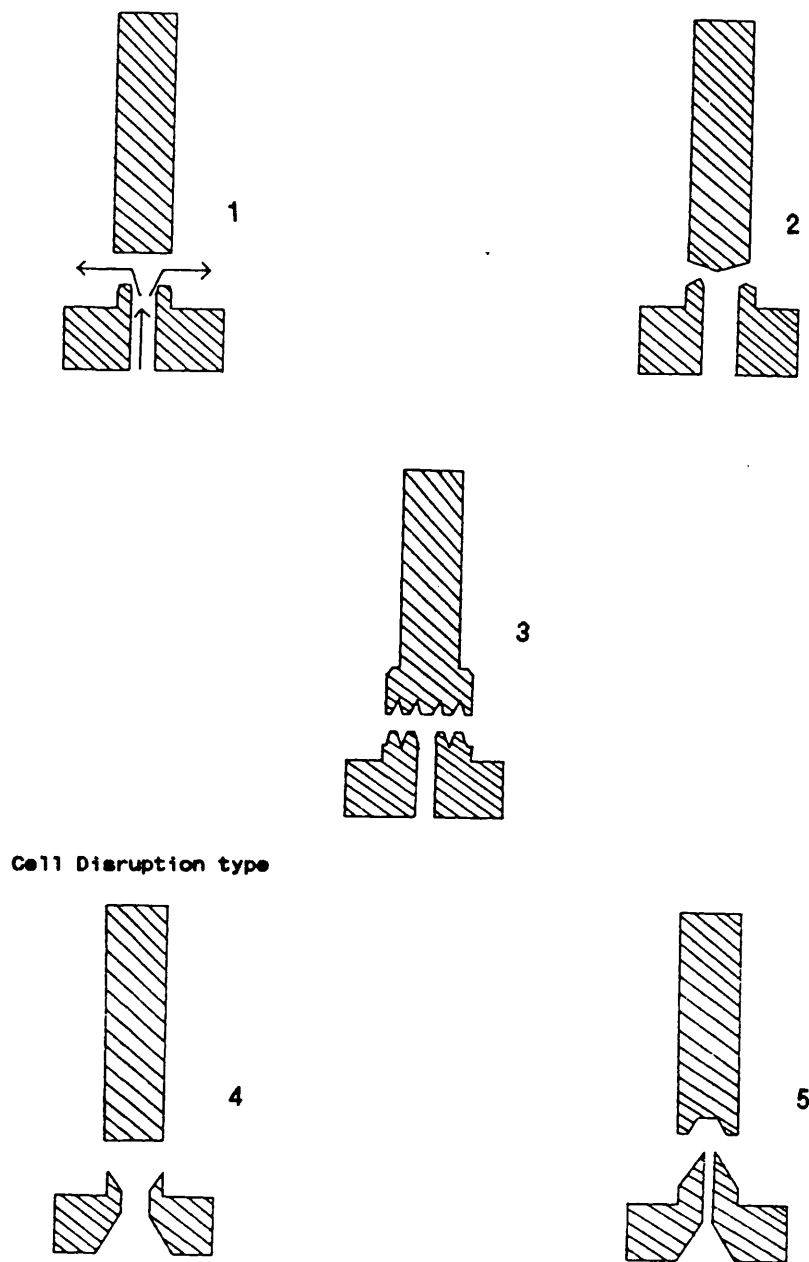
#### 1.2.4 Effect of operating parameters

Operating parameters which may affect the kinetics of disruption in high pressure homogenisers are a) machine related, e.g. the valve design; b) product related, e.g. cell characteristics and concentration; and c) conditions related, e.g. pressure, number of passes, flow rate and temperature.

#### 1.2.4.1 Valve design

Little research has been reported in the open literature on the effect of valve unit design. Two studies (Hetherington et al. 1971; Gray et al. 1972) compared the performance of the flat-edge and knife-edge valve units (Figure 1.3). Both valves and impact rings were dimensionally identical, but the valve seat of the knife-edge model had a substantially reduced seating area. The protein release was improved by 38% after 4 passes using the knife-edge unit (Hetherington et al. 1971). This model suffers from rapid wear; however as mentioned in Section 1.1.3.1, recently introduced ceramic materials are much more resistant to wear. APV-Gaulin Inc. have investigated the effects of homogenising valve geometry on the cell disruption efficiency (APV-Gaulin 1985). Results were monitored by measuring the percentage of the total available protein released after disrupting a 10% dry weight slurry of bakers' yeast. Five valve designs were tested with pressures up to 138 MPa (Figure 1.3). Results indicated that a knife-edge 'Cell Disruption' unit was superior to other valve designs. The design of the unit is not the same as that used by Hetherington et al. (1971), but entails a valve seat giving a narrow gap nearer the periphery. No correlation was reported to relate the rate of cell disruption with the geometry of valve designs.

Research carried out in recent years on the effect of valve geometry on milk homogenisation have also indicated better efficiency with knife-edge valves (Kurzahls 1977; Mohr 1987a, 1987b). However, the correlation between cell disruption and emulsification, if any, is not clear.



**Figure 1.3** Homogeniser valve designs (APV-Gaulin 1985)  
 Hetherington *et al.* (1971) used valve units (1)  
 and (2), except that in their case (2) had a flat  
 valve rod.

#### 1.2.4.2 Cell Characteristics

##### 1.2.4.2.1 Conditions of cell growth

Conditions of growth have a major effect on disruption kinetics. Engler (1979) attempted to derive a general kinetics expression for all microorganisms but concluded that such generalisation even at the level of microorganisms of the same group may be misleading. In the case of Saccharomyces cerevisiae differences have been observed between disruption rates of bakers' yeast and spent brewers' yeast (S. cerevisiae) (Table 1.1), the latter showing a lower value for the pressure exponent in equation 1.1 (Section 1.2.1).

Results obtained for the disruption of E.coli cells indicated that batch cultures grown on a synthetic medium were easier to disrupt than those grown on complex medium (Gray et al. 1972). In another study (Engler and Robinson 1981a) it was shown that cells grown at a higher specific growth rate were easier to disrupt than cells grown at a lower specific growth rate. Similarly, cells harvested during the log phase of growth were more susceptible to homogenisation than those from the stationary phase. It is well known that cells from the stationary phase commonly have a stronger wall structure than those in the log phase. Furthermore, cells grown at a higher specific growth rate probably direct the available energy towards reproduction rather than synthesis or strengthening of wall structure. Complex media may provide additional nutrients for such synthesis, which are not available in simple synthetic media.

##### 1.2.4.2.2 Effect of cell wall structure

Wall structure of microorganisms differ in their composition depending on genetic and environmental factors. However, similarities in overall structural aspects are observed within

Table 1.1 Cell characteristics and conditions of growth versus pressure exponent

<u>Microorganism</u>	<u>Source/conditions of growth</u>	<u>exponent</u>
<u>Bakers' yeast</u>		
Hetherington <u>et al.</u> 1971	commercial yeast. Probably batch or fed batch. Complex medium	2.9
Doulah <u>et al.</u> 1975	as above	1.72-1.79
Dunnill and Lilly 1975	as above	2.9
<u>Spent Brewers' yeast</u>		
Whitworth 1974a	from brewery. Complex medium	1.2-1.3
Engler 1979	from brewery. Complex medium	1.87
<u>Saccharomyces cerevisiae</u>		
Engler 1979	aerobic, continuous culture specific growth rate $0.1 \text{ h}^{-1}$ Synthetic medium	0.86
<u>Candida utilis</u>		
Engler and Robinson 1981a	cyclic batch max. growth rate $0.5 \text{ h}^{-1}$ . Synthetic medium	1.17
	continuous culture specific growth rate $0.1 \text{ h}^{-1}$ . Synthetic medium	1.77
<u>Candida lipolytica</u>		
Whitworth 1974b	batch. Harvest after 55 h Complex medium	n.a.
<u>Bacillus brevis</u>		
Augenstein <u>et al.</u> 1974	batch. Late lag phase then frozen at $-20^{\circ} \text{ C}$ . Complex medium	1.8
<u>Bacillus subtilis</u>		
Engler and Robinson 1981b	continuous culture specific growth rate $0.2 \text{ h}^{-1}$ . Complex	1.07

groups of microorganisms which may explain some of the trends observed in cell disruption. Table 1.2 shows the degree of susceptibility of microorganisms to disruption in a high pressure homogeniser. It indicates that Gram - negative bacteria are easier to disrupt than Gram - positive bacteria which in turn are easier to break than yeasts. Fungal walls are classified as more resistant to disruption but their rupture depends greatly on the mechanism employed. To help understand the basic differences in wall structures, a brief review is given below.

### Bacterial cell wall

The rigid matrix of the walls of nearly all bacteria (except halophilic bacteria and Mycoplasma species) is composed of a network of glycan chains cross-linked by short peptides called peptidoglycan. It provides both cellular shape and strength. There are however significant differences in the wall structure formed by Gram - positive and Gram - negative bacteria.

The walls of Gram - positive bacteria are relatively thick (15-50 nm) and contain 40 to 90% peptidoglycan with the remainder being primarily polysaccharides and teichoic acids (Figure 1.4). The degree of cross-linking can be very high. The peptidoglycan has been considered to form a single macromolecule encompassing the whole cell.

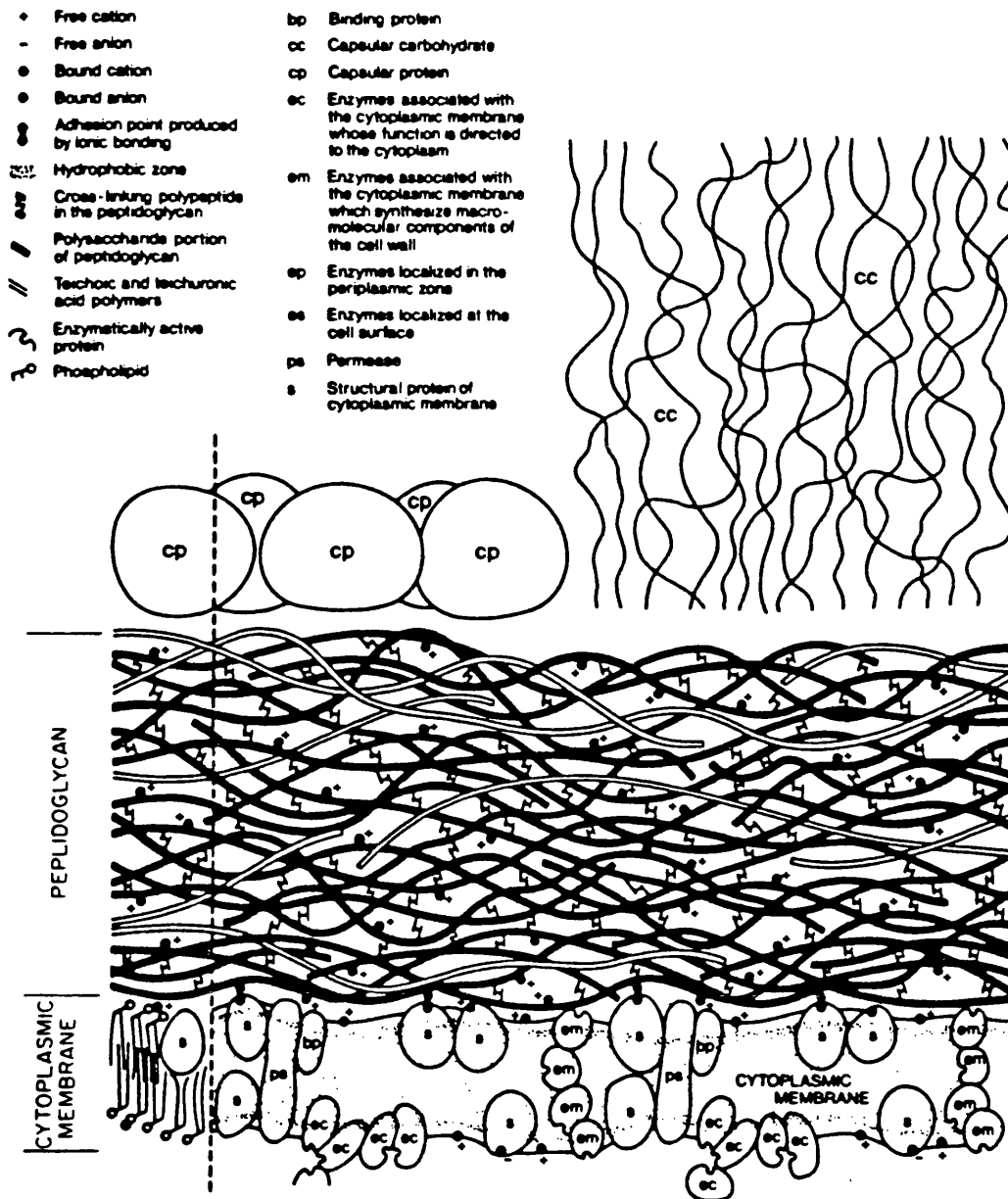
The wall of Gram - negative bacteria consists of a much thinner peptidoglycan layer (1.5-2.0 nm) which contains lipo-proteins covalently attached to it, and an outer membrane similar in appearance in electron micrographs to the cytoplasmic membrane (Figure 1.5). The outer membrane is rich in lipopolysaccharide.

Table 1.2 Protein release from microorganisms in a high pressure homogeniser.

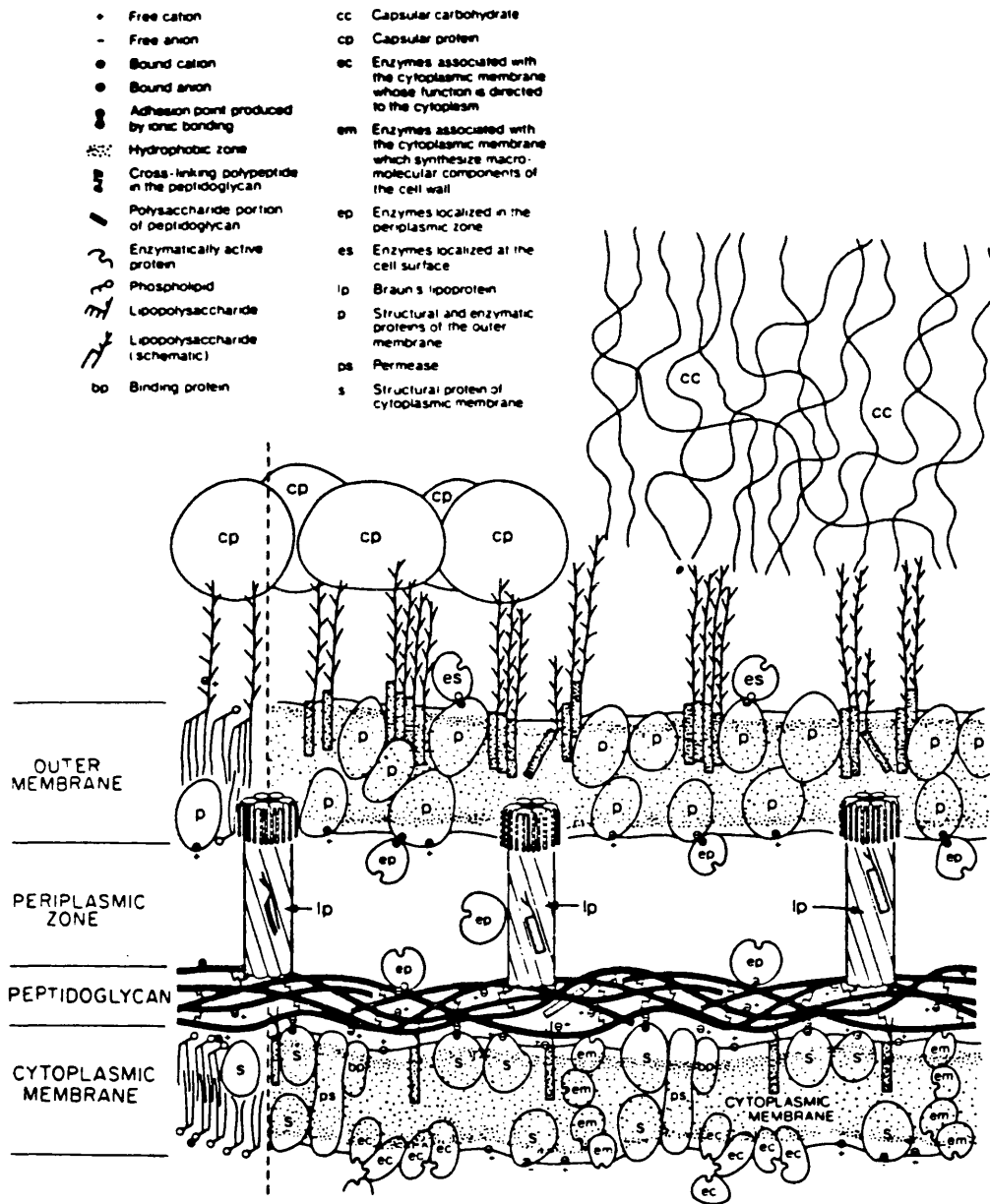
<u>Microorganism</u>	<u>Rate constant K</u>
Pseudomonas putida	0.41
Escherichia coli	0.39
Bacillus brevis	0.28
Saccharomyces cerevisiae	0.23
Norcadia rhodochrous	0.0085

In all cases the microorganisms were harvested near or at the end of growth. Homogenisation was at 50 MPa, 5° C in a model 15M APV-Gaulin homogeniser.





**Figure 1.4** Structure of the cell wall of gram-positive bacteria (Ramaley 1979).



**Figure 1.5** Structure of the cell wall of gram-negative bacteria (Ramaley 1979).

### Yeast cell wall

Cell wall structures of yeasts have been much more difficult to elucidate than those of bacteria. The basic structural components are glucans, mannans and proteins, but the way in which these are combined to form the structure is not known. The overall structure is thicker than that of Gram - positive bacteria. The cell wall of bakers' yeast was reported to be approximately 70 nm thick and the thickness is known to increase with age (Engler 1985). Although the structure of glucan varies from species to species, it is believed that glucans are moderately branched molecules. Mannans from bakers' yeast cell wall have been extensively studied and consist of mannose residues in  $\alpha(1\rightarrow6)$  linkage with short oligosaccharide side chains composed of mannose residues in  $\alpha(1\rightarrow2)$  and some  $\alpha(1\rightarrow3)$  linkages. Phosphodiester links also occur in the mannan. The majority of protein found in yeast cell wall have formed complex structures with mannans and many are enzymes rather than structural components (Figure 1.6). The position of mannan-enzyme complexes has been disputed in the literature (Engler 1985). It has been hypothesised that they may be between cytoplasmic membrane and the glucan-mannan layer rather than in the wall itself.

### Cell walls of other fungi

The fungal cell wall composition and structure are very diverse and no generalisation from one species to another can be made. The most widely studied are the walls of the hyphal growth form (Engler 1985).

In most fungi the cell wall is composed primarily of polysaccharides with lesser amounts of proteins and lipids. The polysaccharides occur in pairs and can be directly related to the taxonomic classification of fungi. The most commonly occurring pair is chitin and glucan. Neurospora crassa wall has been studied in detail

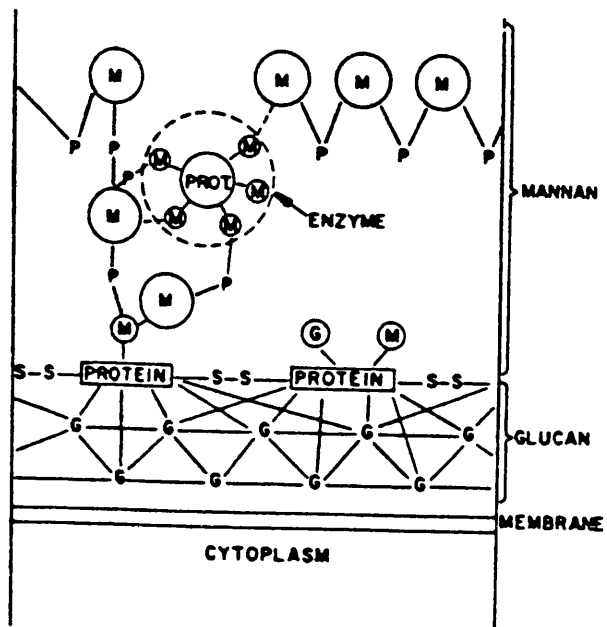


Figure 1.6 Schematic structure of yeast cell wall  
(M), mannans; (P), phosphodiester; (G), Glucans  
(Engler 1985).

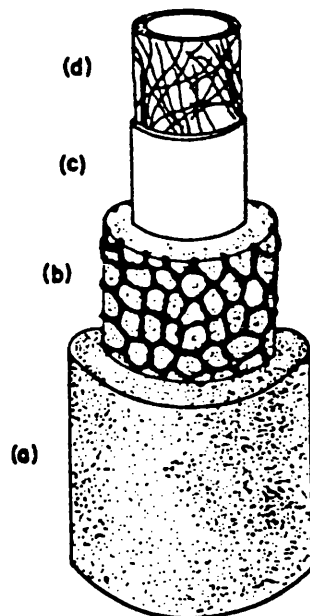


Figure 1.7 Schematic structure of the cell wall of *Neurospora crassa*. (a), outer mixed  $\alpha$ - and  $\beta$ -glucans; (b), glycoprotein reticulum; (c), proteinaceous material; (d), inner chitinous region (Engler 1985).

(Figure 1.7). In the mature wall, glucan, chitin and glycoprotein predominate in concentric layers. The wall is thinner at the hyphal apex and the glycoproteins do not form a recognisable network in this region (Engler 1985). The strength of fungal cell wall appears to be related to polymer networks as in bacterial and yeast cell walls. In addition, the fungal walls which contain fibrous structures of either chitin or cellulose may contribute added strength (Coakley et al. 1977).

The wall structure and composition of Rhizopus species well illustrate the diversity in fungal systems. The study of enzymic lysis of Rh. delemar suggested that the wall structure might be composed of chitin fibres held together by chitosan and protein or peptides scattered in mosaic layers (Tominaga and Tsujisaka 1981). Difficulty in protoplast formation in Rh. nigricans using commercial polysaccharases further suggested that chitosan may have replaced glucan in this fungal wall structure (Broad unpublished).

Although, as mentioned earlier fungal walls are classified as more resistant to disruption than bacterial cell walls, fungal breakage does not always follow such a pattern. Edebo (1983) reported that mycelia are less resistant to breakage than other microorganisms (Table 1.3). This may be attributed to the morphology of filamentous fungi. These cells are much longer in one dimension. Furthermore, for non-septate fungi it may prove less difficult to release their intracellular material than for septate species, as only a few breaks or tears in the hyphal walls would be required.

Table 1.3 Susceptibility of various kinds of cells in suspension to disintegration by various methods.

	<u>Liquid</u> <u>pressing</u>	<u>Freeze</u> <u>pressing</u>	<u>Agitation</u>	<u>Sonication</u>
Animal cell	7	7	7	7
Gram - ve bacilli & cocci	6	6	5	6
Gram + ve bacilli	5	4	(4)	5
Yeast	4	2.5	3	3.5
Gram+ve cocci	3	2.5	(2)	3.5
Spores	2	1	(1)	2
Mycelium	(1)*	5	6	1

The numbers show the ranking within the group. A high number indicates that the cells are sensitive. Parentheses indicate that the number is very uncertain.

\* clogging of orifice may occur

Source: Edebo (1983)

Doulah et al. (1975) have examined the relationship between protein releases and cell size and have considered it likely that it is the larger cells which will be easier to disrupt. For example, they predict for a high pressure homogeniser the minimum size,  $d_m$ , of cell which will be disrupted, will be given by:

$$d_m \propto \frac{\delta}{\sigma P} \quad (1.2)$$

where  $\delta$  is the cell wall strength,  $\sigma$  is the cell density and  $P$  is the homogenising pressure. However, the cell wall strength is poorly defined and is unlikely to be independent of the cell age and size. This model does go some way to indicate why different maximum levels of protein release may be experienced (e.g. as observed by Whitworth et al. 1974b), the value of  $d_m$  decreasing with increased homogenising pressure.

#### 1.2.4.2.3 Cell concentration

The cell disruption rate for bakers' yeast has been reported to be independent of concentration in the range 28–224 kg m<sup>-3</sup> cell dry weight (Brookman 1974). Hetherington et al. (1971) had reached a similar conclusion for bakers' yeast in the range 35–168 kg m<sup>-3</sup>. However, above this range, at pressures greater than 30 MPa, a reduction in the disruption rate and deviation from first order was reported. This was attributed tentatively to inadequate power being provided by the single piston homogeniser. Only one study (Doulah et al. 1975) reported that the release of protein is dependent on concentration at lower pressures. Their model predicts that the power exponent is a function of the cell concentration. No rigorous data covering a wide range of concentrations are available for other unicellular microorganisms.

On the effect of viscosity on cell disruption, Hetherington et al.

(1971) disrupted yeast in the presence of glycerol. The disruption rate decreased with increased glycerol concentration. However, the interpretation of the results was complicated by the fact that yeast metabolised the glycerol and that the effect of glycerol on cell wall strength and solubilisation of protein was unclear.

In the study of the effect of cell concentration on filamentous microorganisms, Thomas (1988) indicated that for Rhizopus nigricans cell dry weight up to 22 g/L had no effect on disruption. This upper limit is governed by the fact that, due to its network structure, the suspension can no longer flow under gravity, and blockage of the homogeniser results. This is of particular importance in industrial scale operations where, due to economic considerations, volumetric throughput is to be minimised. Higher concentrations could be achieved with pelleted cells. This was attributed to the Ostwald rheological behaviour of the pelleted suspension (Thomas 1988). Nevertheless, since concentrations achieved are not comparable to those obtainable with unicellular microorganisms, the recovery of intracellular products from filamentous microorganisms is less satisfactory. Reloading of homogenate with new batches of cells proved effective at increasing the dry weight content of the suspension but did not appear applicable to the extraction of labile enzymes due to their loss of activity during processing (Thomas 1988).

#### 1.2.4.3 Pressure and number of passes

There is general agreement amongst studies on bakers' yeast that the kinetics of disruption are first order and that the exponent of pressure does not vary within the range 10–50 MPa. The validity of the disruption versus pressure relation above the pressure range of the commercially available machines was tested by examining yeast disruption in an experimental homogeniser with a flat-edge valve up to 120 MPa. Above 70 MPa the slope fell below 2.9. This was



attributed to the non-optimal design of the valve for the high pressure used (Dunnill and Lilly 1975). Engler and Robinson (1981a) also postulated the possibility that the pressure exponent in Equation 1.1 may depend on the range of operating pressures studied. With the design of new homogenisers capable of producing pressures well above 100 MPa, it remains to be seen whether the first order kinetics are still applicable at very high pressures. It is worth noting that at such pressures, the suspension may become compressible thus affecting the disruption.

The data however clearly indicate the desirability of operating at the maximum allowable pressure to achieve maximum disruption, possibly minimising the number of passes through the homogeniser. Multi-pass operation is generally undesirable due to the comminution of cell debris, which reduces the efficiency of downstream separation process. It also accelerates the rate of wear on the valve unit, and increases the temperature of the suspension requiring extra cooling. Furthermore the production rate reduces with each additional pass. In the absence of available data, further research is required to compare the effects of size reduction and temperature generation between high pressure, single pass and low pressure, multi-pass operations.

The differences observed between the effect of pressure and number of passes on the disruption kinetics of unicellular and filamentous microorganisms are already outlined in Section 1.2.3 .

#### 1.2.4.4 Temperature

The disruption rates obtained for bakers' yeast were reported to be 1.5 times higher when the temperature of the suspension at the inlet to the homogeniser was increased from 5° C to 30° C ( Hetherington et al. 1971). Attempts were made to correlate this effect to the change in the suspension viscosity. Experimental difficulties led to

inconclusive results (Section 1.2.4.2.3). High temperature operation are not generally desirable in view of resultant protein denaturation and loss of enzymic activity.

Temperature increase generated by heat dissipation during disruption was shown to be a function of the homogenisation pressure (Hetherington et al. 1971; Whitworth 1974b; Brookman 1974; Dunnill and Lilly 1975). A 4° C rise in the temperature of the process stream was detected for a single passage through a single piston machine, at a pressure of 46 MPa; in a three piston model, approximately 8° C rise was observed under the same conditions (Hetherington et al. 1971). Such temperature rises necessitate precooling and inter-passage cooling of the process material.

#### 1.2.4.5 Flow rate

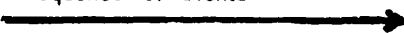
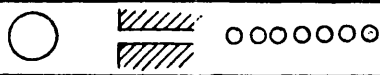
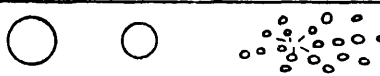
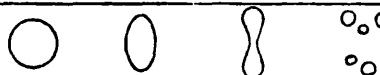
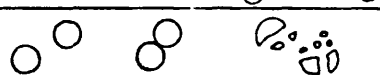
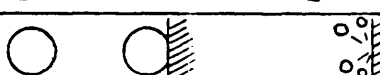
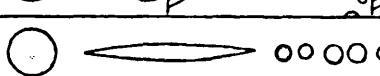
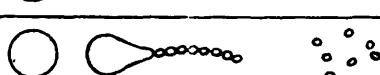

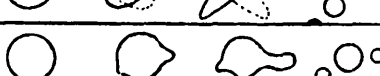

High pressure homogenisers are designed to operate at constant flow rate for a given range of pressures. The effect of flow rate on disruption has therefore not been widely studied. Brookman (1975) found that the flow rate was constant over the recommended pressure range but fell sharply with increased pressures. The effect was attributed to the stalling of the pump. In order to vary the flow rate, an extreme hydraulic pressure pump was connected to a needle valve. Constant pressure peak was obtained by varying both the inlet air pressure and the needle valve aperture. A range of flow rates were thus obtained. It was reported that the soluble protein release was relatively independent of the velocity of the yeast suspension passing through the needle valve. It must be added that the author indicated that it was difficult to measure the needle valve gap with accuracy so that the results may not be highly reliable.

### 1.3 Disruption mechanism in high pressure homogenisers

Over the years many researchers have attempted to analyse the homogenisation process. The close association of this process with the dairy industries has resulted in most investigations being carried out on milk with the view to homogenising the fat content. The approach to the problem has been to make approximations and models of how the flow might proceed through a valve unit and to analyse these conditions with respect to the end product of emulsification. In spite of the volume of work carried out, no consensus exists on the mechanism of homogenisation. Many different theories have been proposed some of which have attracted greater support. Mulder and Walstra (1974) have reviewed these theories based on experimental work carried out on milk emulsions (Figure 1.8). In later years, the application of the technique to cell disruption resulted in some empirical investigations, however the extent of research in this area remains limited. Theories pertaining to milk homogenisation have also been applied to cell disruption. In this section work on the mechanism of cell disruption is reviewed.

#### 1.3.1 Stress

Engler (1979) argued that the hydrodynamic phenomena occurring in high pressure homogenisers were too complex to allow an analysis of the mechanism of disruption, and therefore a well defined, controlled experimental apparatus was required to elucidate the mechanisms of cell disruption. For this purpose, a high pressure intensifier capable of generating pressures up to 350 MPa was designed. Various nozzles could be fitted to the discharge of the pressure intensifier to allow the study of the effects of three types of stress; normal, impact and shear on cell disruption. For impact studies, a flat surface was positioned near the orifice discharge. The orifice created a high velocity jet which then impinged on the flat surface. For the shear stress studies, nozzles

	Theory	Sequence of events 	Essential prerequisites	Does it happen?
1	Crush		valve opening < globule size	no
2	Explosion after compression		globule compressible	no
3	Acceleration		various	no
4	Erosion		globules hard and brittle	no
5	Impact		$\sigma(\text{globules}) \gg \sigma(\text{plasma})$	no
6	Shear		$\eta(\text{fat})/\eta(\text{plasma}) < 4$ ; shear rate $> 10^7 \text{ sec}^{-1}$	probably not
7	Wittig		high shear in convergent flow, then turbulence	probably not
8	Vibration		sufficient time for several oscillations	no
9	Turbulence		eddy size $\approx$ globule size	yes
10	Cavitation		$\frac{1}{2} \rho v^2 > \text{homogenizing pressure}$	probably

**Figure 1.8** Theories explaining globule disruption in a homogeniser (Mulder and Walstra 1974).

made of capillary tubing were used.

Although the study was well conceived, it makes a priori assumption that the system recreates the conditions and thus the relevant forces within the homogeniser. The author in fact recognises this fact during the course of his study and does indicate in conclusion that the system may not be very similar to that of a high pressure homogeniser. Nevertheless the findings are of interest as they may at least partially relate to the mechanism of cell disruption in a high pressure homogeniser.

#### 1.3.1.1 Normal stress

Normal stress manifests itself in high velocity jet flow of viscoelastic fluids through an orifice. Engler (1979) derived the equation

$$P = K_o \cdot \sigma \cdot U^2 + (P_{11} - P_{22}) \quad (1.3)$$

where  $P$  is the operating pressure;  $K_o$ , the parameter including kinetic energy and viscous losses;  $\sigma$ , fluid density;  $P_{11} - P_{22}$ , normal stress difference; and  $U$  the mean velocity at the orifice.

At low velocities, or with Newtonian fluids, the term  $P_{11} - P_{22}$  becomes negligible.

Considerable difficulty was encountered in collecting reliable samples. The limited data obtained showed that normal stress was one fifth the impingement stress, i.e., very small. It must be noted that the viscoelastic nature of the suspension of cells (100 mg dry weight/mL of Candida utilis) was never established. Furthermore it is not easy to separate the effect of viscous forces from that of normal stresses. Due to experimental difficulties, normal stress computation for other cell suspensions (yeast, E. coli and B.

subtilis) was abandoned in the study.

#### 1.3.1.2 Impingement

The effect of impingement was studied by Engler (1979) and also very briefly by McKillop et al. (1955). Engler showed that stresses arising from impingement of a high velocity jet of cell suspension on a flat plate caused disruption. Furthermore, he demonstrated that impingement was the major cause of disruption, shear and normal stresses not being of large enough magnitude to result in significant cell breakage. For laminar flow, the maximum stress to which cells are subjected during impingement was given by

$$P_s = \frac{1}{2} \rho U^2 \quad (1.4)$$

where  $P_s$  is the stagnation pressure and  $U$  the velocity at the orifice.

The rapid deceleration and change in direction of flow during impingement may produce deformations of the cells so that actual stresses may be considerably larger than the stress shown by the equation.

McKillop et al. (1955) investigated the effect of impingement on milk homogenisation in a three piston homogeniser with a flow rate of around 1500 L/h, over a pressure range of 6 to 20 MPa. Two tests compared the effect of removal of impact ring. The results indicated that the elimination of the impact ring did not reduce the effectiveness of homogenisation even though the liquid stream emerging from the space between the valve rod and the valve seat had about ten times farther to travel before striking a surface. Mulder and Walstra (1974) commented that liquid velocities of around 250 m/s are needed to disrupt milk fat globules by impingement. Since the exit velocities from the homogenisation zone were in the region of 50 m/s, no direct disruption was observed. However, the presence or absence of the impact ring may alter flow conditions upstream.

#### 1.3.1.3 Shear

Shear stress is caused by frictional forces generated during flow. Brookman (1975) and Engler (1979) disrupted cells by high pressure extrusion of the cell suspensions through capillary tubes. Brookman's experiments were carried out with a range of capillary tube lengths from less than 10 mm to around 90 mm, with a bore diameter of 0.152 mm. It was reported that the soluble protein release decreased with increasing capillary length. This was taken as an indication that shear is not responsible for cell breakage. This however overlooks the fact that, as the pressure drop was held constant, following the general equation

$$\tau = \frac{P r}{2 L} \quad (1.5)$$

where  $\tau$  is the shear stress;  $P$ , the pressure drop across the capillary due to viscous effects;  $r$ , the radial position; and  $L$ , the length of the capillary, the decrease in capillary length would increase the shear stress which in fact argues for and not against the importance of shear in cell disruption.

Further experiments with a French Press type of equipment consisting of a high pressure pump and a needle valve (which was considered as a variation of the high pressure homogeniser theme) indicated that at constant pressure, disruption was independent of flow rate (Brookman 1977). This was taken as further evidence against the shear theory. Changes in the needle valve aperture necessary to maintain a constant pressure peak were not considered relevant in the development of a disruption theory. Shear results reported by Engler (1979) were inconclusive.

### 1.3.2 Magnitude and rate of pressure drop

The above observations made by Brookman (Section 1.3.3) were interpreted as support for the mechanism relating disruption to the magnitude of pressure drop and the rate at which this occurs. This was taken to be in agreement with previous work on milk homogenisation (Walstra 1969) indicating that the most important determinants of homogenisation are pressure and the time scale of the process. It has been suggested that the more rapid pressure drop may also explain the observed better performance of the knife-edge valve unit relative to the flat type (Chisti and Moo-Young 1986).

### 1.3.3 Turbulence and velocity changes

Experiments related to the effect of turbulence on cell breakage are few. Doulah et al. (1975) (Section 1.2.4.2.2) suggested that turbulent eddies of dimensions smaller than a cell cause the cell fluid to oscillate with enough kinetic energy to disrupt the cell wall. This necessitates an assumption about a minimum cell diameter which would be disrupted, which was discussed in Section 1.2.4.2.2.

Work carried by Engler (1979) using two different nozzle designs to allow greater turbulence in the high velocity jet, suggested that the turbulence was not a primary cause of disruption but may enhance the process near the point where the jet impinges on the impact surface.

Phipps (1971) experimented on milk homogenisation by varying the dimensions of the valve unit so that the effect of both laminar and turbulent flow regimes could be studied. It was reported that turbulent condition did not affect the homogenisation process in any way. It was however suggested that at the slit entrance, the globules are drawn into threads before they disintegrate. There is a steep velocity gradient as the flow converges inside the valve



region where the rupture occurs. However, the length of the disrupting zone may not favour the greatest break up effect possible and thus a single passage of the emulsion through the valve may not produce the maximum dispersive effect.

According to Mohr (1987a), under the conditions of high pressure homogenisation, the energy input into the system is converted into turbulence energy in the dissipating chamber. A spectrum of eddies are formed in the turbulent flow which consists of large and small eddies. Particle dispersion - in an oil in water or milk homogenisation system - takes place in two stages. Primary dispersion is affected by large eddies of high energy content. Secondary dispersion takes place as a result of pressure fluctuations of the smallest energy-dissipating eddies if the particle diameter is much larger than the dimensions of the eddies. In the case of very high energy densities, secondary dispersion takes place by viscous shearing between two convergent small energy dissipating eddies if the particle diameter is roughly equal to the dimensions of these eddies. This treatment presupposes the existence of turbulence in the homogeniser and bases some of the findings on a dispersing system consisting of a nozzle with a subsequent turbulent chamber.

#### 1.3.4 Cavitation

Cavitation is the formation and subsequent collapse of small cavities (vapour bubbles) in a liquid. Cavities form as soon as the local pressure falls below the vapour pressure of the liquid. This may happen when a high velocity produces a negative pressure which cannot persist for long. It is also possible for energy from sound waves or ultrasonic waves of not too high a frequency to set up local negative pressures. A dissolved gas or volatile liquid also favours cavity formation. Cavities may be filled with vapour or with gas. The collapse of these cavities causes high pressure gradients

which may cause cell disintegration.

In the case of milk homogenisation, cavitation is one of the most discussed theories (Loo and Carlton 1953; McKillop 1955; Phipps 1974; Kurzhals 1977; Mohr 1987b). In cell disruption however it is not believed to be a major mechanism. Brookman (1974) could not detect any oscillatory phenomena other than the cyclic operation of the valve due to pressure pulses generated by the pump.

#### 1.3.5 Explosive decompression

Brookman (1975) reported on the suggestion made two decades earlier that the most important factor in disrupting cells of E.coli was explosive decompression- i.e., cell wall expansion during rapid decompression due to sudden application and then release of external hydrostatic pressure- and not the flow characteristics of the cell suspension through a narrow orifice. The theoretical treatment of this idea was taken up further (Scully 1975). During rapid decompression, compressive strain is transformed into tensile strain. The compressive energy of the intracellular water transforms into kinetic energy since water cannot sustain a tensile strain. This energy impacts upon the cell wall, increasing the tensile strain in the wall. Scully (1975) derived an equation in which the tensile strain increased linearly with the applied hydrostatic pressure. The experimental evidence that cell breakage increases more rapidly with the pressure was explained in terms of the additional kinetic energy released by intracellular water. However it is unclear whether this extra energy is adequate to account for the empirically deduced power relationship between disruption and pressure.

#### 1.4 Cell particle and cell debris formation

The separation of cellular fragments from soluble proteins after cell disruption is a major challenge to the biochemical engineer. The desired product is in a crude, dilute state and must be concentrated and purified before use. This requires the removal of cell debris. Solid-liquid separation methods such as centrifugation and filtration are based on density difference and particle size criteria. The size and density of the cellular fragments and the homogenate viscosity, which are dependent on the homogenisation conditions, are therefore crucial to the performance of the separation process. However, the cell debris size is much smaller than the whole microorganism and its distribution much wider; the density difference is also small. The selection, operational conditions and success of a separation process are therefore dependent on the disruption stage.

The desired protein is not however, always water soluble, nor is it always stable enough, as in the case of globular proteins (Virkar et al. 1981), to withstand shear forces in separation processes. Many reactions of industrial interest, such as highly selective hydroxylations, are catalysed by enzyme complexes embedded in cellular lipid membranes. These membrane bound enzymes are insoluble and shear sensitive (Talboys and Dunnill 1985). Their purification necessitates the development of low-energy cell disruption techniques and new processing methods (Hoare and Dunnill 1986; Thomas 1988).

With the advent of genetic engineering, numerous genes which encode prokaryotic, viral or eukaryotic proteins have been cloned into a variety of plasmids and expressed in various microorganisms or tissue culture cells; the most commercially significant proteins being from eukaryotic sources (Kane and Hartley 1988). In many cases, however, the proteins produced are not soluble in the cell but form insoluble, denatured aggregates known as inclusion bodies.

The recovery of these particles free of cell debris and other contaminants and their resolubilisation has led to new research and development in separation processes (Hoare and Dunnill 1986).

#### 1.4.1 Cell debris

The characterisation of cell debris is a new area of research prompted by firstly, the need for the design of separation procedures to recover novel products such as recombinant proteins; and secondly, the attempt to further improve the efficiency of existing purification processes.

In a major study of the unit operations involved in the continuous flow isolation of  $\beta$ -galactosidase from E. coli (Higgins et al. 1978), it was shown that irrespective of the type of industrial centrifuge used, the throughput has to be lowered considerably in order to reduce the percentage of unsedimented solids in the recovered product stream (e.g. a 10 fold reduction in the flow rate in order to decrease the percentage unsedimented solids by a factor of 20). This longer residence time leads to significant temperature rise of the process stream which may adversely affect the quality of the product. This problem is even more acute with yeast cell debris where a 10 fold reduction in the throughput would reduce the percentage unsedimented solids by only a factor of 10 (Mosqueira et al. 1981). Clearly further information on cell debris formation at the disruption stage could help optimise the separation process.

The removal of yeast cell debris by filtration resulted in a rapid increase in filter cake resistance due to blinding of the precoat (Gray et al. 1973). A study of the effect of homogenisation conditions on filtration indicated that the cake resistance increased with the number of disruption passes and was accompanied by a reduction in the amount of soluble protein transmitted of up to 30% (Su et al. 1987). This is probably due to the fact that the

smaller the cell debris, the smaller are the interstitial spaces, resulting in an increased resistance to the process flux. Furthermore, the filter cake has poor mechanical stability and is easily compressed by moderate pressures, which leads to a further reduction in the porosity of the cake. The need for a better understanding of homogenisation process in order to optimise downstream operations is, once again, apparent.

#### 1.4.2. Inclusion bodies

Protein inclusion bodies have been commonly described as dense, insoluble bodies which may be recovered by centrifugation (Marston et al. 1984). However the obvious inadequacy of such a description in process design has led to significant research to characterise these particles. It is now evident that different types of inclusion bodies have different size and density characteristics. For example, the  $\delta$ -interferon and the prochymosin-based inclusion bodies have an average diameter of 0.81 and 1.28  $\mu\text{m}$  respectively (Taylor et al. 1986). Furthermore, a decrease in the density of prochymosin inclusion bodies with increasing particle size is observed, whilst this trend is not detected in the case of  $\delta$ -interferon inclusion bodies (Gardiner et al. 1987). A further factor to consider in separating inclusion bodies after cell disruption is the presence of cell debris. Whilst cell debris is shown to settle at a slower rate than the inclusion bodies, the degree of overlap and the relative closeness of the settling rates indicates the difficulties which may be encountered when this recovery is implemented on an industrial scale (Gardiner et al. 1987).

#### 1.4.3 Microsomal fractions

For the utilisation of membrane bound enzymes it is necessary to isolate the entire subcellular structures in which the enzymes are

located (Smeds and Enfors 1985). These may be photophosphorelating membrane vesicles called chromatophores, or endoplasmic reticulum bound enzymes. Endoplasmic reticulum is extensively disrupted even by gentle homogenisation, resulting in closed vesicles ( Depierre et al. 1980) named microsomes by Claude (1940).

The labile nature of membrane bound enzymes necessitate a rapid, gentle separation process. The PEG precipitation and two phase aqueous extraction systems are believed to be both quicker and more amenable to scale up than other methods (Thomas 1988). Even though there has been some evidence that microsomes resulting from different homogenisation conditions precipitate differently (Sadler et al. 1985; Broad unpublished data), and that in aqueous two phase systems, the adsorption of particles to the interface is dependent on particle size (Smeds and Enfors 1985), little information is available on the effect of homogenisation on microsomal characteristics. Data presented in literature on the size of subcellular particles obtained following laboratory scale separation procedures are summarised in Table 1.4. They may serve as a general guideline.

Table 1.4 Particle characteristics of some cellular fragments

<u>Cell component</u>	<u>Size and shape</u>	<u>reference</u>
Fungus ( <u>N.crassa</u> )	4 -7 $\mu\text{m}$ spherical	Wiley (1974)
Spheroplast ( <u>N.crassa</u> )	4-20 $\mu\text{m}$	as above
Vescicles ( <u>N.crassa</u> )	0.05-1 $\mu\text{m}$	as above
Fungus ( <u>P. chrysosporium</u> )	5-10 $\mu\text{m}$	Greene & Gould (1984)
Spheroplast ( <u>P. chrysosporium</u> )	5-10 $\mu\text{m}$	as above
Vesicle ( <u>P. chrysosporium</u> )	20-50 $\mu\text{m}$	as above
Plasma membrane ( <u>S. cerevisiae</u> )	11-20 $\mu\text{m}$	Blanchardie <u>et al.</u> (1977)
Endomembranes ( <u>S. cerevisiae</u> )	7.5-8.5 $\mu\text{m}$	as above
Round vesicles	0.1-0.3 $\mu\text{m}$ density 1.13-1.18 regular shape	as above
Large membranes containing microsomes high in NADPH cytochrome C reductase activity	irregular shape density 1.20-1.26	as above
Vacuolar membrane	spherical $\leq 0.5 \mu\text{m}$	Aldermann & Hofer (1984)
Mitochondrial fraction	less regular	as above
Microsomes ( <u>Metschnikowia reukaufii</u> )	spherical $\leq 0.2 \mu\text{m}$ $\approx 0.75\mu\text{m}$	as above

### 1.5 Scope of the study

The central aim of this study was to broaden the understanding of the high pressure homogenisation process. In view of the fact that most available research on this topic had been carried out in the early 1970's, there was a need to readdress some of the unresolved problems and also investigate the effect of some of the new developments which had since occurred in the disruption technology.

The disruption study of filamentous microorganisms had been largely neglected until very recently when Thomas (1988) investigated the release of soluble protein and the membrane bound enzyme progesterone 11 $\alpha$ -hydroxylase from Rhizopus nigricans. In the present study, further work was carried out to characterise the disruption kinetics of this microorganism with the view to investigate some of the difficulties previously reported by other workers (Section 1.2.3), and compare the findings with a reference unicellular microorganism namely bakers' yeast.

Against a background of wide ranging theories available to explain cell disruption, the mechanism of cell disruption has been investigated using the above mentioned microorganisms. New evidence is presented to explain some aspects of the complex disruption process. A theoretical approach is thus put forward.

In order to gain a more complete picture of the cell disruption process, cellular particles obtained under different homogenisation conditions, and homogeniser configuration were characterised.

Finally, a new integrated, hygienic homogenisation system comprising a recently developed homogeniser and ancillary equipment (e.g. hoppers, heat exchanger) was designed with the view to future work and possible retrofittability for containment.



## 2. MATERIALS AND METHODS

### 2.1 Materials

Dextrose monohydrate was obtained from Tunnel Refineries (Greenwich, London, UK) and yeast extract from Bovril Ltd. (Burton on Trent, Staffs, UK). Potato dextrose agar and Sabourauds dextrose agar were purchased from Oxoid Ltd. (Basingstoke, Hants., UK). Progesterone was a gift from Glaxo Research Ltd (Greenford, Middlesex, UK). Bovine serum albumin, glutathione and NAD (grade III) were from Sigma Ltd. (Poole, Dorset, UK). Polypropylene glycol (PPG 2025), ethanol and semicarbazide hydrochloride (Alanar) were supplied by BDH Ltd. (Poole, Dorset, UK). Folin and Ciocalteu's phenol reagent, sodium dihydrogen phosphate, disodium and dipotassium hydrogen phosphates and all other chemicals used were obtained from Fisons plc (Crawley, West Sussex, UK).

### 2.2 Microorganisms

Rhizopus nigricans 6227b (listed as R. stolonifer in the ATCC catalogue) was a gift of Glaxo Research Ltd. (Greenford, Middx., UK). Blocks of Bakers' yeast were obtained from the Distillers Co. Ltd. (Sutton, Surrey, UK).

Spores of R. nigricans were kept freeze dried in 20% (w/v) skimmed milk at a concentration of  $7 \times 10^7$  spores/mL. Agar slopes consisting of 2.78 g potato dextrose agar and 1.16 g Sabourauds dextrose agar dissolved in 100 mL deionised water were prepared in 500 mL medical flat bottles fitted with foam bungs. The use of high quality deionised water was found to be important in the dissolution of the agar constituents and subsequent healthy growth of the spores. Approximately  $1 \times 10^8$  spores were suspended in 5 mL of deionised water and then transferred onto the agar slopes. These were

incubated at 28° C until heavy sporulation was achieved (up to 14 days). Spores were then harvested into 50 mL deionised water and counted using a haemocytometer. They were stored at 4° C and used within a week. In the above procedure all materials and instruments were sterilised (at 121° C for 15 minutes) and handled under aseptic conditions. One exception was the skimmed milk which could not be autoclaved due to protein denaturation. This problem was overcome by using a fresh unopened container of skimmed milk in each freeze drying operation.

### 2.3 Growth medium for *Rhizopus nigricans*

The spores of *R. nigricans* were grown in a medium containing 2.5% dextrose monohydrate, 2.0% yeast extract and trace minerals. The trace mineral solution prescribed by Elsworth et al. (1968) was used. However it was found that the recommended 0.1% solids content did not readily dissolve. The proportion of solids was therefore reduced by a factor of ten as recommended by Thomas (1988). Fermentation medium was supplemented with 0.01% PPG 2025 to control foam formation. The pH of all media was adjusted to 4.5 with 5M orthophosphoric acid. Media sterilisation was carried out at 121° C for 15 minutes.

### 2.4 Growth of *Rhizopus nigricans* in shake flasks

Twelve 2 L Erlenmeyer flasks, each containing 250 mL of sterile medium, were inoculated with a spore suspension of  $5 \times 10^8$  per flask, giving a final concentration of  $2 \times 10^6$  spores/mL. The shake flasks were siliconised beforehand in order to eliminate wall growth. Cultures were grown in a reciprocating shaker incubator (New Brunswick, N.J., USA) with a 50 mm throw set at 100 strokes/min held at 29° C for 24 h. In the case where progesterone 11 $\alpha$ -hydroxylase had to be induced in the cells, progesterone was added at 2 g/L after 21 h.

## 2.5 Growth of Rhizopus nigricans in fermenters

### 2.5.1 Equipment

#### 2.5.1.1 Fermenters

Fermentations were carried out in 4 different size vessels as described below. However the majority of the work was done in the 42 L fermenter.

<u>Vessel</u> (L)	<u>Total capacity (L)</u>	<u>Working volume</u>
14 L (Alfa Laval, Middx., UK)	14	10
20 L (LH Eng., Bucks, UK)	20	15
42 L (LH Eng., Bucks, UK)	42	30
150 L (LH Eng., Bucks, UK)	150	100

The baffles in these fermenters were positioned in such a way as to avoid splashing which may result in wall growth. Furthermore the liquid level was well below the top plate. This prevented the blockage of the air exit due to cell growth.

#### 2.5.1.2 Instrumentation and sterilisation

All vessels were equipped with Ingold steam sterilisable pH and DOT electrodes (Life Science Labs., Beds., UK). Exit gases were recorded and analysed using a microprocessor controlled VG MM-80 mass spectrometer (VG Gas Analysis, Cheshire, UK). Via a link up to a PDP minicomputer it was possible to monitor the physical parameters and

compute the OUR, CER and RQ values throughout the fermentation period.

Except for the 150 L fermenter, all components of the media were sterilised together in situ at 121° C for 15 minutes. In the case of the large fermenter, dextrose monohydrate was separately dissolved in 10 L deionised water and the pH of the solution adjusted to 3 using 5 M orthophosphoric acid. It was then sterilised in the same manner and aseptically added to the remaining medium which had already been sterilised in the fermenter.

#### 2.5.2 Conditions of growth

The physical parameters for fermentations carried out in the 20 L and 42 L vessels were as follows. The temperature was held at 29° C, aeration rate was at 0.1 VVM, the pH was set at 4.5 and the tip speed at 2.0 m/s. In the 14 L fermenter, the aeration rate was maintained at 0.12 VVM. The aeration rate in the 150 L vessel was increased to 0.2 VVM.

##### 2.5.2.1 Filamentous growth

Fermentations below 100 L were inoculated from shake flask cultures grown for 10 hours at which time visible filamentous growth could be noted. Conditions were as specified in Section 2.4. For the 100 L fermentations, the 14 L vessel was used as seed fermenter to grow the inoculum. The size of inoculum, depending on the fermenter varied between 7 to 10% (v/v). The fermentations lasted for 15 to 18 h until the stationary phase was reached.

#### 2.5.2.2 Pelleted growth

Pelleted growth was achieved by reducing the inoculum size for the shake flasks to one third, from  $2 \times 10^6$  to  $6.7 \times 10^5$  spores/mL. It was also possible to obtain pelleted cells if the inoculum was transferred at an earlier stage i.e. less than 10 h growth in the shake flask when the mycelia were not fully visible.

### 2.6 Harvesting

#### 2.6.1 Nylon mesh

All shake flask grown cells were harvested by transferring them into a funnel lined with coarse nylon mesh. The cells were washed 3 times in a total of 3 volumes of 50 mM sodium phosphate ( $\text{Na}_2\text{HPO}_4/\text{NaH}_2\text{PO}_4$ ) buffer (pH 7.4) at 4° C and pressed dry.

One 100 L fermentation was harvested using the same procedure as above. It was found to be more time consuming than harvesting using a basket centrifuge.

#### 2.6.2 Basket centrifuge

Fermentation cultures generally were harvested in a basket centrifuge (MSE model 10.65 -now obsolete- MSE Ltd., West Sussex, UK) running at 1000 to 1500 rpm, and washed 3 times in a total of three fermenter working volumes of the above buffer (Section 2.6.1).

## 2.7 Preparation of microorganisms for disruption

### 2.7.1 Bakers' yeast

Fresh blocks of yeast (about 1 kg/block) were stored in a cold room and used within 3 days of purchase. The packed yeast was crumbled and suspended in 4 mM  $K_2HPO_4$  at 4° C to give a concentration of 45% w/v of packed cells. The concentration of phosphate buffer was chosen to maintain constant pH of the disrupted suspension of 5.6 over a wide range of protein concentrations (Hetherington et al. 1971).

### 2.7.2 Rhizopus nigricans

R. nigricans cells from either shake flask or fermentation cultures were resuspended immediately after harvesting in 50 mM phosphate buffer at 4° C to the required concentration. It was important to carry out this step as quickly as possible as the storage time of harvested cells affected the ease of resuspension.

## 2.8 High pressure homogenisation

### 2.8.1 Equipment

The equipment was an APV-Gaulin 15 M single piston positive displacement pump, incorporating a single adjustable, restricted orifice discharge valve assembly, the design and operation of which is already described in Section 1.1.2.2 . The homogeniser had a capacity of 57 L/h and operated within a nominal pressure range of up to 56 MPa. The equipment was coupled to an APV Junior plate heat exchanger (APV Baker, Crawley, West Sussex, UK). A 70% aqueous solution of ethylene glycol at -5° C was used as coolant. The flow was controlled by means of a manual valve. Inlet and outlet

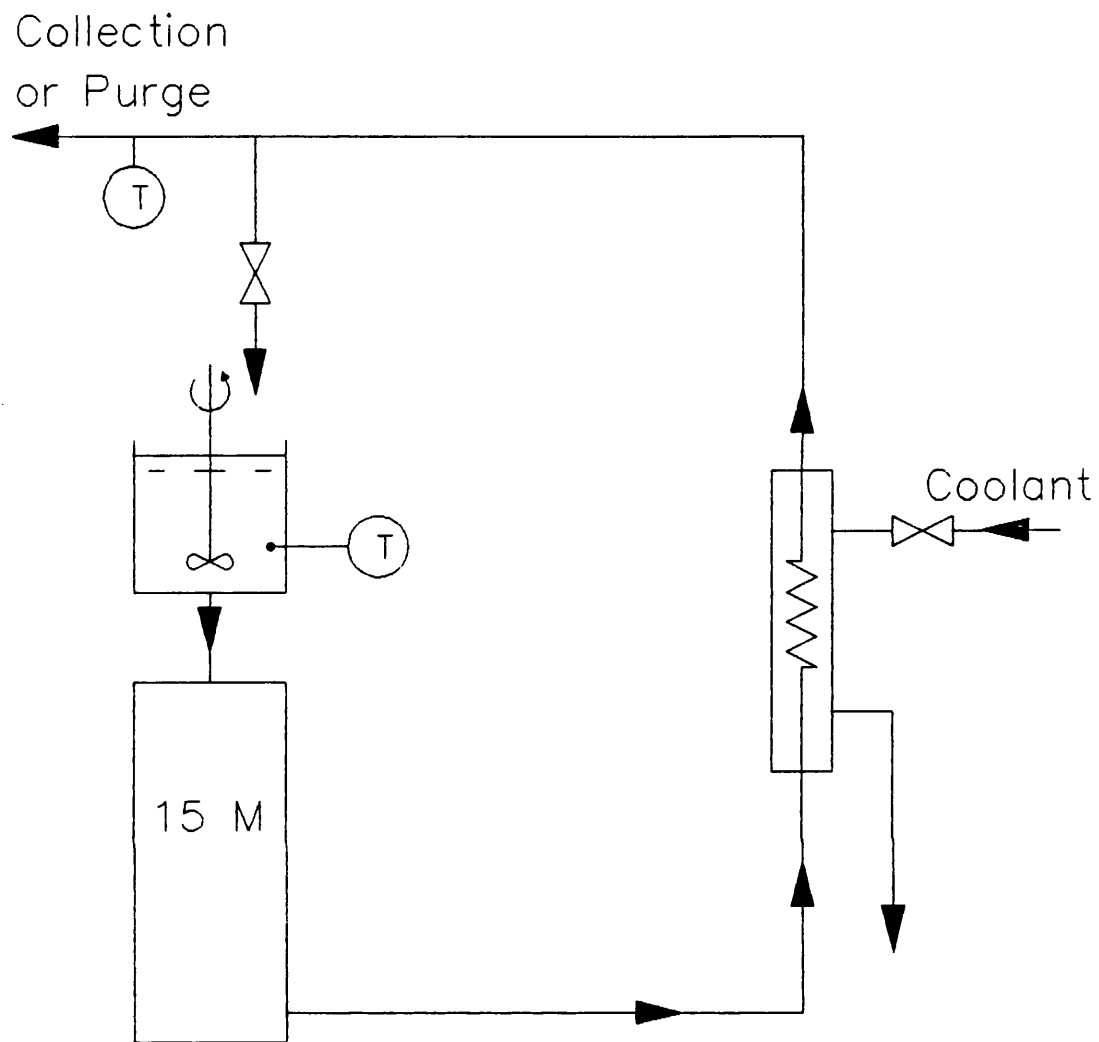
temperatures were monitored using platinum resistance probes (model 3745 PT 100, Digitron Instrumentations Ltd, Hertford, Herts., UK) connected to a Digitron multi selector unit.

The stainless steel container attached to the homogeniser to hold the process batch had a 5 L working volume. The pressure was indicated by a gauge mounted on top of the cylinder block. The fluctuations in measurement caused by the operation of the single plunger were reduced by means of a manually adjusted dampener. An ammeter was installed to identify pressure gauge malfunction. Figure 2.1 gives a schematic outline of the experimental arrangement.

#### 2.8.2 Changing of valve assembly

Depending on the nature of the experiment, five different valve unit configurations were examined, the details of which are given in Table 2.1. This included three types of knife-edge units (CRF, CD, KE), and a flat valve unit (FV). As the dimensional characteristics of these units are essential in the analysis of the results obtained, their details are described in full in Chapter 4 (Section 4.1). Furthermore the impact distance was also varied by using four impact rings of varying bore sizes in the valve geometry CD (Cell Disruption). Details of these dimensions are discussed in Chapter 4 (Section 4.1).

As the homogeniser is not specifically designed for frequent disassembly of the valve unit other than routine inspection, the changing of the components of the valve unit proved to be an involved operation necessitating careful handling. It was essential to ensure that the o-rings and the components of the valve unit were correctly fitted. Failure to do so could result in damage to the unit and leakage, which would impair the disruption process. Furthermore, even though the ceramic composite material of the CD unit was resistant to wear it was nevertheless brittle.



**Figure 2.1** Schematic diagram of homogenisation equipment



Table 2.1 Valve unit configuration

<u>Type of unit</u>	<u>Symbol</u>	<u>Material</u>
Flat valve seat & flat valve rod	Flat valve (FV)	tungsten carbide
Knife-edge valve seat & flat valve rod	Cell Disruption (CD)	ceramic composite
Knife-edge valve seat & coned valve rod	Cell Rupture (CR)	tungsten carbide
Knife-edge valve seat & flat valve rod	Cell Rupture type (CRF)	tungsten carbide
Knife-edge valve seat & flat valve rod	(KE)	stellite

### 2.8.3 Disruption procedure

The homogenisation was performed on a discrete pass basis, for up to 5 passes. The cells were continuously stirred in the hopper throughout the procedure. This was particularly important in the case of filamentous R.nigricans cells which settle easily under gravity. In order to minimise the amount of mixing between two consecutive passes, it was necessary to purge a suspension volume equivalent to the hold up volume in the system. However, it was also desirable to minimise the amount of suspension loss. The following procedure was therefore adopted.

Step 1- The hold up volume was obtained using a colour tracer. This was found to be equivalent to 30 seconds of flow.

Step 2- After pass 1, the system was purged for 30 seconds before collection began.

Step 3- After pass 2, the output from the homogeniser was returned to the hopper for 15 seconds, and purged for the following 15 seconds, before collection started. The logic of this procedure was that for the initial 15 seconds, the hold up volume was the remnant of the pass 1 homogenate and could therefore be returned to the hopper. The following 15 seconds were to be purged due to mixing of the passes in the pipework.

Step 4- Step 3 was repeated for the next passes.

Although it was possible to purge the total hold up volume after each pass for microorganisms available in large quantities, such as Bakers' yeast, it would have been impractical to do so for smaller volumes of cell suspension such as fermenter grown R. nigricans cells. In the case of shake flask cultures where the amount of available cells was even more limited, each pass was followed by buffer to avoid dry running of the homogeniser under pressure which damages the valve unit. The dilution effect was then taken into account by measuring the dry weight of the cells after each pass. The temperature of the process stream was maintained at  $4^{\circ}\text{C} \pm 1$  by controlling the aqueous ethylene glycol supply. It is possible to

cool down the initial suspension prior to homogenisation by recirculating it in the homogeniser without applying any pressure. However this was avoided when dealing with R. nigricans suspensions to prevent possible damage to the cells. As mentioned in Section 2.7, cells were suspended in buffer already cooled to 4° C. Care was taken to achieve reproducible pressures for different experiments carried out at the same pressure. Samples of 30 mL were taken after each pass for further analysis.

## 2.9 Microsomal preparation

### 2.9.1 Homogenate

Shake flask grown cells of R. nigricans were disrupted at 15 MPa and samples were collected after 1, 2, or 4 passes depending on the nature of the experiment.

### 2.9.2 Gel filtration

Samples of disrupted cells were spun at 2000 g in a centrifuge (MSE Ltd, Crawley, West Sussex, UK) for 10 minutes. The supernatant was then spun at 50000 g in a Pegasus 65 ultracentrifuge (MSE Ltd, Crawley, West Sussex, UK) for 45 minutes. The top surface of the supernatant was covered with a lipid layer. Care was taken not to resuspend this layer when removing the supernatant which was then loaded onto a high performance gel filtration column using Superose 12 (Pharmacia Ltd, Uppsala, Sweden) as the Separation medium (range  $10^3 - 3 \times 10^5$  MW). The first peak was collected for particle sizing.

### 2.9.3 'Sugar cushioning'

The homogenate was spun down at 12000 g in an MSE 21 high speed centrifuge for 20 minutes. The supernatant was then gently poured into centrifuge tubes which already contained 1 mL of 4 M sucrose solution. These tubes were then spun at 105000 g for 1 h. The microsomal fraction collected on the top of the sucrose solution was pipetted out and resuspended in 50 mM phosphate buffer for further analysis.

## 2.10 Particle size measurement

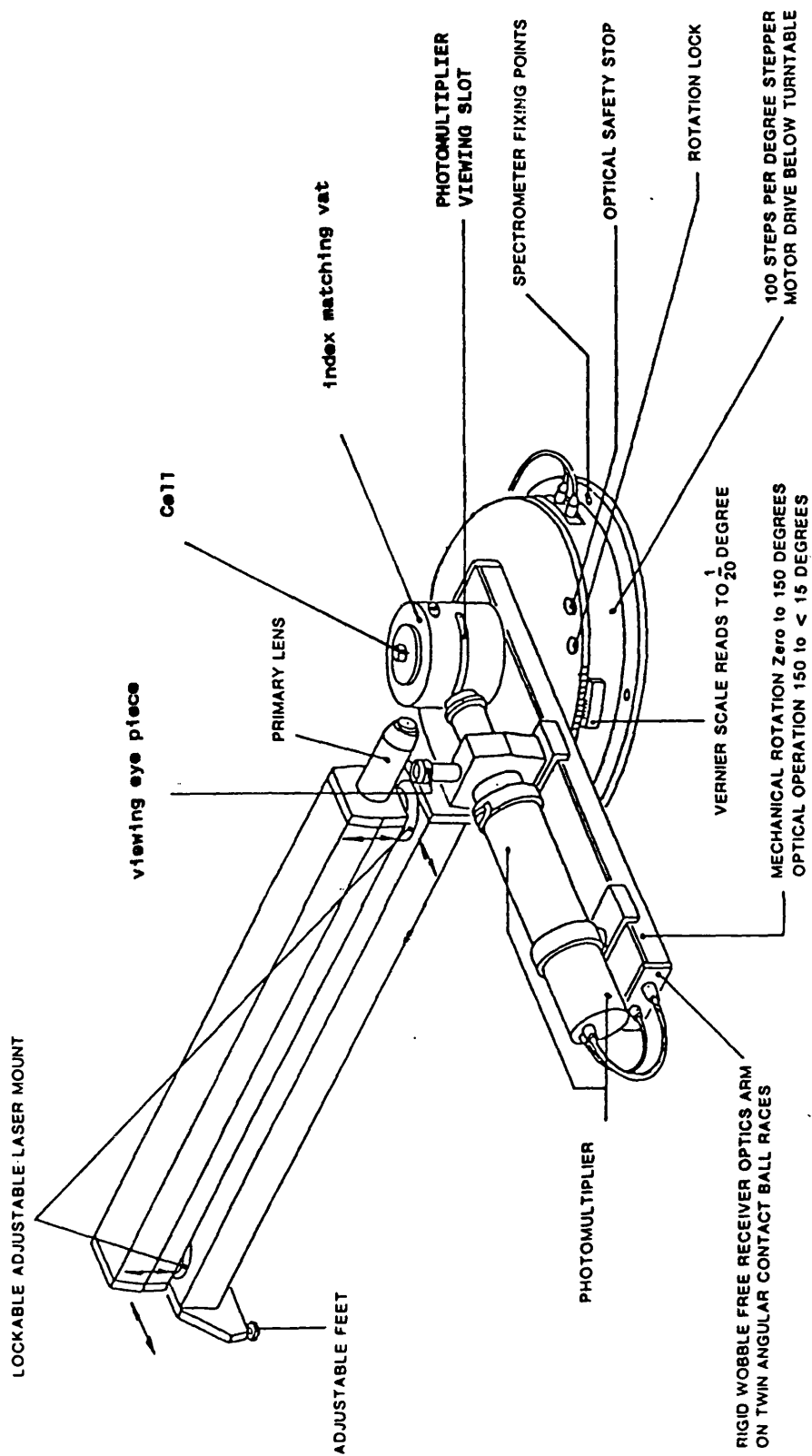
### 2.10.1 Sample types

Particle size analysis of samples obtained from two different sources were carried out. Firstly, microsomal fractions obtained from R. nigricans cells described above were measured using Photon correlation spectroscopy. Secondly, particles obtained from yeast homogenisation were measured. Several different conditions were tested. Yeast homogenate samples obtained as described in Sections 2.7.1 and 2.8 were sized using an electrical sensing zone technique. These included samples after different passes with different valve unit configurations.

### 2.10.2 Photon correlation spectroscopy

#### 2.10.2.1 Equipment

A Malvern 4700 Photon correlation spectroscope (PCS) (Malvern Instruments Ltd, Malvern, Worcests., UK) was used. This equipment is based on a helium-neon continuous wave laser and is capable of measuring particles in the size range 0.003 to 3.0  $\mu\text{m}$ . Figure 2.2 gives a schematic outline of the equipment. Further details about



**Figure 2.2** Schematic outline of photon correlation spectroscope  
(correlator and computer not shown)

the equipment are given in Appendix B.

#### 2.10.2.2 Sample preparation

Sample preparation is a very important step in operating the Malvern 4700. Prior to measuring a sample, the index matching fluid ( i.e. water in these experiments) in which sample cuvettes were immersed was filtered and recirculated using the filter pump available for this purpose. The fluid served to reduce the refractive index change at the surface of cuvette and also acted as a constant temperature bath. The cuvettes and their stoppers were rinsed several times with filtered water to clean them of dust particles. It was possible to overcome the problem of atypically large particles by allowing them to settle, although this was not found necessary when measuring microsomes.

The presence of high concentration leading to multiscatter was detected by visual inspection through the viewing slit. A clean bright light line from the laser passing through the sample indicated an acceptable concentration level. If the beam was shrouded in a halo of light, the concentration was evidently too high and more dilution was required. The temperature difference between the sample and the instrument was eliminated by either preparing the sample at the same temperature as the ambient temperature or allowing it to settle in the instrument for at least 2 minutes. The problem of temperature rise during prolonged experimentation was eliminated by passing aqueous ethylene glycol at 0° C around the walls of the water bath. A heating element installed in the walls was connected to a control unit which adjusted the temperature of the water to a selected set point.

### 2.10.2.3 Instrument settings

The settings were controlled by changing the photomultiplier aperture, the sampling time. These parameters were altered to achieve an acceptable count rate (80000 to 350000 counts/s), "signal to noise" ratio (20-80%) and "within range" value (>80-90%).

### 2.10.3 Electrical sensing zone method

The cell debris from yeast homogenisation were sized using an electrical sensing method (Elzone model 80 XY, Particle Data Ltd, Cheltenham, Gloucs, UK) with 128 channels and a statistics computing accessory. The analyser was fitted with a 30 µm orifice tube and calibrated using latex standards (Particle Data Ltd) of sizes 2.02 µm and 10.18 µm. The current was set at 4.5 A and the gain at 1.5.

The debris suspensions (initial whole yeast concentration of 45% w/v packed cells) were diluted in 1%, 5% and 10% (w/v) sodium chloride to give a coincidence count of less than 1% during size analysis. The sodium chloride had been filtered through 0.1 µm filter and vacuum degassed to avoid bubble formation. Good dispersion was maintained during the dilution process and care was taken to use clean dust free glassware. Particle size data was corrected for an electrolyte background count.

### 2.11 Gel electrophoresis

Sodium dodecyl sulphate-polyacrylamide gel electrophoresis (SDS-PAGE) was performed on samples of filamentous, fermenter grown R. nigricans cells which were disrupted at different pressures for 5 passes. The electrophoresis equipment was a Pharmacia model GE 2/4 LS ( Pharmacia Fine Chemicals AB, Uppsala, Sweden). A modified Laemmli technique (1961) was adopted.

Homogenate samples were spun down at 14000 g for 30 minutes. The supernatant, 0.6 mL, was added to 0.2 ml sample buffer (4 x concentration). The sample buffer was prepared by adding 5 mL glycerol to 2.5 mL 2-mercaptoethanol, 1.5 g SDS, 0.38 g Tris and 12.5 mg bromophenol blue and made up to 12 mL with deionised water. After thorough mixing the pH of the buffer was adjusted to 6.8 with HCl. The samples were then boiled for several minutes, and 35 µL aliquots were placed in the sample wells of the gel slabs. A protein marker in the MW range 12300-78000 was used. After electrophoresis, the gel slabs were scanned in an ultrascan laser densitometer ( LKB Bromma, Uppsala, Sweden).

## 2.12 Protein assay

### 2.12.1 Bakers' yeast

Samples of disrupted cells were spun at 14000 g in an MSE 21 High Speed centrifuge (MSE Ltd, Crawley, West Sussex, UK) for 30 minutes. The supernatant layer was then diluted in the range 0-1.0 mg/mL protein with deionised water. The diluted samples were analysed for their soluble protein content by the Folin-Lowry method (Lowry et al. 1951) using a Technicon Auto-Analyser (Technicon Instruments, Basingstoke, Hants, UK).

For a given suspension the solids content decreased with the degree of disruption. To bring the analytical results to the common basis of protein released per gramme of yeast, it was necessary to compensate for the change in the solids content of samples. The fraction of aqueous phase in a suspension was obtained using the method described by Hetherington et al. (1971).



### 2.12.2 Rhizopus nigricans

Samples were diluted with 50 mM phosphate buffer to the range 0–0.7 mg/mL protein. Care was taken to ensure that the homogenates were well mixed as the debris settles very quickly. The diluted samples were then spun down in an MSE High Speed centrifuge (Europa 24M, MSE Ltd, Crawley, West Sussex, UK) at 14000 g for 30 minutes. Cut-off auto-pipette tips were used to obtain representative samples at low disruption levels. The soluble protein content of the supernatant was then analysed as described in Section 2.11.1 above.

### 2.13 Alcohol dehydrogenase activity assay

The assay was according to Bergmeyer et al. (1983). The assay mixture (3.0 mL) consisted of 6.2 mM semicarbazide hydrochloride, 1.0 mM glutathione, 1.8 mM NAD and 700 mM ethanol in Tris-HCl buffer (0.05 M, pH 8.8). The sample consisted of 0.05 mL of the supernatant solution of disrupted cells previously prepared for soluble protein assay. After addition of the sample mixture the reaction was monitored at 340 nm in a spectrophotometer (model SP 8400, Pye Unicam, Cambridge, England).

In the assays stated in the above sections where appropriate each result was the mean of at least five independent determinations from separate experiments and each determination was the mean of at least two replicate samples.

### 2.14 Dry weight measurements

Homogenised samples (4.5 mL) from each pass together with initial undisturbed samples (approximately 2 g) were transferred to porcelain crucibles and dried at 90° C to constant weight. In the case of R. nigricans cells, samples of the buffer were also measured

for dry weight to account for the contribution to the dry weight of the disrupted cell samples. Yeast data were expressed in terms of wet weight of packed cells. however, dry weight measurements were also taken to monitor the consistency of different batches.

## 2.15 Microscopy

Micrographs of disrupted and whole cells were taken with an Olympus camera (Olympus Optical Co., London, UK) connected to an Olympus BH2 stereoscopic light microscope. Samples were stained with lactophenol blue prior to slide preparation.

### 3. DISRUPTION CHARACTERISTICS OF RHIZOPUS NIGRICANS

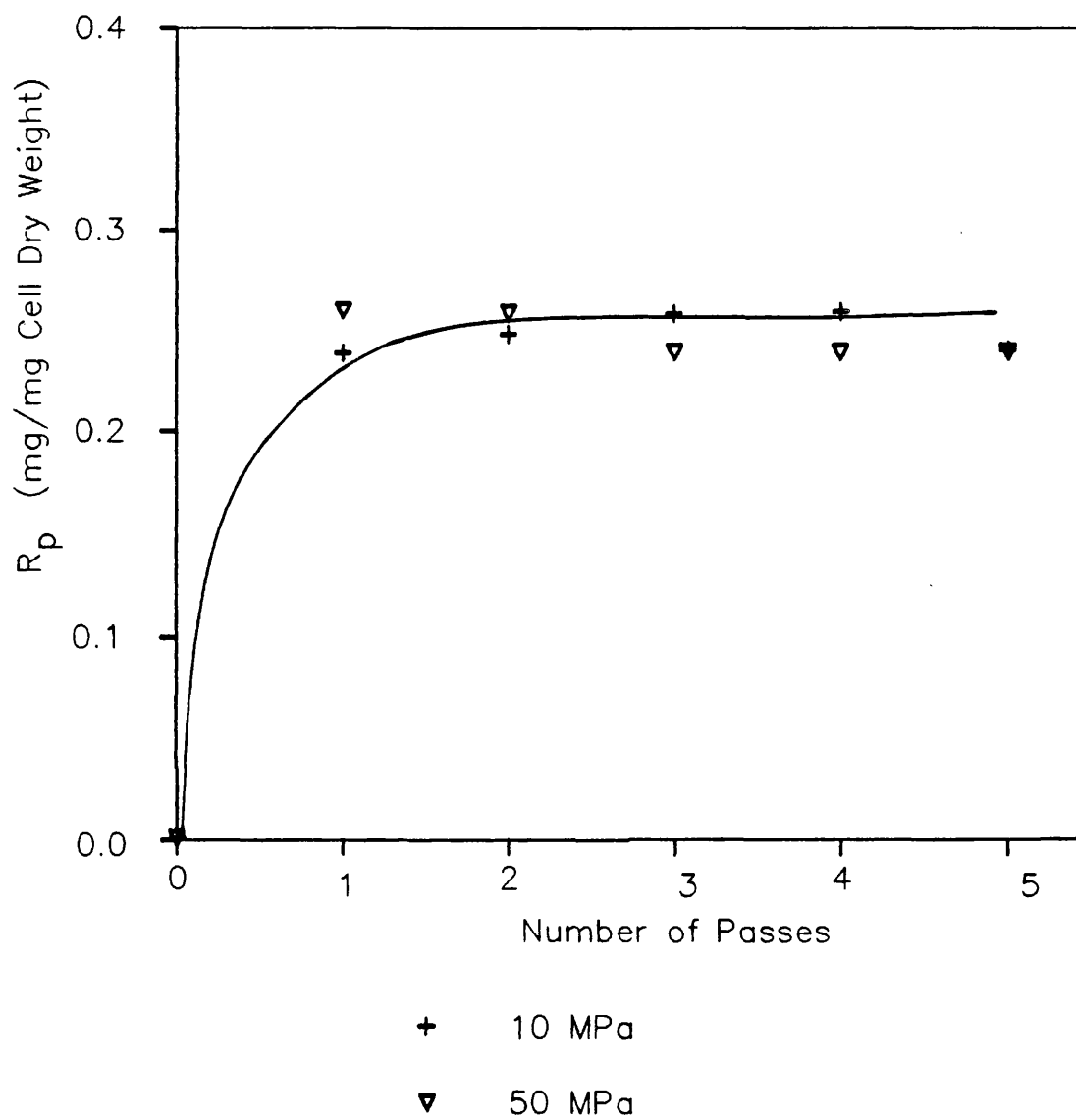
The disruption characteristics of the filamentous fungus Rhizopus nigricans in a high pressure homogeniser was studied. The effect of operating conditions, namely, pressure and the number of passes, cell related conditions, i.e. cell concentration and cell growth, and equipment parameters, i.e. valve unit design were investigated.

#### 3.1 Effect of pressure and number of passes

Within the limited framework of data available on disruption of filamentous microorganisms, high pressure homogenisation has been considered by some researchers as an unfavourable method of cell disruption (Zetelaki 1969, Hanisch 1978), whilst it has been reported by others to be a more effective technique than bead milling (Thomas 1988). Further work was therefore required to substantiate the effectiveness of high pressure homogenisation in disrupting filamentous microorganisms such as R. nigricans.

##### 3.1.1 Shake flask culture

Multi-pass experiments were carried out with filamentous shake flask cultures of R. nigricans, at a low pressure of 10 MPa, and a high pressure of 50 MPa which is close to the limit of operability of the single piston homogeniser used. The release of soluble protein obtained at these pressures is shown in Figure 3.1. The results indicate that there is a sharp and almost complete release of soluble protein after the first pass. No increase in the amount of



**Figure 3.1** Effect of pressure on release of soluble protein from shake flask-grown filamentous cells.

protein released was observed at the higher pressure of 50 MPa versus 10 MPa.

### 3.1.2 Fermenter cultures

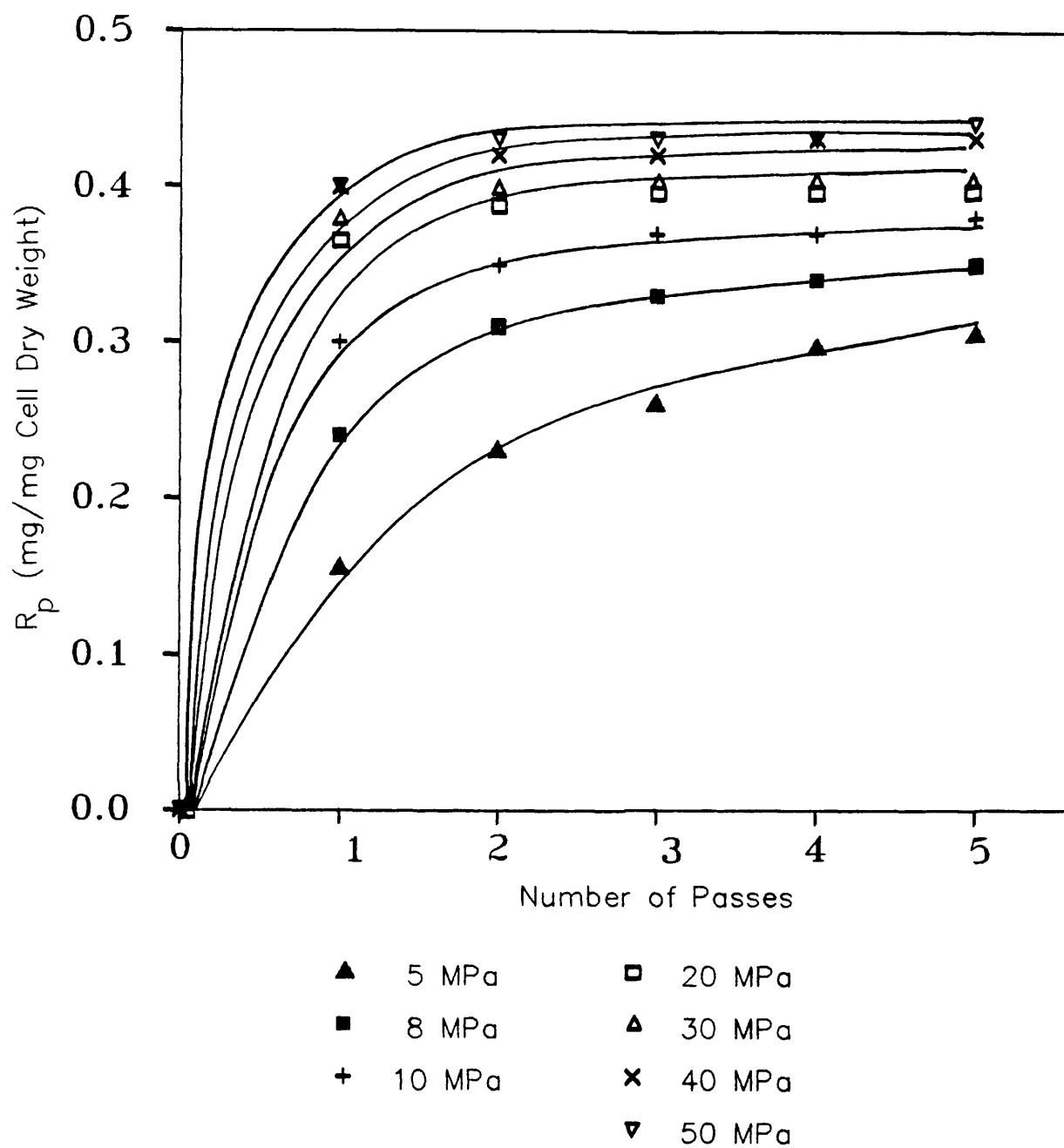
Filamentous cells grown in a fermenter were disrupted over a range of pressures from 5 MPa to 50 MPa. The soluble protein released up to 5 passes was measured (Figure 3.2). The maximum amount of protein released ( $R_m$ ) was reached after 3 passes for pressures above 10 MPa. However,  $R_m$  was observed to be dependent on pressure. This result was contrary to the observations made for high pressure homogenisation of unicellular microorganisms, where  $R_m$  was independent of pressure (Hetherington et al. 1971; Gray et al. 1973).

Fermenter grown pelleted cultures of the cells were also disrupted at pressures in the range 5 MPa and 20 MPa. Similar results to those for filamentous cultures were obtained as shown in Figure 3.3.

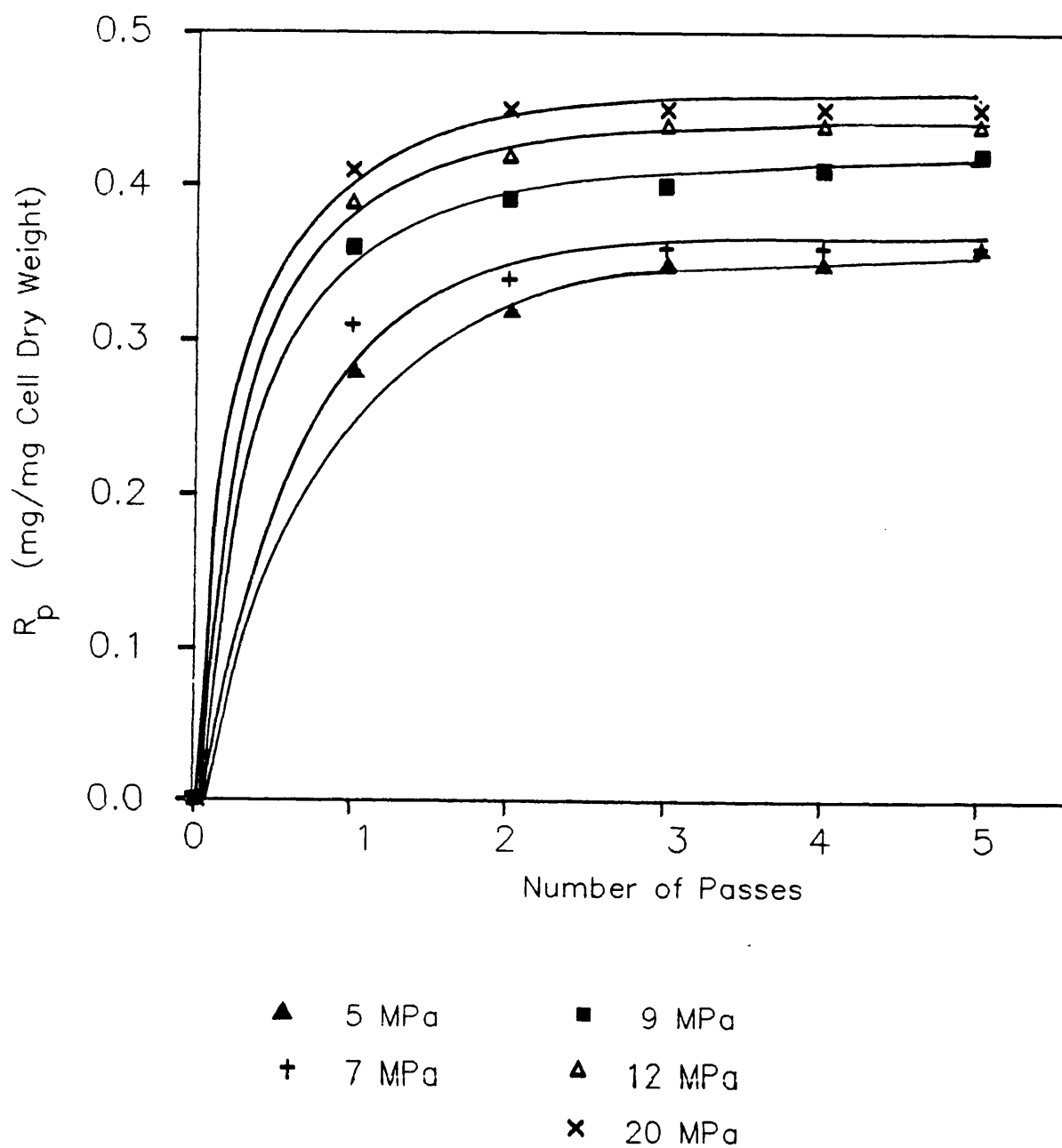
### 3.1.3 Maximum protein release

The dependency of  $R_m$  on pressure had been previously observed for Candida lipolytica and was attributed to the mixed morphology of the culture consisting of filamentous and elongated ovoid cells (Whitworth 1974b), but no further work was carried out to clarify these findings (Section 1.2.2). However, this explanation could not be applied to the observations made in this study as cultures, whether filamentous or pelleted, were of uniform morphology.

Previous work by Limon-Lason et al. (1979) on disruption of Bakers' yeast in a bead mill showed variable values of  $R_m$ . This was explained by the possible release of insoluble complex proteins and other Folin-positive materials such as peptide, glycopeptide and amino-acids by micronisation of the cell debris. As this could be a



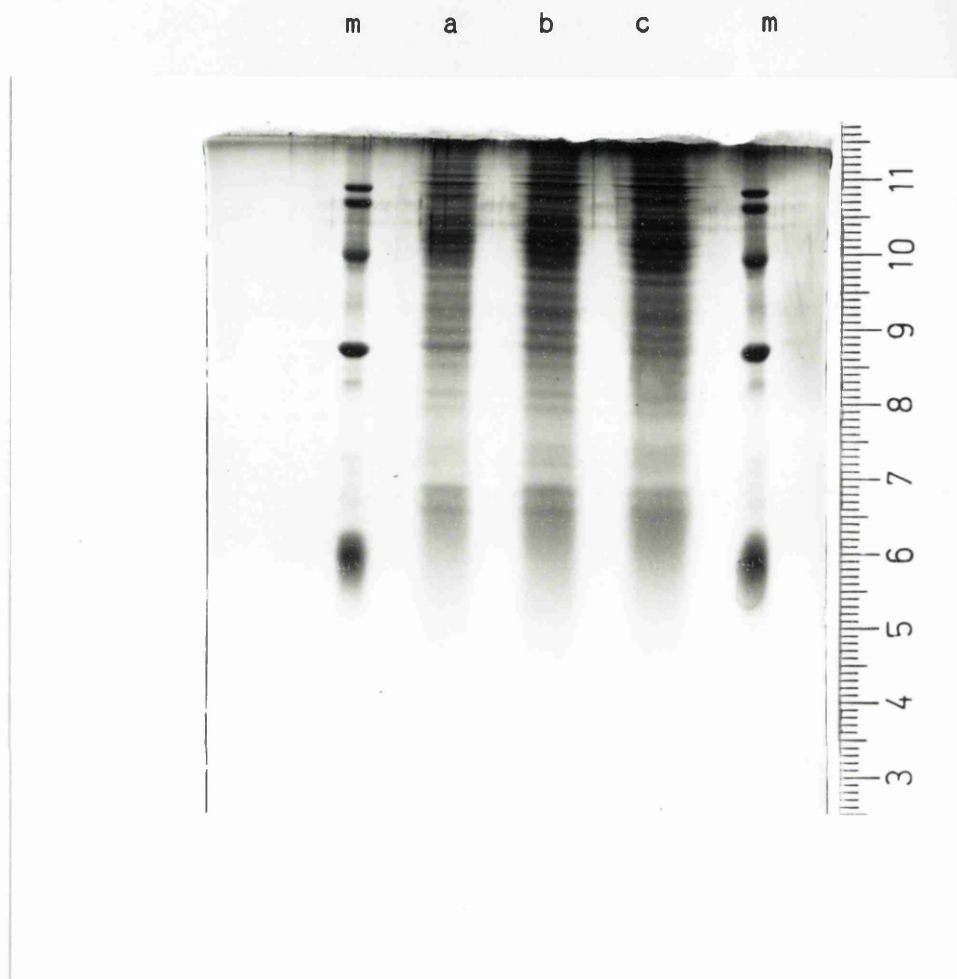
**Figure 3.2** Effect of pressure on release of soluble protein from filamentous fermenter-grown cells.



**Figure 3.3** Effect of pressure on release of soluble protein from pelleted fermenter-grown cells.

plausible explanation for the observations made in this study, the possibility of micronisation of R. nigricans cell debris was investigated. An attempt was first made to detect the presence, if any, of the released proteinaceous material from the cell debris. This was carried out by assaying the released proteins of the disrupted cells at two different pressures by discontinuous gel electrophoresis. The technique is a powerful tool for identifying and distinguishing different proteins which are seen as stained bands on the gel slabs. If micronisation had occurred the released extra protein would appear as extra bands on the gel. Samples used were from filamentous fermenter-grown cells which were disrupted at 10 MPa and 15 MPa for 5 passes. The results obtained (Figure 3.4) did not reveal the presence of any extra protein released at the higher pressure of 15 MPa as compared to that released at 10 MPa. Furthermore, no quantitative differences could be detected between comparable protein bands obtained for the two pressures by scanning the gels in an Ultrascan (Section 2.11). Although this was some indication that the  $R_m$  value was not pressure dependent, it could not be taken as a conclusive result. It was suspected that small molecules of Folin - positive material might have been released which were difficult to detect. It was therefore necessary to find an alternative approach to test the apparent variability of  $R_m$  with pressure. This required an independent measure of cell disruption. In the case of Bakers' yeast, Follows et al. (1971) had shown that alcohol dehydrogenase (ADH) had the same rate of release as that of the mean rate for total soluble protein. For the Rhizopus species, the existence of ADH has been established (Gleason 1971) and the enzyme has been characterised and shown to be similar to that of yeast (Gleason 1976; Yoneya and Sato 1980). Alcohol dehydrogenase was therefore used as an independent measure of disruption. Figure 3.5 illustrates the release of ADH activity from a fermenter-grown, filamentous culture of R.nigricans, over a wide range of pressures (10 MPa-50 MPa) for up to 5 passes. Results indicated that the maximum level of activity released remained constant for all pressures studied.



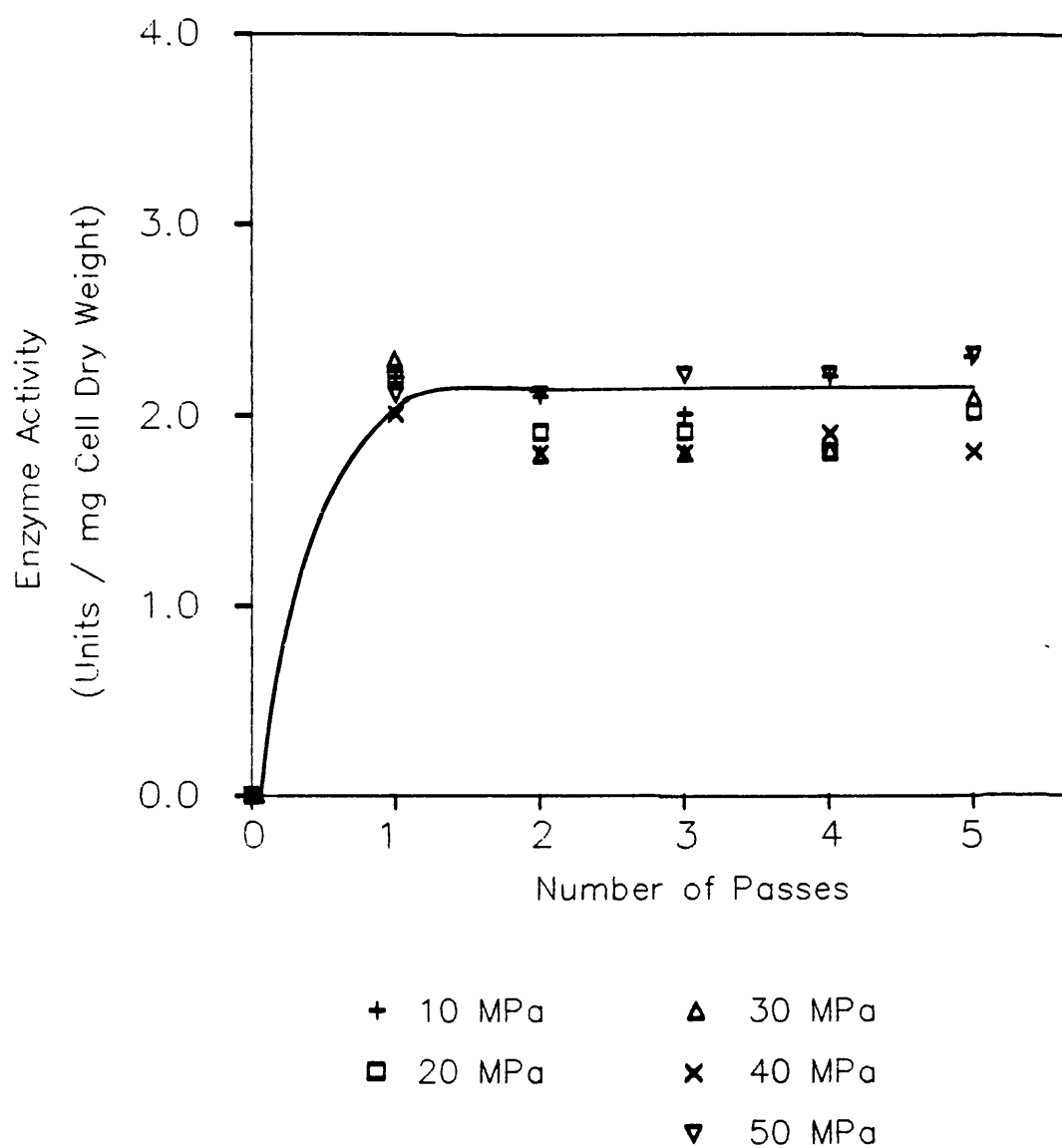


Source of cells

- a 8 g/L dry wt, (15 MPa)
- b 13 g/L dry wt, (15 MPa)
- c 13 g/L dry wt, (10 MPa)
- m marker protein

Release of protein for up to 50 MPa was also examined but similar inconclusive results were obtained.

**Figure 3.4** Gel electrophoresis of proteins released from R.nigricans at 15 MPa and 10 MPa after 5 passes.



**Figure 3.5** Effect of pressure on release of ADH activity from filamentous fermenter-grown cells.

### 3.2 Effect of cell concentration

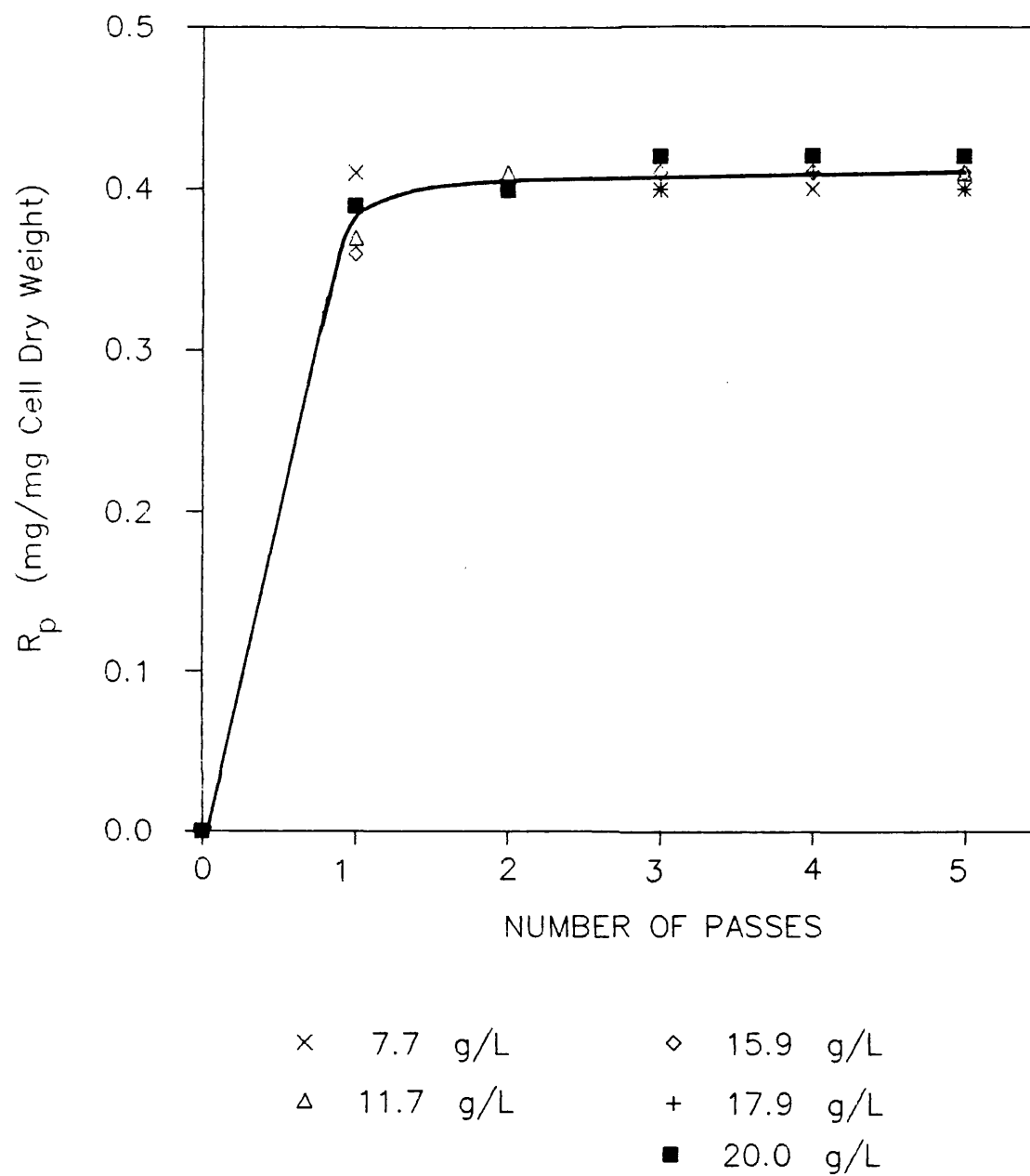
Cell concentration was reported to have no effect on the kinetics of disruption of unicellular microorganisms (Hetherington et al. 1971; Brookman 1974). The disruption of filamentous microorganisms, on the other hand, may be affected, in the case of high cell concentration, by the network structure of the cells resulting in the blockage of the equipment (Edebo 1983, Thomas 1988). It was therefore necessary to investigate the effect of cell concentration in the system under study. Figure 3.6 shows that filamentous fermenter-grown cell concentrations in the range 7.7 g/L to 20 g/L (dry weight of cells) did not influence the disruption kinetics observed. The cell concentration, however, could not be increased beyond the upper limit of 22 g/L due to homogeniser blockage. The experiment was repeated with pelleted cells in an attempt to increase this limit. A maximum of 30 g/L (dry weight of cells) was achieved prior to blockage.

### 3.3 Effect of up-stream processing conditions

Although it was not the aim of this study to investigate and optimise fermentation and harvesting conditions, several aspects of these processes were found to be of importance in the disruption of R.nigricans.

#### 3.3.1 Cell growth

Cells were grown in different size vessels (Section 2.5.1.1 ) ranging from 10 L to 100 L (working volume). Appendix A describes the fermentations carried out in detail. It was found that whilst the disruption characteristics of cell biomass obtained from 15 L and 30 L fermentations were consistent, the filamentous cells grown in the pilot scale 100 L vessel demonstrated different properties.



**Figure 3.6** Effect of cell concentration on release of soluble protein from fermenter-grown cells at 20 MPa.

The cells consisted of highly entangled hyphae matted together to form clumps which did not dissociate on resuspension. Furthermore, homogeniser blockage occurred even though the cell concentration used was reduced from over 15 g/L to below 10 g/L (dry weight of cells). One factor which may have caused these results was thought to be the change in morphology of the cells, affected by changes in the growth conditions of the cells (Appendix A). Although tip speed was kept the same as smaller fermenters, it is possible that different shear patterns were set up as a result of different geometry, which influenced the morphology and thus the disruption characteristics of the cells. Furthermore, this also appears to have resulted in the formation of a drier cell cake after harvesting, which was more difficult to resuspend. Such a change in morphology was also observed by other researchers (Talboys 1983), although direct comparison is difficult as different growth conditions were used (Appendix A).

### 3.3.2 Harvesting and storage

It was noted that the dewatering of the cells in the harvesting stage affected the ease of resuspension which in turn influenced disruption. Centrifugation in a basket centrifuge above 1500 rpm (289 g) resulted in clumps of cells which did not dissociate easily. This led to non uniform distribution of cells in buffer, settling of cells in the homogeniser hopper and unrepresentative samples. Centrifugation was therefore carried out between 1000 and 1500 rpm (128 g to 289 g).

Another important factor was the effect of storage time on the network structure of R.nigricans. Cells harvested and stored dry overnight at 5° C were very difficult to resuspend. Reduction of storage time to only few hours did not alleviate the problem even when the cells were deliberately centrifuged at low speed (500 rpm i.e. 32 g) to ensure that the cake was wet and therefore cells

easier to dissociate. This meant that not only was it not possible to follow the common practice of storing the biomass for further experimentation at a later date, but it was necessary to resuspend the cells for disruption soon after harvesting.

### 3.4 Discussion

#### 3.4.1 Micronisation

It was found in this study that the maximum level of ADH activity released remained constant for all pressures studied. These findings indicated that cytoplasmic proteins were released at low pressures, as no increase in ADH activity was recorded at high pressures (above 10 MPa), and the maximum soluble protein release ( $R_m$ ) therefore could not be pressure dependent over the pressure range studied. Therefore, the apparent rise in the  $R_m$  value with pressure was evidently the result of micronisation of cell debris and release of materials detectable by the Folin-Lowry protein assay. Micrographs of disrupted cells further confirmed these findings. Figure 3.7(a) shows the undisrupted cells. In Figure 3.7(b), filamentous cells are broken after 2 passes at 10 MPa. The filamentous structure of the cells is preserved even though the contents are emptied. In Figure 3.7(c), the cells are disrupted at 50 MPa after only one pass. No cellular structure remains and the cells are completely micronised.

In the case of shake flask cultures (Figure 3.1) however, no difference in the  $R_m$  values was observed at 10 and 50 MPa. This may be explained by the fact that micronisation of debris occurred even at low pressures due to weak wall strength of cells grown in shake flasks. Cells grown in fermenters are subjected to conditions of increased shear and this may have resulted in enhanced wall toughness as reported by Talboys (1983). This was supported by the microscopic examination of disrupted shake flask - grown cells, which showed micronisation at both pressures.

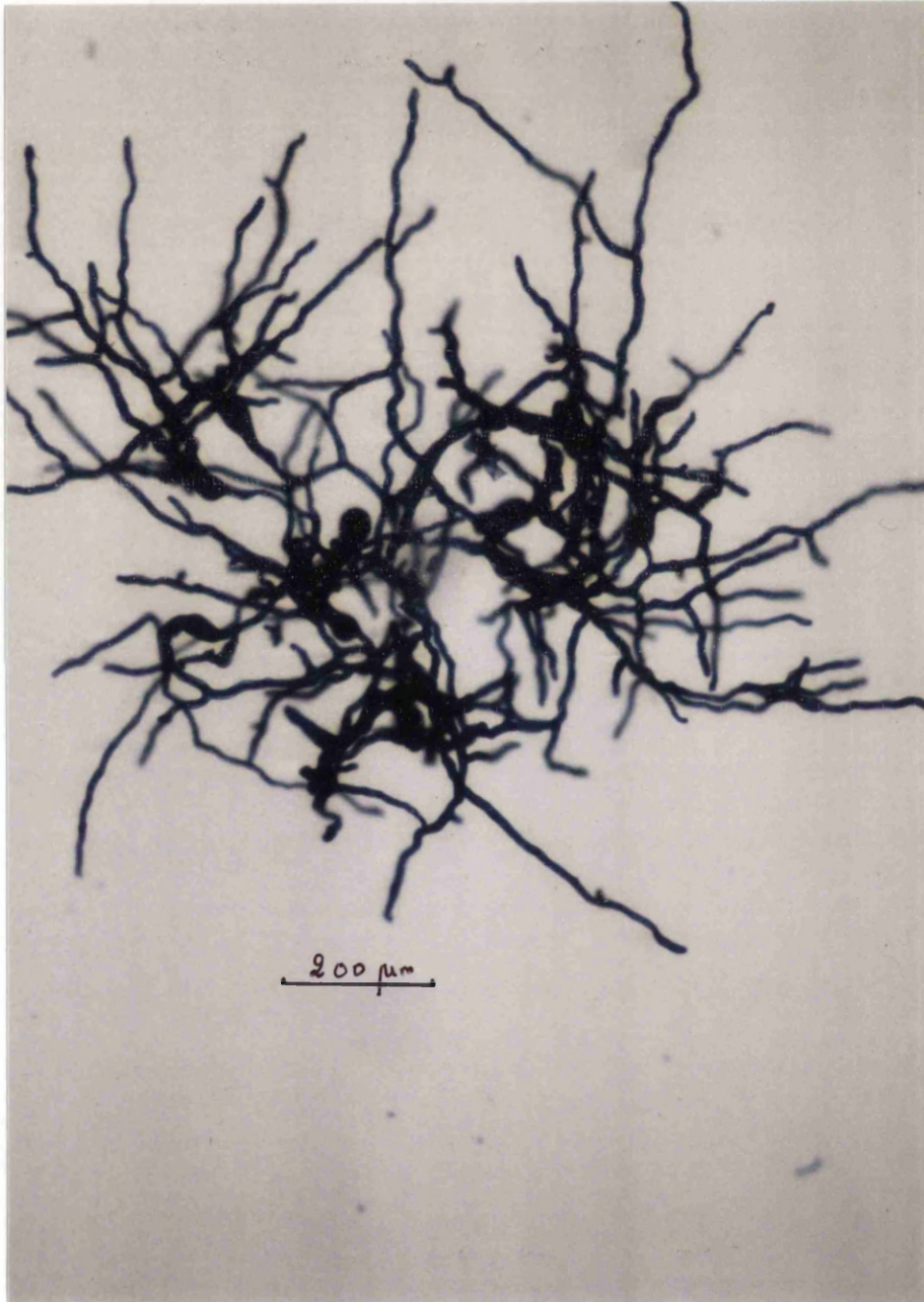


Figure 3.7(a)      Undisrupted Rhizopus nigricans cells.

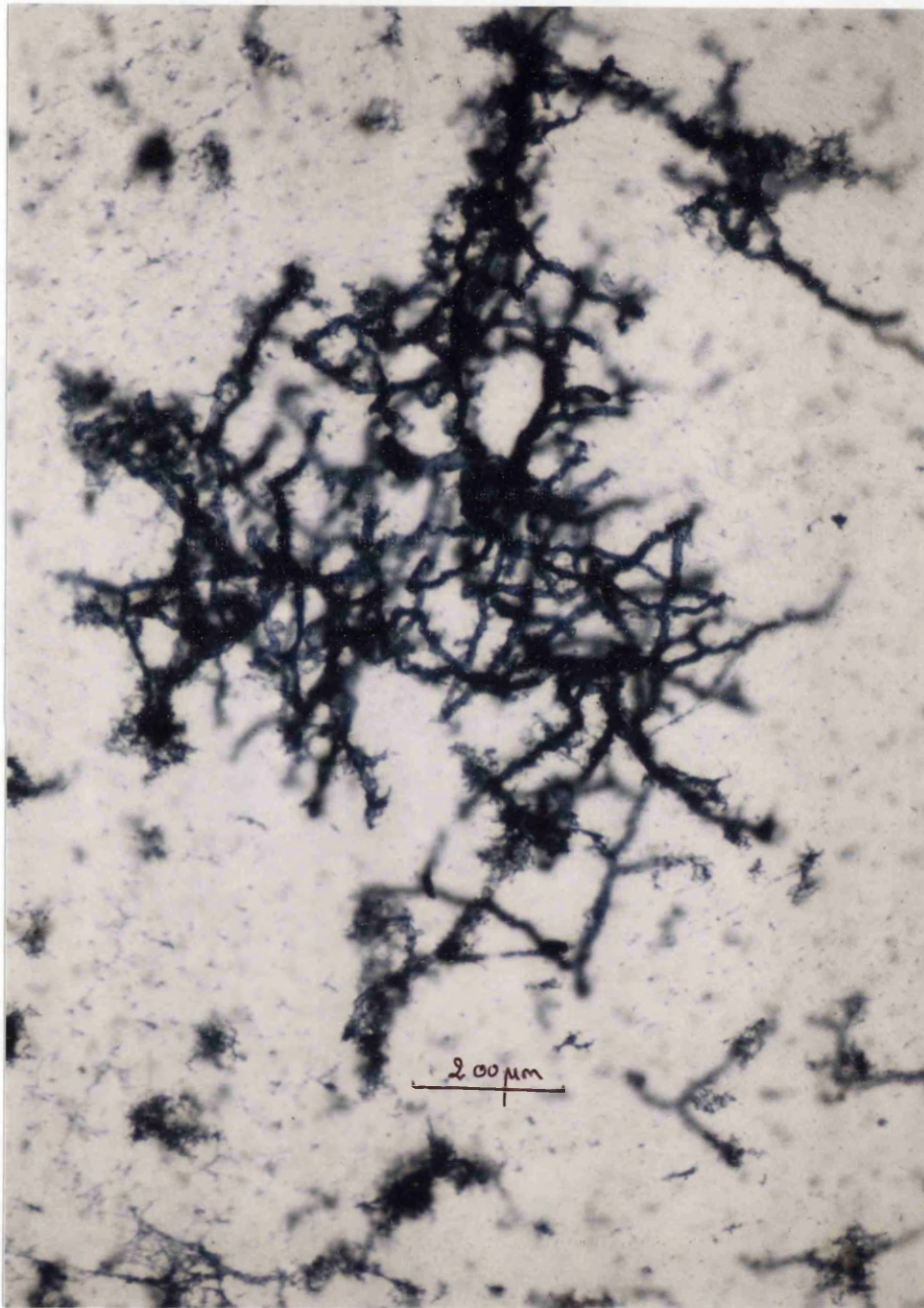


Figure 3.7(b)      Disrupted Rhizopus nigricans cells at  
10 MPa, 2 passes.  
x 100 magnification



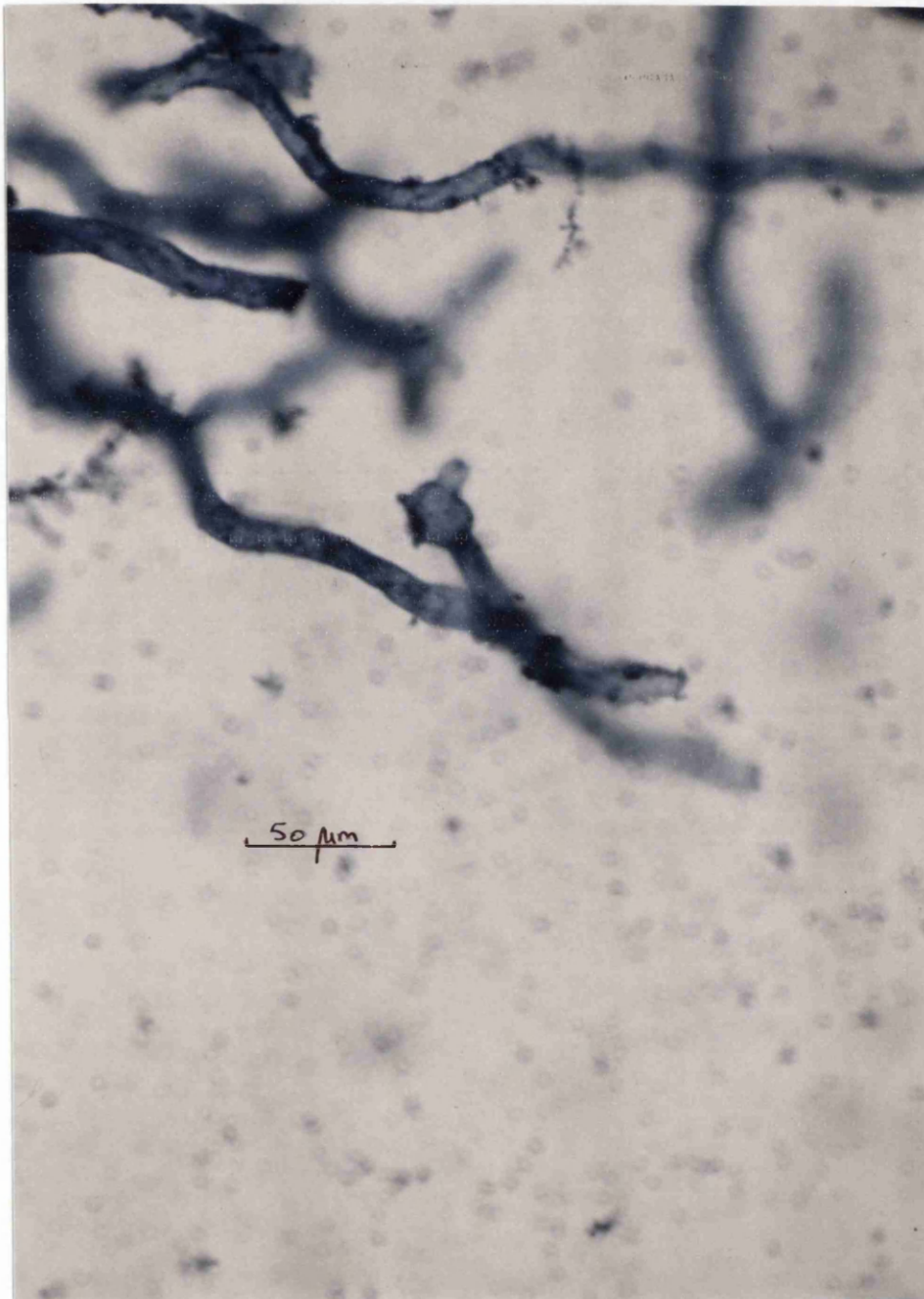


Figure 3.7(b)      Disrupted Rhizopus nigricans cells at  
10 MPa, 2 passes.  
x 400 magnification

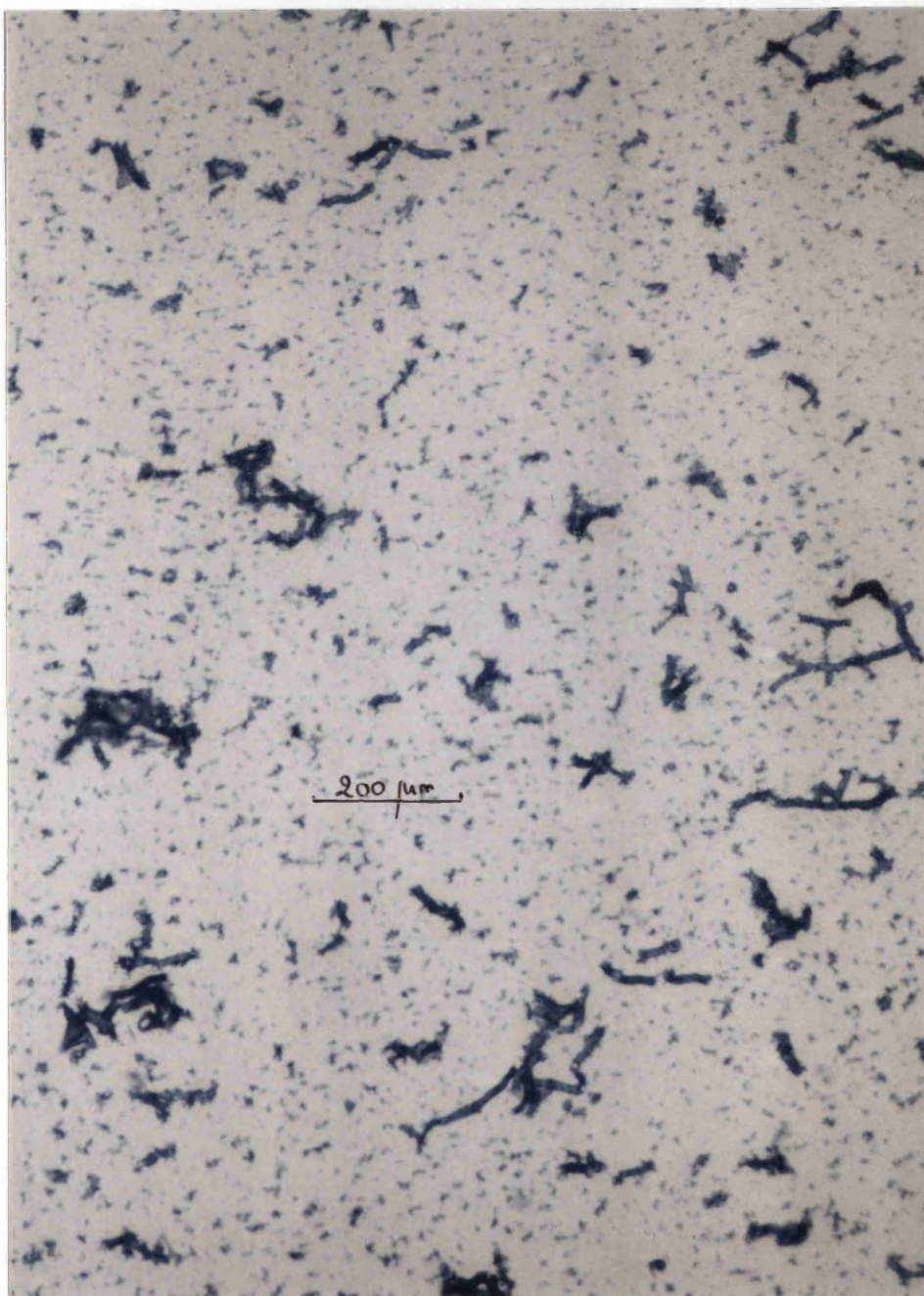


Figure 3.7(c)      Disrupted Rhizopus nigricans cells at  
50 MPa, 1 pass.  
x 100 magnification

#### 3.4.2 Cell related conditions

The major effect of cell concentration was not on disruption kinetics observed but on structural characteristics of the suspension. Above 20–22 g/L (cell dry weight), cells formed closely intertwined structures which easily settled into cellular mats blocking the homogeniser. For pelleted cells it was possible to disrupt the cells at up to a maximum of 30 g/L (cell dry weight) prior to blockage. Pellets form homogeneous suspensions similar to those of unicellular microorganisms. Little interaction exists between these cells, which may avoid blockage until relatively high concentrations are reached. The morphology and the structural characteristics of Rhizopus nigricans were affected by growth conditions in the fermenter and by harvesting parameters. Further study of these effects was beyond the scope of this study, but may be required to further increase the understanding of the behaviour of filamentous microorganisms in downstream processes.

#### 3.4.3 Disruption kinetics

The study of homogenisation of Rhizopus nigricans showed that the kinetics of disruption of this filamentous fungus differ significantly from those of unicellular microorganism as examined by previous researchers (Hetherington et al. 1971; gray et al. 1973) in that the soluble protein release was a weak function of pressure. Other features of the kinetics which were shared with such unicellular microorganisms as bakers' yeast still showed characteristics specific to filamentous cells. Cell concentration was one such feature. It did not affect the disruption kinetics. However, homogeniser blockage occurred at relatively low concentrations. With bakers' yeast, concentrations as high as 224 g/L (cell dry weight) have been reported (Brookman 1974) without equipment blockage.

One aspect of cell disruption largely neglected in the open literature is the effect of mechanical parameters, namely valve assembly configuration, on the disruption of both unicellular and filamentous microorganisms (Section 1.2.4.1). In this study attempts were made to redress the balance by examining the consequence for disruption of both types of cells of changes in homogeniser valve unit geometry. Thus, the objective was to better understand the rupture mechanism and the performance of homogenisers for the purpose of cell disruption. The results obtained are reported in the following chapter.

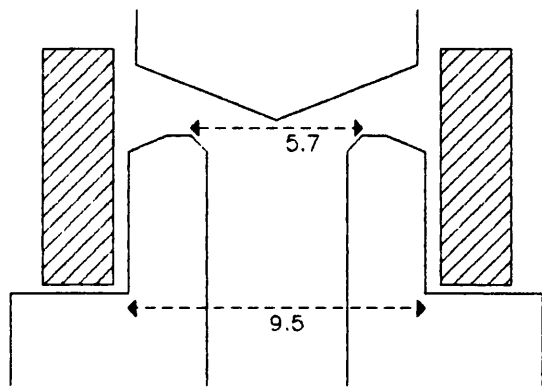
#### 4. SIGNIFICANCE OF MECHANICAL PARAMETERS IN CELL DISRUPTION

The part of the high pressure homogeniser equipment involved in cell disruption is the valve unit assembly (Section 1.1.2.2). An essential feature in studying the effect of equipment configuration on cell rupture was therefore the precise characterisation of the geometry of the valve unit.

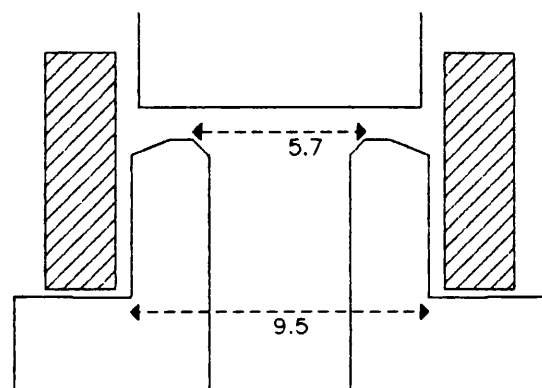
##### 4.1 Valve unit characterisation

The valve unit was housed in the homogeniser block assembly and comprised a valve seat, a valve rod and an impact ring. As explained in Section 1.1.2.2, on the power stroke of the piston, the suspension was forced between the valve seat and the valve rod and impinged on the impact ring on exit. The pressure was adjusted by means of a spring loaded handwheel set against the valve rod.

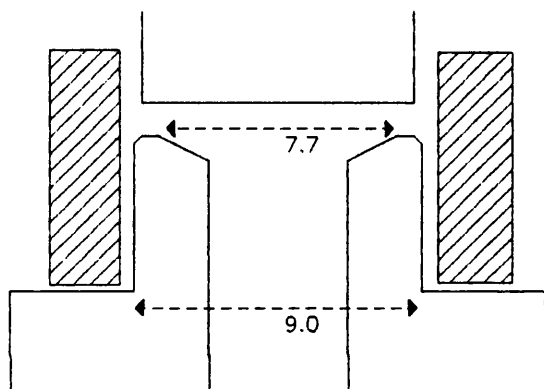
In the experiments carried out in this study, a range of valve geometries were examined (Section 2.8.2, Table 2.1). This included three types of knife-edge units designated as CRF, CD and KE respectively (Figure 4.1(b-d)) and a flat valve unit (FV) (Figure 4.1 (e)). All these valve seats were used with a flat valve rod. Further experiments were carried out with the valve seat of the CRF unit but the valve rod was changed to a coned rod (CR) (Figure 4.1(a)). The CR unit was widely used in the USA, whilst the CRF unit was commonly used in the UK. These two valve seats have been superseded by the CD unit (Cell Disruption) (Section 1.1.3.1).



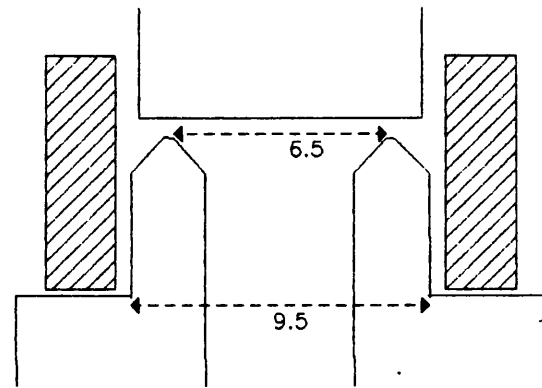
(a) CR, Cell Rupture  
(coned valve Rod)



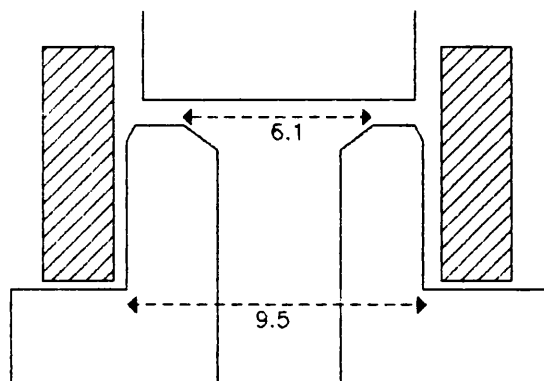
(b) CRF, Cell Rupture  
(flat valve rod)



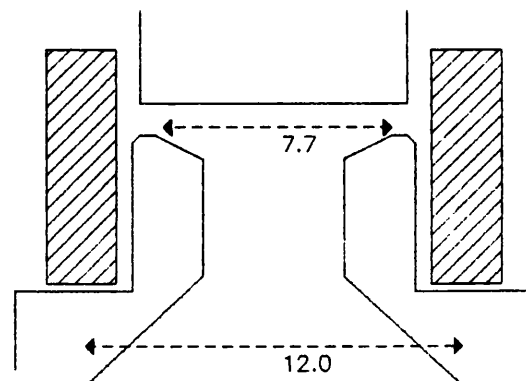
(c) CD, Cell Disruption



(d) KE, Knife-edge



(e) FV, Flat Valve



(f) CD, coned entry

All dimensions in mm.

**Figure 4.1** Schematic diagram of valve units used.

Further experiments were undertaken where the impact distance was varied using a series of impact rings of varying bores together with the valve geometry CD. Table 4.1 describes the impact distances and respective bore sizes employed.

#### 4.2 Effect of valve unit geometry on disruption of *R.nigricans*

Initially shake flask grown cultures of *R.nigricans* were disrupted at 20 MPa using the CD and the KE valve units (Figure 4.2). No differences could be detected between the levels of soluble protein released when these two configurations were used. Given the weak dependence of disruption on pressure for this microorganism (Section 3.4.3), it was thought that a lower pressure of 10 MPa should be used to better demonstrate the effect of different valve geometries. Figure 4.3 illustrates the results of soluble protein release at 10 MPa using CD, KE and FV valves. Similar results as before were obtained for the former two valve units. However, the FV unit did not appear to perform as well. The fall in the soluble protein content after several passes may be attributed to the dilution effect caused by the addition of buffer after each pass (thus avoiding damage to the homogeniser when the suspension volume was limited (Section 2.8.3)), specially as the initial cell concentration of the suspension was already low (8 g/L dry weight). In order to corroborate the above findings, fermenter-grown cells which were less fragile than shake flask grown cultures (Section 3.4.1) were used. Results are shown in Figure 4.4. In all cases a standard impact ring was used.

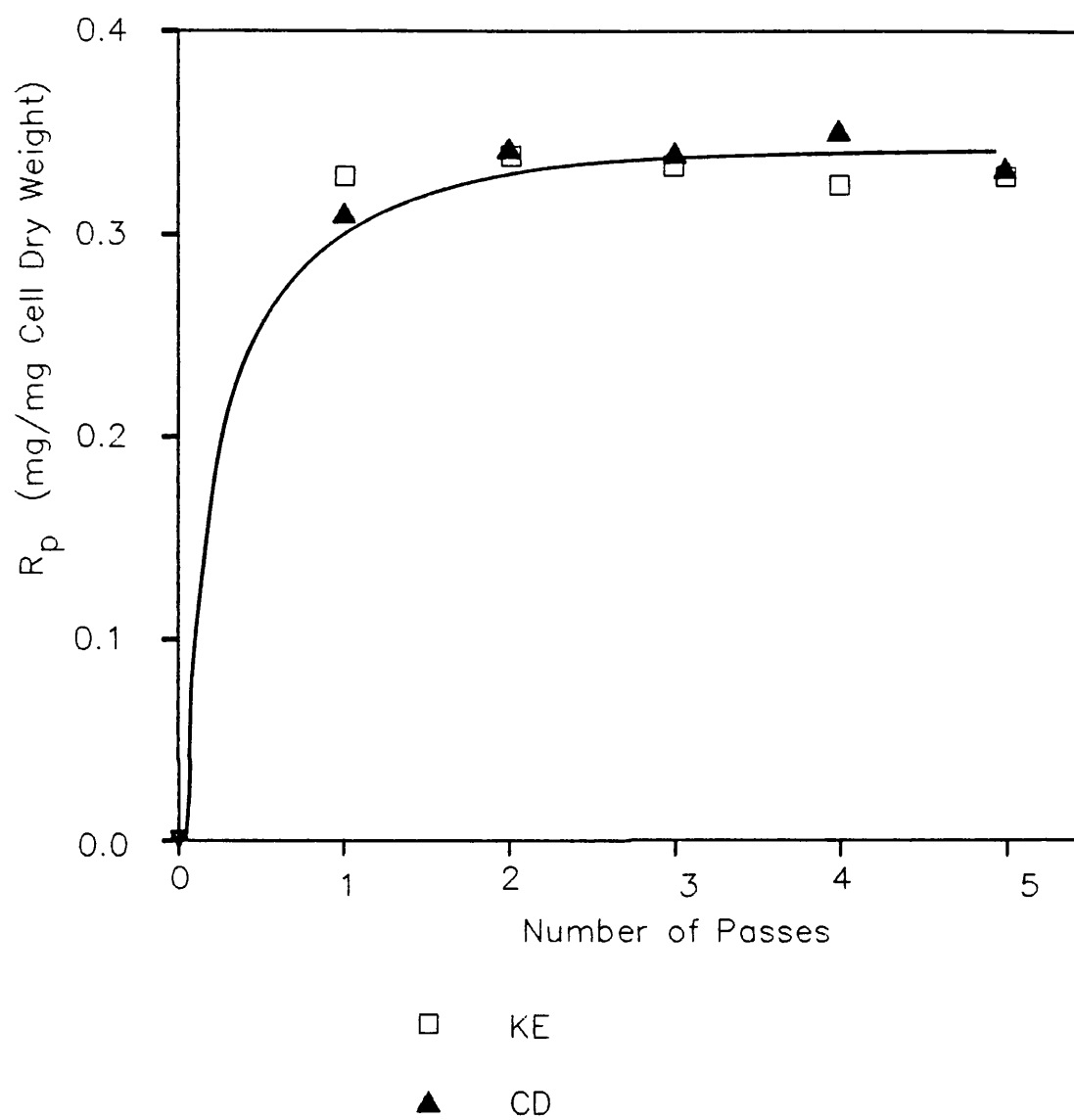
It should be noted that at this stage of experimentation, other valve units illustrated in Figure 4.1 were not tested as they were not yet made available by the manufacturers.

**Table 4.1 Impact ring dimensions and corresponding  
impact distance for a CD valve**

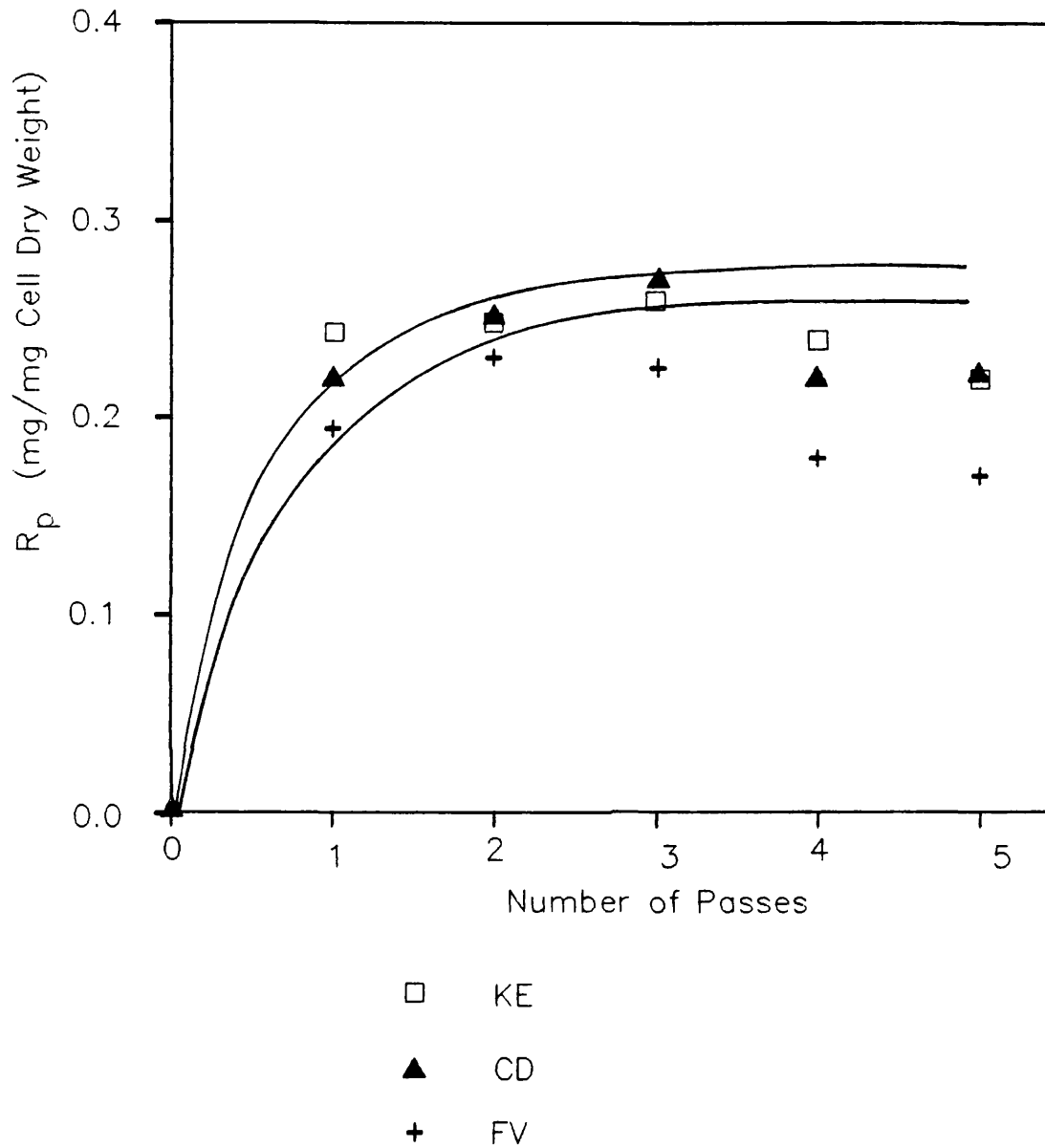
<b><u>impact ring bore</u></b>	<b><u>impact distance<sup>a</sup></u></b>
<b>(mm)</b>	<b>(mm)</b>
10.16	0.33
10.56	0.53
11.00	0.75
11.50	1.00
13.50	2.00
no impact ring (18.90)	4.70

<sup>a</sup> Impact distance was measured from the exit point of the valve rod to the impact ring surface (Figure 6.1)

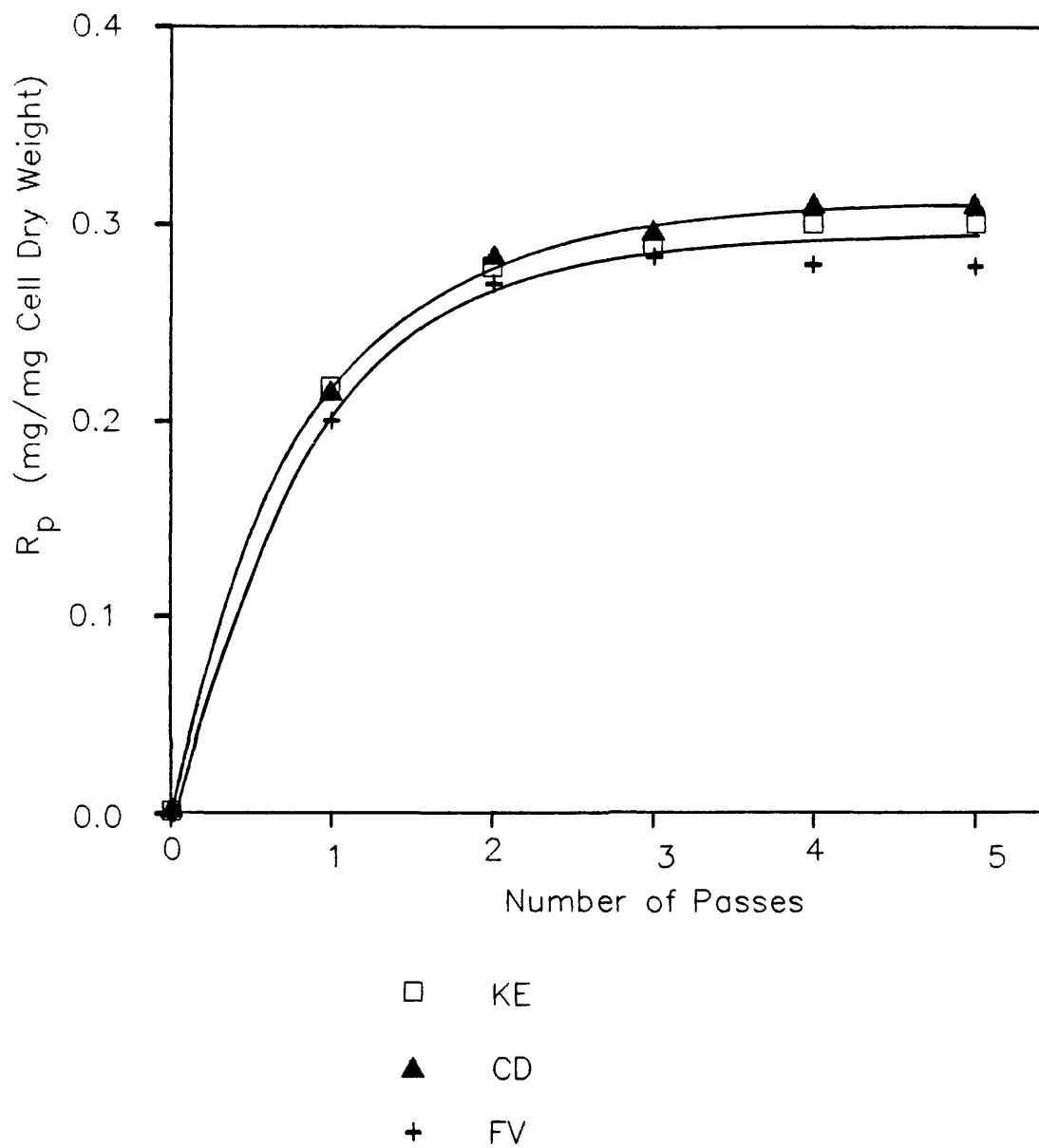




**Figure 4.2** Effect of valve geometry on disruption of shake flask-grown *Rhizopus nigricans* at 20 MPa.



**Figure 4.3** Effect of valve geometry on disruption of shake flask-grown *Rhizopus nigricans* at 10 MPa.



**Figure 4.4** Effect of valve geometry on disruption of fermenter-grown Rhizopus nigricans at 10 MPa.

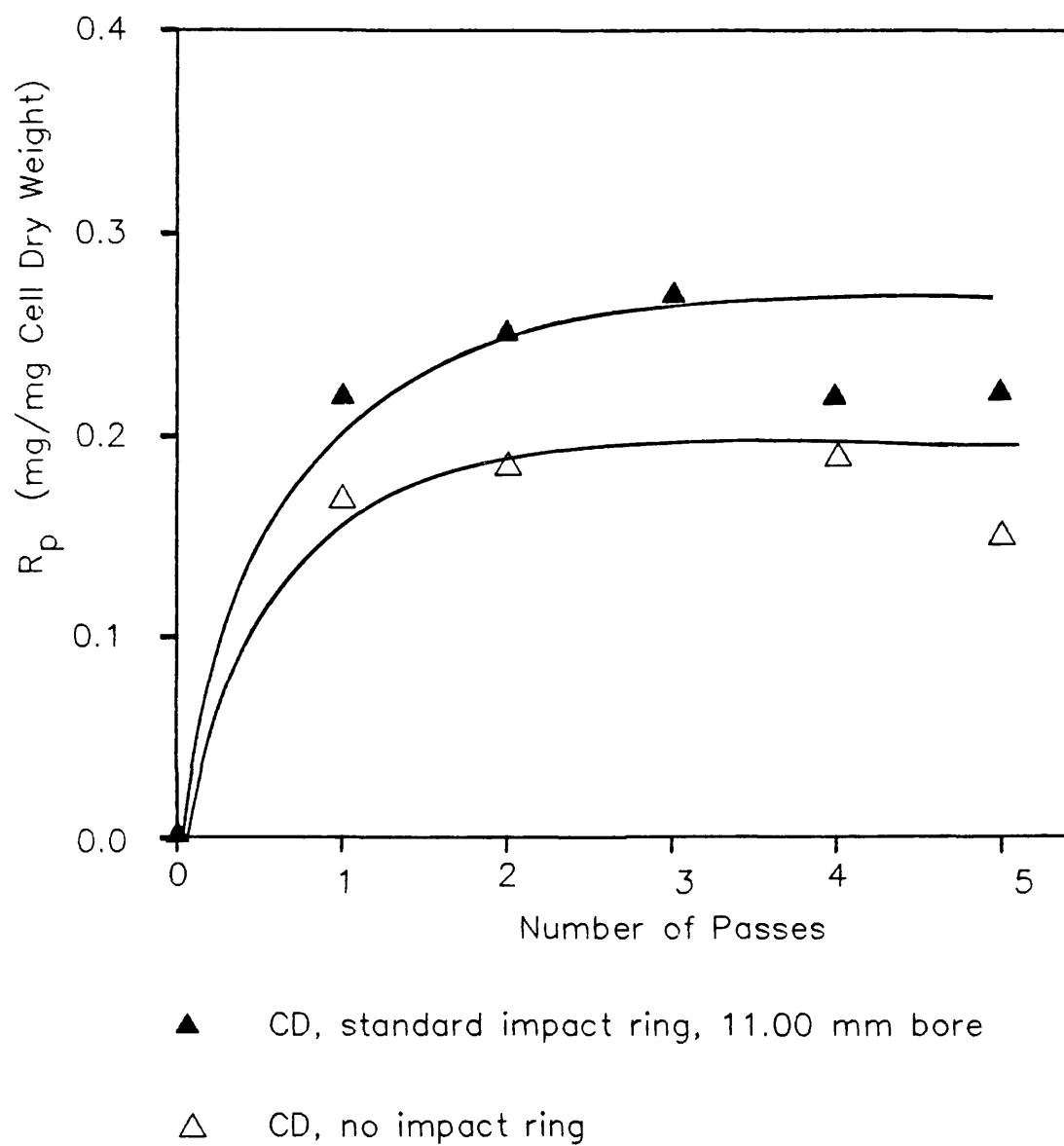
### 4.3 Effect of impact distance on disruption of *R.nigricans*

On exit from the homogeniser, the suspension impinged on an impact ring which also served to protect the wall of the block from wear. To assess the effect of impingement on the disruption of *R.nigricans*, following a similar rationale as that in the above experiments, cells from both shake flask and fermenter sources were disrupted at 10 MPa using a CD valve unit with and without an impact ring (Figures 4.5 and 4.6). Similar results were observed for both types of cultures. The yields obtained when the impact ring was present was higher than when it was removed. The possible reason for the fall in the protein content of shake flask cultures after several passes is given in Section 4.2 above.

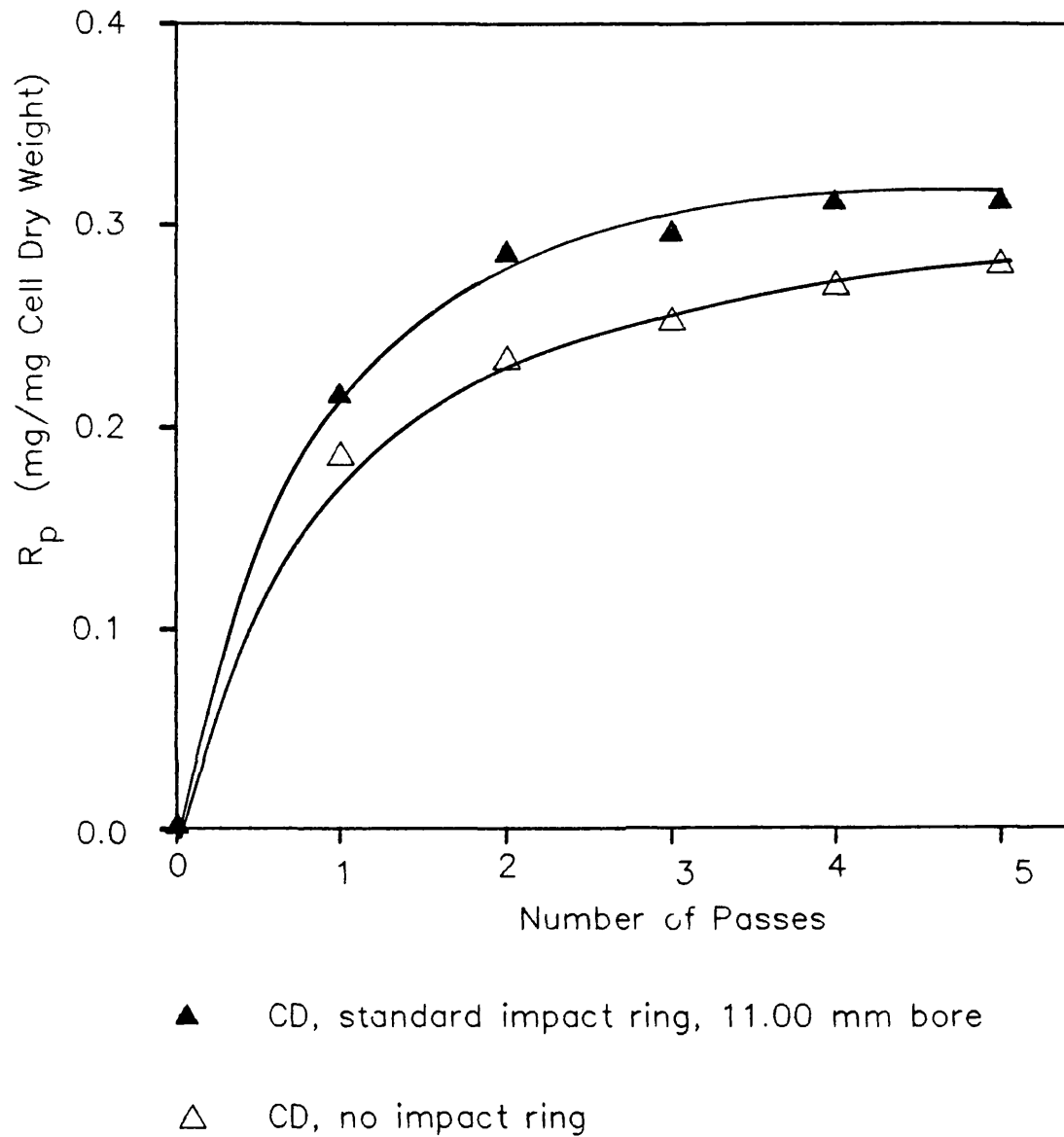
### 4.4 Discussion

The results of disruption with different valve unit configurations indicated that impact distance was a significant factor in the rupture of the filamentous *R. nigricans* cells. Less soluble protein was released when the impact ring was removed i.e., increasing the impact distance from 0.75 mm to 4.70 mm, whilst keeping the valve geometry constant. Changing of valve geometry did not appear to have affected the disruption significantly. The FV unit exhibited poorer disruption characteristics than either KE or CD valves; although the effect was marginal.

In view of the special disruption kinetics displayed by *R.nigricans*, it was difficult to infer from the findings in the above sections what effect mechanical parameters such as valve unit configuration might have on unicellular microorganisms. It was therefore decided to examine the corresponding disruption characteristics of bakers' yeast since it was a well defined, reproducible unicellular microorganism.



**Figure 4.5** Effect of impact distance on disruption of shake flask-grown Rhizopus nigricans at 10 MPa.



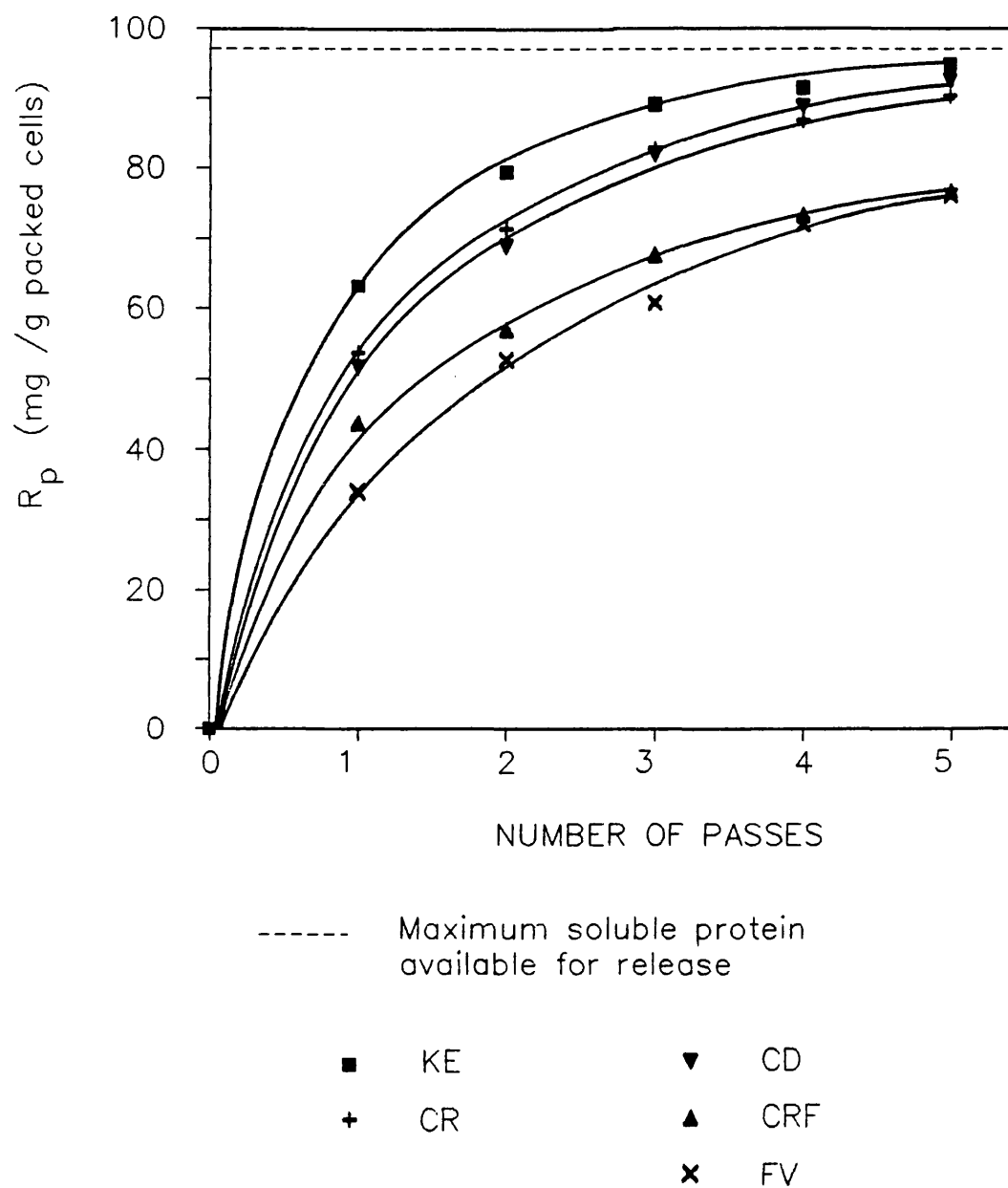
**Figure 4.6** Effect of impact distance on disruption of fermenter-grown Rhizopus nigricans at 10 MPa.

#### 4.5 Effect of valve unit geometry on disruption of bakers' yeast

Bakers' yeast cells were disrupted at 46 MPa for up to five passes using five valve unit configurations described in Figure 4.1(a-e). All units were fitted with a standard size impact ring. The results are illustrated in Figure 4.7 and summarised in Table 4.2. Maximum performance was observed with the knife-edge (KE) configuration whilst the valve geometries consisting of the flat valve seat and flat valve rod (FV and CRF) gave similar lowest yields. Changing the valve rod to a cone shape (CR) resulted in considerably higher protein release, comparable to that obtained for the CD unit which had a reduced seat surface. This last finding did not support the claim by the manufacturers that CD unit performed as much as 50 % better than CR unit after one pass at a similar pressure (APV-Gaulin 1985). The results, however, confirmed the general findings of the pioneering work carried out by Hetherington *et al.* (1971) in which knife-edge geometry was reported to perform better than flat valve unit.

##### 4.5.1 Effect of geometry of valve seat central orifice

In order to assess whether the geometry of the central orifice of the valve seat influenced cell disruption, a unit was used consisting of identical knife-edge dimensions to those of the ceramic CD unit except that the entry orifice was widened from 5 mm diameter to 12 mm, into a conical shape (Figure 4.1(f)). The amount of soluble protein released at 46 MPa for up to five passes did not differ from those obtained under the same conditions with the CD unit (Figure 4.8). Clearly the geometry of the central orifice did not contribute to the disruption process.



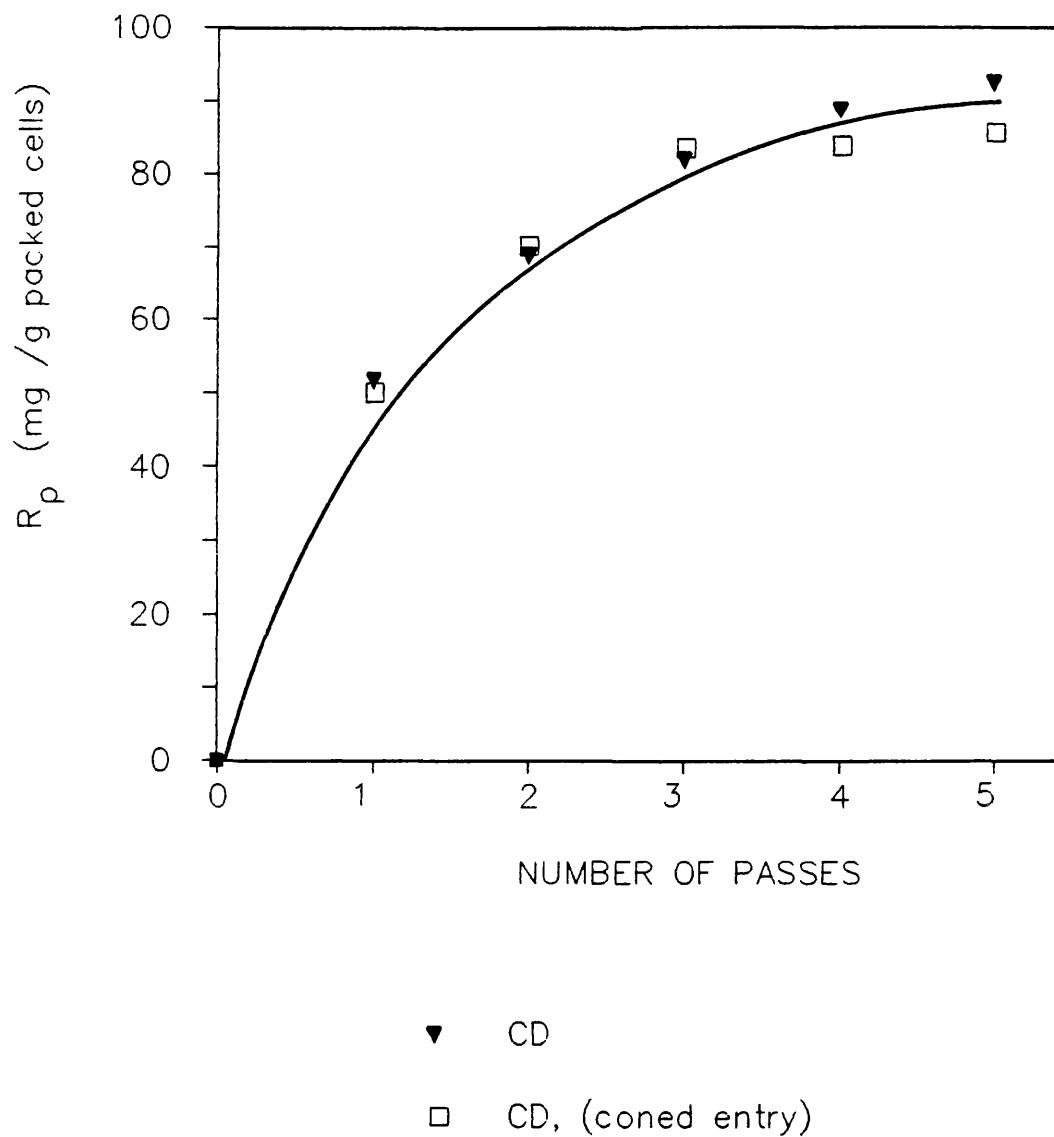
**Figure 4.7** Extent of disruption of bakers' yeast using 5 valve units at 46 MPa.



**Table 4.2 Disruption yields of five valve units**  
**at 46 MPa**

<u>valve unit</u>	<u>pass 1<sup>a</sup></u>	<u>pass 5<sup>a</sup></u>
KE	66	99
CD	54	96
CR	56	94
CRF	46	80
FV	35	79

<sup>a</sup> Figures given as % total soluble protein released.



**Figure 4.8** Effect of geometry of valve seat central orifice on disruption of bakers' yeast at 46 MPa.

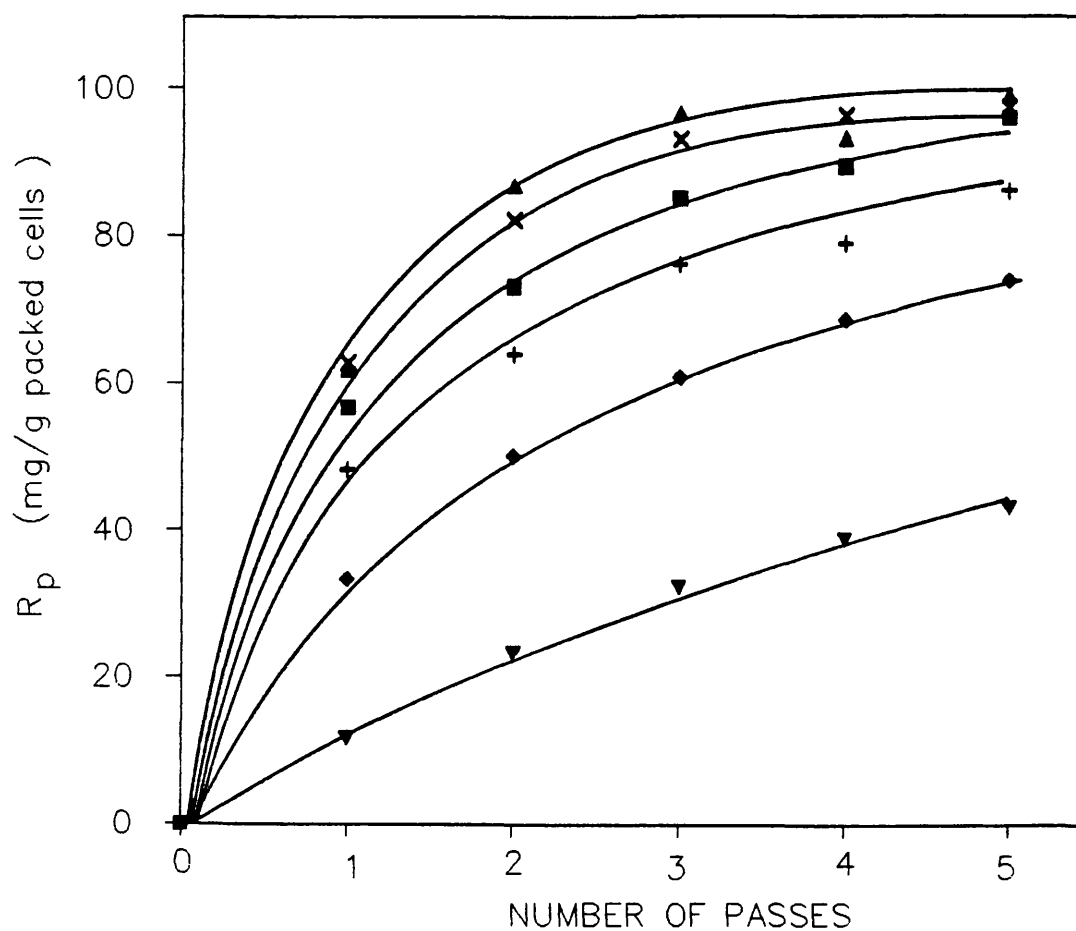
#### 4.6 Effect of impact distance on disruption of bakers' yeast

To assess the effect of impingement on the disruption of bakers' yeast, the CD unit was tested with impact rings of varying bore sizes (10.16 mm to 13.5 mm corresponding to impact distances 0.33 mm to 2.00 mm respectively (Table 4.1). The standard bore size was 11.0 mm. Figure 4.9 illustrates the variation of soluble protein release with the impact ring bore size. The smaller the bore, the more efficient the disruption became. The removal of the impact ring (corresponding to 4.7 mm impact distance) resulted in the lowest release of soluble protein from cells. In Figure 4.10 the effect of impact distance on the extent of disruption is shown. Maximum disruption was obtained over a range of impact distances corresponding to 10.16 mm to 11 mm bore sizes. The extent of disruption dropped markedly as the impact distance was increased.

The importance of the impact ring in the disruption process was further demonstrated by comparing the extent of disruption of cells using an FV unit (i.e. the least effective of geometries) with a standard impact ring, and a CD unit (a highly effective geometry) with no impact ring (Figure 4.11). The absence of an impact ring for the CD unit resulted in over 50% less disruption after the first pass even though the geometry of the valve unit was shown to be superior (Figure 4.7).

#### 4.7 Effect of scoring of the valve seat

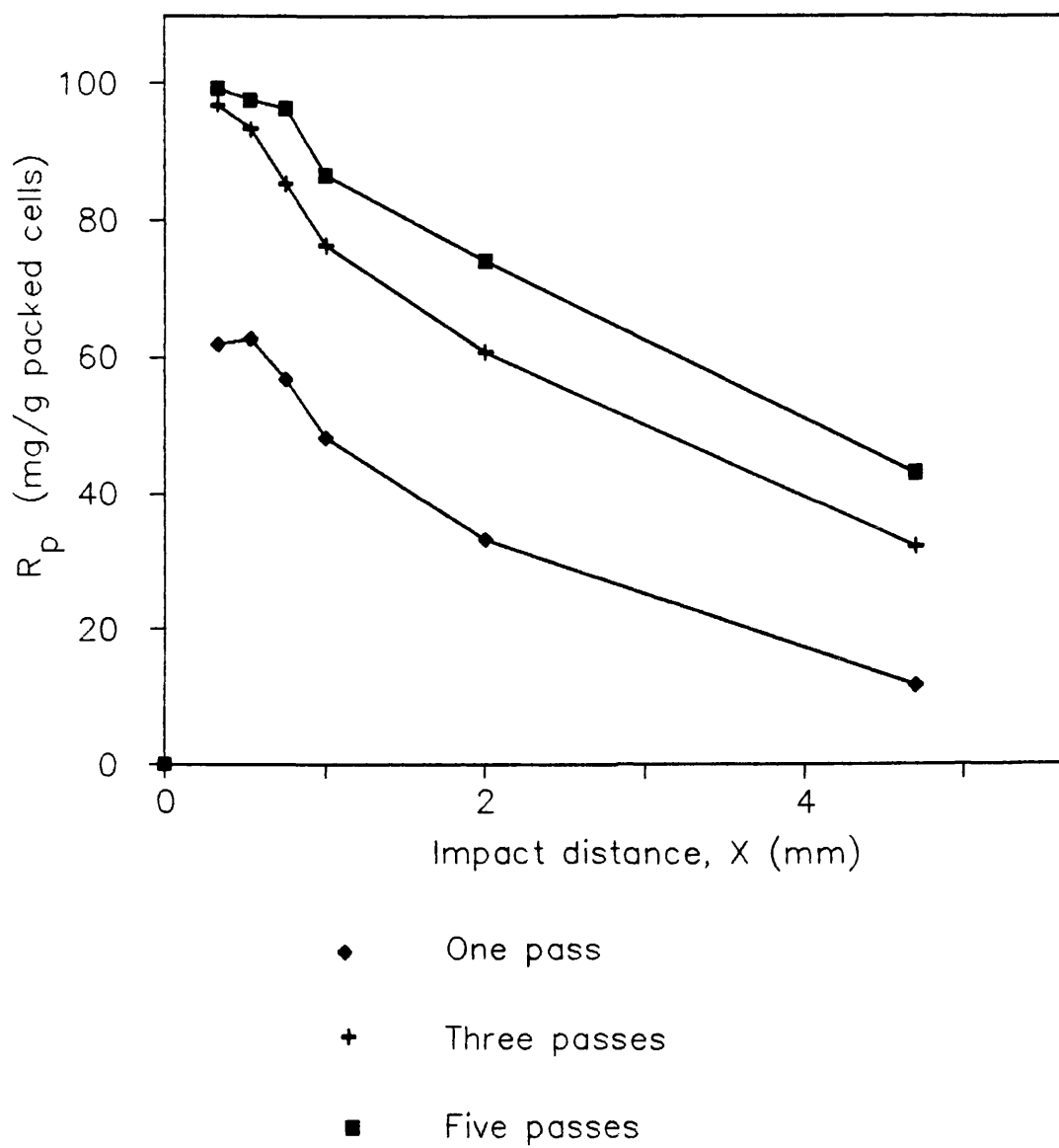
The ceramic material of the CD valve unit, even though resistant to every day wear, was brittle and therefore prone to scoring. In the experiments carried out, new sets of valve units were employed for all geometries, and regular inspections ensured that defective components were not used. Nevertheless, since an already flawed CD valve seat was made available by the manufacturers, it was of interest to check the performance of this particular unit.



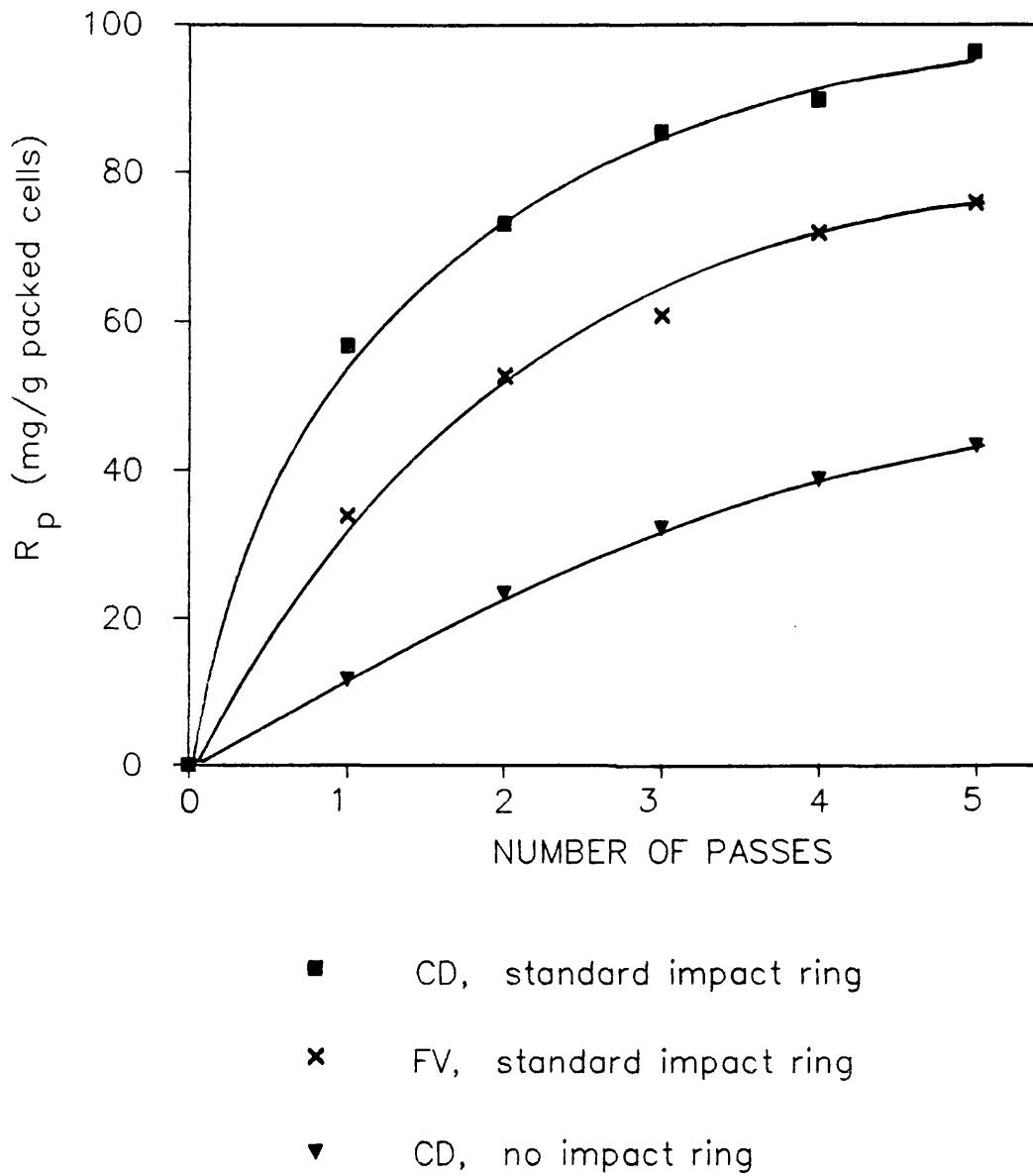
Impact ring bore diameter and impact distances are:

- ▲ 10.16 mm; 0.33 mm
- × 10.56 mm; 0.53 mm
- 11.00 mm; 0.75 mm (standard)
- + 11.50 mm; 1.00 mm
- ◆ 13.50 mm; 2.00 mm
- ▼ no impact ring (i.e. 18.90 mm); 4.70 mm

**Figure 4.9** Extent of disruption of bakers' yeast using a CD unit with different impact rings at 46 MPa.



**Figure 4.10** Effect of impact distance on disruption of bakers' yeast at different passes, (46 MPa).



**Figure 4.11** Comparison between the effect of impact ring and valve geometry for bakers' yeast, (46 MPa).

Figures 4.12(a) and 4.12(b) show the photographs of the perfect and imperfect valve seats respectively. The place where the seat was chipped is shown with an arrow. It indicates that the defect was on the inner edge of the seat. The amount of soluble protein released for these two valves were compared (results not shown). No differences were observed indicating that the entry zone geometry did not affect the disruption of the cells.

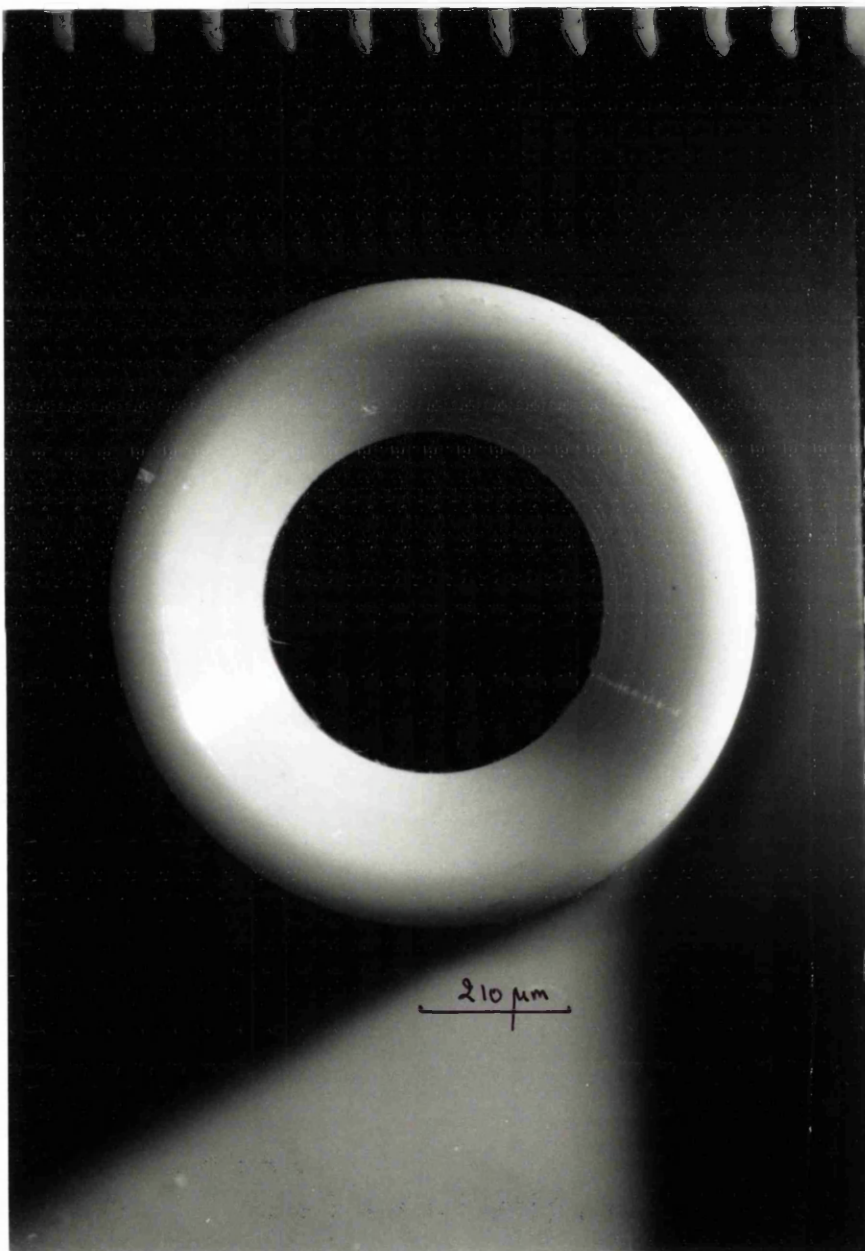


Figure 4.12(a) CD ceramic valve seat (perfect).



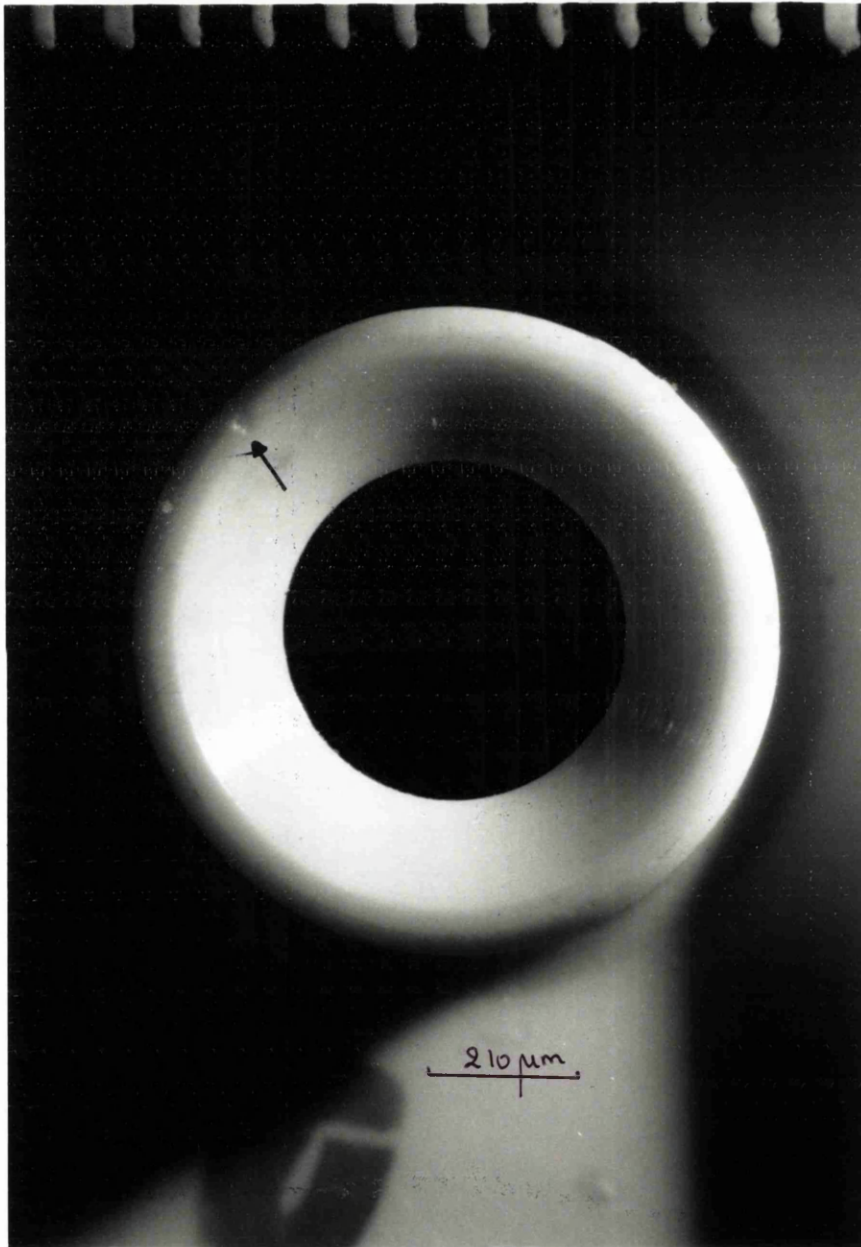


Figure 4.12(b) CD ceramic valve seat (flawed).

## 5. PARTICLE AND CELL DEBRIS FORMATION

The importance of characterisation of cell particles and cell debris was outlined in Section 1.4.1. Homogenisation is the downstream step in which cell fragments are formed and intracellular contents, and on occasions particles (e.g. inclusion bodies) are released. It is therefore evident that data on the resultant cell particles and debris would provide invaluable information relevant to the subsequent downstream processing stages.

### 5.1 Microsomal fractions from *R.nigricans*

The interest in the microsomal fractions of *R.nigricans* stemmed from the fact that the enzyme complex progesterone 11 $\alpha$ -hydroxylase is believed to be located on the endoplasmic reticular membrane which, upon disruption, forms microsomes (Section 1.4.3). This enzyme complex is capable of hydroxylating progesterone and thus producing a precursor of cortisone used in the pharmaceutical industry. In this part of the study an attempt was made to provide some preliminary information on the effect of disruption on microsomal formation.

#### 5.1.1 Microsomal preparation

The well established laboratory scale procedure for microsomal preparation reported in the literature (e.g. Talboys 1983) is the differential centrifugation of the cell homogenate. The disrupted cells are spun for two minutes at 800 g; the resultant supernatant is then respun at 10000 g for 20 minutes to separate the post-mitochondrial fraction. This is followed by the ultracentrifugation

of the supernatant at 105000 g for one hour. The presence of cytochrome P450, which is believed to be a constituent of the enzyme complex, was detected by some workers (Breskvar and Hudnik-Plevnik 1981) in the 105000 g pellet which was thus considered as the portion containing the enzyme bound microsomal fraction.

This protocol was repeated in the present study but no 11- $\alpha$  progesterone activity was detected in the microsomal pellet. This was attributed to shear sensitivity of the enzyme complex (Talboys 1983). It was thought likely that one of the components of the enzyme complex, NADPH-cytochrome P450 reductase was solubilised during the microsomal separation process. This, according to Gosh and Samanta (1981), is the result of the dissociation of NADPH reductase from the cytochrome P-450 during ultracentrifugation. It was therefore decided to follow an alternative method to minimise the loss of enzyme activity. This was based on reducing the number of enzyme damaging centrifugal steps and using gel filtration. Thus cells were centrifuged at 2000 g for ten minutes and spun at 50000 g for 45 minutes. The supernatant was then passed through a gel filtration column. This method was based on work by Tangen et al. (1973) who developed a rapid technique for isolation of liver microsomes. Gel filtration of the post-mitochondrial supernatant had resulted in the elution of the microsomal fraction in the void volume, which appeared in the first absorbance peak. The presence of microsomal marker enzymes and cytochrome P450 was detected in this fraction; furthermore the spectra of P450 from gel filtered samples and control samples obtained by traditional techniques were similar. The second peak contained the solutes of the supernatant. The authors further justified the validity of their method on the basis of the size of the microsomes reported by Claude (1969), which range from 0.06  $\mu\text{m}$  to 0.2  $\mu\text{m}$  in diameter, thus allowing them to readily pass through the spaces between the gel beads, which were estimated to vary between 9  $\mu\text{m}$  and 38  $\mu\text{m}$ . In the present work, this method was used to separate the microsomes. Figure 5.1 shows a typical elution curve obtained. However, attempts to detect the activity of the

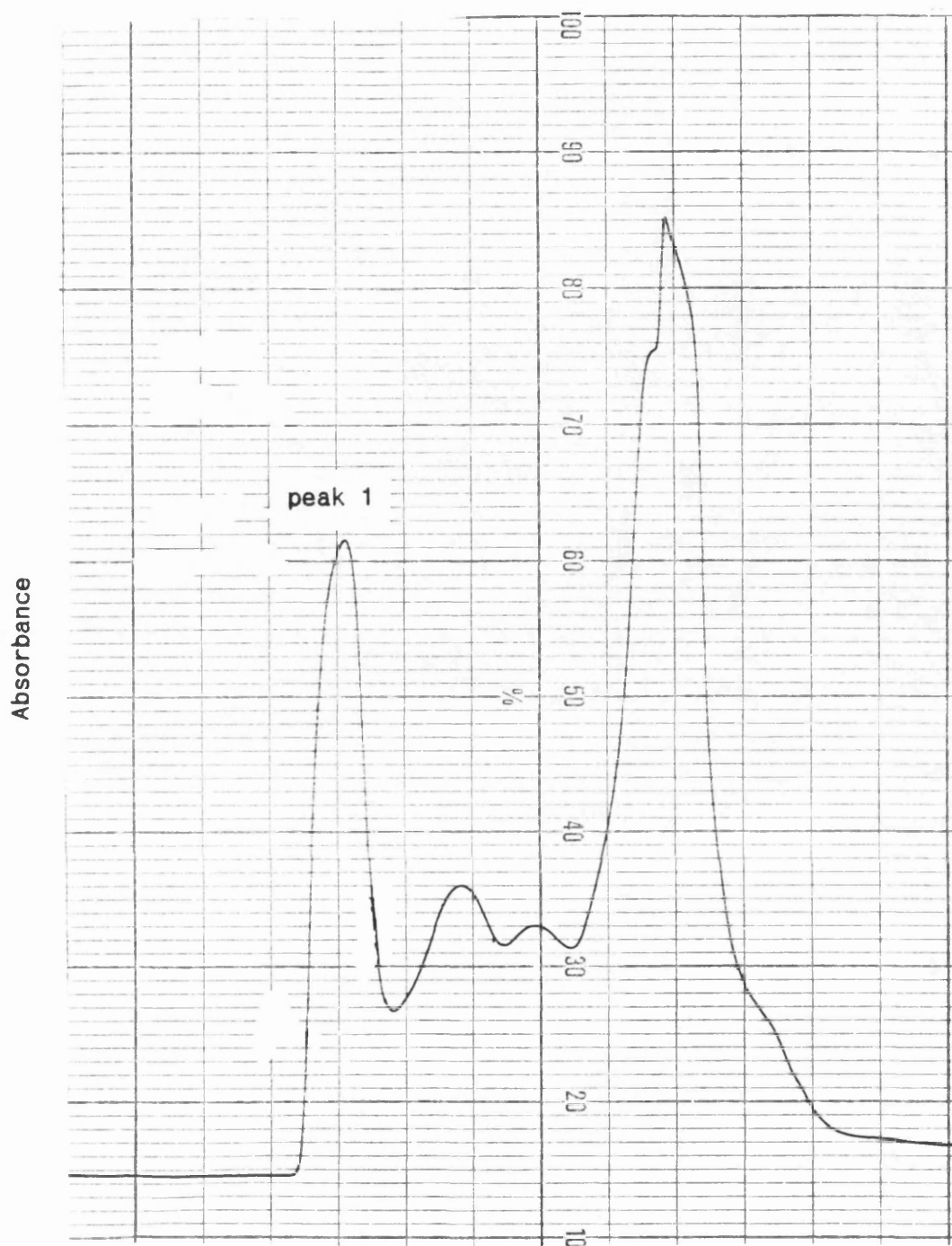


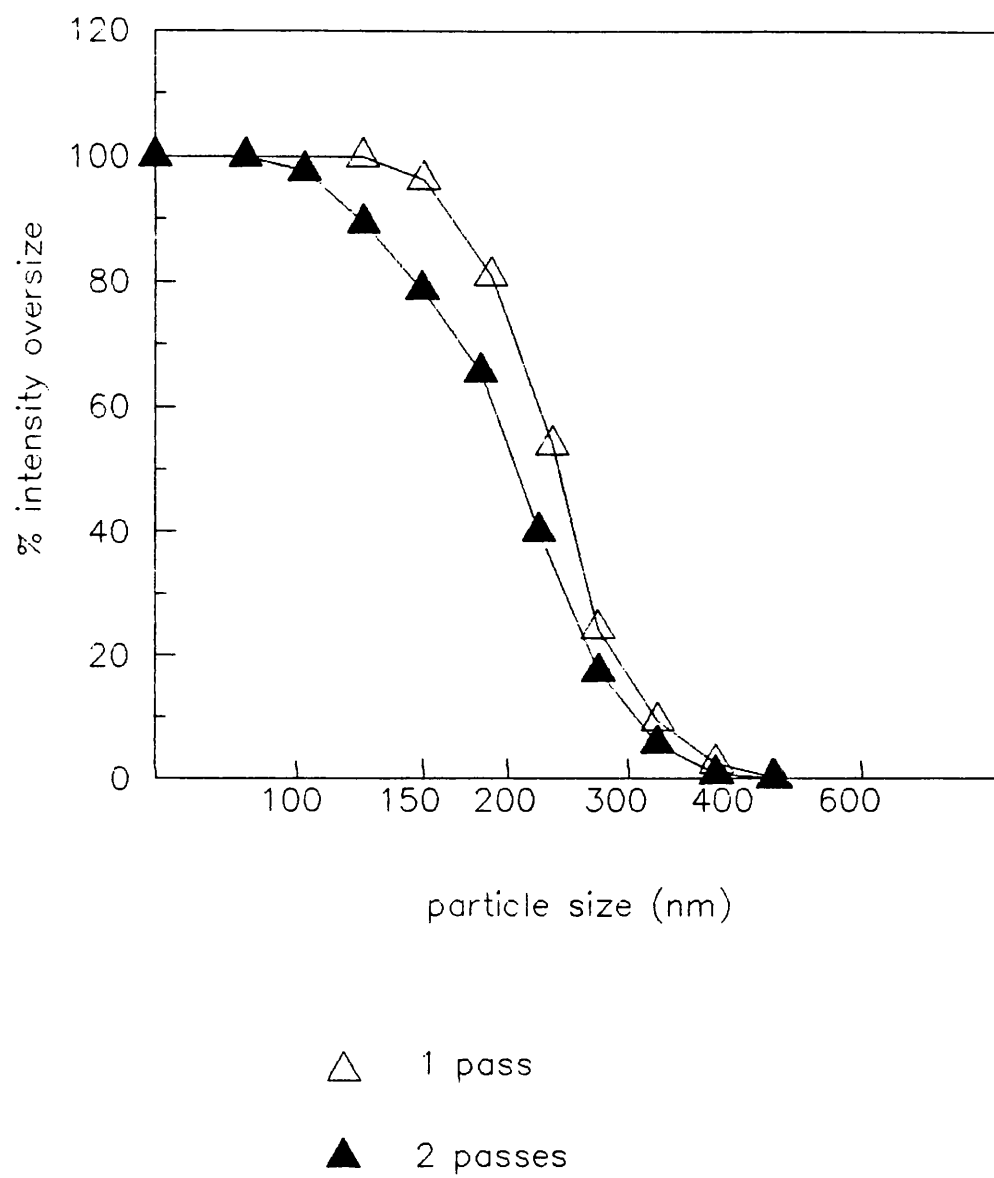
Figure 5.1 Typical elution curve from gel filtration column. Cells disrupted at 15 MPa, after 2 passes.

enzyme and also the presence of cytochrome P450 in samples before gel filtration and in the fractions obtained in the peaks were not successful. Nevertheless, it was decided to proceed with the characterisation of the microsomal fractions in order to gain insight into the effect of cell disruption on vesicle formation.

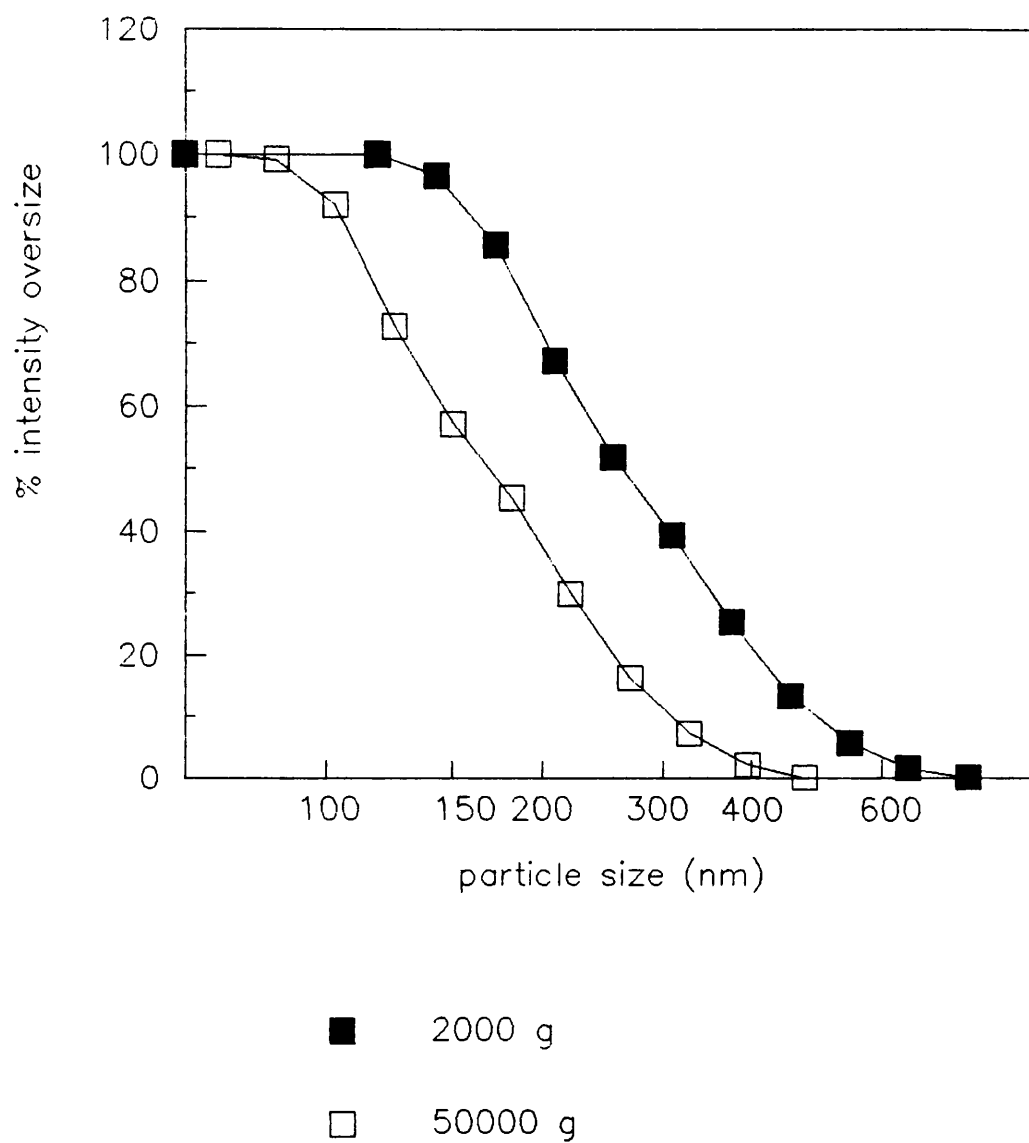
#### 5.1.2 Effect of cell disruption on microsomes

The intensity distributions of microsomal fractions from cells disrupted at 15 MPa after one, two and four passes through the homogeniser were obtained (Section 2.10.1) and results compared (the applicability of light intensity distribution to particle size measurements is discussed in Appendix B). The transition from the first pass to the second pass indicated a reduction in the size of the particles of at least 10 % (Figure 5.2). However no significant further reduction was observed from two to four passes (data not shown here). The distributions were monomodal (but not narrow) with a mean of  $0.26 \pm 0.02 \mu\text{m}$  and  $0.22 \pm 0.02 \mu\text{m}$  for one and two passes respectively. These values were within the range reported by other workers (Table 1.4). Furthermore they provided an independent means of confirming the findings that the initial passes through the homogeniser were the most important in disrupting R.nigricans cells (Chapter 3).

The intensity distributions from the intermediary centrifugation steps i.e. supernatants from 2000 g and 50000 g spins were also measured. The results showed a reduction in the size of the particles after the second spin (Figure 5.3). Evidently, the larger particles were removed but the microsomal fractions remained, together with smaller particles, in the supernatant.



**Figure 5.2** Intensity distribution of microsomes. Cells disrupted at 15 MPa after 1 and 2 passes.



**Figure 5.3** Intensity distributions of particles obtained from the intermediary centrifugation steps.  
Cells disrupted at 15 MPa, after 2 passes.

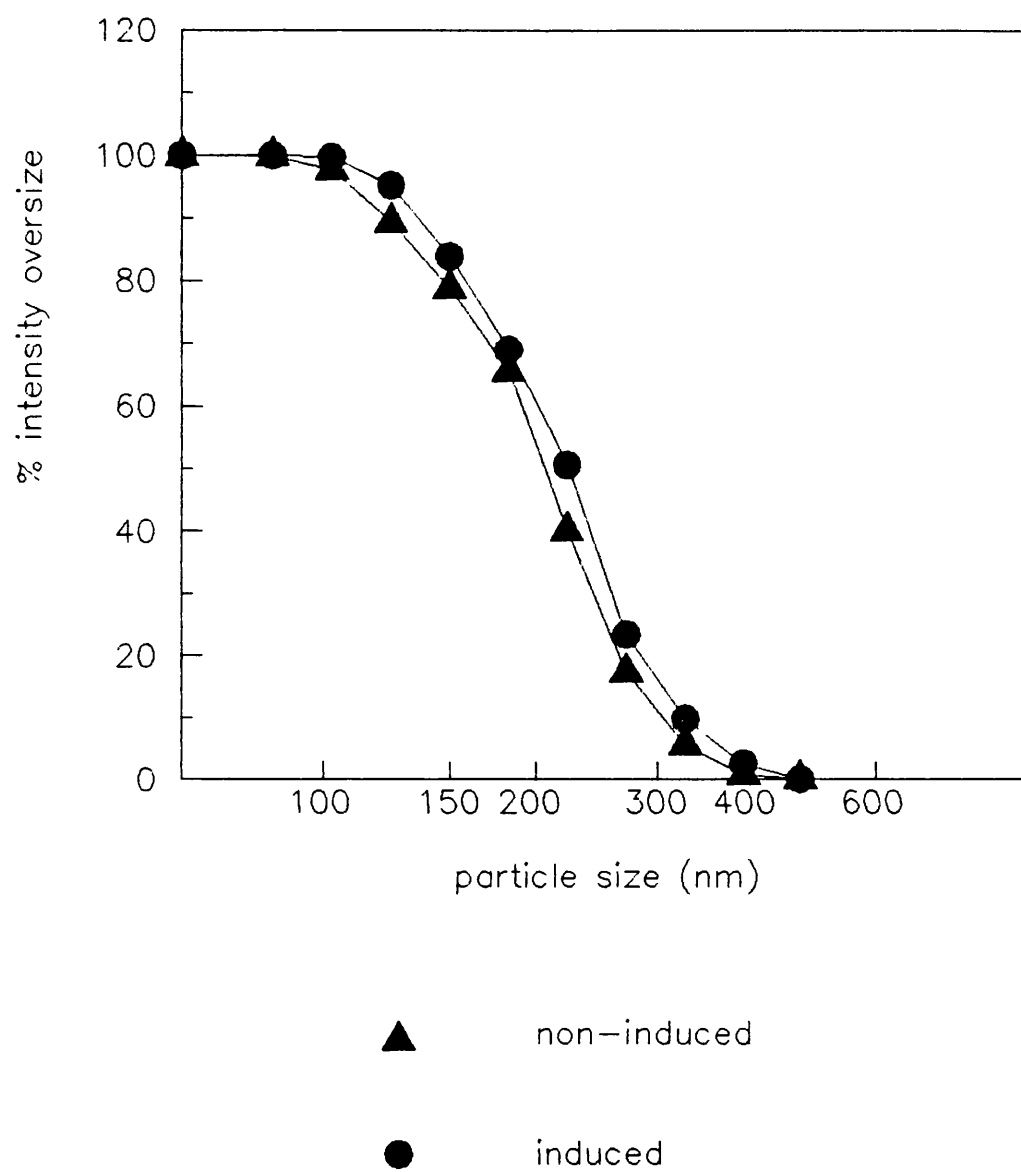
After gel filtration, the microsomal fraction appeared in the first peak and the remaining smaller particles in the second peak. In the absence of activity data it was, however, difficult to say with certainty that the content eluted in the second peak was not part of the microsomal fraction.

Further experiments were carried out to establish whether the induction of cells with progesterone would make any difference to the size of microsomes obtained. As shown in Figure 5.4, no significant changes were detected.

#### 5.1.3 'Sugar cushioning' for microsomal separation

The lack of enzyme activity observed in the above experiments were attributed to two possible factors. Firstly, the shear effect was thought to be still a significant element even though the separation stages were modified to reduce it. Secondly, the enzyme was recovered from the supernatant fraction i.e. from a very dilute state. In order to substantiate the results obtained from the gel filtration work, it was necessary to recover enzymatically-active microsomal fractions. Therefore, it was therefore decided to obtain the concentrated microsomes from the pellets of the 105000 g ultracentrifugation as outlined in Section 5.1.1. However, in order to minimise the shear effect, the bottom of the centrifuge tubes for the ultracentrifugation stage were covered with a layer of saturated sucrose and the sample carefully added to the tubes. The microsomal pellet could then gently settle on the layer of saturated solution, avoiding shear and impact. Microsomal fractions thus obtained were easily resuspended in buffer and were enzymatically active even though 70 % loss in specific activity was detected. The intensity distribution of the dissolved pellet obtained showed two peaks ( $0.18 \pm 0.02 \mu\text{m}$  and  $0.33 \pm 0.04 \mu\text{m}$ ). The first peak size was in reasonable agreement with that found in the first elution peak of the gel filtration experiment for cells homogenised after two





**Figure 5.4** Intensity distributions of microsomes obtained from induced and non-induced cells. Cells disrupted at 15 MPa, after 2 passes.

passes. However, it was not possible to attribute the enzymatic activity to only one peak.

## 5.2 Effect of homogenisation on yeast debris formation

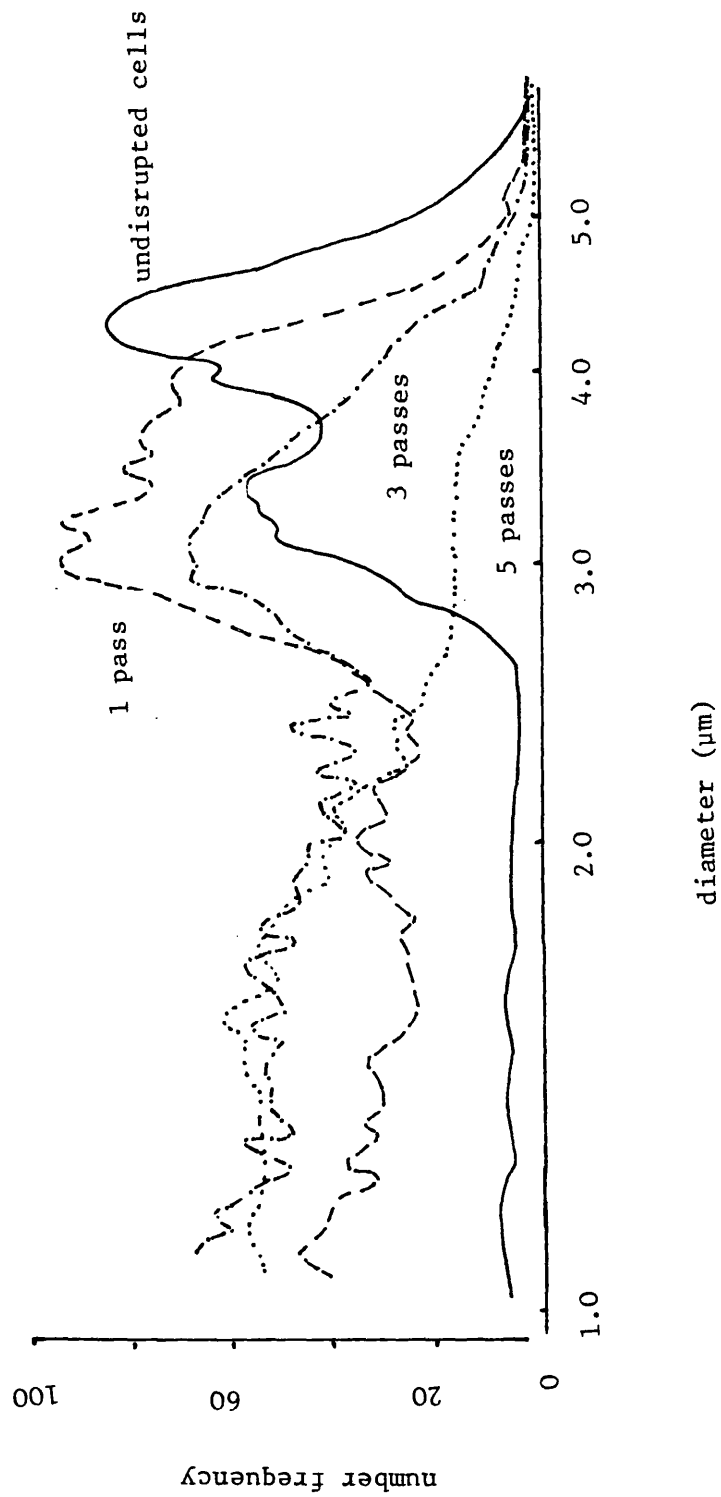
Published studies on cell disruption mainly address the issue of release of enzymes from microorganisms. However, in order to obtain a complete description of the homogenisation process it is also necessary to obtain information on the effect of homogenisation on cell debris formation (Section 1.4). In this study, in conjunction with work on the effect of valve geometry and impact distance on protein release, the effect of these parameters on yeast cell debris formation was also investigated.

### 5.2.1 Effect of multiple passes

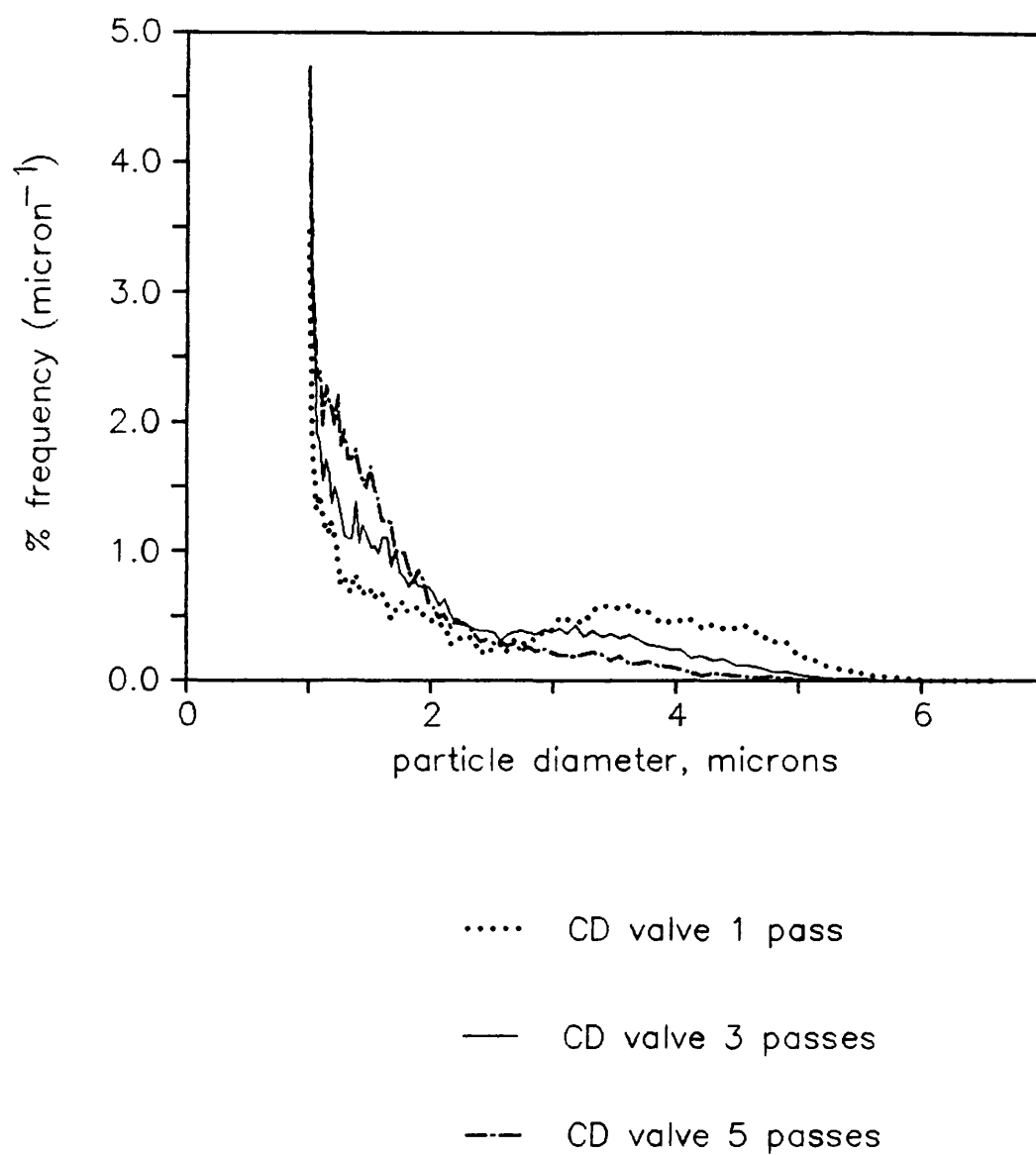
Particles obtained after 1, 3, and 5 passes through the homogeniser were sized for each of the five valve unit configurations (CR, CRF, CD, FV and KE) shown in Figure 3.1(a-e). These units were all fitted with the standard impact ring. Raw data for the CD unit are illustrated in Figure 5.5. The data were recalculated to obtain the corresponding frequency distributions. For all the valve units tested, a consistent trend was observed where a reduction in the proportion of larger particles was noted together with an increase in the proportion of smaller sizes. Figures 5.6 and 5.7 show representative results for the CD and FV valves.

### 5.2.2 Effect of valve unit geometry

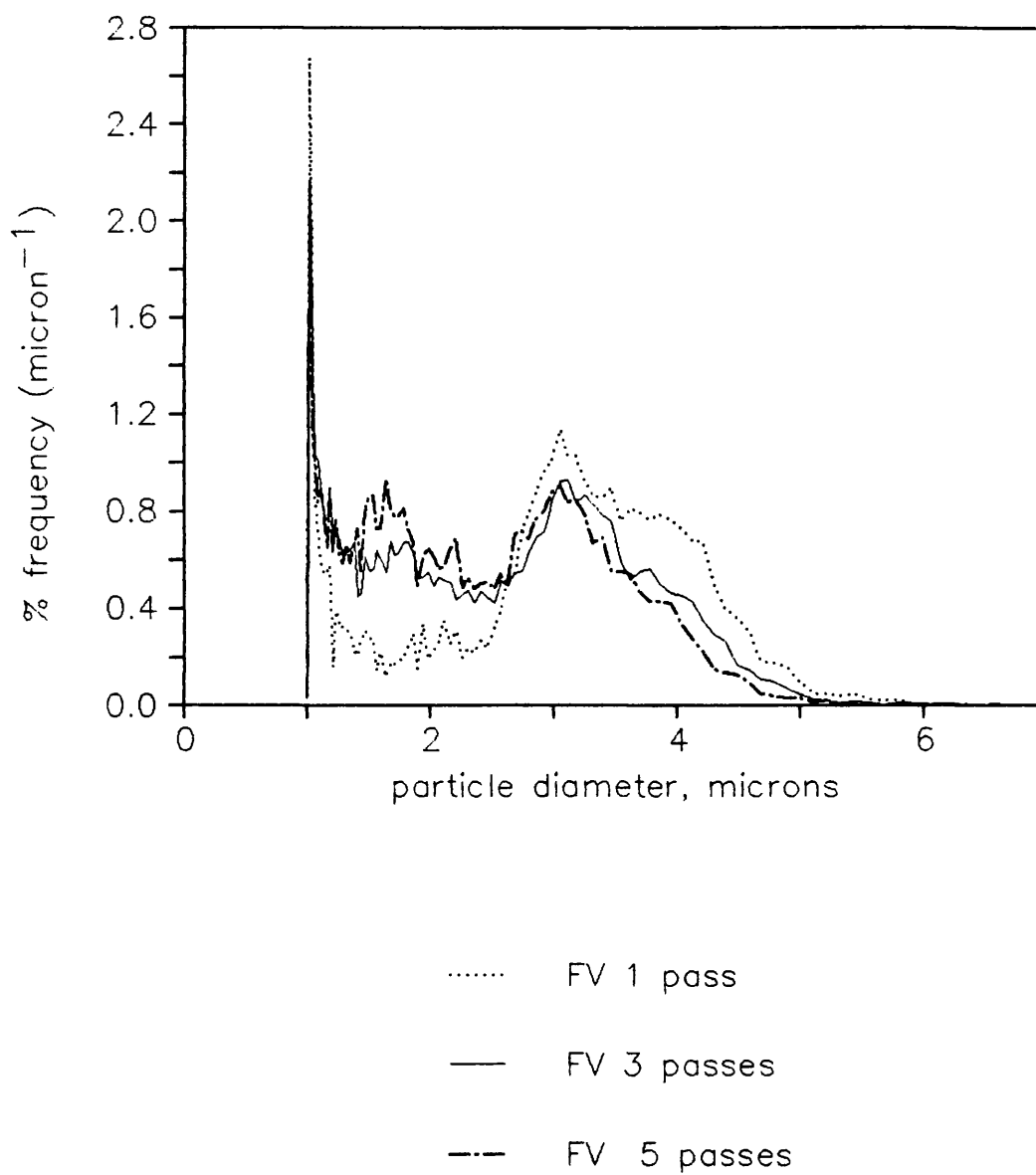
The effect of valve configuration on the debris formation was first investigated by examining the results of protein release versus percentage particle size by number (Table 5.1 and Figure 5.8). The findings indicated that as the soluble protein content of the cells



**Figure 5.5** Representative data output from the electrical sensing zone equipment (CD unit).



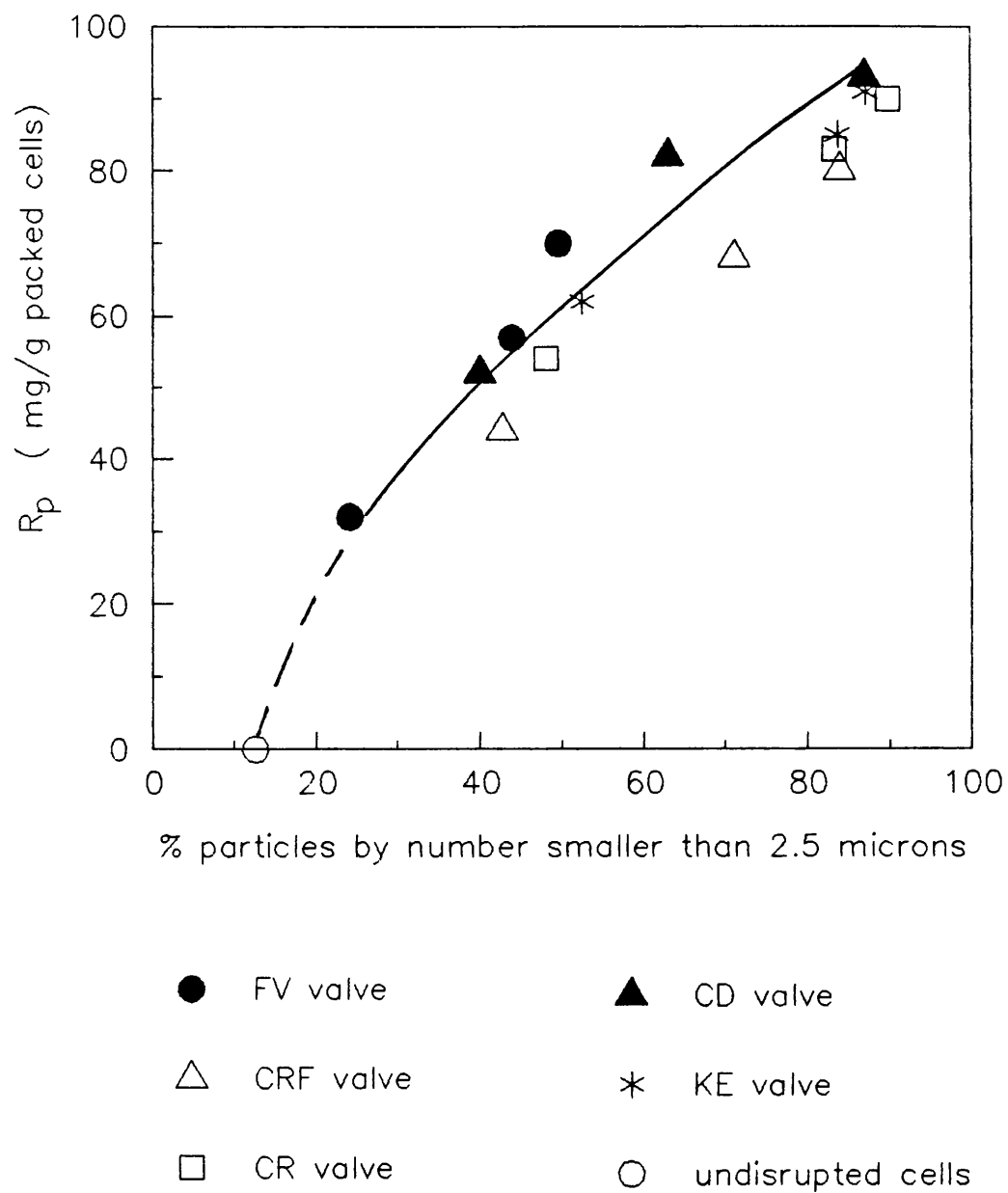
**Figure 5.6** Frequency distribution for CD unit, 46 MPa.



**Figure 5.7** Frequency distribution for FV unit, 46 MPa.

Table 5.1 Protein release versus % particle size (by number)

<u>pass 1</u>			<u>pass 3</u>		<u>pass 5</u>	
<u>valve</u> <u>unit</u>	<u>protein</u> (mg/g)	<u>%&lt;2.5u</u>	<u>protein</u> (mg/g)	<u>%&lt;2.5u</u>	<u>protein</u> (mg/g)	<u>%&lt;2.5u</u>
undisrupted cells		12.6				
KE	63	53	89	84	91	87
CR	54	48	83	83	90	90
CD	52	40	83	63	93	87
CRF	44	43	68	71	77	84
FV	33	24	61	44	70	50



**Figure 5.8** Protein release versus percent particle by number.

increased, the proportion of smaller sized particles rose as well. Furthermore, all the valve geometries studied remained on the same curve. There was a strong indication that although it may be possible to reduce the number of passes by replacing the valve geometry whilst releasing the same quantity of soluble protein, the particle size distribution did not shift towards larger sizes. This is of importance in the downstream step of centrifugation where larger particles are more desirable as they are easier to remove from the process stream. However, the analysis of data on the basis of percentage particle size by number should be made with caution. At the fine end of the particle size distribution, as the limit of operability of the instrument is approached, the results become prone to equipment error specially as the interpretation of the data by the equipment software at such a fine level is not clear. An alternative means of presenting the results was therefore sought. In centrifugation, it is the particle size distribution below a critical size which determines the centrifuge capacity. Representative values are best taken at the fine end of the size distribution, for example where 90, 95, or 99 % of the particles are of greater size; i.e.  $d_{90}$ ,  $d_{95}$  or  $d_{99}$  respectively. Table 5.2 and Figures 5.9(a-d) summarise the results of percentage volume oversize distributions for the different valve units under study. In general, it may be argued that irrespective of the type of valve geometry used, higher protein release was related to a higher proportion of smaller particles. However, the comparative merits of using fewer passes with different types of valves needed further scrutiny. This was investigated by examining the frequency and cumulative volume oversize distributions of valve units which showed similar levels of protein release at different number of passes through the homogeniser. Three sets of data were compared. The first set (Set A) presents particle data after 1 pass with KE valve versus those after 3 passes with FV valve. The second set (Set B) compares those after 3 passes with CD valve versus those after 5 passes with CRF valve, and the third set (Set C) matches the data for FV valve after 5 passes against those for CRF valve after 3 passes. The results are



Table 5.2 % volume oversize cut for different valve units

<u>KE</u>			
<u>% cut</u>	<u>pass 1</u>	<u>pass 3</u>	<u>pass 5</u>
	(63 mg/g)	(89 mg/g)	(91 mg/g)
99	1.26	1.04	1.04
95	1.98	1.29	1.26
90	2.51	1.53	1.47
50	3.70	3.32	2.74

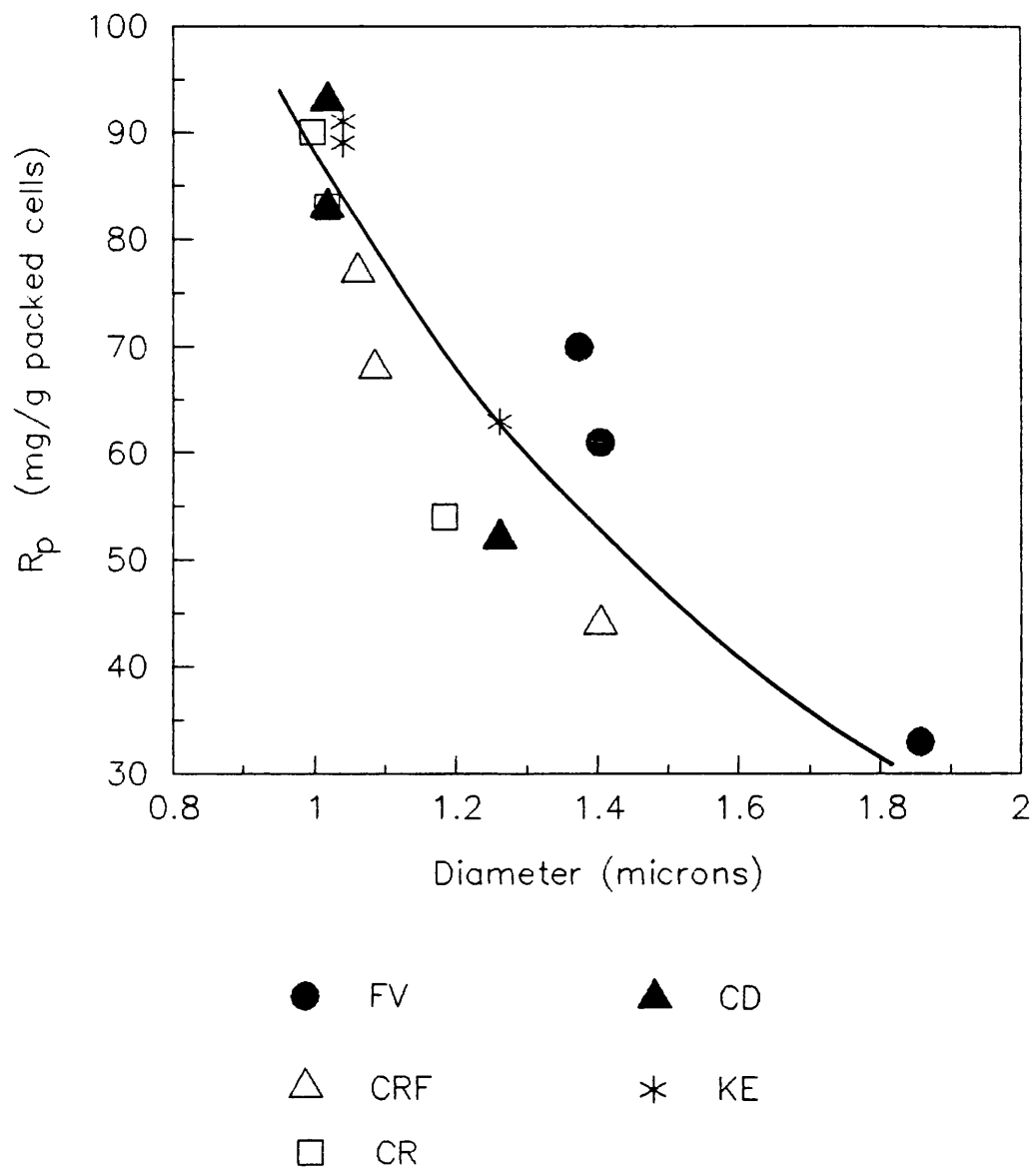
<u>CD</u>			
<u>% cut</u>	<u>pass 1</u>	<u>pass 3</u>	<u>pass 5</u>
	(52 mg/g)	(83 mg/g)	(93 mg/g)
99	1.26	1.02	1.02
95	2.07	1.43	1.24
90	2.57	1.82	1.44
50	3.54	3.10	2.74

<u>CR</u>			
<u>% cut</u>	<u>pass 1</u>	<u>pass 3</u>	<u>pass 5</u>
	(54 mg/g)	(83 mg/g)	(90 mg/g)
99	1.18	1.02	0.99
95	1.86	1.29	1.11
90	2.35	1.53	1.26
50	3.37	2.92	2.30

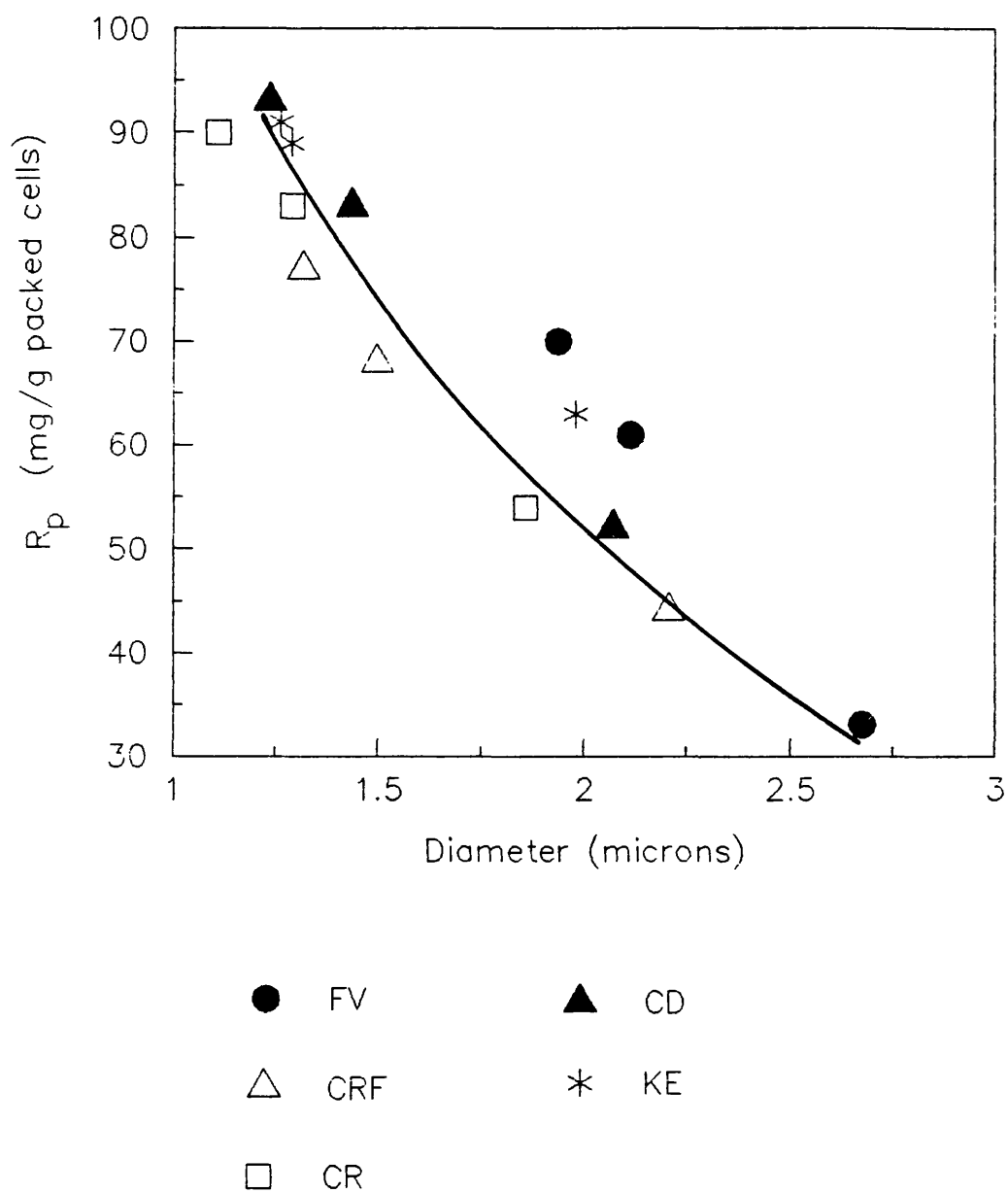
Table 5.2 (continued)

<u>% cut</u>	<u>CRF</u>		
	<u>pass 1</u>	<u>pass 3</u>	<u>pass 5</u>
	(44 mg/g)	(68 mg/g)	(77 mg/g)
99	1.40	1.09	1.06
95	2.20	1.50	1.32
90	2.73	1.82	1.53
50	3.78	3.18	2.79

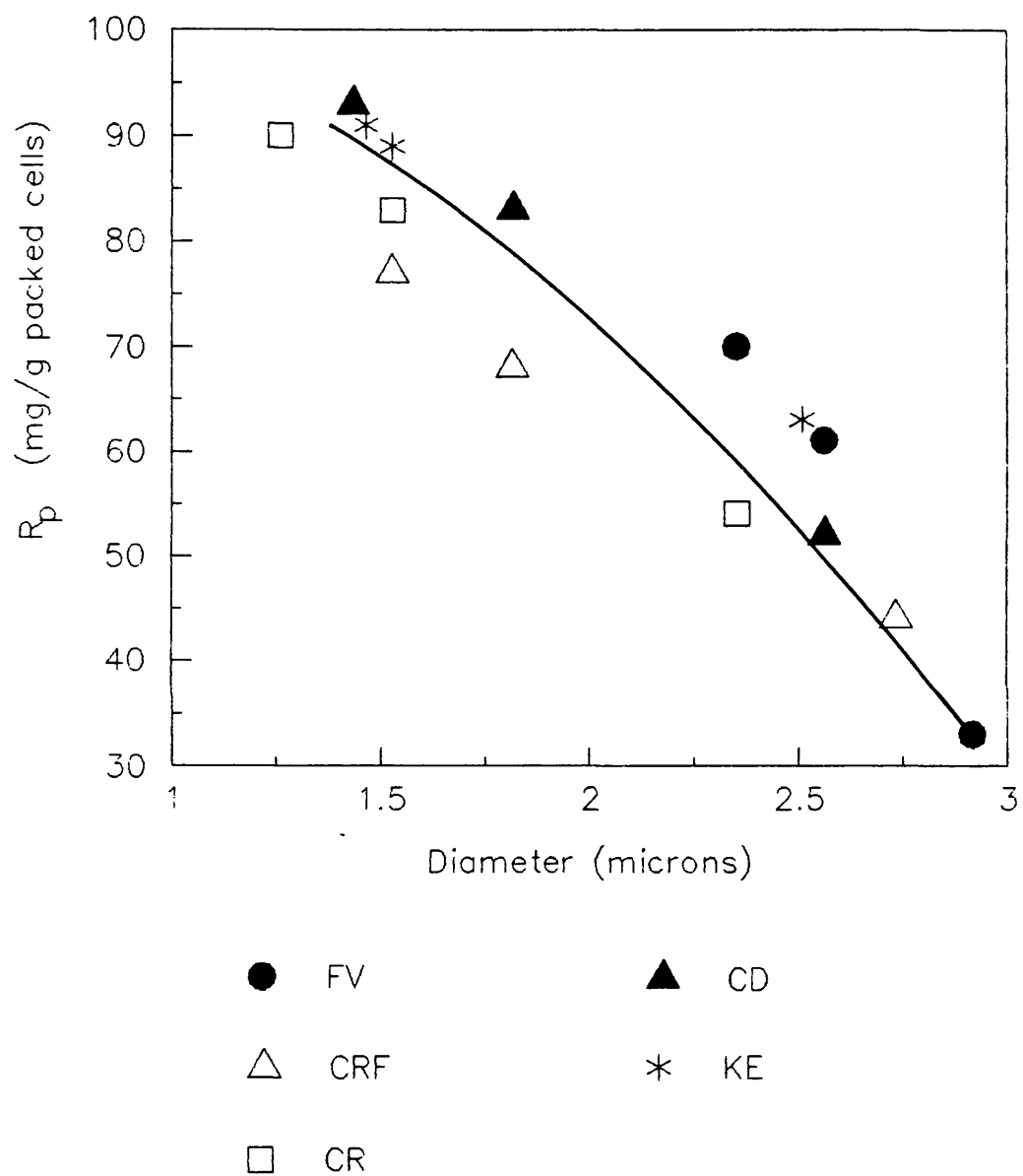
<u>% cut</u>	<u>FV</u>		
	<u>pass 1</u>	<u>pass 3</u>	<u>pass 5</u>
	(33 mg/g)	(61 mg/g)	(70 mg/g)
99	1.86	1.40	1.37
95	2.67	2.11	1.94
90	2.92	2.56	2.35
50	3.86	3.62	3.42



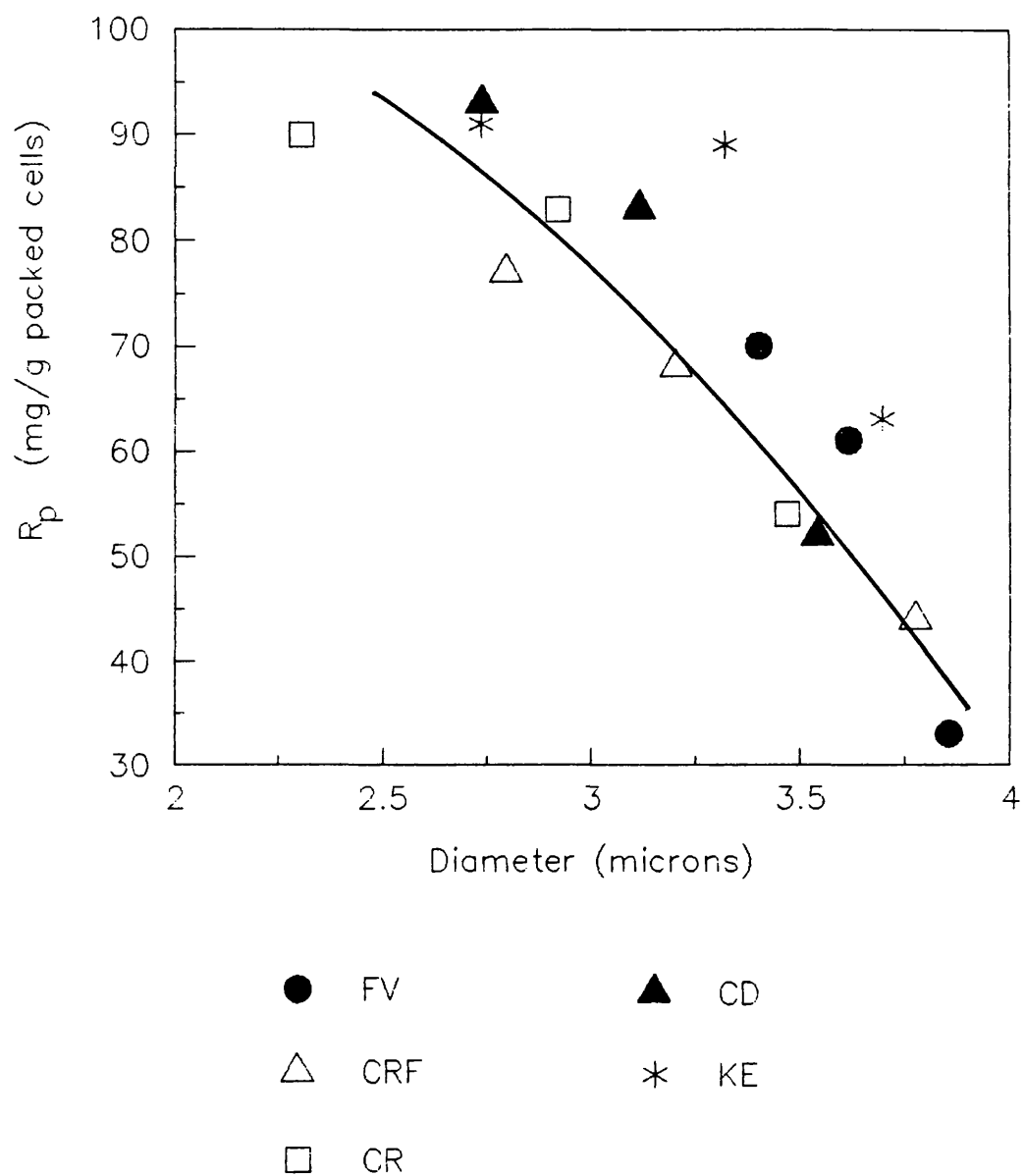
**Figure 5.9(a)** Protein released versus particle size  $d_{99}$ .



**Figure 5.9(b)** Protein released versus particle size  $d_{95}$ .



**Figure 5.9(c)** Protein released versus particle size  $d_{90}$ .



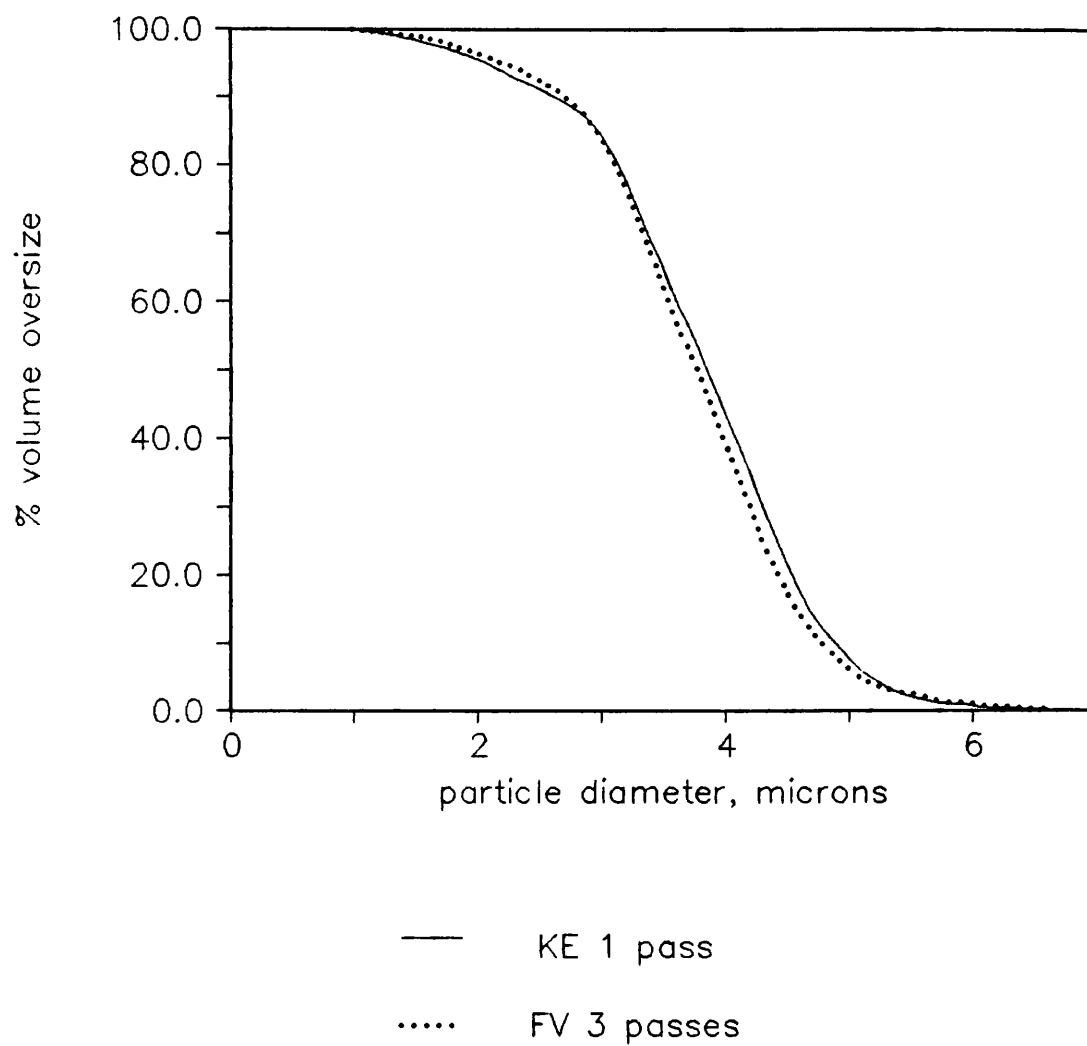
**Figure 5.9(d)** Protein released versus particle size  $d_{50}$ .

illustrated in Figures 5.10, 5.11 and 5.12 respectively. In the first set (Figure 5.10), the two valve geometries at the given passes correlated closely in terms of protein release and size distributions. However other valve geometries in the other sets (Figures 5.11 and 5.12) showed distinct differences.

In general, the analysis of the data reported in this section shows a small but distinct trend to the FV and the KE valves giving larger particles for equivalent protein release compared to other homogenisation valves. It is interesting to note that the FV valve has the longest "land" width and the KE valve, the shortest (Figure 4.1 and Table 6.1). This observation seems to imply that the land width is a contributing factor in particle attrition.

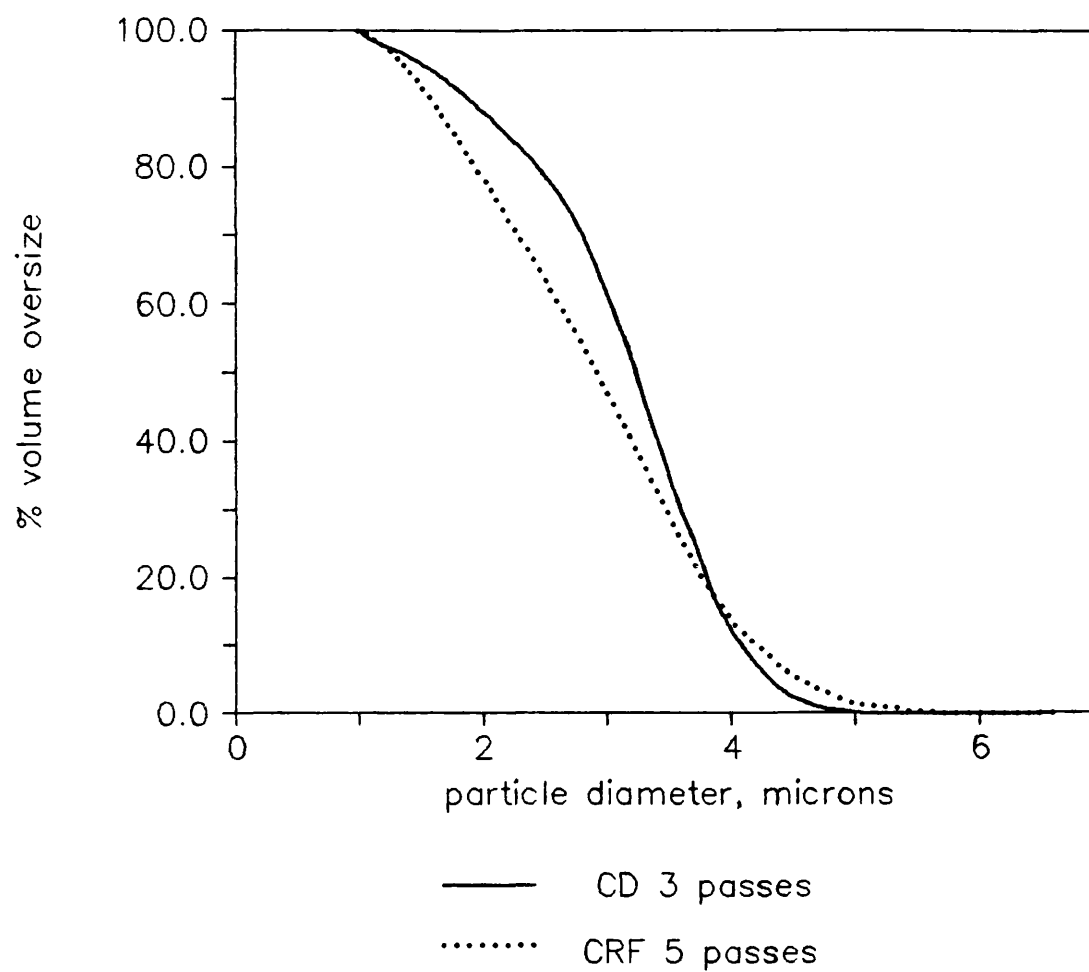
#### 5.2.3 Comparison between CD and CR valve units

Within the knife-edge category of valve geometries, this study showed that there was no significant difference between the performance of the CD and the CR valve units, expressed in terms of soluble protein release (Section 4.5). The particle size distributions of the homogenate obtained using these two valve configurations are illustrated in Figures 5.13(a,b). The CR unit resulted in a larger proportion of smaller particles, whilst the cumulative volume oversize distributions further demonstrated that although the released protein levels were similar, the 95% cut for the CR valve corresponded to a smaller particle size (1.29 microns) than that for the CD unit (1.43 microns). This gave an added advantage to the ceramic CD valve which was designed to give a better performance and longer life.

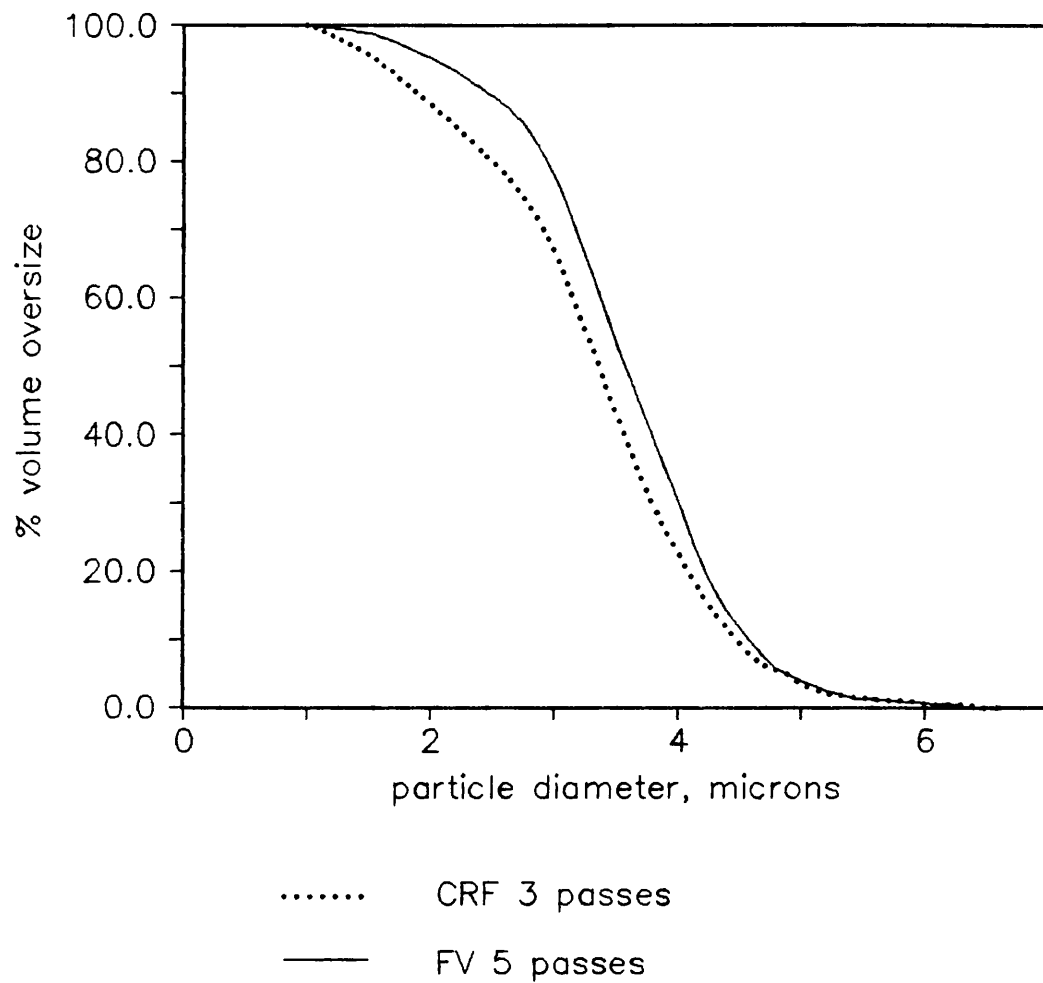


**Figure 5.10** Cumulative volume oversize distribution  
Set A

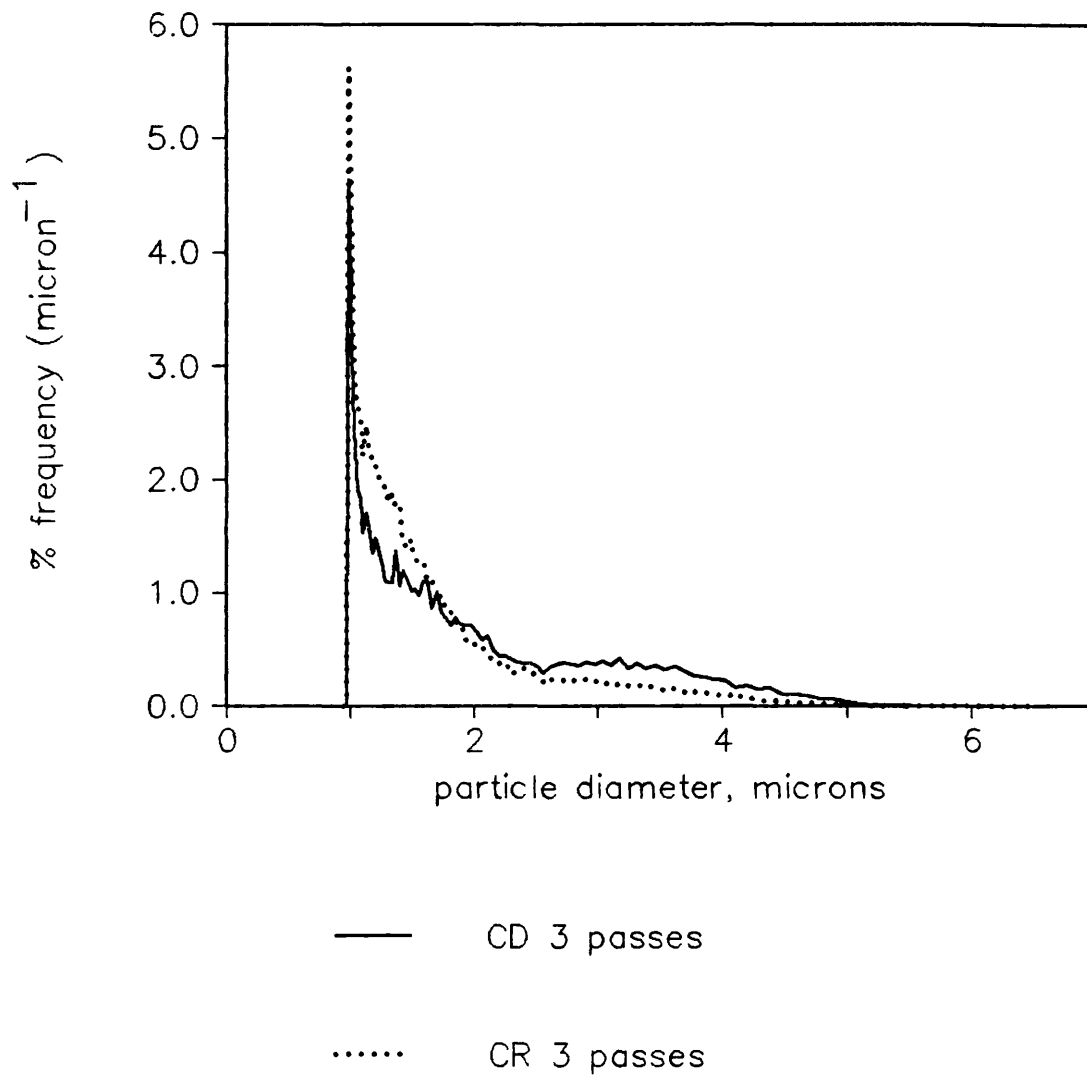




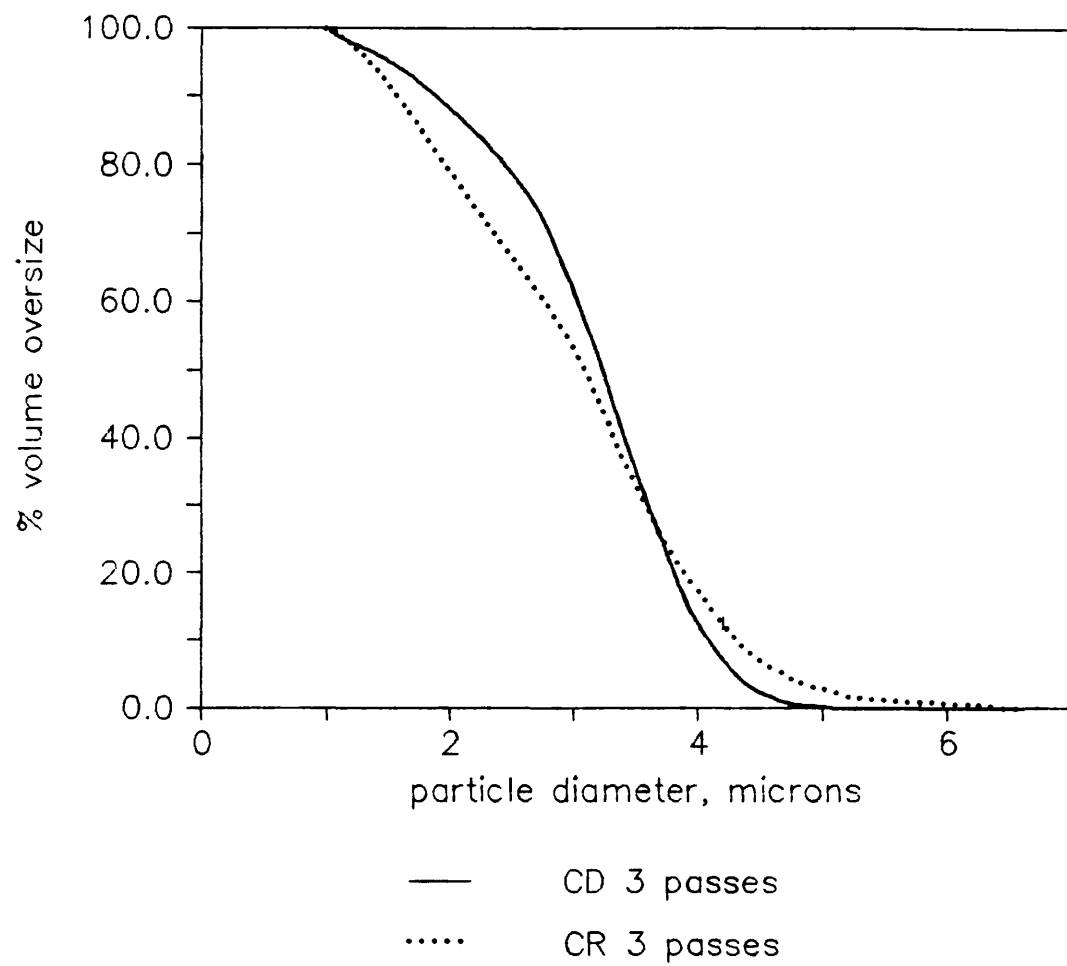
**Figure 5.11 Cumulative volume oversize distribution  
Set B**



**Figure 5.12** Cumulative volume oversize distribution  
Set C



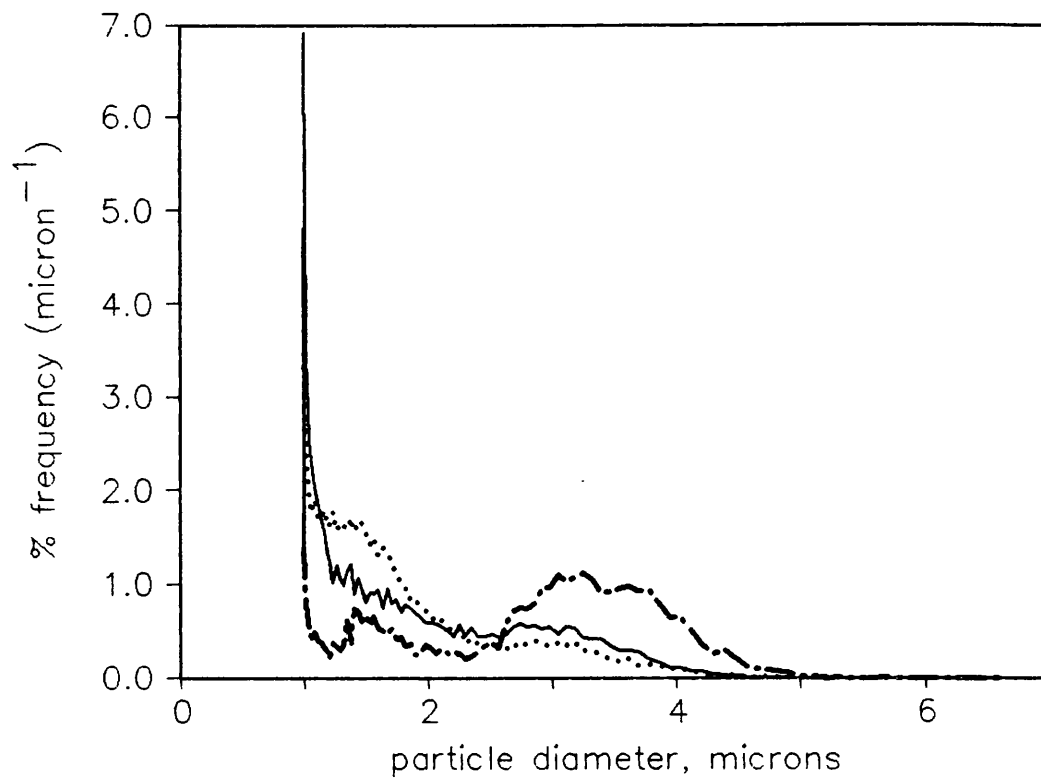
**Figure 5.13(a)** Frequency distributions for CD and CR units. 46 MPa, 3 passes



**Figure 5.13(b)** Cumulative volume oversize distributions for CD and CR units. 46 MPa, 3 passes

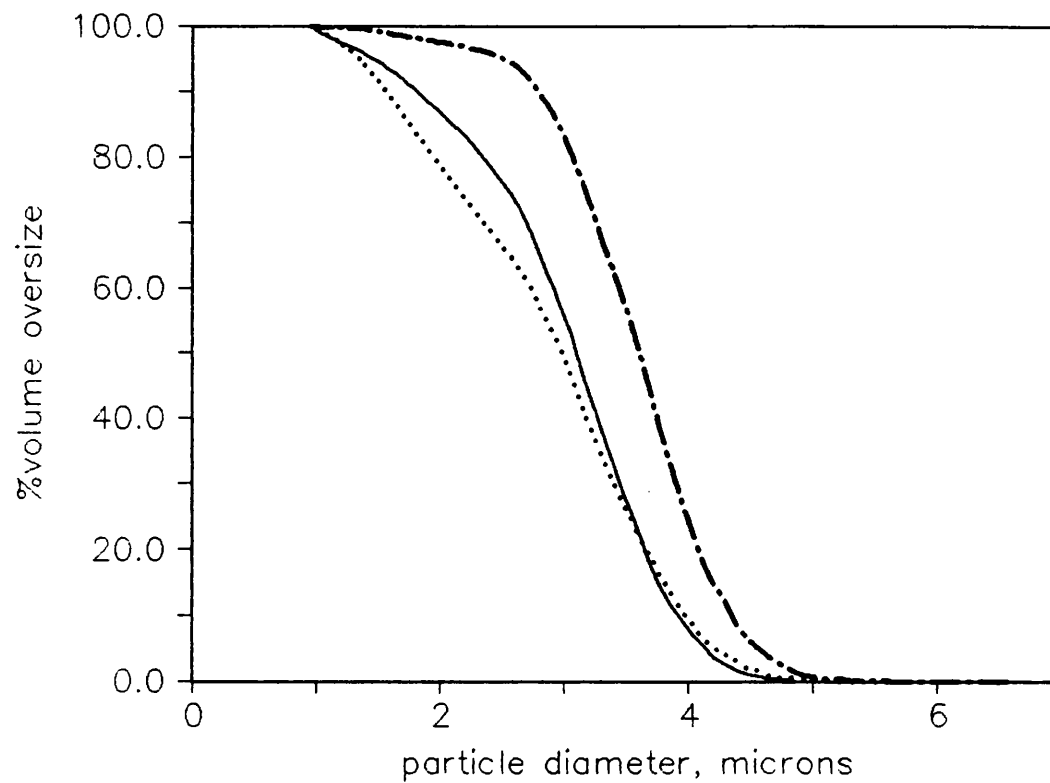
#### 5.2.4 Effect of impact distance

The effect of impact distance on debris size was investigated by measuring the size distribution of particles formed after homogenisation with CD valve using a standard impact ring, no impact ring, and the smallest available impact ring (Table 4.1). The results are shown in Figures 5.14(a,b), 5.15 and 5.16. As expected the proportion of smaller particles increased with decreasing impact distance as more cells were being disrupted. By the fifth pass through the homogeniser, most of the cells were ruptured with both standard and the smaller (10.16 mm bore) impact rings. This was illustrated in the particle size cuts at 99%, 95%, 90% and 50% remaining very close for both of these impact rings after 5 passes (Figures 5.15 and 5.16).



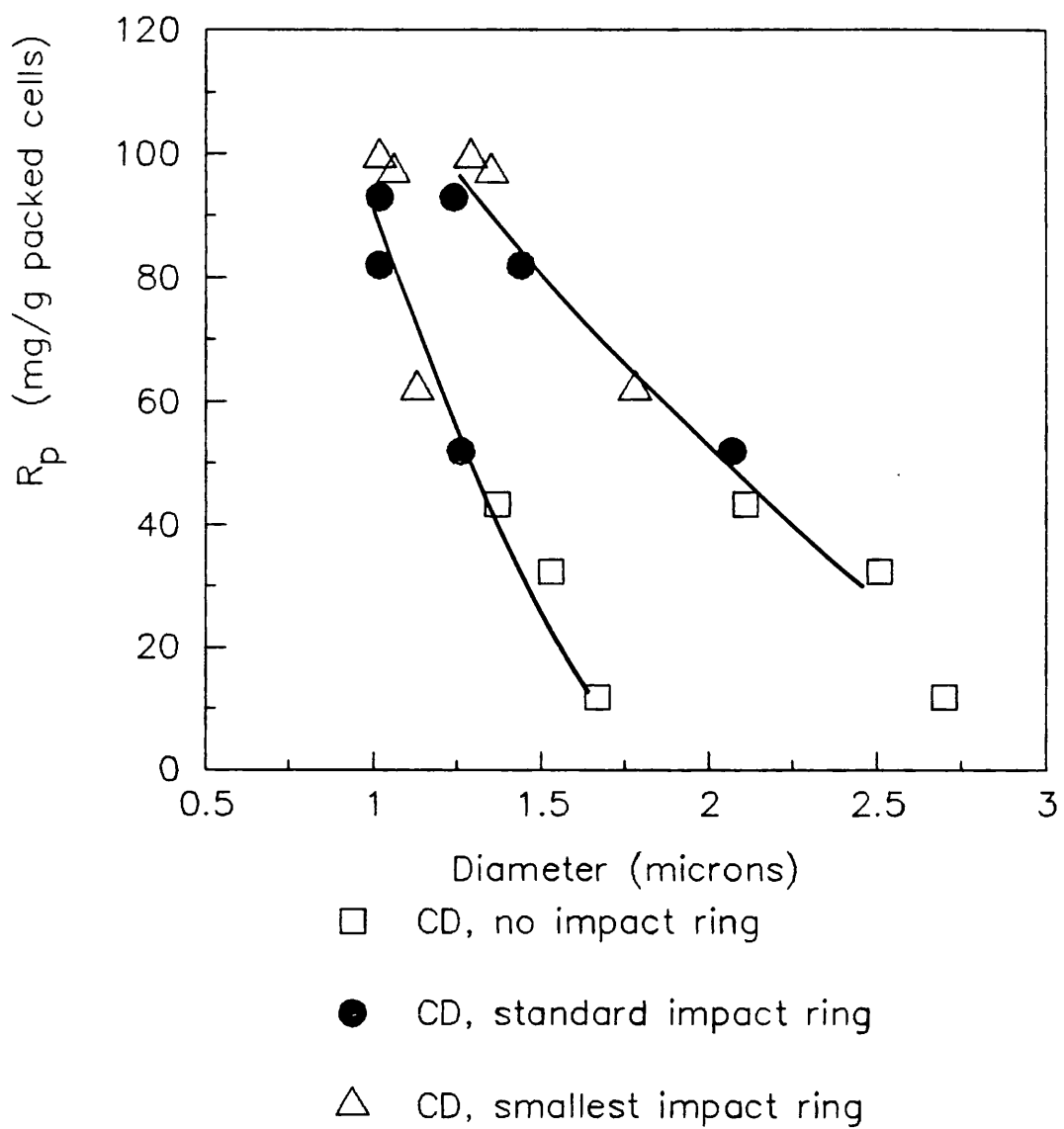
- CD, no impact ring, 3 passes
- CD, standard impact ring, 3 passes
- ..... CD, smallest impact ring, 3 passes

**Figure 5.14(a)** Frequency distributions for CD using a standard impact ring, no impact ring and the smallest impact ring. 46 MPa, 3 passes.



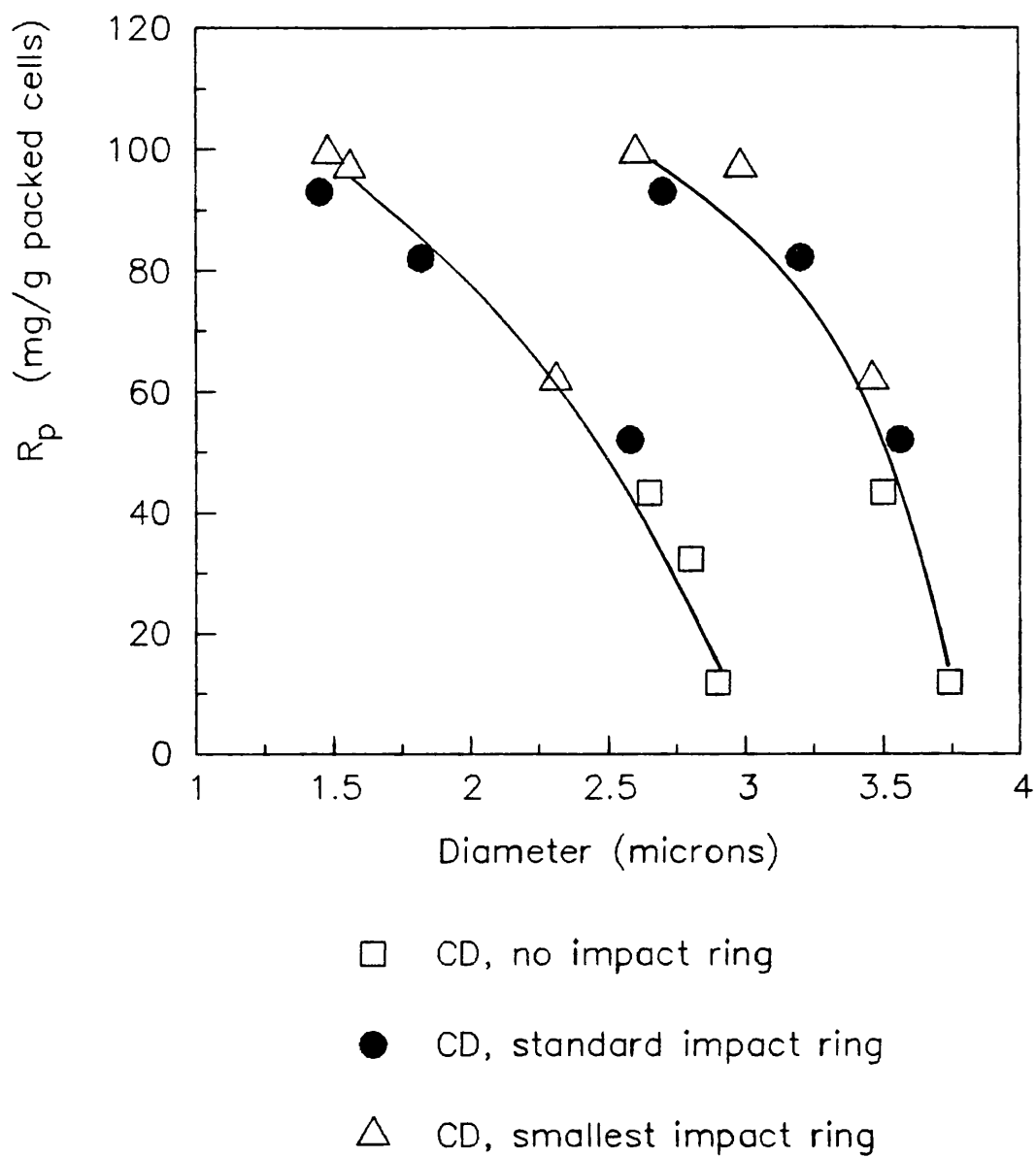
- · — · — · — CD, no impact ring, 3 passes
- CD, standard impact ring, 3 passes
- ..... CD, smallest impact ring, 3 passes

**Figure 5.14(b)** Cumulative volume oversize distributions for CD using a standard impact ring, no impact ring and the smallest impact ring. 46 MPa, 3 passes



**Figure 5.15** Protein release versus particle size  $d_{99}$  and  $d_{95}$ .





**Figure 5.16** Protein release versus particle size  $d_{90}$  and  $d_{50}$ .

## 6. MECHANISM OF CELL DISRUPTION

The investigation of the effect of mechanical parameters on cell disruption described in Chapter 4 revealed new information previously unreported in the literature. This was found to be of importance in explaining the mechanism of cell disruption. In this chapter, these findings are discussed and evidence is put forward for a better understanding of cell rupture in high pressure homogenisers.

### 6.1 Theoretical considerations

It was mentioned earlier (Section 4.1) that an essential feature of this work was the precise characterisation of the geometry of the valve unit. This is particularly important in elucidating the theoretical argument in the study. A generalised diagram of the valve unit is shown in Figure 6.1, identifying the dimensions of importance. The diagram is approximately to scale except, as will be discussed later, that the valve gap width  $h$ , is considerably smaller than shown. The impact distance,  $X$ , is defined from the radius at which the annular liquid jet leaving the valve geometry is allowed to expand freely on both sides.

The suspension flow path through a homogenisation valve is through the central orifice of the valve seat, across the "land" – which is the length  $(R - R_o)$  – where at a given pressure a gap (width  $h$ ) is created between the valve rod and the valve seat. The fluid then impinges on an impact ring a distance  $X$  from the valve. The various valve unit geometries (Figure 4.1) mainly differed in the values of  $R$ ,  $R_o$  and "land". The valve rod dimensions (except for the CR unit)

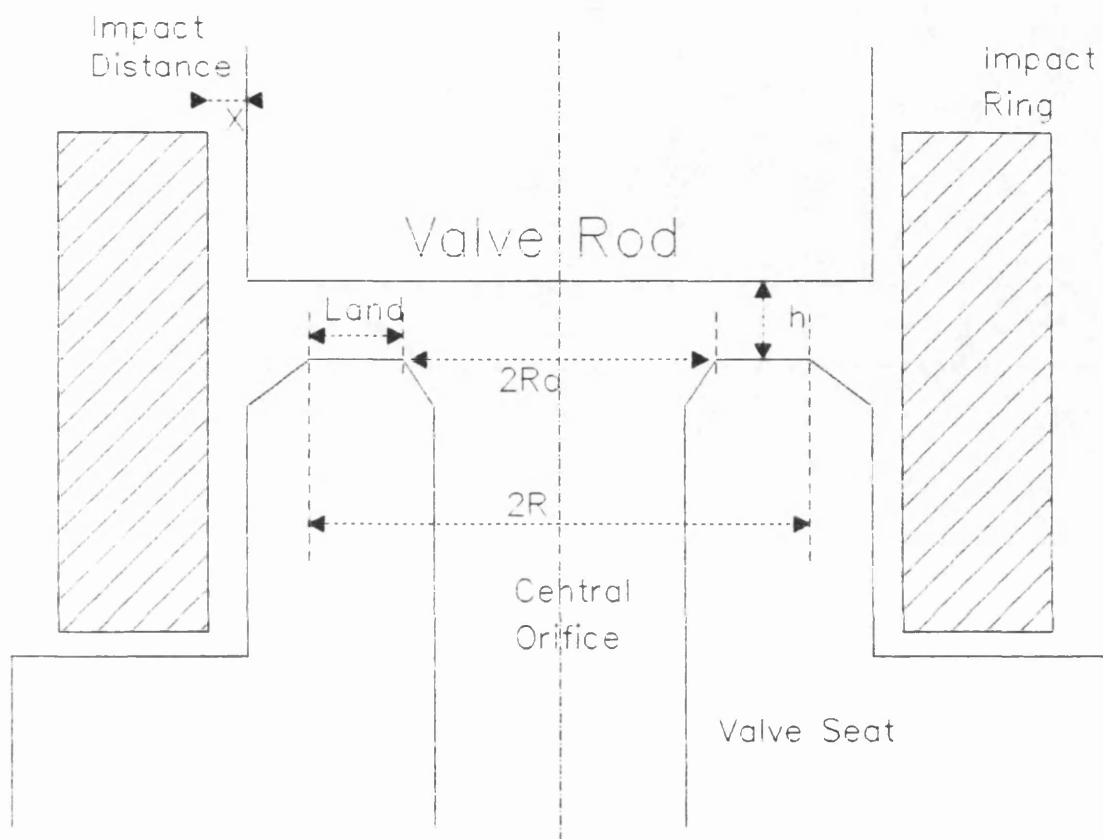


Figure 6.1 Schematic diagram of a typical valve unit.

were identical, similarly the bore size of the standard impact ring was the same. The land distance varied from near zero (0.1 mm) for the KE unit to 1.5 mm for the FV unit. The principal energy losses in the valve unit consisted of an entry zone loss (radius  $>R_o$ ), a friction loss across the land, and an exit zone loss (radius  $>R$ ). However, empirical data on these losses are scarce because of the physical difficulties encountered in experimentation in the valve zone of a high pressure homogeniser. The only available information was put forward by Phipps (1975) in the form of a Bernoulli type expression for the sum of the losses in the valve. For turbulent flow the following equation was given:

$$\frac{P}{\sigma U_o^2/2} = a + \frac{10 R_o}{h Re^{3/5}} \left[ 1 - \left\{ \frac{R_o}{R} \right\}^{2/5} \right] + a' \left[ \frac{R_o}{R} \right]^2 \quad (6.1)$$

i.e. total pressure loss = entry zone loss + friction loss + exit zone loss

$$Re = \frac{\sigma U_o h}{\mu}$$

where  $P$  is the total pressure drop,  $U_o$  is the mean velocity at radius  $R_o$ ,  $\sigma$  is the fluid density,  $\mu$  is the fluid viscosity,  $a$  the entry loss taken as 0.5 for sharp entries,  $h$  is the gap width between the valve rod and the valve seat,  $R_o$  and  $R$  are respective entry and exit diameters as shown in Figure 6.1,  $Re$  the Reynolds number at the entry into the homogenisation zone of the valve unit and  $a'$  is the exit loss factor taken as unity. The pressure drop  $P$  is taken as the homogenisation pressure, the homogeniser discharging to atmosphere.

The friction loss term is an empirical modification of the friction loss determined by Kawaguchi (1971) for turbulent flow between two parallel plates to allow for smaller dimensions in a homogeniser.

According to Kawaguchi (1971) and Phipps (1975), the change from a laminar to a turbulent regime for radial flow occurs at around Re equal to 500.

Equation (6.1) may be rewritten as:

$$P = \frac{\sigma}{4} \left[ \frac{Q}{2\pi R_o h} \right]^2 + \frac{5 \sigma \eta^{3/5}}{h^3} \left[ \frac{Q}{2\pi} \right]^{7/5} \left( \frac{1}{R_o^{2/5}} - \frac{1}{R^{2/5}} \right) + \frac{\sigma}{2} \left[ \frac{Q}{2\pi R h} \right]^2 \quad (6.2)$$

where Q is the flow rate and  $\eta$  is the kinematic viscosity of the fluid. It is thus possible to calculate the gap width h for a given valve geometry at a given pressure. The application of this equation to milk homogenisation by Phipps (1975) predicted a decrease in h, with increasing homogenisation pressure. This was found to be in agreement with independent experimental observations by other workers (McKillop et al 1955; Kurzahls 1977).

The above equation provided a basis for relating the valve unit geometry with the flow characteristics. However, it attempted to describe the events in the valve zone alone and did not carry any information on the effects of the impact ring. Beyond the exit from the valve zone, the fluid impinges on an impact ring. The impact distance X is measured from the valve rod to the impact ring because the valve rod overlaps the valve seat, from which point jetting occurs. From the results obtained on the effect of varying the impact distance on soluble protein release (Sections 4.3 and 4.6), it was evident that impingement affected cell breakage and had to be considered in the investigation of cell disruption mechanism. Based on experiments on jet impingement from a circular orifice, Beltaus and Rajaratnam (1974) reported that, for subsonic impinging air jets in the turbulent flow region, the stagnation pressure ( $P_s$ ) at the point of impact is a function of exit jet velocity from the orifice, U, the distance from the orifice to the impingement wall, X, and the orifice diameter d:

$$P_s = \frac{25 \sigma U^2 d^2}{\chi^2} \quad (6.3)$$

It was also shown that the maximal wall shear stress  $\tau_m$  in the impingement region occurs at a radial distance equal to  $0.14 X$  from the central impingement point and is given by:

$$\tau_m = \frac{0.16 \sigma U^2 d^2}{\chi^2} \quad (6.4)$$

The equations (6.3) and (6.4) are developed on the basis of dimensional analysis of a circular orifice where  $U \propto d^{-2}$ , and hence:

$$P_s \text{ or } \tau_m \propto \frac{1}{\chi^2 d^2} \quad (6.5)$$

The fluid suspensions will be exposed to a range of pressures or wall stresses. However, the pressure and shear profiles are reported to be approximately independent of variations in  $X$  and  $d$  (Beltaus and Rajaratnam 1974). Therefore, the value of  $P_s$  or  $\tau_m$  may be taken as representative of flow conditions in a particular jet. Hence in the case of cell disruption, if impingement were a significant breakage mechanism it would be expected that disruption rate would be directly proportional to an equivalent stagnation pressure or maximum wall shear stress. A certain fraction of the cells nearest to the centre of the impacting jet will be disrupted, this resulting in a first order process as was observed experimentally by Hetherington *et al.* (1971) (Section 1.2.1). The first order process was described by:

$$\frac{dR_p}{dN} = K (R_m - R_p) \quad (6.6)$$

or  $\ln \left\{ \frac{R_m - R_p}{R_m - R_p} \right\} = K N$

where  $R_p$  is the amount of released soluble protein after  $N$  discrete passes through the homogeniser,  $R_m$  is the maximum amount of soluble protein available for release, and  $K$  is the rate constant or the disruption yield which is a function of homogenisation pressure and valve geometry.

With the assumption that the dimensional analysis for an impinging air jet may be applied to the more complex particle liquid suspension under consideration here, the relationship as derived in equation (6.5) may be used to describe impaction effects in the high pressure homogeniser. In this case the dimension,  $d$ , the jet diameter will be replaced with the valve gap width,  $h$ :

$$P_s \text{ or } \tau_m \propto \frac{1}{\chi^2 h^2} \quad (6.7)$$

## 6.2 Discussion

The application of a Bernoulli type expression (equation 6.1 or 6.2) to describe the flow velocities through the valve unit and the definition of the properties of the impinging jet (equation 6.7) required a number of assumptions which need further comment. The expressions used are for turbulent flow (i.e.  $Re$  in the region of 500 or more). Table 6.1 describes the gap width as derived from equation (6.2) and the valve geometry, and also the resulting flow conditions in the valve unit. Based on the entry velocity, the required Reynolds numbers for turbulent flow were attained. However, due to the cylindrical geometry of the orifice, it is evident that the Reynolds number will decrease on flow through the valve seat, in the case of the flat valve seat to less than 500. Turbulent flow conditions may still be assumed as the presence of yeast cells which are only 2 to 4 fold smaller than the valve gap

Table 6.1 Flow characteristics with different valve geometries<sup>a</sup>

valve unit	KE	CD	CRF	FV
<hr/>				
gap width, h (μm)	12.55	15.15	19.10	21.61
entry velocity, U <sub>o</sub> (m/s)	206.0	144.1	154.4	127.5
exit velocity, U (m/s)	200.0	127.6	124.0	85.5
entry Reynolds number, Re	517.1	436.6	589.8	551.1
mean velocity gradient x 10 <sup>7</sup> , $\bar{G}$ (s <sup>-1</sup> ) <sup>b</sup>	13.7	5.0	4.2	2.5
<hr/>				

<sup>a</sup>

Assumptions: Q = 57 L/h  
 pulse rate = 1 pulse/s for 0.3 s  
 $\sigma = 1000 \text{ kg m}^{-3}$   
 $\mu = 5 \times 10^{-3} \text{ Pa s}$   
 concentration = 45% w/v  
 P = 46 MPa

<sup>b</sup>

$$\bar{G} = \frac{P_v^{1/2}}{\mu}$$

where  $P_v$  is the power dissipated per unit volume

$$P_v = \frac{P Q}{\pi (R^2 - R_o^2) h}$$



width would tend to promote the formation of turbulent eddies. The valve unit configuration with a 90° change in flow direction on entry would also promote turbulence. Hence it seems reasonable to assume that equations (6.1), (6.2) and (6.7) may be used to identify flow conditions within the homogeniser valve.

In determining the flow rate, it was important to take account of the pulsating nature of the flow which is a characteristic of single piston homogenisers. One pulse per second (0.3 second duration) was used as the basis for the calculations. This was in accordance with data reported by (Brookman 1975). Data on the viscosity of the suspension was based on preliminary experimental work carried out on whole and disrupted yeast cells.

#### 6.2.1 Effect of impact ring

A major finding of this study was the significance of impingement in cell disruption in high pressure homogenisers. Previous theories pertaining to cell disruption in the type of equipment used in this work do not account for the importance of the impact ring (Doulah et al. 1975; Brookman 1975). Impingement has only been considered in equipment directly designed to test the impact effect (Engler 1979; Kramer and Bomberg 1988a, 1988b).

Impact distance has two possible effects on homogeniser operation. Firstly, it contributes to the back pressure of the system and secondly it is involved in the impingement phenomenon. The effect of back pressure is not significant because an increase in impact distance at constant total pressure should result in lower back pressure and therefore better disruption. This is however, contrary to the observations made (figure 4.9) where smaller impact distance resulted in better homogenisation. Furthermore the annular cross sectional area for the exit flow parallel to the impact ring was at least 50 times larger than the flow area in the homogenisation zone of the valve unit, based on the impact distance and gap width values

(Table 6.1). The back pressure due to the impact ring has therefore a minor effect on the valve gap width and hence for any particular valve configuration impingement effects are an important parameter.

Early studies on milk homogenisation (McKillop et al. 1955) had shown that the removal of the impact ring (i.e. an increase in impact distance) did not reduce the effectiveness of homogenisation. This observation is at variance with that made for cell disruption. The failure to observe similar results may be attributed to the fact that milk homogenisation was shown to be complete before the fluid left the area between the valve rod and valve seat (Loo and Carlton 1953) and that high velocities of over 250 m/s were required to disrupt milk on impact (Mulder and Walstra 1974). Evidently the mechanism of cellular breakage is different from that of homogenisation of dairy products. This could explain the negative results obtained in studies attempting to correlate milk homogenisation with cell disruption (Brookman 1975).

#### 6.2.2 Effect of valve geometry

The finding that knife-edge geometries yield better disruption than the flat-edge configuration is in accordance with previous studies in which at least one of three types of knife-edge units (CD, CR and CRF) were tested against a flat valve unit (Hetherington et al. 1971; APV Gaulin 1985). Within the knife-edge range of units, the experimental KE, which has the sharpest edge, was the most efficient. CD and CR valve units were similar in performance despite claims by the manufacturers that the CD unit resulted in better yield.

For the KE, CD, CRF and FV configurations it was possible to estimate flow conditions in terms of mean velocity gradient or velocities of flow in the valve (Table 6.1). The ascending trend of the disruption yields follows that of the corresponding flow values

although it is not possible to identify whether the mean velocity gradient or velocity of flow was the relevant correlating parameter. Similarly decreased valve gap width leads to increased disruption rate and, since the yeast cell sizes are of similar dimension (approximately 5  $\mu\text{m}$  diameter for a whole cell), then the effects of cell distortion on flow through the valve may also contribute considerably to the disruption rate. However, it should be noted that the land width is yet another variable in the valve configurations studied and is not possible to distinguish between various contributory effects of the valve geometry without further research.

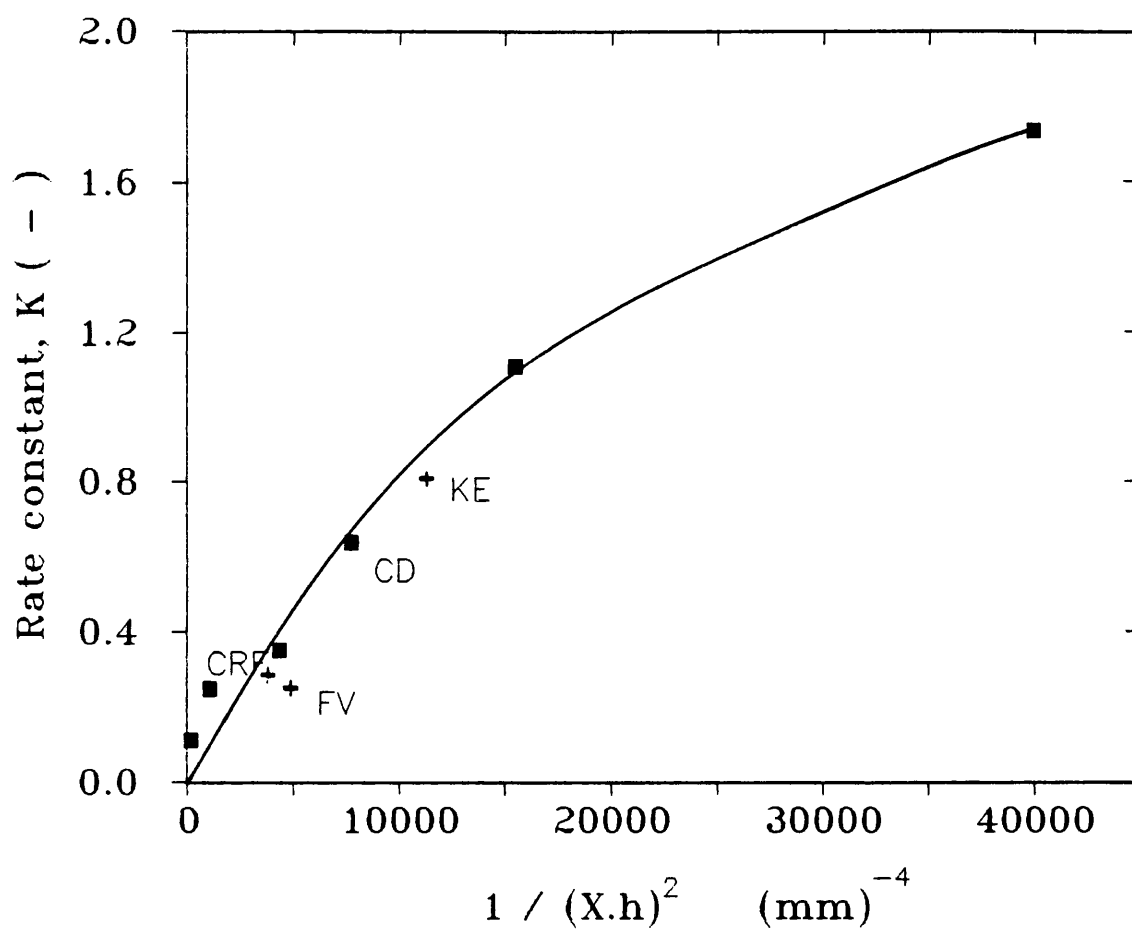
As far as the effect of mechanical parameters on cell debris formation is concerned, no simple correlation may be drawn between the mechanism of cell disruption and debris size distribution. It is however possible to speculate on the implications of the results reported in Chapter 5. The effect of impact ring is mainly related to the breakage of whole cells on impaction. The reduction in debris size however is most likely a function of the valve unit geometry and the dimensions in the valve zone. Repeated passages through the homogeniser would not only break the undisrupted cells but also micronise the cell debris.

### 6.3 Concluding remarks on the mechanism of cell disruption

The variation of disruption yield with impact distance,  $X$ , and gap width,  $h$ , expressed as  $1/(X^2 h^2)$ , is shown in Figure 6.2, firstly at constant  $h$ , where one valve geometry was used at constant pressure with a range of impact distances, and secondly at constant  $X$ , where different valve geometries were used at constant pressure with the same impact ring, resulting in variation in  $h$ . The two cases correlate well as data for constant  $X$  and then constant  $h$  lie on the same curve. The relationship therefore describes well the operation of the homogeniser within a narrow range of gap widths studied i.e.

$12.6 \mu\text{m} < h < 21.6 \mu\text{m}$  which relate to 46 MPa pressure.

The results of the study therefore indicate that both valve geometry and impact ring are relevant to the disruption process. Two mechanisms are involved, that relating to the homogenisation zone within the valve unit, and that connected with the impingement in the exit zone. Impingement is the predominant mechanism as illustrated in Figure 4.11. For the CD unit it is estimated that only 20% of the disruption obtained after the first pass under normal working conditions (i.e. with a standard impact ring) is due to the valve unit geometry; the rest (80%) is achieved by impingement.



**Figure 6.2** Effect of impact distance and valve geometry on soluble protein yield from bakers' yeast at 46 MPa. Yield is the rate constant  $K$  in the equation 6.6.

## 7. BIOCHEMICAL ENGINEERING DESIGN OF AN INTEGRATED HOMOGENISATION SYSTEM

### 7.1 Background

At the initial stages of the study, decisions had to be made regarding possible ways of conducting the investigation of the mechanism of disruption in high pressure homogenisers. Previous researchers had been faced with the problem of dealing with essentially a 'black box' since the crucial features of a high pressure homogeniser, namely the components of the valve unit, are encased in the assembly block. High operational pressures, very small flow paths and valve unit dimensions made reliable measurements within the unit virtually impossible. Alternatively, other researchers had attempted to use experimental equipment with the intention to recreate the conditions within the homogeniser (Brookman 1977; Engler 1979). In this study, initial experiments were carried out using equipment similar to that devised by Brookman (1977). This consisted of an air driven liquid pump capable of pumping 9 L/h at 69 MPa connected to an adjustable relief valve. The system proved unsatisfactory because of difficulties to control the air supply and the aperture of the relief valve. Furthermore the unit could not be used with filamentous microorganisms due to severe blockage. The design of a system consisting of a high pressure intensifier attached to an exit aperture of well defined dimensions was feasible (Engler 1979). However, since it was never possible to claim with certainty that the conditions within high pressure homogenisers were accurately emulated, it was decided to discontinue the search for an experimental equipment and instead investigate the high pressure homogeniser itself by varying the operating parameters and geometric configurations (Chapters 3 to 6).

During the course of the study, however, it became clear that the design of the homogenisation system could be improved in many ways.

The homogeniser itself was a single piston device with a high degree of pulsation which made reproducible experimentation difficult. At the time, other three piston homogenisers available on the market were of high operating capacity (well above 200 L/h). The range of operating pressures was also limited. Other researchers, who had extended the pressure range by altering the pump unit, noted variations in their results which were attributed to the non-optimal design of the equipment (Dunnill and Lilly 1975). Furthermore, the homogeniser did not have any provision for containment at any level. Even for non contained processes, safety regulations required operation with covered containers for feed and collection to avoid splash back and possible aerosol discharge. Another aspect of the system which required much improvement was the need for suitable integration of ancillary equipment such as the heat exchanger, pipework and instrumentation with the homogeniser. The manufacturers do not provide a total integrated system. The ancillaries, therefore, were usually fitted in house 'piece - meal'.

## 7.2 Design philosophy

In view of the above considerations, it became clear that there was a need for a new integrated homogenisation system which would satisfy the following overall guidelines.

- a- A homogeniser that could be operated over a wide range of pressures, from very low to very high (eg. beyond 100 MPa), with moderate flow capacity commensurate with pilot scale process requirements.
- b- Auxiliary equipment based on hygienic design and fitted as one single unit with the homogeniser.
- c- Some degree of built-in containment with provision for future full containment of the total system.

d- Provision for CIP (cleaning in place) operation.

Discussions with APV Gaulin revealed that a new homogeniser (designated model 30 CD) was being developed and specifically designed for the biotechnology industry and therefore in some ways met the stated criteria. However, there was a need for some extra features (Section 7.3.2). Other recently marketed homogenisers such as Lab 60 (APV Baker Ltd, Crawley, West Sussex, UK) did not have any provisions for containment. The 30 CD was to be marketed, as all other homogenisers, without any auxiliary units. It was therefore decided to design and construct a complete integrated homogenisation system using the 30 CD as the centre piece. The work was carried out with the help of APV Gaulin and APV Baker. The system has been intended for future research in the pilot plant.

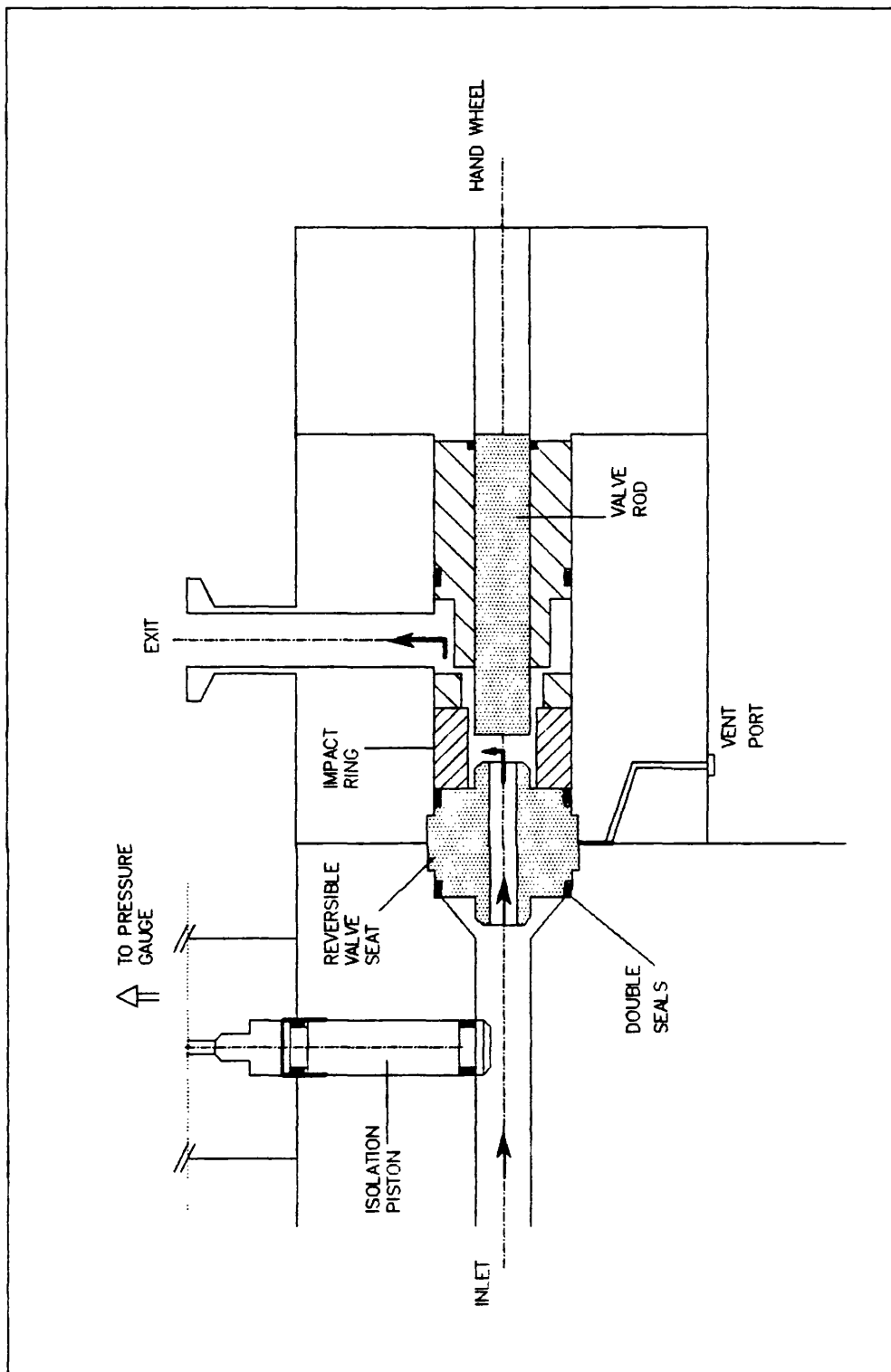
### 7.3 The homogeniser

#### 7.3.1 Main features

The 30 CD is a three piston homogeniser which is based on the same general principle of operation as that of a single piston described in Section 1.1.2.2. It has, however, some unique features. It has a capacity of 113 L/h at a maximum operating pressure of 105 MPa in continuous operation mode. The pressure may be increased by another 20 % for intermittent runs of maximum 20 minutes duration. The CD valve assembly which is made of a ceramic composite material, is designed such that the valve seat is reversible, providing two workable surfaces which can be interchanged in case of damage (Figure 7.1). The pressure gauge is not coupled directly to the discharge manifold but is isolated by a piston in order to prevent the mixing of the pumped product with the hydraulic fluid.

Another feature which makes the equipment particularly suitable for use in the biotechnology industry is the prevention of leakage and





**Figure 7.1** Schematic diagram of the valve assembly for the 30 CD.

aerosol formation by means of double seals with drain ports between them at locations of high pressure. These occur at several points in the system. Double seals and drain ports are provided at the coupling of the homogeniser valve assembly to the pump block (Figure 7.1), and the cylinder packing box to the block (not shown). Similar arrangements are positioned in the suction and discharge valve assemblies. Furthermore, a rupture disc assembly is fitted to release any over pressure in the discharge manifold through a safety relief port (not shown).

### 7.3.2 Additional features for the integrated system

Although the flow capacity of the homogeniser at 113 L/h was much lower than those of other three piston homogenisers available in the market, nevertheless it was well above smaller homogenisers (57 to 60 L/h). Given the small quantities of process material available from fermentation sources, it was desirable to be able to reduce the flow rate of the 30 CD. This was achieved by decreasing the speed of the pump motor by means of a variable frequency inverter (IMO Jaguar, VL550, IMO Ltd, London, UK). The inverter principle is to vary motor frequency along with motor supply voltage to achieve the most efficient means of altering motor speed. It was thus possible to vary the flow rate from 113 L/h to 70 L/h. Although in theory it is possible to reduce the speed further to allow for lower flow rates, in practice the operation is limited by the pumping action (pulsed flow instability), large hold up volume in the pump and oil accessibility to the gear box.

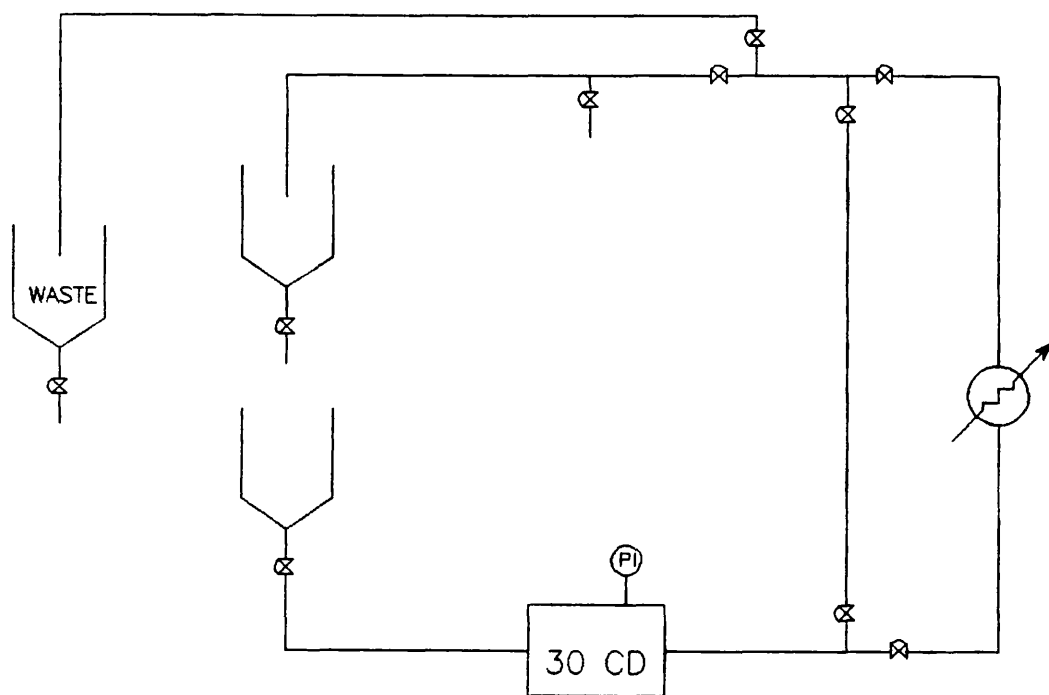
Another feature of the homogeniser which needed some modification was the pressure gauge. It was desirable to be able to set the pressure over the whole range from few MPas up to the maximum. The existing pressure gauge was not sensitive to the small changes at the lower end of the scale. It was however in principle possible to use a pressure transducer and adjust the pressure by means of a

hydraulically operated actuator. Since this mechanism was not fully developed by the manufacturers at the time of this study, an alternative design consisting of two pressure gauges was conceived covering the low and high pressure ranges respectively. A cut off mechanism was installed to protect the low pressure gauge from over pressurisation.

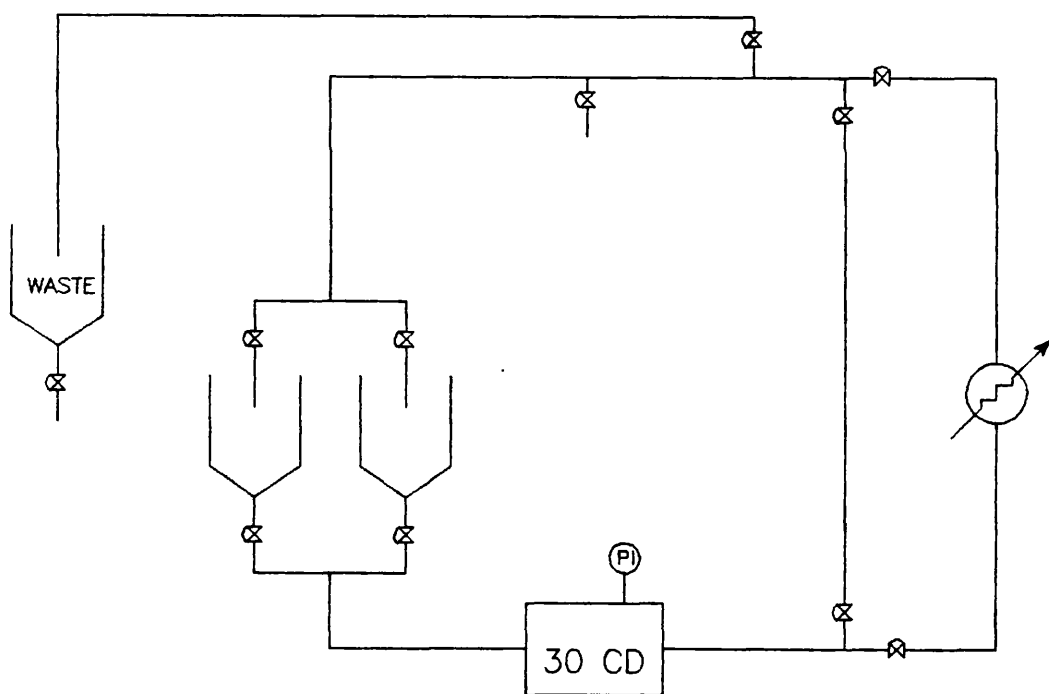
#### 7.4 Plan of the auxiliary equipment

The first step in the design of the integrated system, once the homogeniser was selected, was to identify the auxiliary items. These consisted of hoppers for feed, collection and waste, pipework and valves, heat exchanger unit, and instrumentation. The lay out of the plant was the next important step. This was based on the requirements for discrete pass disruption whilst taking account of several constraints. The space availability was a major consideration, limiting the dimensions of the plant to 1.53 m x 1.2 m. The height, weight and ability to physically transport the equipment through the building into the pilot plant were also considered. It was also necessary to ensure accessibility of various units for operation and maintenance by the operator. The total package was to be assembled on a stainless steel skid with all termination points taken to the edge of the package.

The logic behind the discrete pass operation was based on the methodology used in the study as outlined in Section 2.8.3. Two basic layouts were considered. One option to arrange the feed and collection receptacles in series (Figure 7.2 (a)) allowed for a simpler homogenisation procedure but excluded the possibility of interchanging the hopper usage. The system also had to allow for the collection hopper to empty within 20 seconds to prevent the mixing of process fluids between different passes. This was based on the assumption that the hold up volume would be around 600 ml and that the equipment was running at full flow capacity. Therefore, fast



(a) Hoppers in series



(b) Hoppers in parallel

**Figure 7.2** Alternative hopper layout

acting, full bore valves were to be considered together with exit pipes with a diameter greater than 3/4 inch to allow an average flow rate of about 1000 L/h.

An alternative layout was to arrange the feed and collection hoppers in parallel (Figure 7.2 (b)). This was more practical as it allowed the interchange of the two tanks, it did not necessitate the stringent requirement for rapid discharge of the vessels and alleviated the associated problem of aerosol formation when an empty hopper is being filled. It was therefore selected as the basis for the rest of the design work.

## 7.5 Design of hoppers

Three stainless steel hoppers were required, each with 5 L working volume ( 8.3 L total volume). In the case of contained operation it would be necessary to fully seal the hoppers and also be able to steam sterilise the contents. In such a case the hoppers would be pressurised vessels similar to stirred tank fermenters with the same design considerations. For the purpose of the present work, simple atmospheric conical bottom hoppers were used with appropriate connections (Section 7.6) for retrofitting with pressurised vessels. The conical shape of the lower part of the hopper would allow easy and quick release of the process fluid. The feed and collection hoppers were to be jacketed to allow for cooling.

### 7.5.1 Level control

The operator has to be aware of the level of the process fluid inside the feed and collection hoppers in order to open and close the appropriate valves (Section 7.6). One alternative was to incorporate a level sensor which, at a given level, would automatically initiate the opening and closing of designated valves.

Three possibilities were considered which consisted of a load cell operating on the basis of weight changes in the hopper content, a conductivity probe responding to a break in fluid contact, and an ultrasonic sensor detecting the change in the sound velocity through air and liquid. All these options were costly and had operational drawbacks, and given that non contained hoppers were selected, were thought to be unnecessary at this stage but would be reassessed when retrofitting for fully contained operation. Visual observation was the alternative solution. The use of a sight glass was considered. However, past experience had shown that the glass could easily get covered with particles and cellular matter obscuring a clear view of the fluid level. Observation from the top was the most reliable method, but the hoppers had to be covered. Even though the vessels were not contained, nevertheless it was necessary to comply with the safety regulations which required the process fluid to be fully enclosed. In order to satisfy both safety and operational requirements, a lid made of perspex was designed with appropriate ports for instrumentation. The lid consisted of two halves so that access to the contents would be easy without the need for dismantling all attached instrumentation.

#### 7.5.2 Instrumentation

In order to preserve the consistency of the homogenised process fluid, to prevent the cells from sedimentation in the hoppers which may lead to homogeniser blockage - especially in the case of filamentous microorganisms - and to prevent a filter mat of filamentous organisms forming in the outlet pipe from hopper, an overhead stirrer unit with mechanical variable speed control and a stainless steel 2-blade impeller rotor was installed ( SS1, Stuart Scientific Co Ltd, Redhill, Surrey, UK) in both feed and collection hoppers. The height and the angle of the stem could be easily adjusted by means of a retort stand clamp ( Climpex, Arnold Howell Ltd, London, UK). The stirrer would be positioned at a minimum

height from the exit of the hopper, and would be turned off as soon as the fluid fell below this level to avoid aerosol formation. The control of the stirrer speed was important to prevent frothing and disruption of fragile cells. In order to increase mixing at the exit to the hopper, a stainless steel cross shaped removable baffle was positioned over the orifice.

The temperature of the suspension fluid in the feed and collection hopper was monitored by means of a 63 mm dial thermometer ( type VRS, Knowsley Instrument services Ltd, Liverpool, UK) with 3/8 inch compression gland, installed in each container.

To prevent damage to the homogeniser valve assembly, it is essential to ensure continuous flow of fluid to the equipment. An alarm mechanism was therefore installed in the hoppers to inform the operator of the low level of fluid in the receptacles. This was an emergency measure and was not intended as part of the routine operational procedure. The system consisted of a conductivity probe with the tip close to the fluid exit point in the hopper, and earthed via the body of the hopper. If the level of the process fluid were to fall below the tip of the probe, the circuit contact would break and an alarm would sound to alert the operator. Addition of fluid would reconnect the circuit and stop the alarm. A mute mechanism allowed the operator to temporarily override the alarm if necessary.

The process fluid downpipe into each hopper was positioned on the side of the vessel with a discharge near the base of the cone away from the stirrer. This arrangement prevented splash back and aerosol formation.

## 7.6 Pipework, fittings and valves

All pipings were in corrosion and pitting resistant 316 stainless steel. All the joints were fully welded. Where connecting seals were unavoidable such as for the hoppers and the homogeniser inlet connection, sanitary fittings were used to eliminate accumulation of residual process suspension in the pipework. These fittings were Tri-Clover clamp type unions (Metior Hygienic fittings Ltd, Stainless Fittings, Dudley, West Midlands, UK) designed to give smooth, hygienic, crevice - free seals suitable for CIP. Pipes connecting the feed and collection hoppers to the homogeniser had a 3/4 inch BSP external diameter to prevent blockage, whilst the rest of the pipework had a 1/2 inch BSP diameter.

The valves selected to perform the discrete pass operation were APV diaphragm valves (APV Baker, Crawley, West Sussex, UK) suitable for hygienic systems. They could be cleaned in place, steam sterilised and dismantled. Four valves operating the inlets and outlets to the hoppers were fast acting pneumatically operated, whilst the sample point valves and the exit to the waste hopper were manually controlled (Figure 7.2) (later in the study, the latter valve was retrofitted with a pneumatic version) as there was no need for fast release. The bulk of the valves was of stainless steel and the product contact seals, of Virgin PTFE. A molded PTFE diaphragm provides a barrier to the interspace of the containment chamber. Above this interspace a steam chest is provided allowing for steam sterilisation. The valves may be retrofitted with feed back information on valve seal positioning and electrical interlocking facilities. Calculations indicated that the hold up volume was around 12 mL in the valves. Two sample ports operated by manual APV valves were positioned after the homogeniser and after the heat exchanger before the hoppers.

One important unit was an APV hygienic pressure release valve (APV Gaulin, Crawley, West Sussex, UK) which was installed immediately after the homogeniser in order to provide a safeguard against back



pressure built up in the case of blockage in the heat exchanger whilst the homogeniser was running. Although the homogeniser had its own built-in burst disc (Section 7.3.1), this was designed to release overpressure due to blockage within the valve itself (ie upstream). A pressure indicator comprised of a 63 mm hygienic diaphragm gauge graduated in the range 0 - 0.4 MPa (Knowsley Instrument services Ltd, Liverpool, UK) was also added in order to allow the measurement of any back pressure. This also had the unanticipated advantage of indicating the malfunction of the process valves as some built up of pressure (although not large enough to activate the release valve) could be easily detected.

In addition to the instruments related to the heat exchanger unit (Section 7.7), two 100 mm dial thermometers (type VRS, Knowsley Instrument services Ltd, Liverpool, UK) with 3/4 inch tri-clamp flanges were installed in the pipeline, one after the homogeniser to measure the temperature rise during homogenisation, and one at the exit from the heat exchanger.

## 7.7 Heat exchanger unit

The design of the heat exchanger unit was based on several criteria. It was to be used for cooling the process stream and the jacketed hoppers. No freezing of the product was permitted, minimum hold up volume was desired and the unit had to fit within the space allocated to the entire homogenisation system. Hygienic operation was required with consideration for possible containment.

The use of glycol as the cooling fluid was considered. However, from previous experience it was known that unless a reliable, fast responding control mechanism was used, the process stream was liable to freezing in the heat exchanger. Furthermore the glycol was supplied from a communal source in the plant and any possible leakage of the process fluid could not be contained. It was

therefore decided to use chilled water instead. A self contained chilled water unit was designed with glycol as the coolant Figure (7.3). This consisted of a glycol containing coil in a water bath. Allowance was made for possible built up of an ice film on the coil without blockage of the shell. The top of the water bath was covered with a removable perspex lid to allow for the inspection of the liquid level. Water was recirculated by means of a centrifugal pump suitable for low temperature fluids (CR 2-20 vertical in-line pump, Grundfos Pumps Limited, Leighton Buzzard, Beds, UK). Due to fluctuations in the glycol line pressure, a booster pump identical to that used for water recirculation was installed as it was resistant to glycol corrosion. The temperature of the chilled water was kept constant at 3° C by controlling the flow of glycol with a Sarco temperature control unit (SBRA, Spirax Sarco Cheltenham, Gloucs, UK). It consists of a sensor containing a temperature sensitive fluid which is connected via a capillary tube to a control valve actuator. The sensor was positioned in the outlet pipe from the water heat exchanger. The expansion or contraction of the sensor fluid would move the actuator piston to open or shut the control valve installed in the glycol inlet pipe. A manual valve on the sensor allowed for set point adjustment.

Within the constraints imposed by the initial criteria, several process heat exchangers were assessed. Based on data from other APV three piston homogenisers (Hetherington et al. 1971), a temperature rise of 17.5° C per 100 MPa was expected. The process stream was to be cooled to around 6° C. A coil type heat exchanger was considered with the product passing through 10 meters of 1/4 inch coil. Using reducers, the coil ends would be welded to the larger 1/2 inch process pipeline. This would be a contained operation. Any possible leak from the process stream into the water could also be contained as the cooling water was recirculated and could be discharged into a kill tank. The drawback of the design was large hold up volume (over 160 mL). This could be reduced at the expense of an increase in pressure drop creating a back pressure of around 0.2 MPa on the

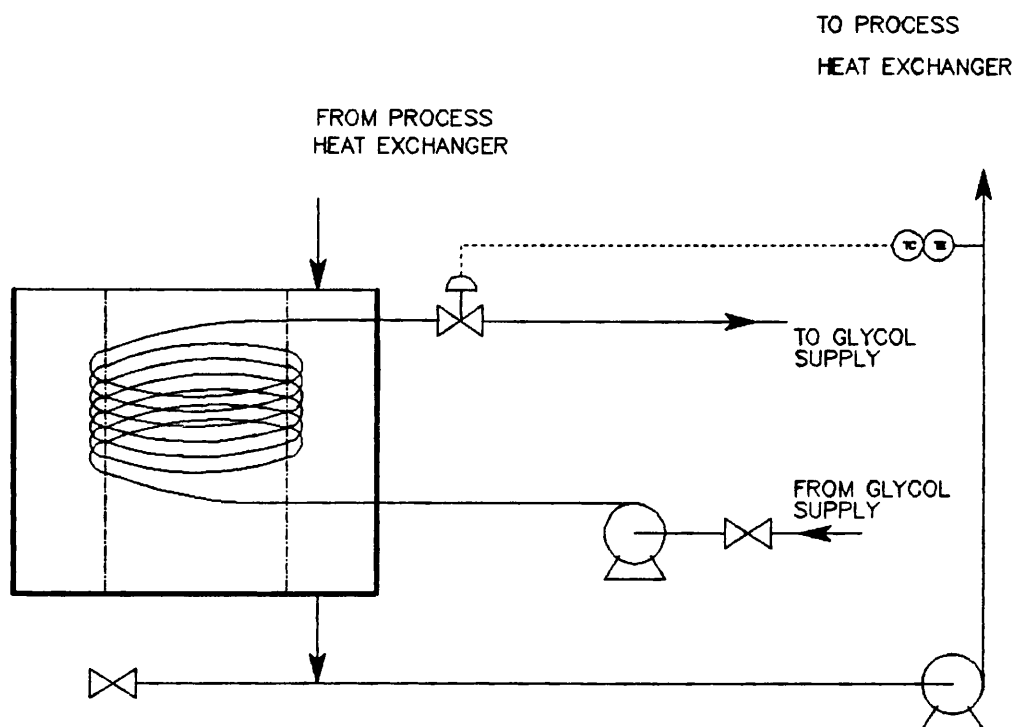


Figure 7.3 Chilled water unit.

homogeniser. In normal operation this does not cause any problems. However, for research studies on homogenisation, it was desirable to minimise extra variables.

Another possibility was to use a miniature plate heat exchanger (with a total height of about 15 cm) which was to be marketed by APV Baker for the home central heating market. Its main feature was that the plates were welded together, thus making the unit suitable for contained operation. This option had to be abandoned since, due to the rationalisation plans of the company, the manufacture of the unit was put under review. It was however considered to weld the plates of an existing small heat exchanger. The only reservation about such a unit was the difficulty to clean the plates.

In view of the fact that the present operation was not contained, it was decided to choose a simple but functional 'off the shelf' heat exchanger with the view to retrofitting the coil type heat exchanger in the future. Based on the experience with the existing heat exchanger used with single piston homogeniser, a Junior Paraflow plate heat exchanger (JNLLP/1784, APV Baker Ltd, Crawley, West Sussex, UK) was selected consisting of a single rising pass (1 of 1 for process, 1 of 2 for service). The advantages were small hold up volume (56 mL) and hygienic design. The possibility of blockage with filamentous microorganisms was ruled out since previous experience with Rhizopus nigricans and other mycelia had been without any significant problems. After commissioning, initial tests indicated that with this particular homogeniser the temperature increase was around 25° C per 100 Mpa which was much higher than expected even though the pump power was the same as that of the three piston homogeniser previously used (Hetherington *et al.* 1971). This was attributed to poor heat dissipation to the environment by the 30 CD. The extra heat load was removed by increasing the heat transfer area (1 of 2 for process, 1 of 3 for service). The hold up volume was increased to 100 mL. However this was still reasonably small in comparison to other alternatives previously considered.

A line diagram of the overall homogenisation system is illustrated in Figure (7.4). A photograph of the integrated system prior to installation is shown in Figure (7.5).

#### 7.8 Control panel

It was desirable to allow the operator to control the homogenisation process from a single monitoring position. For this purpose, a control panel was designed consisting of a frequency gauge together with an adjustment dial to enable flow rate regulation. Manual switches to activate the pneumatic valves – including one for the manual opening of the pressure release valve – and starters for the glycol and the water pumps were also operated from the panel. Additional features included the alarm light and mute connected to the conductivity probe in the hoppers (Section 7.5.2) and an ammeter which was thought essential for routine checking of the pressure gauge accuracy. The panel size was kept to minimum so that it could be mounted together with other parts of the homogeniser on a skid. The only piece of equipment separate from the integrated system was the frequency drive unit and the main starters which could be positioned anywhere in the plant.

#### 7.9 Steam sterilisation and CIP

Provisions for steam sterilisation of the system were made at two points. The first was positioned at the most elevated position in the pipeline above the hoppers (figure 7.5). This made the back steaming of the process heat exchanger possible. It also provided steam access for future pressure vessels which would replace the hoppers. It was envisaged that these vessels would be steamed through their air inlet filters. The second steam point was positioned along the pipeline to the homogeniser in order to sterilise the 30 CD. A steam trap at the lowest point in the

Figure 7.4 Line diagram of the integrated homogenisation system

## Legend to Figure 7.4

AV Actuated Valve  
HV Hand Valve  
PRV Pressure Relief Valve  
TCV Temperature Control Valve

TC Temperature Controller  
TE Temperature Element  
TI Temperature Indicator

LS Level Signal  
M Mixer  
P Pump  
PI Pressure Indicator  
ST Steam Trap  
TP Termination Point  
V Vent

All pipes are identified by a letter indicating the type of fluid they contain. The letter is preceded by the size of the pipe in mm followed by an arbitrary pipe number

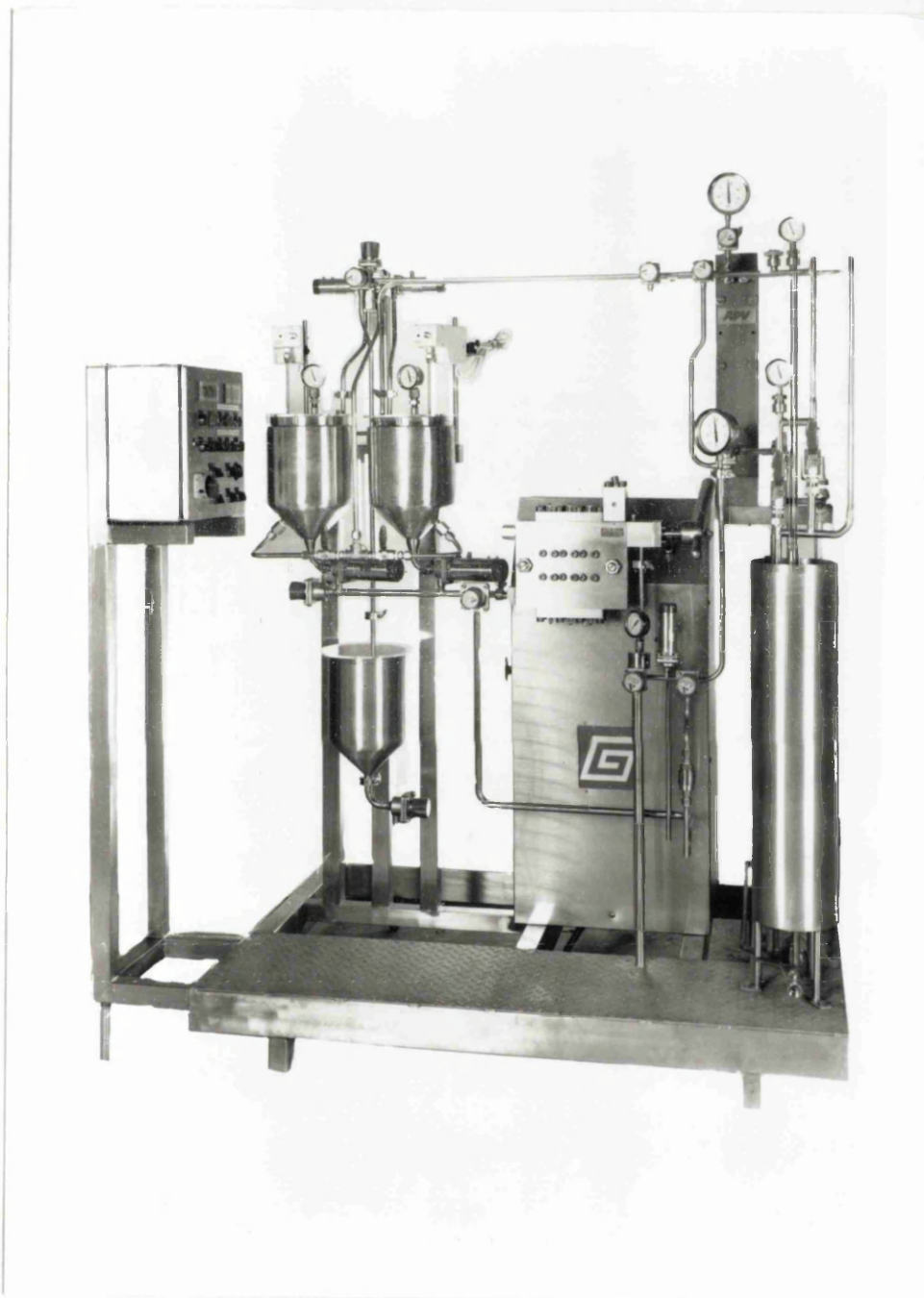


Figure 7.5 Photograph of the integrated homogenisation system (prior to commissioning).



pipework allowed for condensate collection from both steam lines. The water line for the lubrication and cooling of the homogeniser pistons, which was made of thin plastic tubing, would be retrofitted with steel piping to accommodate the steam sterilisation of the packing box.

At the steam termination points a three way valve and a non return valve (not shown in Figure (7.4)) were installed to give access to both soft water in the plant and steam. A by pass over the homogenisation unit allowed for an increase in velocity necessary for cleaning the pipework. Drainage was provided to the edge of the skid. For future CIP, it was envisaged that a contained tank and pipe would be necessary to recirculate 1% sodium hydroxide.

#### 7.10 Conclusion - Future containment

In designing the present integrated homogenisation system, where necessary, provisions were made or guidelines were drawn for the future containment of the homogenisation process. Where appropriate, these were referred to in the design of individual units in this chapter. In this final section, some of the salient points are summarised.

The 30 CD is one of few medium size homogenisers currently available for applications in the biotechnology industry. Double gaskets with leak detection at high pressure points minimise aerosol formation and allow the immediate discovery of failed seals. All the leak pipings could be taken to one contained kill tank. Furthermore, lubricant water for the pistons could be recirculated within a closed unit. The replacement of the present manually operated pressure handwheel with a hydraulic actuator would enable the remote operation of the homogeniser. This may be achieved in conjunction with the full automation of the existing hydraulic valves to control the flow in and out of the hoppers. These, in turn, would be

replaced by pressure vessels suitable for in situ steam sterilisation. In the case where sampling is needed in between the passes, sampling ports similar to those used with fermenters may be considered. However, further evaluation of this aspect of containment would be necessary, given the dynamics of discrete pass operation. The process heat exchanger may be retrofitted with the coil type equipment as outlined in Section 7.7.

## 8. CONCLUSIONS – FUTURE WORK

### 8.1 Mechanism of cell disruption

The relationships put forward in this work describing the mechanism of cell disruption are derived for a narrow range of gap widths at a given pressure. It is therefore of interest to extend the available data to obtain a unifying correlation encompassing a wide range of pressures and gap widths for the geometric configurations studied. Based on the present work, preliminary theoretical predictions appear to indicate that cells are exposed to a range of impact pressures with a threshold minimum value  $P_{tm}$  below which no disruption occurs. It is expected that as the homogenisation pressure increases, a larger proportion of the jet suspension becomes exposed to impact pressures above  $P_{tm}$  and thus a higher breakage rate is achieved. This would be consistent with a first order disruption process (Hetherington et al. 1971). At higher homogenisation pressures, a maximum threshold may be reached beyond which the proportion of jet suspension exposed to  $P_{tm}$  will not increase significantly, and a decrease in homogenisation efficiency will ensue. Such an argument is consistent with the experimental observations made by Dunnill and Lilly (1975) who reported a fall in the disruption rate constant at very high pressures (Section 1.2.4.3). This also in agreement with the findings of this study which showed the presence of an optimal impact distance below which no further significant increase in disruption is achieved (Section 4.6).

Further work should therefore focus on the compilation and analysis of data for a range of pressures with various valve configurations in order to obtain the value(s) of  $P_{tm}$ . The 30 CD homogeniser which

is designed for cell disruption over a wide range of pressures is well suited for the implementation of such a research programme.

## 8.2 Particle sizing and valve design

The design of very high pressure homogenisers such as the 30 CD has been a response, partly, to the need for higher pressures to break tougher microorganisms or release intracellular materials not easily accessible under milder conditions, and partly, to the demand for increasing efficiency and for minimising damage to the product by reducing the number of passes. Each of these contentions, however, merits close scrutiny and therefore research is needed to establish whether higher pressures with lower number of passes results in optimal disruption conditions. This is particularly relevant in cell debris sizing as it is necessary to investigate the way in which the size distributions of homogenised particles change since, as mentioned in Chapter 5, they are of importance to the centrifugal stage of downstream processing.

In general, smaller cell debris sizes are associated with higher protein release, and knife edge valve units perform better than flat valve units. However, there is some indication that the flat valve (FV) results in larger particles for equivalent protein release compared with other geometries (Section 5.2.2). These findings are interesting in that, together with information on impingement, they can form a basis for further research into the optimised design of a homogeniser which can be used for scaled - down operations.

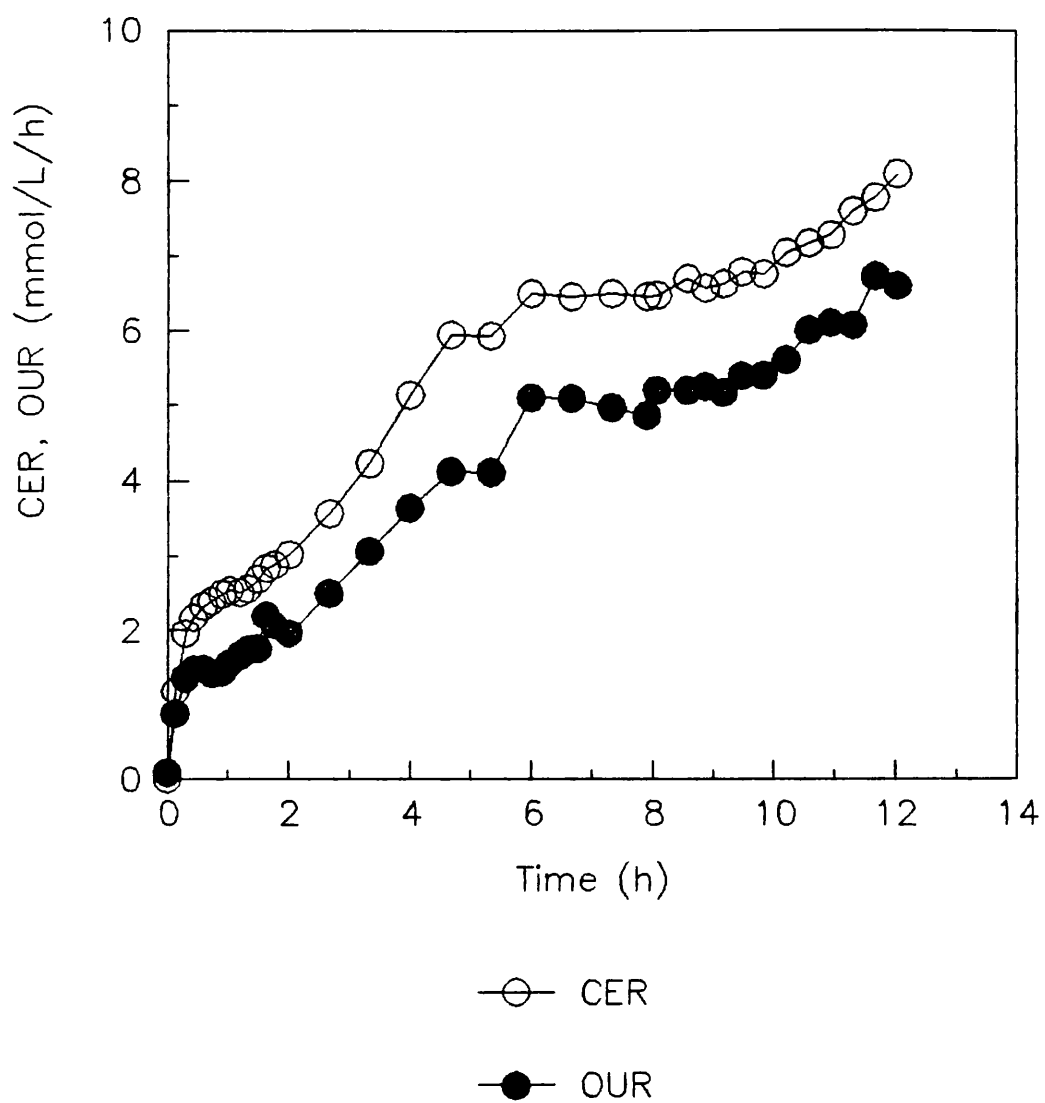
## Appendix A Growth of *Rhizopus nigricans* in fermenters

Fermentations were carried out in several baffled stirred tank reactors of different sizes as outlined in Section 2.5. Small scale fermentations were performed in 14 L and 20 L fermenters corresponding to 10 L and 15 L working volumes respectively. Profiles of these fermentations are illustrated in Figures A1 and A2. For pilot scale fermentations, 42 L and 150 L vessels (working volumes of 30 L and 100 L respectively) were used (Figures A3, A4 and A5).

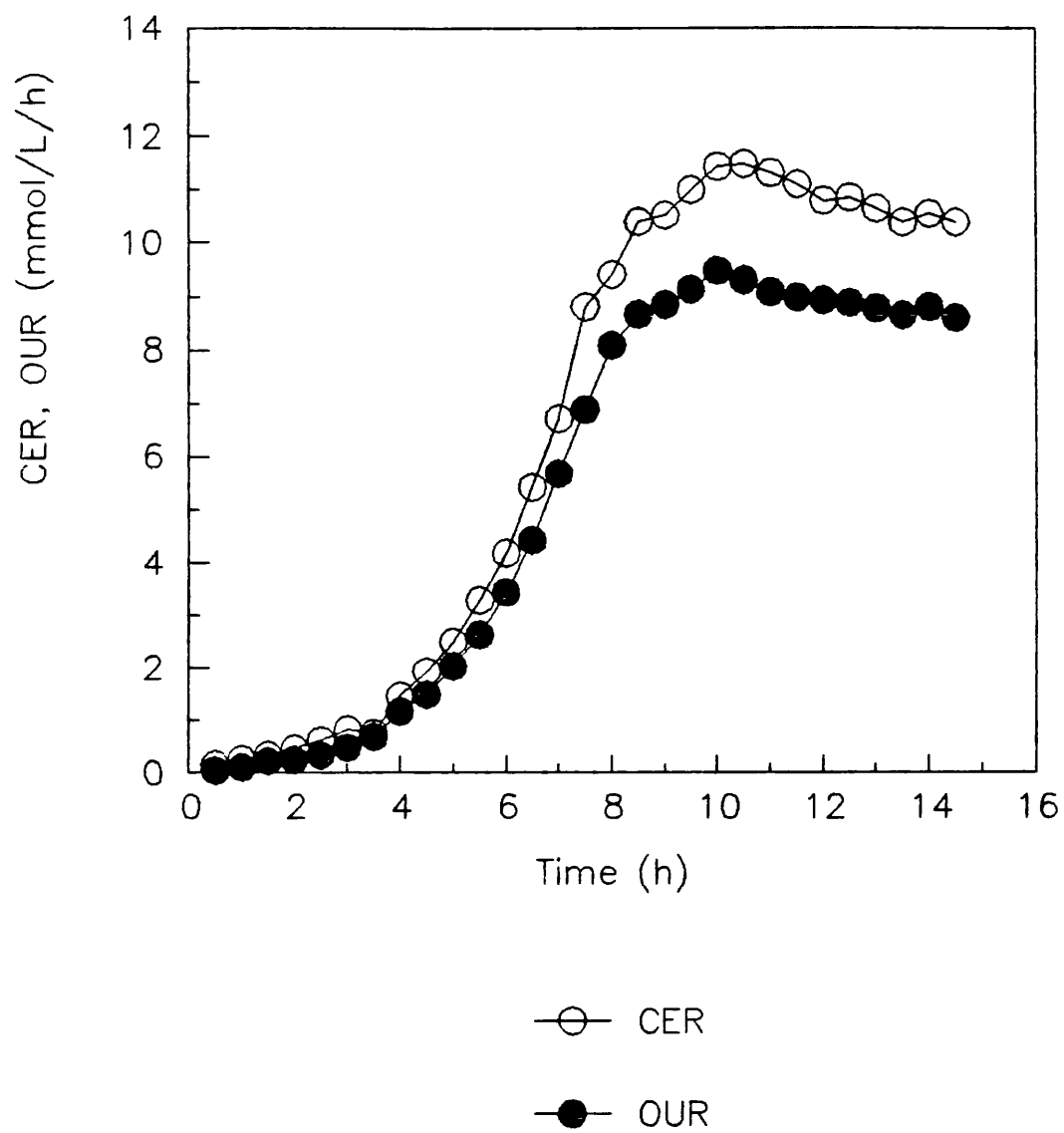
Vigorous cell growth was obtained in the 100 L fermenter which is reflected in the high levels of CER achieved. Furthermore, as explained in Section 3.3.1, the cells harvested from this fermentation showed different morphology, disruption properties and were difficult to disrupt. Few factors may have contributed to the differences observed between the growth pattern of these cells and those cultured in the other fermenters. Firstly, the type of inoculum should be considered. All fermenters except the 100 L, were inoculated with shake flask grown cultures. For the 100 L however, a 10 L fermenter grown seed culture was used. It may be argued that these cells have already adopted to shear forces in the seed fermenter and are therefore more robust when grown in the large fermenter. As mentioned in Section 3.3.1, shear conditions in the fermenter resulting from different vessel geometry could also have contributed to the changes observed. Furthermore, the aeration rate in the 100 L fermenter was higher than in other fermenters contributing to the higher growth rate observed. The scale-up features observed in this study such as changes in cell morphology were also experienced by other workers. Hanisch (1978) attempted to scale up to 600 L (working volume) by using 5 L and 100 L

fermentations as consecutive seed cultures. Pellet formation was obtained. This was ascribed to the high agitation rate. The tip speed was reduced to 2 m/s. This resulted in thick homogeneous growth in the smaller vessels. However, the tip speed reduction to 1.4 m/s in the 1000 L fermenter (600 L working volume) did not alleviate the problem and pellet growth was still observed. Talboys (1983) used shake flask grown cells as inoculum for a 100 L fermentation. The tip speed was set at 2.65 m/s with a low aeration rate (0.1 VVM). Some change in morphology was observed. The cells consisted of fat hyphae forming large matted clumps. However they remained highly branched.

In view of the fact that large quantities of cells are required for disruption studies, the scale-up of Rhizopus nigricans fermentation remains an interesting problem. The use of a 42 L fermenter (30 L working volume) resulted in adequate biomass for use in a single piston homogeniser. For a larger capacity equipment, however, more biomass may be necessary. This may be achieved by detailed optimisation of fermentation in the 42 L fermenter and further scale-up studies of 100 L fermentation.

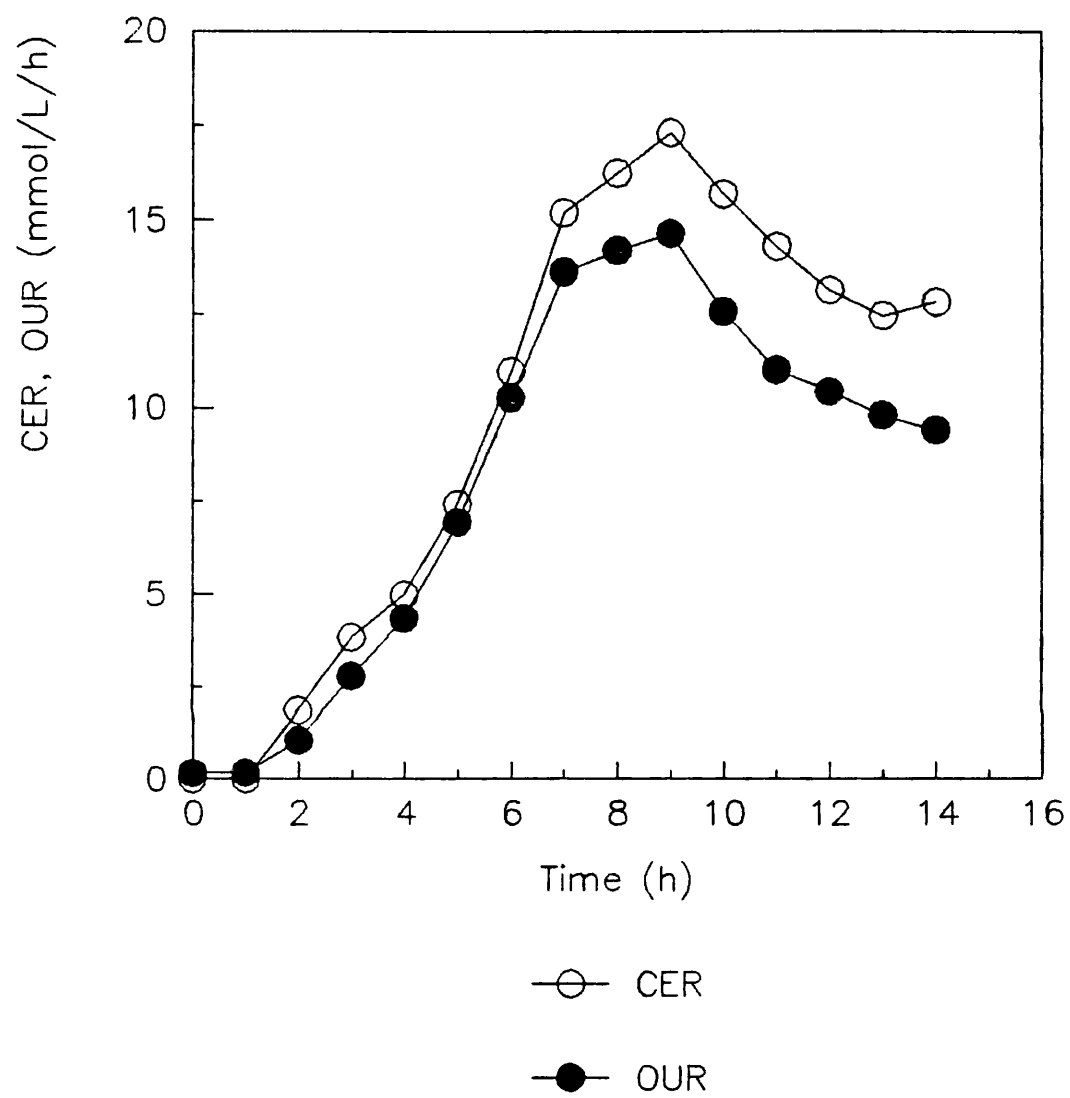


**Figure A1** Profile of a 10 L fermentation

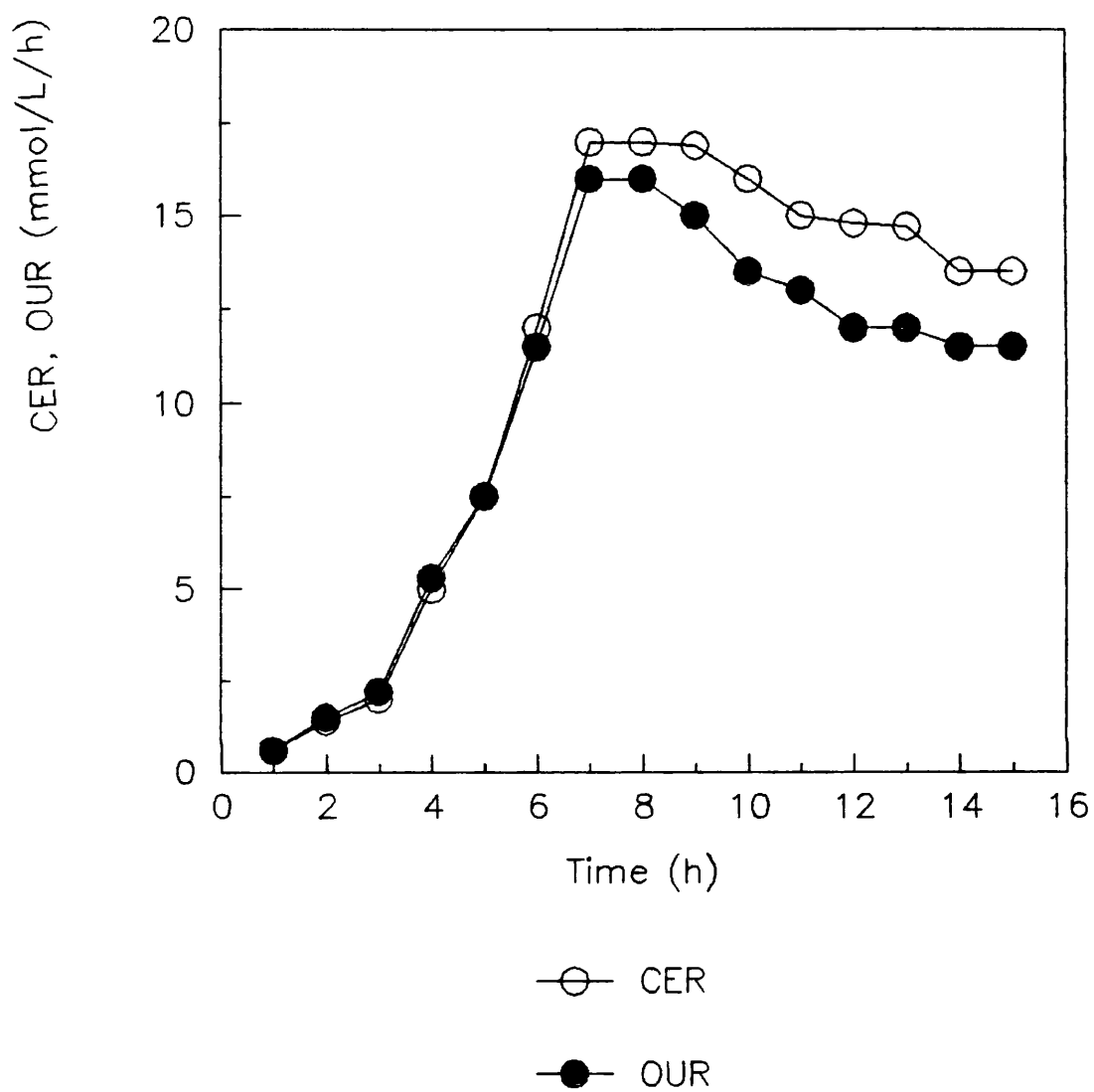


**Figure A2** Profile of a 15 L fermentation

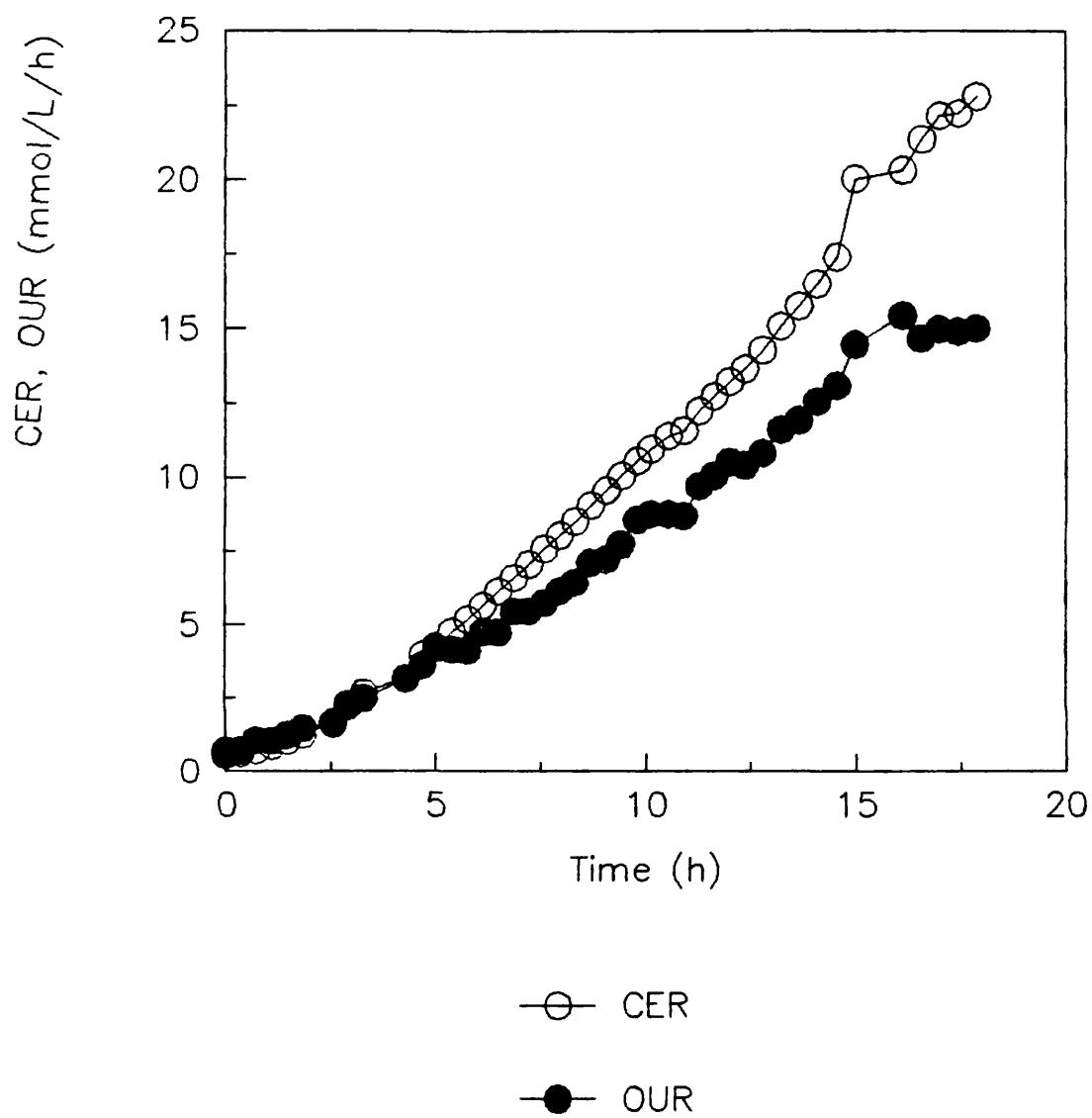




**Figure A3** Profile of a 30 L fermentation



**Figure A4** Profile of a 30 L fermentation (pelleted)



**Figure A5** Profile of a 100 L fermentation

## APPENDIX B Application of Photon correlation spectroscopy (PCS)

The theory of PCS is based on recording the rate of light intensity fluctuations when coherent monochromatic light (eg. laser light) is scattered from particles in Brownian motion. The intensity is indirectly related to the phase of light wave scattered from the particles, which in turn is dependent on the position of the particles. The intensity is detected by a photomultiplier and is converted to an electrical signal. Signals are correlated with delayed versions of themselves (hence, auto-correlation) in a correlator.

The form of a correlation function for a diffusion process is exponential in character. For a monosized particle, it would be a pure exponential. Using a variable time expansion technique, i.e. a process in which the correlator operates at many sample times simultaneously, the correlator measures a summed signal due to many exponential functions combined together by a convolution process. The decay constant of the auto-correlation function is dependent on the diffusion coefficient. The hydrodynamic radius of the particles can therefore be derived via Stokes-Einstein equation.

The Malvern 4700 which is based on a helium- neon continuous wave laser light source, contains a proprietary distribution analysis algorithm which is essentially model free (Malvern 4700 manual 1986). The instrument covers a size range ratio of 100:1 which can be reduced to 10:1 to increase data resolution. the results may be presented as frequency or cumulative distributions of light intensity, particle volume or particle number versus particle size.

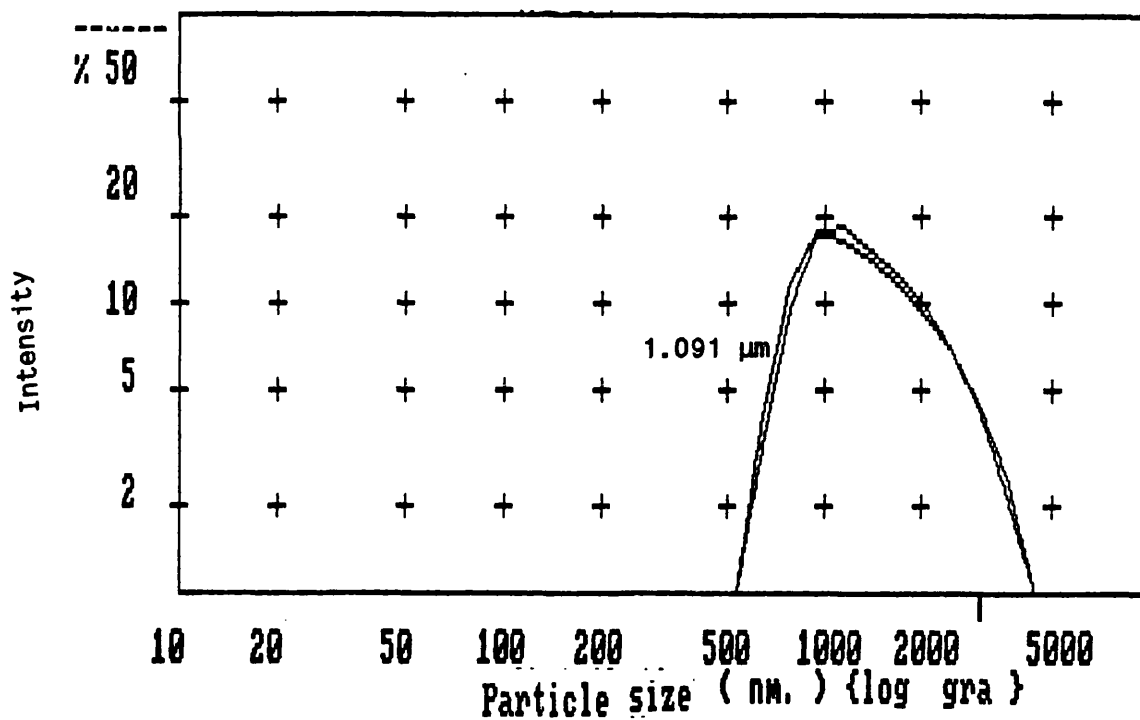
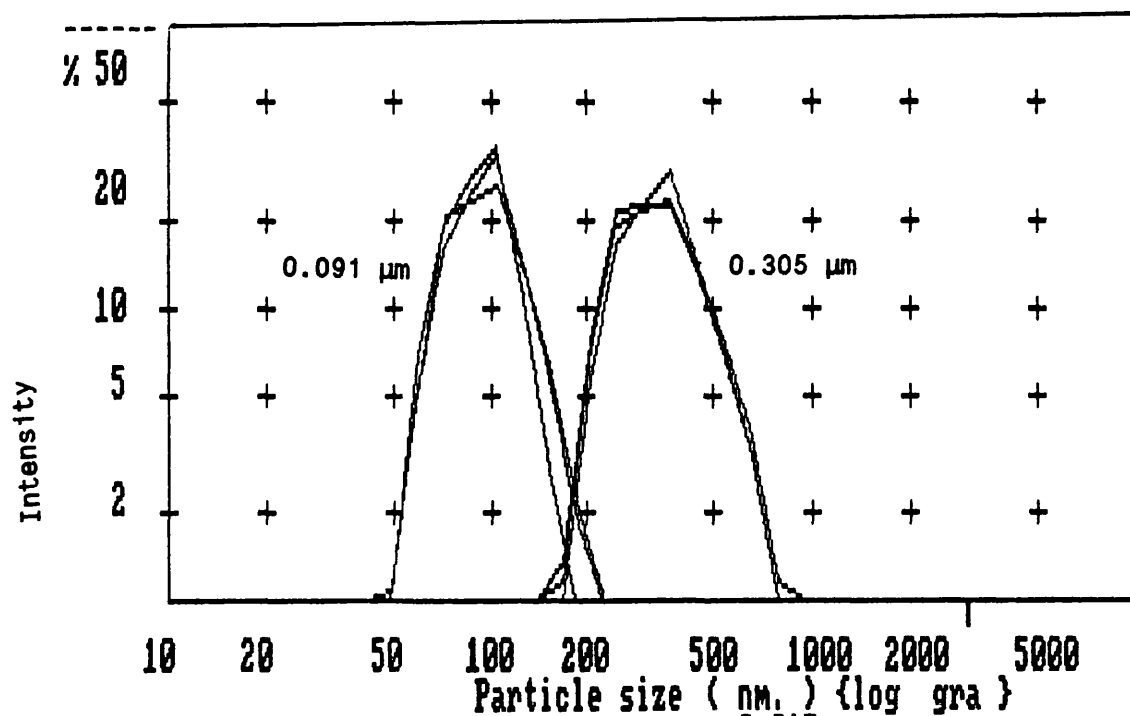
## B.1 Experiments with latex particles

In order to understand and assess the applicability of the PCS technique, a series of experiments with standard latex particles were carried out.

Latex polystyrene particles in the range 0.1 to 1  $\mu\text{m}$  ( $0.091 \mu\text{m} \pm 0.0059$ ,  $0.305 \mu\text{m} \pm 0.008$  and  $1.091 \mu\text{m} \pm 0.0082$ ) were measured. It was possible to test the resolution of a known bimodal distribution of the two closest particle sizes and also test the resolution of a multimodal distribution.

## B.2 Monomodal distributions

The latex particles (10% solid contents) were diluted in deionised water (0.1  $\mu\text{m}$  filtered) 804, 2010 and 5226 fold for 0.091, 0.305 and 1.091  $\mu\text{m}$  sizes respectively. Different dilutions had to be used for different sizes in order to eliminate multiscattering and also particle interaction which masks the Brownian motion of the particles (Section B4). The theory of light scattering which relates the rate of light scatter to the Brownian motion of particles in suspension, assumes infinite dilution. Figures B1 and B2 show the intensity distributions for the three latex particles mentioned above. Figure B3 gives a typical output from the Malvern instrument. It must be noted that although the distributions may be expressed in terms of intensity, volume or number of particles versus particle size or diffusion coefficient, the intensity versus particle size is recommended to be used for comparative studies. This is because the scattering rate is very strongly dependent on particle size. The instrument measures the intensity directly which is then translated into weight or number distributions. The mass transformation assumes solid particles of equal density (since light scattering is actually sensitive to volume and not mass). This transformation utilises a scattering model which may relate very



**Figure B1** Intensity distributions for 0.091 μm, 0.305 μm and 1.091 μm latex particles (all measured in separate suspensions).

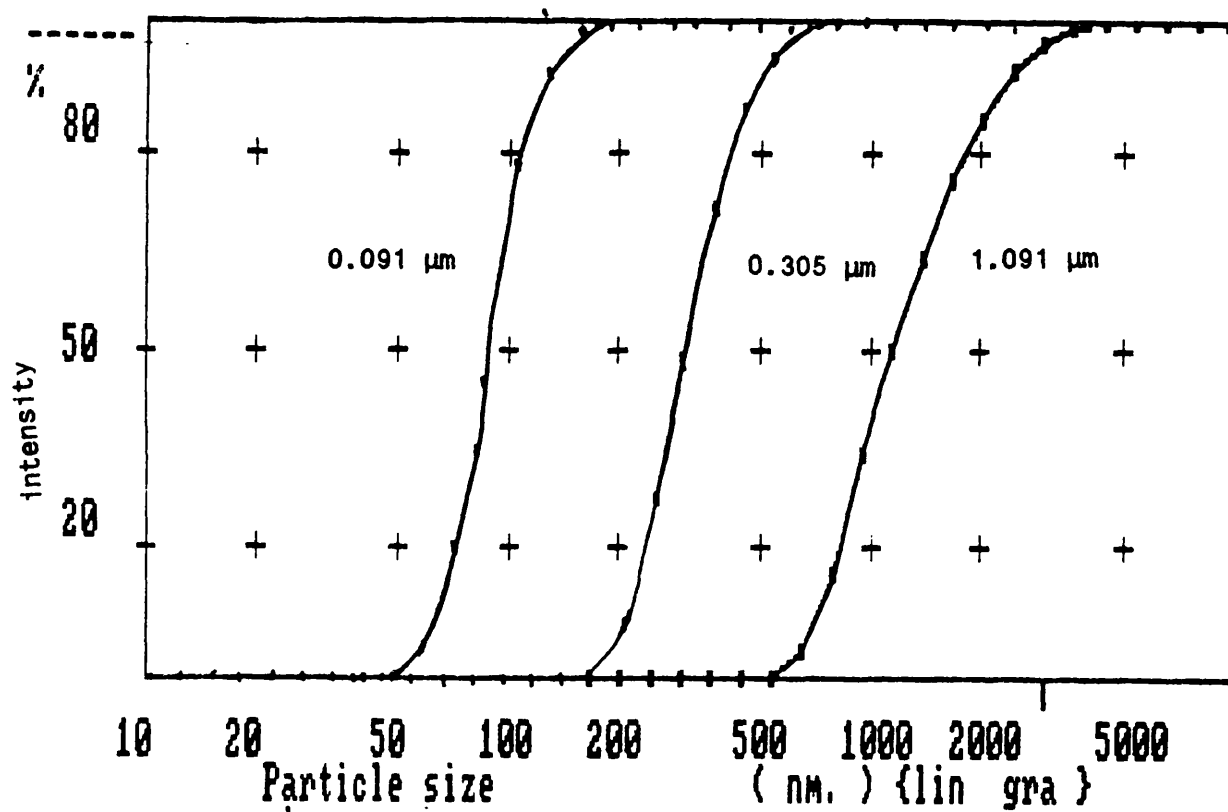


Figure B2 Cumulative intensity undersize distributions for 0.091  $\mu\text{m}$ , 0.305  $\mu\text{m}$  and 1.091  $\mu\text{m}$  latex particles

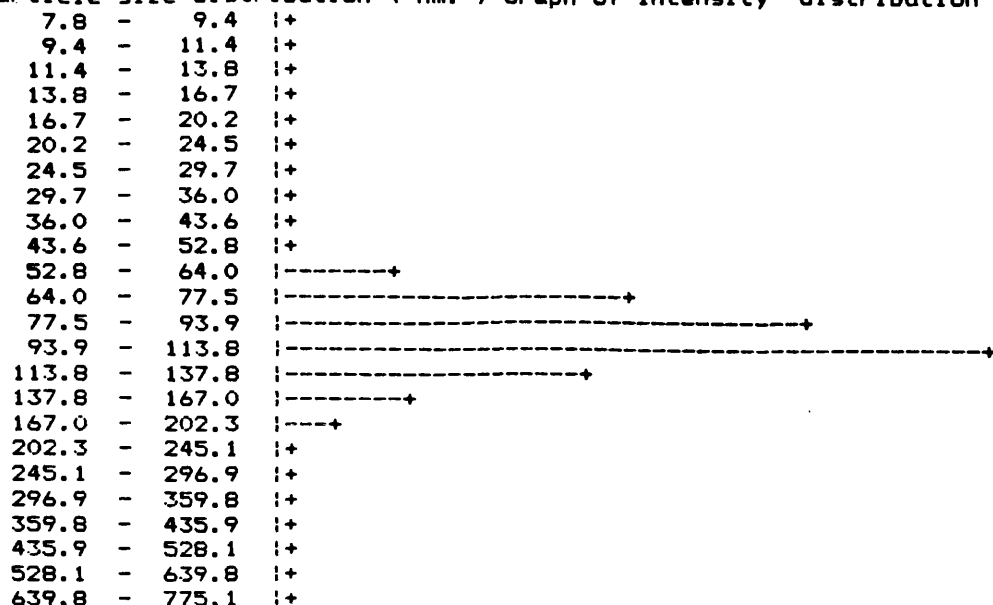
## MALVERN AUTOMEASURE 4700

sample : 91nm latex

Live Data from Correlator

Temperature 27.0 Viscosity 0.8513 Refractive Index 1.330 Angle 90.0

Particle size distribution ( nm. ) Graph of Intensity distribution



Size Class	% by Intensity			% by mass			% by number		
	Under	In	Above	Under	In	Above	Under	In	Above
7.8 - 9.4	0.0	0.0	100.0	0.0	0.0	100.0	0.0	0.0	100.0
9.4 - 11.4	0.0	0.0	100.0	0.0	0.0	100.0	0.0	0.0	100.0
11.4 - 13.8	0.0	0.0	100.0	0.0	0.0	100.0	0.0	0.0	100.0
13.8 - 16.7	0.0	0.0	100.0	0.0	0.0	100.0	0.0	0.0	100.0
16.7 - 20.2	0.0	0.0	100.0	0.0	0.0	100.0	0.0	0.0	100.0
20.2 - 24.5	0.0	0.0	100.0	0.0	0.0	100.0	0.0	0.0	100.0
24.5 - 29.7	0.0	0.0	100.0	0.0	0.0	100.0	0.0	0.0	100.0
29.7 - 36.0	0.0	0.0	100.0	0.0	0.0	100.0	0.0	0.0	100.0
36.0 - 43.6	0.0	0.0	100.0	0.0	0.0	100.0	0.0	0.0	100.0
43.6 - 52.8	0.0	0.3	99.7	0.0	4.8	95.2	0.0	16.9	83.1
52.8 - 64.0	0.3	4.9	94.8	4.8	15.5	79.7	16.9	30.8	52.3
64.0 - 77.5	5.2	16.0	78.8	20.3	24.9	54.8	47.7	27.9	24.4
77.5 - 93.9	21.2	24.2	54.6	45.2	25.4	29.4	75.6	16.0	8.4
93.9 - 113.8	45.4	32.7	21.9	70.6	18.3	11.1	91.6	6.5	1.9
113.8 - 137.8	78.1	14.1	7.8	88.9	8.3	2.7	98.1	1.7	0.3
137.8 - 167.0	92.2	5.9	2.0	97.3	2.2	0.5	99.7	0.2	0.0
167.0 - 202.3	98.0	2.0	0.0	99.5	0.5	0.0	100.0	0.0	0.0
202.3 - 245.1	100.0	0.0	0.0	100.0	0.0	0.0	100.0	0.0	0.0
245.1 - 296.9	100.0	0.0	0.0	100.0	0.0	0.0	100.0	0.0	0.0
296.9 - 359.8	100.0	0.0	0.0	100.0	0.0	0.0	100.0	0.0	0.0
359.8 - 435.9	100.0	0.0	0.0	100.0	0.0	0.0	100.0	0.0	0.0
435.9 - 528.1	100.0	0.0	0.0	100.0	0.0	0.0	100.0	0.0	0.0
528.1 - 639.8	100.0	0.0	0.0	100.0	0.0	0.0	100.0	0.0	0.0
639.8 - 775.1	100.0	0.0	0.0	100.0	0.0	0.0	100.0	0.0	0.0

Average Mean 86.5 Poly 0.046 Dist. mean 98.8 St.Dev. 26.0

Analysis range 100 : fit : 0.0212

Run : counts/1000 : % merit : % in-range : Count rate 1000's /sec

7 23359.4 74.8 99.2 278.1

Figure B3 Typical data output from PCS Malvern 4700.



small signals to very large parts of the particle size distribution expressed by weight or number though not by the amount of light the particles scatter. Errors may therefore be introduced particularly for particles over 0.5  $\mu\text{m}$  in diameter.

### B.3 Significance of parameters obtained in the results

#### Z average mean and polydispersity

The Z average mean of a monodisperse distribution may be thought of as the size corresponding to the mean light scattering response of that distribution. The term "Z average" is used because no account is taken of the fact that particles of different sizes scatter different amounts of light. The Z average mean of a latex particle dispersion is expected to agree well with the arithmetic mean of the distribution because of the narrowness of the distribution. This is generally true for standard latex particles.

The polydispersity index is a model free measure of the variance of the mathematical form of the auto-correlation function. The Z average mean and polydispersity do not describe the form of the distribution (i.e. monomodal or multimodal) except that if polydispersity is low (below 0.1) it means that the distribution is narrow.

#### Analysis range

It is possible to set the range of particle sizes to be measured . This is typically 100:1 , which means that for a particle mean diameter of 0.1  $\mu\text{m}$ , the instrument measures a span of 0.01 to 1  $\mu\text{m}$ . The range selected does not affect the distribution provided it is wide enough to fit all the information from the light scattering data. The reason for varying the range is to control the resolution once the intensity distribution is known.

### Goodness of fit

The goodness of fit gives the difference between the correlation function measured and that corresponding to the calculated model. The smaller the value, the better the fit. It is estimated that values close to or less than  $50 \times 10^{-3}$  give a good fit.

### B.4 Effect of concentration

The concentration of particles may affect the results obtained. At extremely low concentrations, the scattering due to the particle is relatively small and experimental artifacts such as reflection from the sample cell wall and scattering from dust particles are likely to be a problem. At high concentrations, multiple scattering (i.e. detection of photons which scatter from several particles) is likely to be a problem. Furthermore, the interactions between particles cause departure from pure Brownian motion. The threshold concentration at which particle interactions begin to occur has not been well established experimentally. It may vary with particle size. Data reported for  $0.109 \mu\text{m}$  latex particles show conflicting threshold values ranging from 0.0001% solids to 0.1%, whilst for  $0.407 \mu\text{m}$  particles a threshold value of 0.003% has been found (Stock and Ray 1985). It is therefore difficult to assess the optimum sample concentration a priori. One indication is the visual observation of the laser beam passing through the sample, which should be a crisp line without glow (Section 2.10.2.2). The manufactures of the Malvern equipment state a guide line for dilution of less than 0.01% but also stress that this figure is very much dependent on the size of the particle.

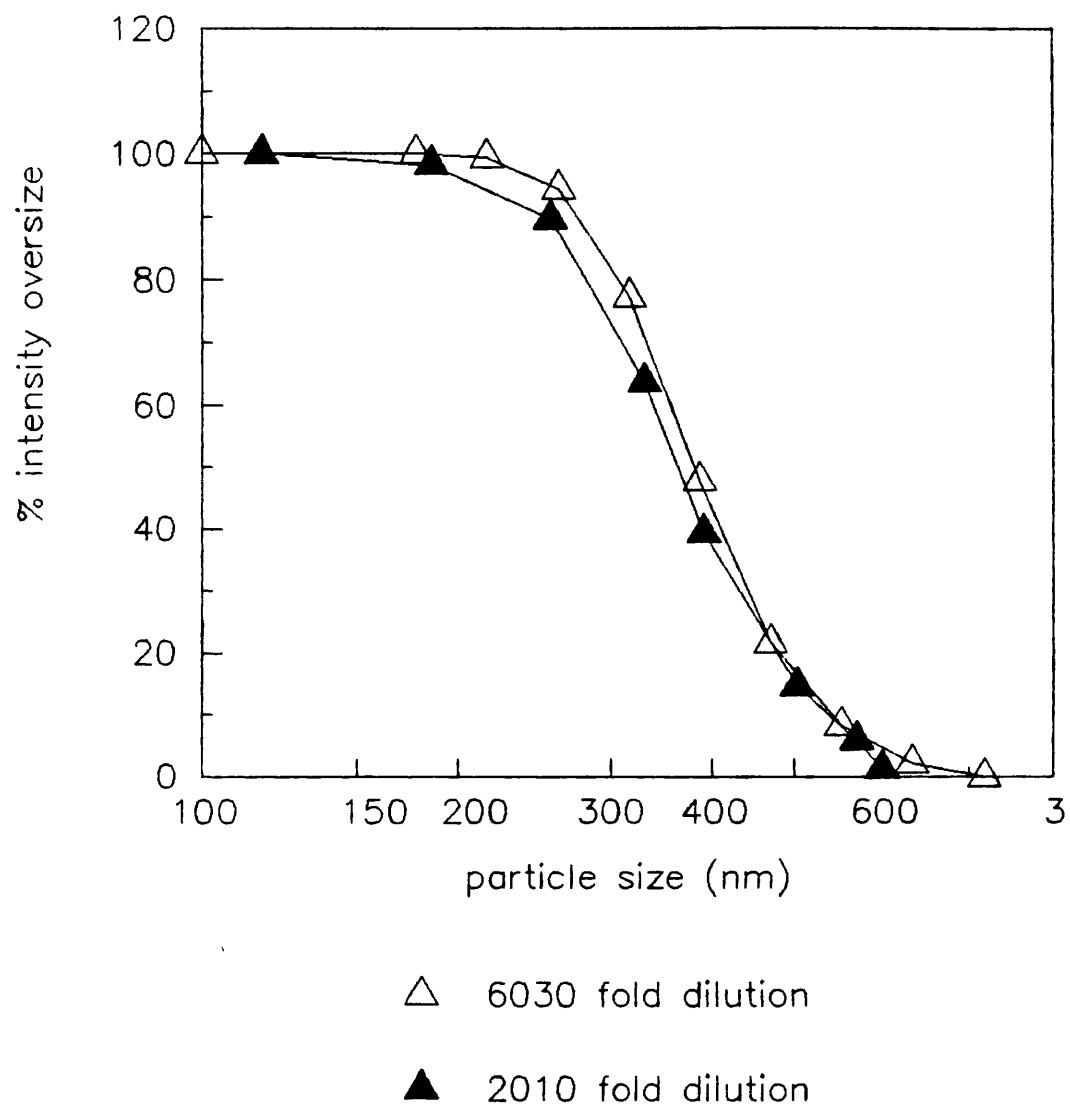
For particles of size less than the wavelength of the incident light (i.e. 623 nm), the intensity is proportional to the 6th power of the particle diameter. For larger particles, this dependence is less strong and the intensity is also a function of the scattering angle.

However, for a given dispersion, the light scattered from few larger particles can mask the scatter from the smaller particles unless enough of these are present to redress the balance.

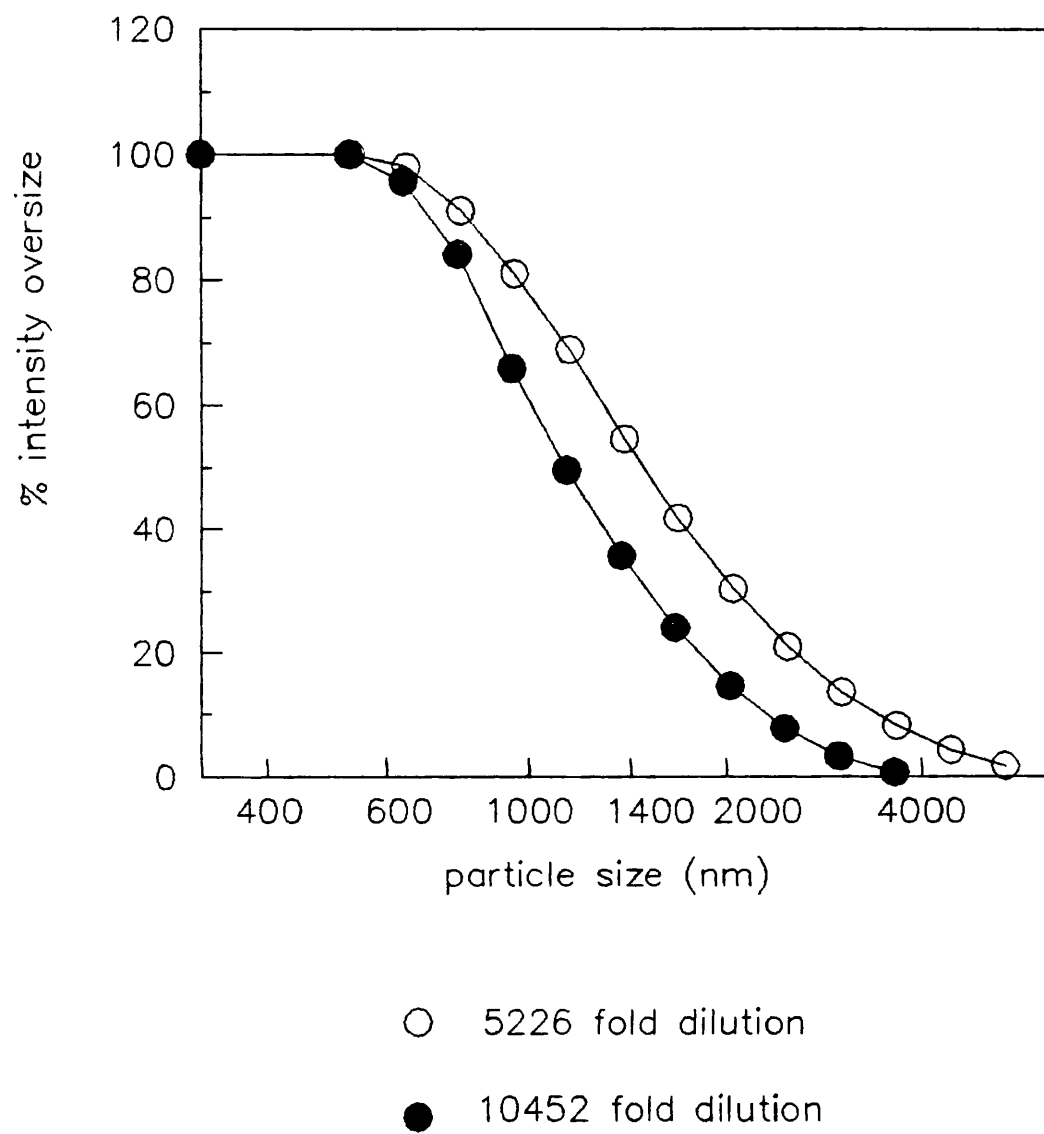
In this study, results indicated that for latex particles of 0.305  $\mu\text{m}$  diameter, a range of 2000 to over 6000 fold dilution did not affect the resultant intensity distribution (Figure B4) (i.e. the solids content of the dispersion was reduced from 10% to 0.005% and 0.0017% respectively). For larger latex particles (1.091 $\mu\text{m}$ ), two dilutions of 5200 and 10400 were tested corresponding to a reduction in the solids content of the dispersion from 10% to 0.002% and 0.001%. Results indicated that the intensity distribution for this particle size is concentration dependent over the range tested (Figure B5). The lower dilution gave the visual threshold for obtaining a clear, glowless beam through the sample. It was therefore expected to obtain a similar intensity distribution at the higher dilution. However, the resultant distribution was broader. The goodness of fit was consistently above the recommended upper limit of  $50 \times 10^{-3}$ . This together with the general wideness of the distribution at all dilutions could be attributed to possible agglomeration of particles in dispersion.

#### B.5 Selection of total experiment duration

The experimental time is the time duration to analyse N number of samples. The selection of sample time depends on the rate of decay of the correlation function. The longer the sample interval, the greater the probability of larger counts per sample. However, the result is that the correlator cannot deal with all the signal information it receives and inevitably some will be lost. Too short a sample interval, on the other hand, results in only a portion of the signal information being examined. the choice of optimum experimental duration is therefore important in order to reduce both statistical error and unnecessarily long experimentation.



**Figure B4** Effect of dilution on the intensity distribution of 0.305  $\mu\text{m}$  latex particles.



**Figure B5** Effect of dilution on the intensity distribution of 1.091  $\mu\text{m}$  latex particles.

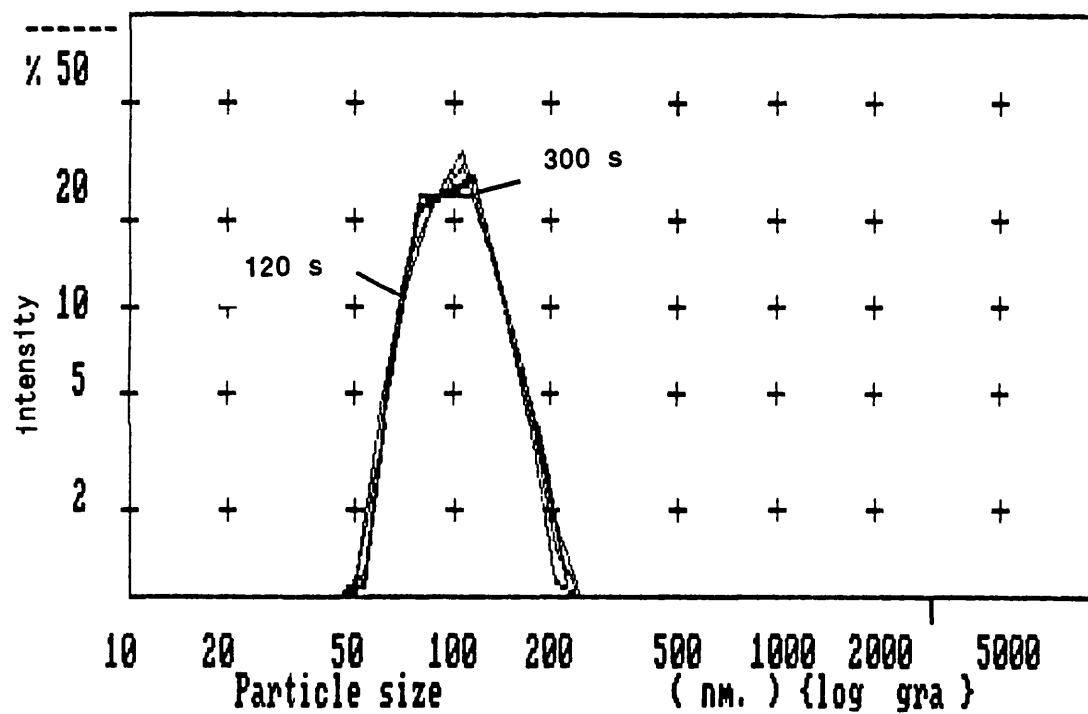
Larger particles by virtue of their slow motion require longer experimental duration to provide adequate data for the correlator. Figure B6 indicates that for submicron size particles (e.g. 0.091 $\mu\text{m}$  diameter), increasing the duration from 120 seconds to 300 seconds did not affect the distribution significantly. However, for 1.091  $\mu\text{m}$  particles, an increase in the time from 120 seconds to 250 seconds resulted in a comparatively better fit ( $66.6 \times 10^{-3}$  against  $75.1 \times 10^{-3}$ ) and less polydispersity (0.110 against 0.201) (Figures B7 and B8).

#### B.6 Bimodal and polymodal distributions

Experiments with latex particles demonstrated that with careful selection of instrument settings, the PCS was able to successfully measure monodisperse distributions (Figures B1, and B2). It was also possible to measure bimodal distributions. However, for polymodal distributions, information was truncated and presented as two peaks. This was to be expected as being the limit of resolution of the installed software.

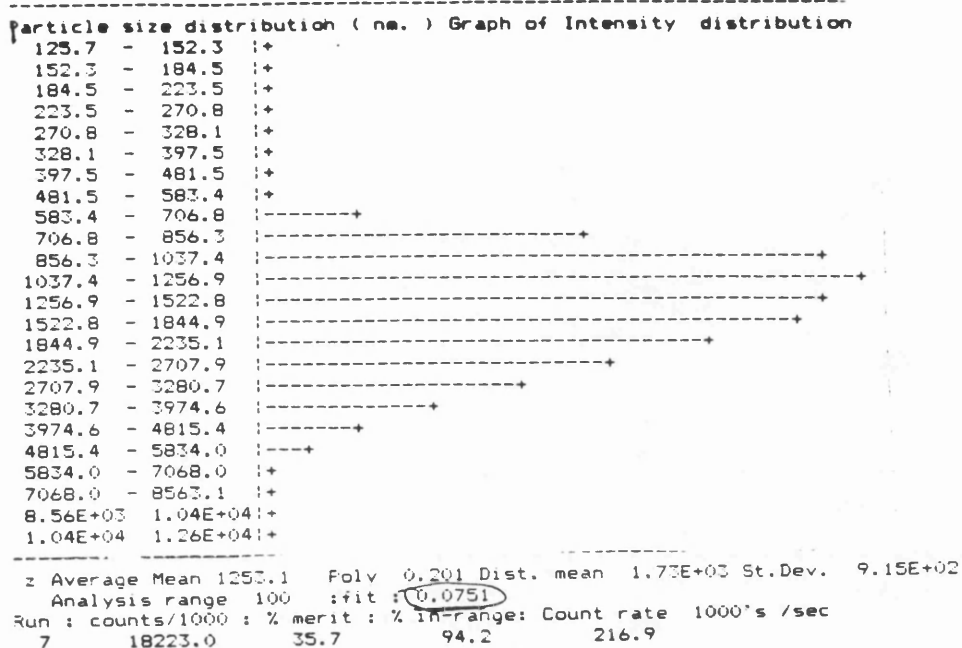
The degree of resolution of two close particle sizes in a bimodal distribution was tested using a dispersion containing 0.091  $\mu\text{m}$  and 0.35  $\mu\text{m}$  particles (size ratio 3.35:1) (Figure B9(a) and B9(b)). It was not always possible to detect the bimodal nature of the distribution and at times it was required to reduce the analysis range from 100:1 to 10:1 before a bimodal trend became apparent.

For a mixture of 3 particle sizes (0.091  $\mu\text{m}$ , 0.305  $\mu\text{m}$  and 1.091  $\mu\text{m}$ ), a bimodal distribution was obtained which truncated the results towards the smaller size particles (Figure B10(a) and B10(b)). It was found necessary to increase the experiment duration in order to obtain sufficient data for the larger particles in the samples.

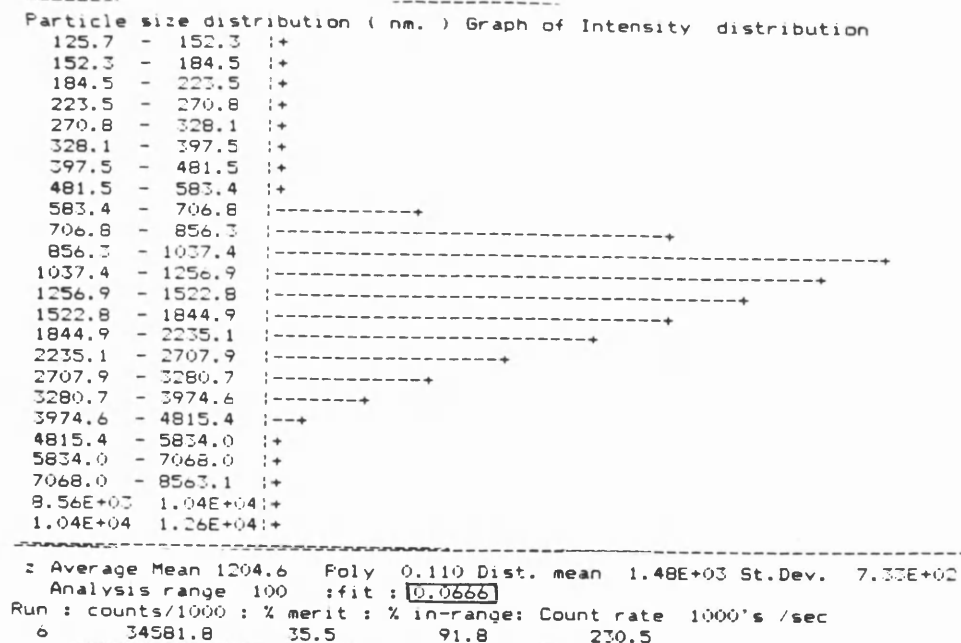


**Figure B6** Effect of experimental duration on the intensity distribution of 0.091  $\mu\text{m}$  latex particles.

120 s



250 s



**Figure B7** Intensity distributions for 1.091  $\mu\text{m}$  latex particles at 120 s and 250 s duration times.



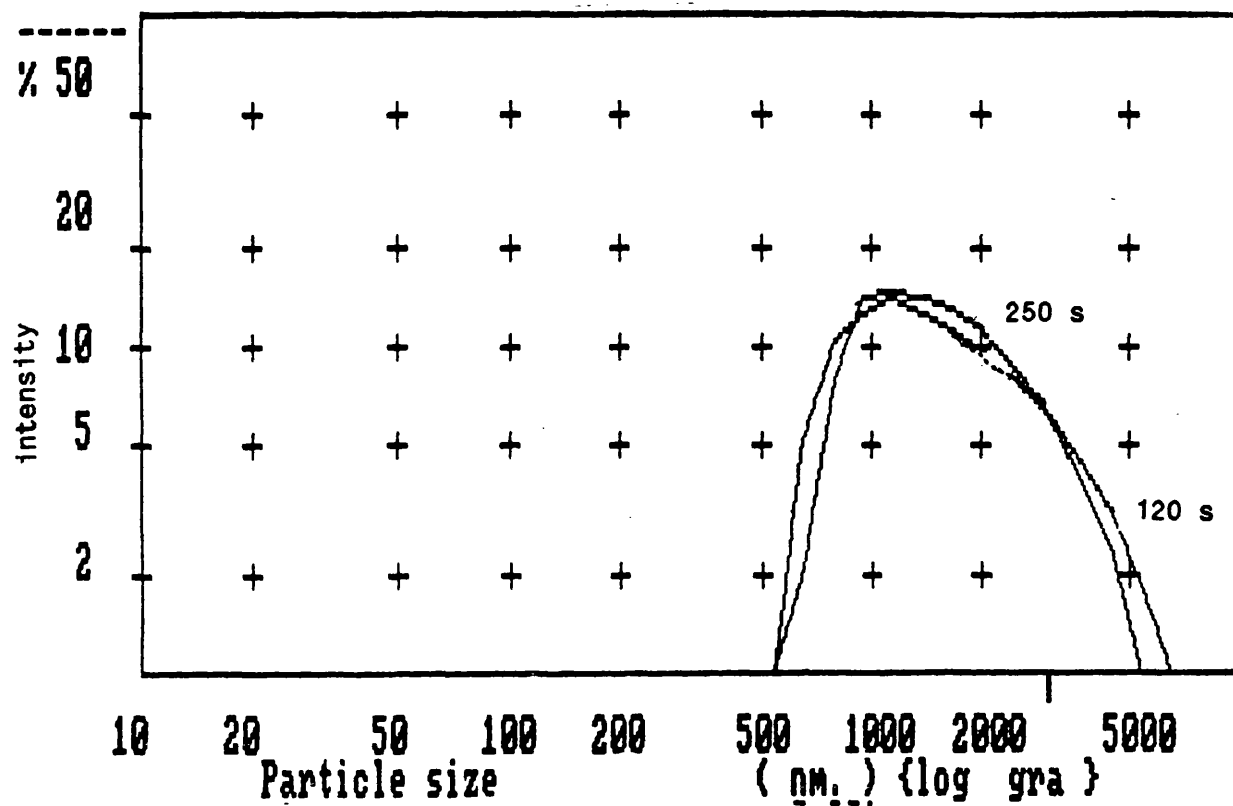
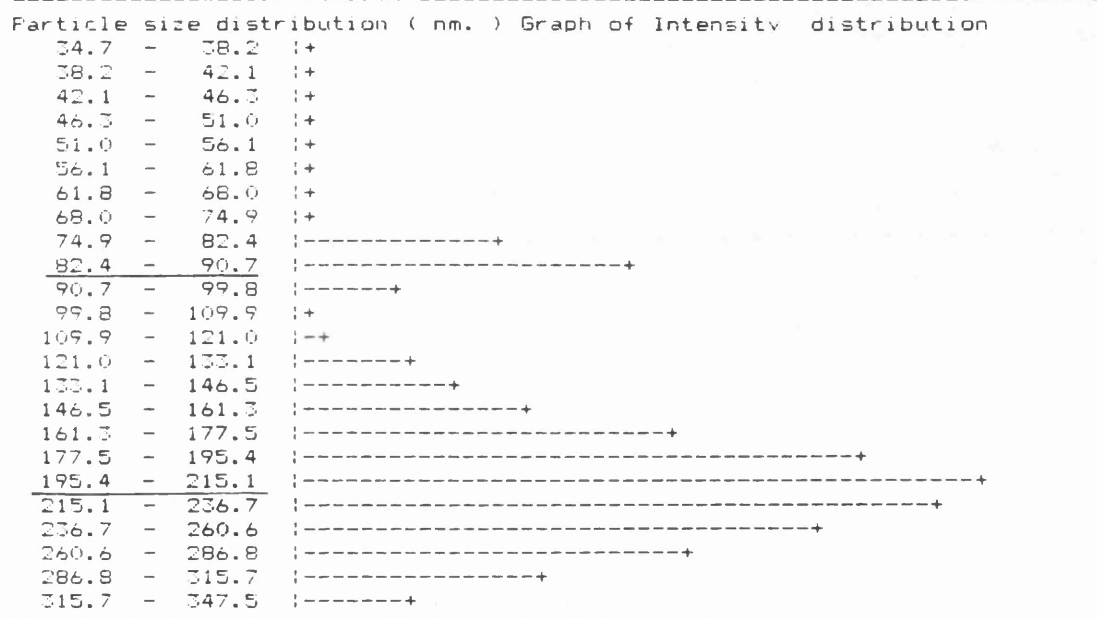


Figure B8 Effect of experimental duration on the intensity distribution of 1.091  $\mu\text{m}$  latex particles.



z Average Mean 121.4 Poly 0.268 Dist. mean 198.3 St.Dev. 62.7  
 Analysis range 10 : fit : 0.0489  
 Run : counts/1000 : % merit : % in-range: Count rate 1000's /sec  
 0 16780.0 75.1 99.5 233.1

Figure B9(a)

Intensity distribution of a mixed  
 suspension of 0.091  $\mu\text{m}$  and 0.305  $\mu\text{m}$   
 latex particles.

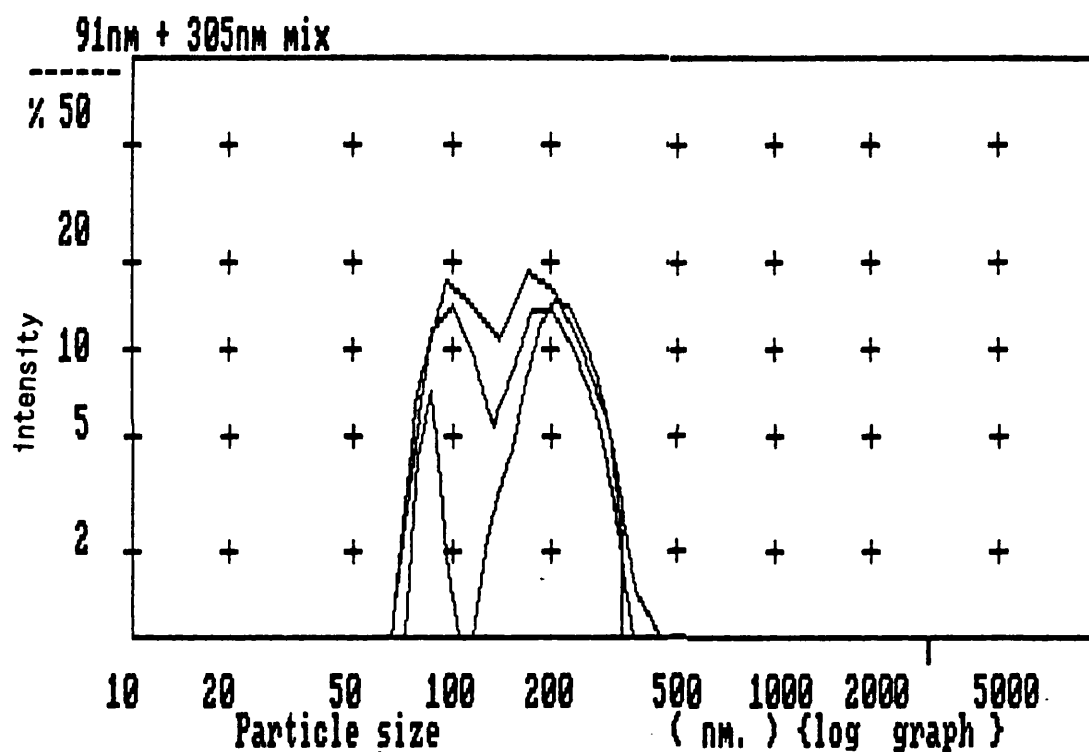
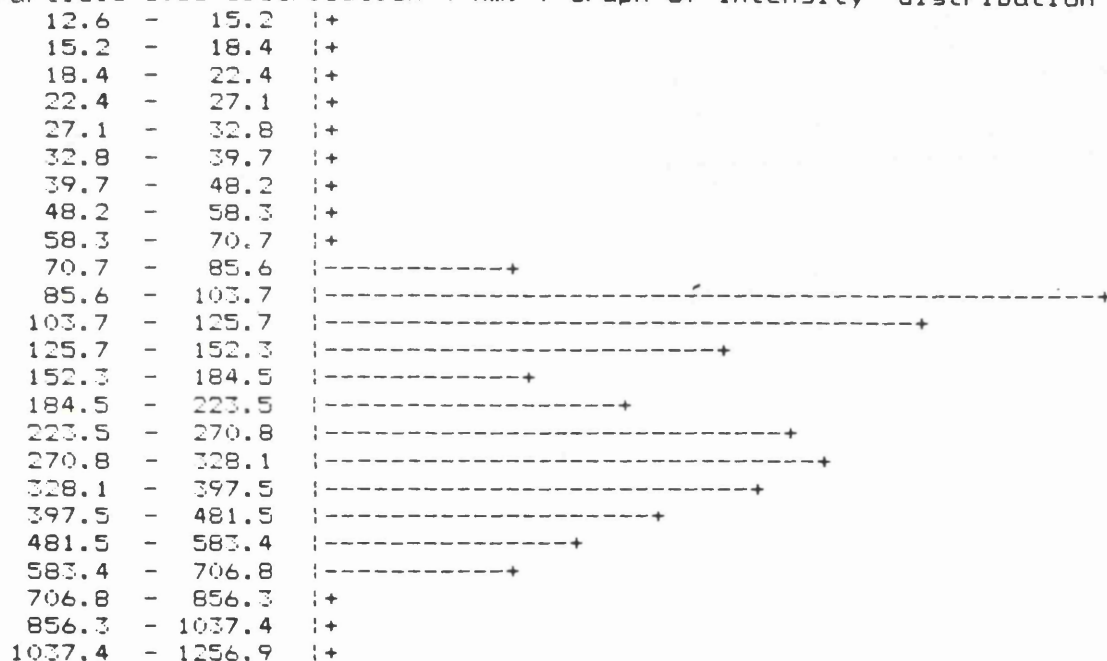


Figure B9(b)

Intensity distribution of a mixed suspension of 0.091  $\mu\text{m}$  and 0.305  $\mu\text{m}$  latex particles (alternative representation).

-----  
Particle size distribution ( nm. ) Graph of Intensity distribution



-----  
 z Average Mean 142.3 Poly 0.385 Dist. mean 242.7 St.Dev. 153.2  
 Analysis range 100 :fit : 0.0258  
 Run : counts/1000 : % merit : % in-range: Count rate 1000's /sec  
 5 17505.5 73.6 95.4 140.0

Figure B10(a)

Intensity distribution of a mixed suspension of 0.091  $\mu\text{m}$ , 0.305  $\mu\text{m}$  and 1.091  $\mu\text{m}$  latex particles.

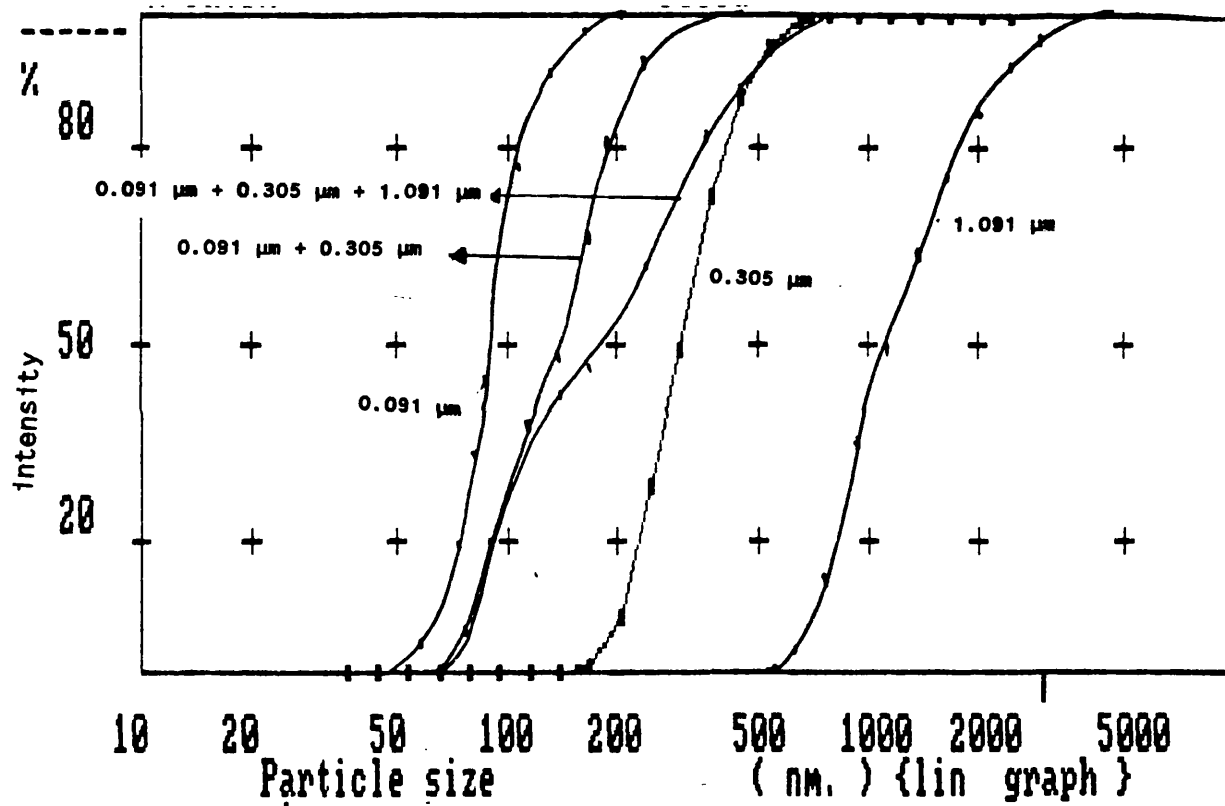


Figure B10(b) Cumulative intensity undersize distributions for single and mixed latex particle suspensions.

## NOMENCLATURE

a	pressure exponent	-
d	diameter	m
$d_m$	minimum diameter	m
$\delta$	cell wall strength	$N\ m^{-2}$
$\bar{G}$	mean velocity gradient	$s^{-1}$
h	valve gap width	m
$K_o$	parameter for kinetic energy and viscous losses (Equation 1.3)	-
K	disruption rate constant	-
k	disruption rate constant (Equation 1.1)	$Pa^a$
L	length of capillary	m
N	pass number	-
P	pressure	Pa
$P_{11}-P_{22}$	normal stress difference	$N\ m^{-2}$
$P_{tm}$	threshold minimum pressure	Pa
$P_s$	stagnation pressure	Pa
$P_v$	power dissipated per unit volume	$W\ m^{-3}$
Q	flow rate	$m^3\ s^{-1}$
r	radial position in a capillary	m
R	exit zone radius (Figure 6.1)	m
Re	Reynolds number	-
$R_m$	maximum protein released	mg/g packed cells or mg/mg cell dry weight
$R_o$	entry zone radius (Figure 6.1)	m
$R_p$	soluble protein released	mg/g packed cells or mg/mg cell dry weight
U	exit velocity	$m\ s^{-1}$
$U_o$	entry velocity	$m\ s^{-1}$
X	impact distance	m

$a$	entry loss factor	-
$a'$	exit loss factor	-
$\eta$	kinematic viscosity	$\text{m}^2 \text{s}^{-1}$
$\sigma$	density	$\text{kg m}^{-3}$
$\tau$	shear stress	$\text{N m}^{-2}$
$\tau_m$	maximum wall shear stress	$\text{N m}^{-2}$
$\mu$	viscosity	$\text{Pa s}$

#### ABBREVIATIONS

ADH	alcohol dehydrogenase
CD	Cell Disruption unit
CER	Carbon dioxide evolution rate
CR	Cell Rupture unit
CRF	Cell Rupture type and flat valve rod
FV	flat valve unit
KE	Knife-edge unit
OUR	Oxygen uptake rate
PCS	Photon correlation spectroscopy

## REFERENCES

- Aldermann, B., Hofer, M. J.Gen.Microbiol. 1984, 130, 711-723
- APV-Gaulin Technical Bulletin 1985, 74
- Augenstein, D.C., Thrasher, K., Sinskey, A.J., Wang, D.I.C. Biotechnol. Bioeng. 1974, 16, 1433-1447
- Asenjo, J.A., Dunnill, P. Biotechnol.Bioeng. 1981, 23, 1045-1056
- Asenjo, J.A., Andrews, B.A., Hunter, J.B., Lecorre, S. Process Biochem. 1985, 20, 158-164
- Bergmeyer, H.V., Grabl, M., Walter, H.E. in Methods of Enzymatic Analysis 1983 (Bergmeyer, H.V., ed.), verlag Chemie, Weinheim, 139-140
- Beltaus, S. and Rajaratnam, S. Proc. ASCE J.Hydraul. Div. 1974, 100, 1313-1328
- Berskvar, K. and Hudnik-Plevnik, T. J.Steroid Biochem. 1981, 14, 395-391
- Blanchardie, P., Carde, J.-P., Cassagne, C. Biol.Cellulaire 1977, 30, 127-136
- Brookman, J.S.G. Biotechnol.Bioeng. 1974, 16, 371-383
- Brookman, J.S.G. Biotechnol.Bioeng. 1975, 17, 465-479
- Brookman, J.S.G. Ph.D. thesis 1977, University of Wales, Cardiff, U.K.
- Chisti, J.A. Moo-Young, M. Enzyme Microb.Technol. 1986, 8, 194-204
- Claude, A., Science 1940, 77, 91
- Claude, A. in Microsomes and Drug Oxidations 1969 (Gillette, J.R. et al., eds.), Academic Press, New York, 3
- Coakley, W.T., Bater, A.J., Lloyd D. Adv. Microb. Physiol. 1977, 16, 279-341



Currie, J.A., Dunnill, P., Lilly, M.D. Biotechnol.Bioeng. 1972, 14, 725-736

Darbyshire, J. in Topics in Enzyme and Fermentation Biotechnology 1981 (Wiseman, A. ed.), 5, Ellis Horwood, Chichester, 147-186

Depierre, J.W., Enster, L., in Microsomes, Drug oxidation and Chemical carcinogenesis 1980 (Coon et al., eds), 1, Academic Press, New York, 431-440

Doulah, M.S., Hammond, T.H., Brookman, J.S.G. Biotechnol.Bioeng. 1975, 17, 845-858

Doulah, M.S. Biotechnol.Bioeng. 1977, 19, 649-660

Dunnill, P. Proc.IV IFS Ferment.Technol. Today 1972, 187-194

Dunnill, P. Process Biochem. 1983, 18, 9-13

Dunnill, P., Lilly, M.D. in Single Cell Protein II 1975 (Tannenbaum, S.R., Wang, D.I.C., eds.), MIT Press, Cambridge, MA U.S.A., 179-207

Edebo, L. Ferment.adv. 1969, 249-271

Edebo, L. in Enzyme Technology 1983 (Lafferty, R.M., ed.), Springer-Verlag, Heidelberg, 93-114

Edebo, L. and Magnusson K.-E. Pure Appl. Chem. 1973, 36, 325-338

Elsworth, R., Miller, G.A., Whitaker, A.R., Kitching, D., Sayer, P.D. J.Appl.Chem. 1968, 18, 157-166

Engler, C.R. Ph.D. thesis 1979, University of Waterloo, Ontario, Canada

Engler, C.R. in Comprehensive Biotechnology 1985 (Moo-Young, M.,ed.), 2, Pergamon Press, Oxford & N.Y., 305-324

Engler, C.R., Robinson, C.W. Biotechnol.Bioeng. 1981a, 23, 765-780

Engler, C.R., Robinson, C.W. Biotechnol. Lett. 1981b, 3, 83-88

Fraser, D. Nature 1951, 167, 33-34

Follows, M., Hetherington, P.J., Dunnill, P., Lilly, M.D. Biotechnol.Bioeng. 1971, 13, 549-560

Gardiner, S.A.M., Olbrich, R., Marston, F.A.O., Fish, N.M., Hoare, M., Proc. 4th European Congress on Biotechnol 1987, 2, 541-544

Gleason, F.H. Mycologia 1971, 63, 906-910

Gleason, F.H. Mycologia 1976, 68, 426-429

- Gosh, D. and Samanta, T.B. J. Steroid Biochem. 1981, 14, 1063-1067
- Gray, P.P., Dunnill, P., Lilly, M.D. Proc.IV IFS Ferment.Technol. Today 1972, 347-351
- Gray, P.P., Dunnill, P., Lilly, M.D. Biotechnol.Bioeng. 1973, 15, 309-320
- Greene, R.V., Gould, J.M. Arch.Biochem.Biophys. 1984, 228, 97-104
- Hanisch, W.H. Ph.D. Thesis 1978, University of London, London, U.K.
- Harrison, J.S. Process Biochem. 1967, 2, 41-45
- Hetherington, P.J., Follows, M., Dunnill, P., Lilly, M.D. Trans.Instn.Chem.Engrs. 1971, 49, 142-148
- Hedenskog, G. and Mogren, H. Biotech.Bioeng. 1973, 15, 129-141
- Higgins, J.J., Lewis, D.J., Daley, W.H., Mosqueira, F.G., Dunnill, P., Lilly, M.D. Biotechnol.Bioeng. 1978, 20, 159-182
- Hoare, M., Dunnill, P. The Chemical Engineer 1986, 39-41
- Hughes, D.E. Brit.J.Exp.Pathol. 1951, 32, 97-109
- Hughes, D.E. J.Biochem.Microbiol.Engng. 1961, 3, 405-433
- Hughes, D.E. and Cunningham, V.R. in Biochem. Soc. Symp. 1963, 23, 8-19
- Hughes, D.E., Wimpenny, J.W.T., Lloyd, D. in Methods in Microbiol.1971 (Norris, J.R., Ribbons, D.W., eds.), 5B, Academic Press, N.Y., 1-54
- Kane, J.F., Hartley, D.L. Trends in Biotechnol. 1988, 6, 95-101
- Kawaguchi, T. Bull. JSME 1971, 14, 355-363
- Kitamura, K. and Tanabe, K. Agric.Biol.Chem. 1982, 46, 553-554
- Kramer, P., Bomberg, A. Poster in Proc. Engineering Foundation IV Conf. on Recovery of Bioproducts 1988a
- Kramer, P., Bomberg, A. Chem.-Ing.-Tech. 1988b, 60, 776-778
- Kurzhaals, H.-A., Ph.D. Thesis 1977, Tech.Univ., Hannover, W.G.
- Liu, L.-C., Prokopakis, G.J., Asenjo, J.A. Biotech.Bioeng. 1988, 32, 1113-1127
- Lilly, M.D. and Dunnill, P. in Fermentation Advances 1969 (Perlman, D., ed.), Academic Press, London, 225-247

- Limon-Lason, J., Hoare, M., Osborn, C.B., Doyle, D.J., Dunnill, P. Biotechnol.Bioeng. 1979, 21, 745-774
- Loo, C.C. and Carlton, W.M. J.Dairy Sci. 1953, 36, 64-75
- Lowry, O.H., Roseborough, N.J., Farr, N.J., Randall, R.J. J.Biol.Chem. 1951, 193, 265-275
- McKillop, A.A., Dunkley, W.L., Brockmeyer, R.L., Perry, R.L. J. Dairy Sci. 1955, 38, 273-283
- Magnusson, K.E. and Edebo, L. Biotechnol.Bioeng. 1976a, 18, 449-463
- Magnusson, K.E. and Edebo, L. Biotechnol.Bioeng. 1976b, 18, 865-883
- Magnusson, K.E. and Edebo, L. Biotechnol.Bioeng. 1976c, 18, 975-986
- Marston, F., Lowe, P.A., Doel, M.T., Schoemaker, J.M., White, S., Angal, S. Bio/Technol. 1984, 2, 800-804
- Mohr, K.-H. Lebensmittelindustrie 1980, 27, 399-403
- Mohr, K.-H. J.Food Engng. 1987a, 6, 177-186
- Mohr, K.-H. J.Food Engng. 1987b, 6, 311-324
- Mosqueira, F.G., Higgins, J.J., Dunnill, P., Lilly, M.D. Biotechnol.Bioeng. 1981, 23, 335-343
- Mulder, H. and Walstra, P. in the Milk Fat globule : Emulsion Science as Applied to Milk Products and Comparable Foods 1974, C.A.B., Farnham Royal and Pudoc, Wageningen, Chapter 9
- Nissinen, V.J., Markkanen P. Poster Third Eng. Foundation in Recovery of Bioproducts 1986, Uppsala, Sweden
- Pandolfe, W.D. J.Dairy Sci. 1982, 65, 2035-2044
- Phipps, L.W. Nature 1971, 233, 617-619
- Phipps, L.W. J.Dairy Research 1974, 41, 1-8
- Phipps, L.W. J. Phys. D: Appl.Phys. 1975, 8, 448-462
- Ramaley, R.F. in Advances in Applied Microbiology 1979 ( Perlam D., ed.), 25, Academic Press, N.Y., 37-55
- Sadler, A.M., Winkler, M., Wiseman, A. Chem.Eng.J. 1985, 30b, 43-49

- Scawen, M.D., Atkinson, A. Darbyshire, J. in J.Applied Protein Biochemistry 1980 (Grant, R.A.,ed.), Applied Science Publishers, London, 281-325
- Schutte, H., Kroner, K.H., Hustedt, H., Kula, M.R. Enzyme Microb.Technol. 1983, 5, 143-148
- Schutte, H. and Kula, M.R. Enzyme Microb. Technol. 1988, 10, 552-558
- Scully, D.B. Biotechnol.Bioeng. 1975, 17, 1545-1550
- Scully, D.B. and Wimpenny, J.W.T. Biotech.Bioeng. 1974, 16, 675-687
- Seva, R., Fieschko, J., Sachdev, R., Mann, M. Proc. Society Ind.Microbiol. 1986
- Smeds, A.L., Enfors, S.-O. Enzyme Microb.Technol. 1985, 7, 601-605
- Stock, R.S. and Ray, W.H. J.Polymer Sci. 1985, 23, 1393-1447
- Su, Z.G., Kleinzen, H.H., van Brakel, J., Weeselingh, J.A. Proc. 4th European Congress on Biotechnol. 1987, 2, 554-557
- Talboys, B.L. Ph.D. thesis 1983, University of London, London, U.K.
- Talboys, B.L., Dunnill, P. Biotechnol.Bioeng. 1985, 27, 1726-1729
- Tangen, O., Jonsson, J., Orrenius S. Anal.Biochem. 1973, 54, 597-603
- Taylor, G., Hoare, M., Gray, D.R., Marston, F.A.O. Bio/Technol. 1986, 4, 553-557
- Thomas, V. Ph.D. thesis 1988, University of London, London, U.K.
- Thorpe, N.O. Cell Biology 1984, J.Wisely & son, N.Y.
- Tominaga, Y., Tsujisaka, Y. Agr.Biol.Chem. 1981, 45, 1569-1575
- Tsang, S., Lee, C.-H., Kyun Rha, C. J.Food Sci. 1979, 44, 97-99
- Virkar, P.D., Narendranathan, T.J., Hoare, M., Dunnill, P. Biotechnol.Bioeng. 1981, 23, 425-429
- Walstra, P. Neth. Milk Dairy J. 1969, 23, 290-292
- Wase, D.A.J. and Patel, Y.R. J.Chem.Tech.Biotechnol. 1985, 35B, 165-173
- Washington, C. Laboratory Equipment Digest 1987

Washington, C., Davis S.S., Intern.J.Pharmaceutics 1988, 44, 169-176

Whitworth, D.A. Compt.Rend.Trav.Lab. 1974a, Carlsbeg, 40, 19-32

Whitworth, D.A. Biotechnol.Bioeng. 1974b, 16, 1399-1406

Wiley, W.R. Methods in Enzymology 1974, 31, 609-626

Wiseman, A. Process Biochem. 1969, 4, 63-65

Wimpenny, J.W.T. Process Biochem. 1967, 2, 41-44

Woodrow, J.R., Quirk, A.V. Enzyme Microb.Technol. 1982, 4, 385-389

Yoneya, T. and Sato, Y. Appl.Environ.Microbiol. 1980, 40, 967-969

Zetelaki, K. Process Biochem. 1969, 4, 19-22 and 27

Zomer, E., Er-El, Z., Rokem, J.S. Enzyme microb. Technol. 1987, 9, 281-284